frontiers | Research Topics

New progress in the treatment of bone and soft tissue tumors

Edited by
Zhiyu Zhang, Xiaomeng You, Yingqi Hua, Xiaoyu Xu and Duoyi Zhao

Published in
Frontiers in Pharmacology
Frontiers in Oncology

ISSN 1664-8714
ISBN 978-2-8325-4978-0
DOI 10.3389/978-2-8325-4978-0

About Frontiers

Frontiers is more than just an open access publisher of scholarly articles: it is a pioneering approach to the world of academia, radically improving the way scholarly research is managed. The grand vision of Frontiers is a world where all people have an equal opportunity to seek, share and generate knowledge. Frontiers provides immediate and permanent online open access to all its publications, but this alone is not enough to realize our grand goals.

Frontiers journal series

The Frontiers journal series is a multi-tier and interdisciplinary set of open-access, online journals, promising a paradigm shift from the current review, selection and dissemination processes in academic publishing. All Frontiers journals are driven by researchers for researchers; therefore, they constitute a service to the scholarly community. At the same time, the *Frontiers journal series* operates on a revolutionary invention, the tiered publishing system, initially addressing specific communities of scholars, and gradually climbing up to broader public understanding, thus serving the interests of the lay society, too.

Dedication to quality

Each Frontiers article is a landmark of the highest quality, thanks to genuinely collaborative interactions between authors and review editors, who include some of the world's best academicians. Research must be certified by peers before entering a stream of knowledge that may eventually reach the public - and shape society; therefore, Frontiers only applies the most rigorous and unbiased reviews. Frontiers revolutionizes research publishing by freely delivering the most outstanding research, evaluated with no bias from both the academic and social point of view. By applying the most advanced information technologies, Frontiers is catapulting scholarly publishing into a new generation.

What are Frontiers Research Topics?

Frontiers Research Topics are very popular trademarks of the *Frontiers journals series*: they are collections of at least ten articles, all centered on a particular subject. With their unique mix of varied contributions from Original Research to Review Articles, Frontiers Research Topics unify the most influential researchers, the latest key findings and historical advances in a hot research area.

Find out more on how to host your own Frontiers Research Topic or contribute to one as an author by contacting the Frontiers editorial office: frontiersin.org/about/contact

New progress in the treatment of bone and soft tissue tumors

Topic editors

Zhiyu Zhang — Fourth Affiliated Hospital of China Medical University, China
Xiaomeng You — Brigham and Women's Hospital, Harvard Medical School, United States
Yingqi Hua — Shanghai Jiao Tong University, China
Xiaoyu Xu — University of Pennsylvania, United States
Duoyi Zhao — Fourth Affiliated Hospital of China Medical University, China

Citation

Zhang, Z., You, X., Hua, Y., Xu, X., Zhao, D., eds. (2024). *New progress in the treatment of bone and soft tissue tumors*. Lausanne: Frontiers Media SA. doi: 10.3389/978-2-8325-4978-0

Table of contents

frontiers | Frontiers in Pharmacology

TYPE Editorial
PUBLISHED 23 May 2024
DOI 10.3389/fphar.2024.1430844

OPEN ACCESS

EDITED AND REVIEWED BY
Olivier Feron,
Université catholique de Louvain, Belgium

*CORRESPONDENCE
Zhiyu Zhang,
zyzhang@cmu.edu.cn

†These authors have contributed equally to this work

RECEIVED 10 May 2024
ACCEPTED 13 May 2024
PUBLISHED 23 May 2024

CITATION
Zhao D, Yu J, Ma C, Xu X and Zhang Z (2024), Editorial: New progress in the treatment of bone and soft tissue tumors.
Front. Pharmacol. 15:1430844.
doi: 10.3389/fphar.2024.1430844

Editorial: New progress in the treatment of bone and soft tissue tumors

Duoyi Zhao[1†], Jiachen Yu[1†], Chengbin Ma[1†], Xiaoyu Xu[2] and Zhiyu Zhang[1*]

[1]Department of Orthopedics, The Fourth Affiliated Hospital of China Medical University, China Medical University, Shenyang, Liaoning, China, [2]McKay Orthopedics Research Lab, University of Pennsylvania, Philadelphia, PA, United States

KEYWORDS

bone and soft tissue tumors, osteosarcoma, chemotherapy, immunotherapy, nanotechnology engineering, clinical transformation

Editorial on the Research Topic
New progress in the treatment of bone and soft tissue tumors

Bone and soft tissue tumors, constitute a heterogeneous group of neoplasms that frequently affect the young. These tumors are highly aggressive, often metastasizing early in the disease's progression, posing a significant challenge to orthopedic oncologists. Treatment strategies for these tumors have evolved, with a mainstay approach combining surgery, chemotherapy, and more recently, the introduction of targeted therapies and immunotherapy. Over the past decade, there have been significant advancements in the molecular understanding of these tumors, leading to the development of innovative therapeutic strategies that hold promise for improving patient outcomes and potentially modifying the prognosis of these malignancies.

This study encompassed a total of 10 articles, comprising 4 original research articles, 5 review articles, and 1 case report.

Chen-xi et al. conducted thorough research into the role of long non-coding RNA PRR7-AS1 in the development of bone sarcoma and evaluated its potential as a therapeutic target. The team discovered that PRR7-AS1 interacts with the protein RNF2, thereby inhibiting the translation of the downstream gene MTUS1, which in turn promotes the proliferation and migration of bone sarcoma cells. Furthermore, the researchers found that the knockdown of PRR7-AS1 significantly suppressed the *in vitro* proliferation and the *in vivo* growth and metastasis of bone sarcoma cells. These findings underscore the oncogenic role of PRR7-AS1 in bone sarcoma and suggest its potential as a novel target for diagnosis and treatment.

Miwa et al. reported on a case of pulmonary giant cell tumor of the bone (GCTB) that was inoperable and successfully treated with Denosumab. The case involved a 49-year-old male who had undergone two surgeries for GCTB in the right proximal ulna. A CT-guided needle biopsy revealed rapid growth and high 18F-FDG uptake, though no histological signs of malignancy were present. Given that the lung lesion was not surgically removable, Denosumab was administered. After 18 months of initial treatment with Denosumab, there were no symptoms or signs of tumor growth. While the long-term efficacy and safety of Denosumab remain to be determined, the authors posit that it may represent a viable treatment option for patients with non-resectable pulmonary GCTB.

Zhang et al. have made a notable advancement in the local drug delivery for bone tumors through the innovative use of a composite scaffold made of poly (3-hydroxybutyrate-co-3-hydroxyvalerate) (PHBV), polyethylene glycol (PEG), and melatonin. This method presents a promising avenue for enhancing bone cancer treatment by minimizing the systemic side effects of chemotherapy.

In another study by Zhang et al., nanoparticles are seen as an emerging drug delivery system that could improve the precision and efficacy of osteosarcoma treatment, reduce the side effects associated with chemotherapy, and enhance patient outcomes through targeted delivery strategies. Although the clinical application of nanoparticles in osteosarcoma treatment is still under investigation, their potential and future prospects are significant and are anticipated to play a crucial role in future clinical practice.

Zhu et al. reviewed the potential of nanomedicine to enhance immunotherapy by targeting bone marrow cells within the tumor microenvironment, highlighting the innovative thinking that is propelling the field forward. By modulating the immunosuppressive effects of bone marrow cells, these therapies aim to maximize the immune system's potential to combat cancer cells, marking a new frontier in the treatment of bone and soft tissue tumors.

Hou et al. emphasized the use of engineered biomaterials to mitigate chemotherapy-related cardiac toxicity, showcasing innovative solutions to improve the safety and tolerability of cancer treatments. These biomaterials, by delivering chemotherapy drugs directly to the tumor site, can reduce systemic exposure and toxicity, making chemotherapy a more feasible option for patients with bone and soft tissue tumors.

Takeshima et al. stressed the critical importance of fertility preservation in young patients undergoing treatment for malignant bone and soft tissue tumors. With the increasing use of alkylating agents, which are known to cause gonadal toxicity, the preservation of sperm prior to the initiation of treatment is a crucial consideration in the comprehensive care of these patients. This aspect of care is vital as it pertains to long-term quality of life and the potential for family planning post-treatment.

Osumi et al. study on the role of proteoglycan synthesis genes in osteosarcoma stem cells offers valuable insights into cellular mechanisms that could be targeted for therapy. Understanding the pathways that govern the self-renewal and differentiation of osteosarcoma stem cells is essential for developing targeted therapies to effectively counteract tumor recurrence and metastasis. These therapies are designed to disrupt specific molecular pathways driving tumor growth, offering a more personalized approach to treatment.

Zhou et al. reviewed the role of hypoxia-inducible factor-1 alpha (HIF-1α) in osteosarcoma metastasis, providing a comprehensive summary of the molecular mechanisms involved. HIF-1α, a key regulator of cellular response to hypoxia, is increasingly recognized as a potential therapeutic target for metastatic osteosarcoma. Disrupting the complex signaling pathways regulated by HIF-1α may inhibit the onset and progression of metastasis, offering renewed hope for patients with advanced disease.

Yang et al. emphasized that the rich vascular system of bone marrow provides favorable conditions for tumor cell growth, and circulating tumor cells can form micrometastases in the early stage of disease and promote metastasis through molecular mechanisms. Symptomatic bone marrow metastasis is associated with severe myelosuppression and poor prognosis. Common symptoms include anemia, thrombocytopenia, and abnormal coagulation. The effect of myelosuppression should be considered in treatment.

In summary, this Research Topic's articles highlight innovative research and clinical progress in bone and soft tissue tumor treatments. Advances in targeted therapies, nanotechnology for drug delivery, and immunotherapy illustrate significant progress. With a deeper understanding of tumor biology, integrating these approaches should improve patient outcomes. Personalized medicine is a continuous pursuit, and these studies are key steps towards it. We hope this Topic encourages further research and interdisciplinary collaboration to develop advanced treatments for these tumors.

Author contributions

DZ: Conceptualization, Writing–original draft, Writing–review and editing. JY: Investigation, Writing–original draft, Writing–review and editing. CM: Conceptualization, Writing–original draft, Writing–review and editing. XX: Methodology, Writing–review and editing. ZZ: Conceptualization, Formal Analysis, Project administration, Writing–original draft, Writing–review and editing.

Funding

The author(s) declare that no financial support was received for the research, authorship, and/or publication of this article.

Acknowledgments

The editors would like to thank the authors, reviewers, and the Frontiers in Pharmacology development team, whose efforts have led to the success of this Research Topic.

Conflict of interest

The authors declare that the research was conducted in the absence of any commercial or financial relationships that could be construed as a potential conflict of interest.

The author(s) declared that they were an editorial board member of Frontiers, at the time of submission. This had no impact on the peer review process and the final decision.

Publisher's note

frontiers | Frontiers in Oncology

TYPE Case Report
PUBLISHED 16 August 2023
DOI 10.3389/fonc.2023.1230074

OPEN ACCESS

EDITED BY
Duoyi Zhao,
Fourth Affiliated Hospital of China Medical University, China

REVIEWED BY
Teruya Kawamoto,
Kobe University, Japan
SongFeng Xu,
Chinese Academy of Medical Sciences and Peking Union Medical College, China
Ran Wei,
Peking University People's Hospital, China

*CORRESPONDENCE
Shinji Miwa
smiwa001@yahoo.co.jp

RECEIVED 08 June 2023
ACCEPTED 18 July 2023
PUBLISHED 16 August 2023

CITATION
Miwa S, Yamamoto N, Hayashi K, Takeuchi A, Igarashi K, Taniguchi Y, Morinaga S, Asano Y, Nojima T and Tsuchiya H (2023) Case Report: Unresectable pulmonary metastases of a giant cell tumor of bone treated with denosumab: a case report and review of literature.
Front. Oncol. 13:1230074.
doi: 10.3389/fonc.2023.1230074

Case Report: Unresectable pulmonary metastases of a giant cell tumor of bone treated with denosumab: a case report and review of literature

Shinji Miwa[1]*, Norio Yamamoto[1], Katsuhiro Hayashi[1], Akihiko Takeuchi[1], Kentaro Igarashi[1], Yuta Taniguchi[1], Sei Morinaga[1], Yohei Asano[1], Takayuki Nojima[1,2] and Hiroyuki Tsuchiya[1]

[1]Department of Orthopedic Surgery, Graduate School of Medical Sciences, Kanazawa University, Kanazawa, Japan, [2]Department of Pathology, Graduate School of Medical Sciences, Kanazawa, Japan

Giant cell tumors of bone (GCTB) sometimes metastasize to distant organs. In this case report, we present pulmonary metastases of GCTB mimicking malignancies. A 49-year-old man underwent two surgical treatments for a GCTB of the right proximal radius. At the time of the second surgery, no lesions were observed on chest radiography. Three years after surgery, the patient presented with cough and dyspnea, and chest radiography and computed tomography (CT) revealed multiple lung nodules. Positron emission tomography/CT revealed a high accumulation of 18F-fluoro-2-deoxy-D-glucose (18F-FDG) in multiple lesions. Based on the rapid growth and accumulation of 18F-FDG, a metastatic malignant tumor was suspected. CT-guided needle biopsy was performed, and the histology showed proliferation of spindle cells and multinuclear giant cells without malignant changes. Denosumab was administered because multiple lung lesions were unresectable. One month after denosumab treatment, CT showed marked shrinkage of the lesions, and the symptoms significantly improved. Eighteen months after the initial treatment with denosumab, the patient had no symptoms or tumor growth. Although its long-term efficacy and safety remain unclear, denosumab may be a treatment option for patients with unresectable pulmonary GCTB.

KEYWORDS

metastasis, giant cell tumor of bone, PET, denosumab, unresectable

1 Introduction

Giant cell tumor of bone (GCTB), a locally aggressive and rarely metastasizing tumor, is classified as intermediate malignancies according to the 2020 World Health Organization (WHO) classification (1–3). Histologically, GCTB consist of ovoid mononuclear cells and

giant osteoclast-like cells (4, 5). Osteoclast-like multinuclear cells and their precursors express receptor activator of nuclear factor-kappa B (RANK), whereas mononuclear stromal cells express RANKL, which is necessary for the formation, function, and survival of the osteoclasts (6–9).

The standard treatment for GCTB is surgical excision, which consists of curettage and en bloc resection (10). In cases of unresectable GCTB, denosumab, a human monoclonal antibody targeting the nuclear factor-kappa B ligand (RANKL), is considered a treatment option (5, 11, 12). Denosumab binds to RANKL and blocks its binding to RANK on osteoclasts and osteoclast precursors, resulting in the inhibition of osteoclast differentiation and bone resorption by the osteoclasts (5, 12). Denosumab is widely used to prevent hypercalcemia, pathological fractures, and spinal cord compression in patients with metastatic bone diseases (13–15). Furthermore, high response rates have been reported in clinical studies on denosumab in patients with GCTB (5, 11). In a phase 2 study of denosumab in patients with GCTB, patients received 120 mg of subcutaneous denosumab (every 4 weeks with a loading dose on days 8 and 15 of the first cycle) (16). In this study, 163 of 169 (96%) patients were progression-free after a median follow-up of 13 months (16). In another study including 43 patients with resectable GCTB and 54 patients with unresectable GCTB, all tumors were controlled by denosumab treatment, whereas 40% of patients who discontinued denosumab showed tumor progression after a median of 8 months (12). Furthermore, it is reported that neoadjuvant treatment with denosumab can downstage the lesions by increasing the thickness of cortical bone and forming new cortical rim around the soft-tissue mass that facilitates joint salvage and decrease surgery invasiveness (1, 17–23). Although denosumab does not have direct cytotoxic effect on neoplastic stromal cells, it can inhibit pulmonary metastases. Denosumab prevents RANKL-mediated formation and activation of multinucleated giant cells from RANK-positive mononuclear preosteoclasts and macrophages, resulting in marked reduction in multinucleated giant cells (5, 24–26). Although denosumab is considered an effective treatment option for patients with unresectable GCTB, the indications, doses, and periods of denosumab use in metastatic GCTB remain unclear. Therefore, investigations into treatment strategies for unresectable metastatic GCTB are required.

In the management of malignant tumors, ^{18}F-fluoro-2-deoxy-D-glucose (^{18}F-FDG) positron emission tomography/computed tomography (PET/CT) is one of the most useful diagnostic tools to assess grading, staging, therapeutic response, surgical planning, and expected prognosis (27). PET/CT can be used to differentiate between malignant and benign lesions (28). However, GCTB has high accumulation of ^{18}F-FDG (27), and the high accumulation of ^{18}F-FDG may mislead the diagnosis of the tumor (29–31). In this report, we present a case of pulmonary metastasis of GCTB that mimicked malignancies on radiographic examinations, which was successfully controlled by treatment with denosumab.

2 Case presentation

A 49-year-old man presented with right elbow pain. Radiography revealed osteolytic lesions and scalloping in the right proximal radius (Figure 1A). Magnetic resonance imaging showed a tumor lesion in the proximal radius with iso intensity on T1-weighted images and high intensity on T2-weighted images, and the lesion was enhanced by gadolinium (Figure 1B). ^{201}Thallium (^{201}Tl) scintigraphy and ^{99m}Tc-methylene diphosphonate (^{99m}Tc-MDP) scintigraphy showed an increased uptake of the ^{201}Tl and ^{99m}Tc-MDP in the proximal radius. Open biopsy was performed, and the histology of the tumor showed proliferation of spindle cells and multinuclear osteoclast-like cells with collagen fibers and deposition of hemosiderin (Figure 1C). Immunohistological staining showed positivity for H3.3G34W in the tumor cells (Figure 1D). Based on the histological findings, the tumor was diagnosed as a GCTB. He underwent curettage with adjuvant treatment with ethanol and phenol, and the bone defect was augmented with α-tricalcium phosphate (αTCP) (Figure 1E). Two years after the initial surgery, radiography and CT revealed tumor recurrence. He underwent denosumab treatment (120 mg on days 1, 8, 15, 29, 56, and 84), curettage with adjuvant treatment with ethanol and phenol, and artificial bone grafting using α-TCP. Histological

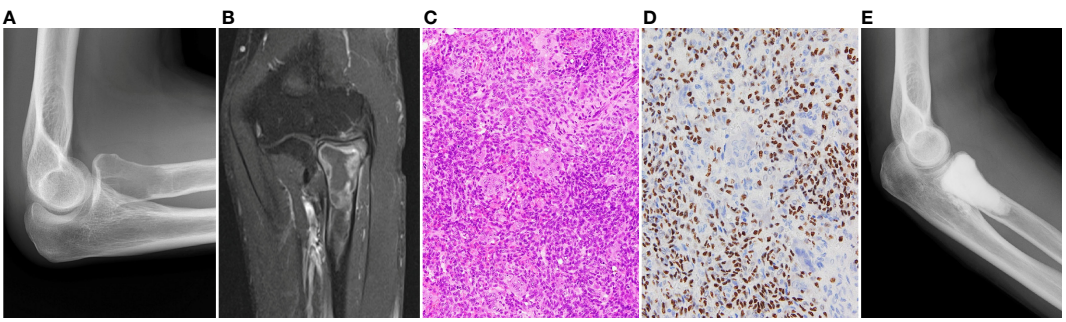

FIGURE 1
(A) Initial radiography shows an osteolytic lesion in the proximal radius. **(B)** In enhanced magnetic resonance imaging, the lesion is enhanced by gadolinium. **(C)** Histology of the specimen of the radius shows proliferation of spindle cells and multinucleated osteoclast-like cells, which is consistent with diagnosis of GCTB. **(D)** Immunohistological staining of H3.3G34W. **(E)** The lesion is curetted and augmented with α-tricalcium phosphate.

examination of the tumor specimen showed proliferation of spindle cells and multinuclear giant cells, consistent with GCTB recurrence. At the time of the second surgery, no pulmonary nodules were detected on chest radiography (Figure 2A).

Three years after the second surgery, the patient presented with cough and dyspnea. Radiography and CT revealed 31 nodules, including the largest lesion (15 × 13 cm) in the lungs (Figure 2B). PET/CT revealed a markedly increased uptake of ^{18}F-FDG in the lesions (SUVmax = 11.8–12.2) (Figures 3A–C). Based on the clinical course and radiological findings, malignant metastasis was suspected. CT-guided needle biopsy was performed to confirm the diagnosis of multiple lung lesions. Histological examination of the specimen revealed proliferation of spindle cells and multinuclear osteoclast-like cells without malignant changes (Figure 3D), and the tumor cells were positive for H3.3G34W on immunohistological staining (Figure 3E). These findings were similar to the histology of the primary lesions of the proximal radius, and the lung lesions were diagnosed as multiple metastases from GCTB. Because the lung nodules were thought to be unresectable, he was treated with denosumab (120 mg subcutaneously on days 1, 8, 15, and 29 and every 4 weeks thereafter). One month after the initiation of denosumab treatment, shrinkages of the lung nodules and gradual improvement in pulmonary symptoms were observed (Figure 4). Then, the denosumab treatment continued every 4 weeks. During the denosumab treatment, the patient underwent chest X-ray every month, blood examination every 3 months, and chest CT every 6 months. After 3 months of denosumab treatment, the patient achieved a partial response according to the Response Evaluation Criteria in Solid Tumors criteria (32). During the treatment 7period, X-ray and CT showed no regrowth of the tumor, and there were no adverse events, such as hypocalcemia and osteoporosis of the jaw. Eighteen months after the initial treatment with denosumab, the patient showed no symptoms or disease progression and continued to undergo denosumab treatment (Figure 4).

3 Discussion

In this report, we presented a case of multiple pulmonary metastases of GCTB. In this case, multiple pulmonary lesions were unresectable; however, these lesions were successfully controlled with denosumab treatment. The incidence of metastasis in GCTB has been reported to be 1–9% (33–37), and the lung is the most common site of metastasis, followed by the brain, kidney, bone, skin, and lymph nodes (34). Although most metastatic lung lesions of GCTB are slow-growing and can be controlled by tumor resection or observation (10, 33), some metastatic GCTB are aggressive and causes mortality (10, 38, 39). Although our follow-up protocol for patients with GCTB did not include chest X-ray, addition of chest X-ray or CT to the follow-up protocol is recommend to diagnose pulmonary metastases of GCTB earlier. Tsukamoto et al. reported that follow-up protocol after surgical treatment for GCTB included chest X-ray or CT every 4 months for the first 2 years, every 6 months for the next 3 years, and then annually (10). Chan et al. investigated the risk factors for pulmonary metastasis from GCTB in 291 patients with benign GCTB (39). In this study, only local recurrence was an independent risk factor for pulmonary metastases. Tsukamoto et al. investigated the outcomes and safety of initial observations in patients with pulmonary metastases of GCTB (10). In this study, 46% of patients with lung lesions ≤ 5 mm and all patients with lung lesions > 5 mm had disease progression. The patients with lung lesions ≤ 5 mm had significantly better progression-free survival than those with lung lesions > 5 mm ($p = 0.022$). Initial observation may be an option for patients with small pulmonary lesions. However, the present case required treatment because the pulmonary metastases were large and symptomatic.

In this case, clinical course and high accumulation of ^{18}F-FDG in PET/CT mimicked malignancies. In previous reports, GCTB had higher accumulation of ^{18}F-FDG (mean SUVmax = 8.4–16.8) than

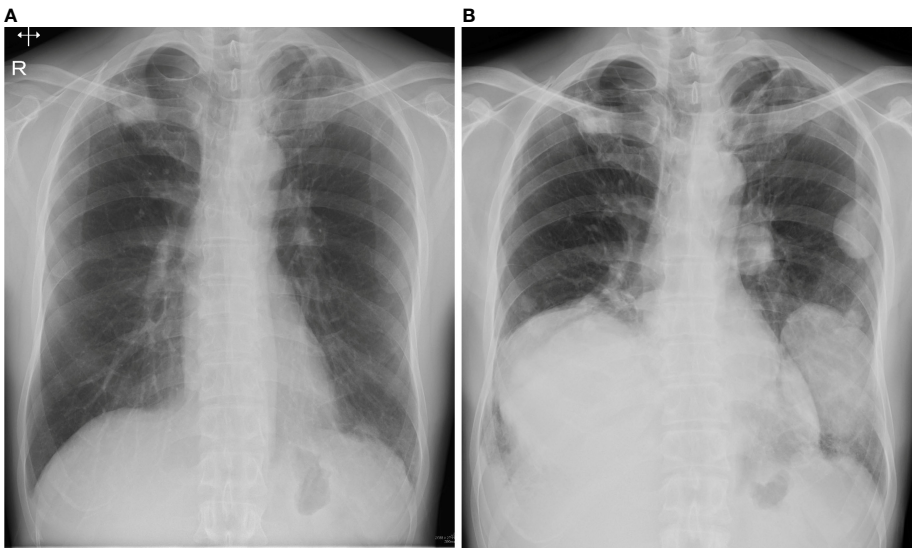

FIGURE 2
(A) At the time of second surgery, no pulmonary lesion was detected on radiography. **(B)** Three years after the second surgery, radiography showed multiple lung nodules.

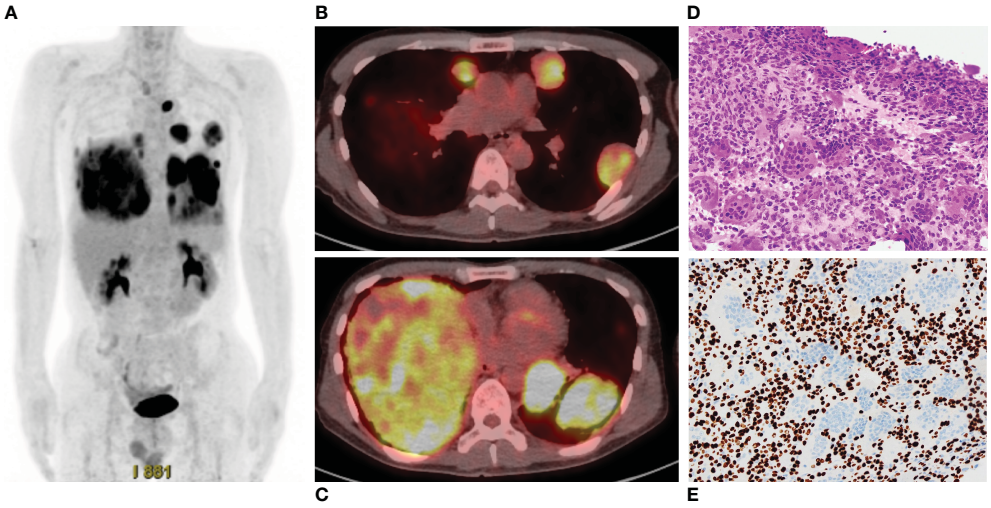

FIGURE 3
(A) Positron emission tomography/computed tomography shows high accumulation of ^{18}F-fluoro-2-deoxy-D-glucose in the multiple lung lesions. **(B, C)**. The maximum standardized uptake values are 11.8–12.2. **(D)** Histology of specimen of the lung nodule shows proliferation of spindle cells and multinuclear cells, which is similar to the findings of specimen of the radius. **(E)** Immunohistological staining of H3.3G34W.

other benign lesions (28, 40–43). Uptake of FDG in tumor cells is associated with expression of glucose transporter protein (GLUT)-1, hexokinase II, and with gene upregulation for these proteins (44, 45). Ong et al. reported significantly greater GLUT-1 and hexokinase II in human cancer cell lines (46). On the other hand, other studies showed upregulation of GLUT-1 in monocyte-derived macrophages (47–49), and the high ^{18}F-FDG uptake may be explained by high monocyte/macrophage content within GCTs (44, 50). Based on the reports, GCT and other lesions containing active macrophages should be considered in differential diagnoses of lesions with high accumulation of ^{18}F-FDG.

There are several reports on systemic treatment for metastatic pulmonary GCTB (Table 1) (51–60). In a retrospective study of denosumab treatment in 7 patients with pulmonary GCTB, 3 patients showed partial response and 4 patients had stable disease (54). Based on the previous reports, denosumab can be one of the treatment options in patients with unresectable pulmonary GCTB (54, 56, 59, 60). However, denosumab can cause severe side effects, including hypocalcemia, hypophosphatemia, increased risk of atypical femoral fracture, and osteonecrosis of the jaw (5, 16). Therefore, long-term treatment with denosumab is not ideal therapeutic option, and discontinuation, dose reduction, or extension of the treatment interval, may be needed to avoid severe adverse effects of denosumab. Although denosumab can reduce tumor size by inhibiting osteoclastic differentiation and reducing giant cells, it is not cytocidal in the neoplastic stromal cells of GCTB, and discontinuation of the treatment may cause regrowth of the tumor (12). Tanikawa et al. reported a case treated with extended interval of the denosumab treatment for GCTB in the sphenoid bone (61). In their report, denosumab treatment (120 mg) for the first 2 years was performed every 4 weeks. Subsequently, the treatment interval was gradually extended, with 4 monthly dosing for the next 1 year, followed by a 6 monthly dosing for 2 years. During the extension of the treatment interval, slight growth of the lesion was observed, but it was thought to be acceptable range. They concluded that optimal extended dosing interval of denosumab

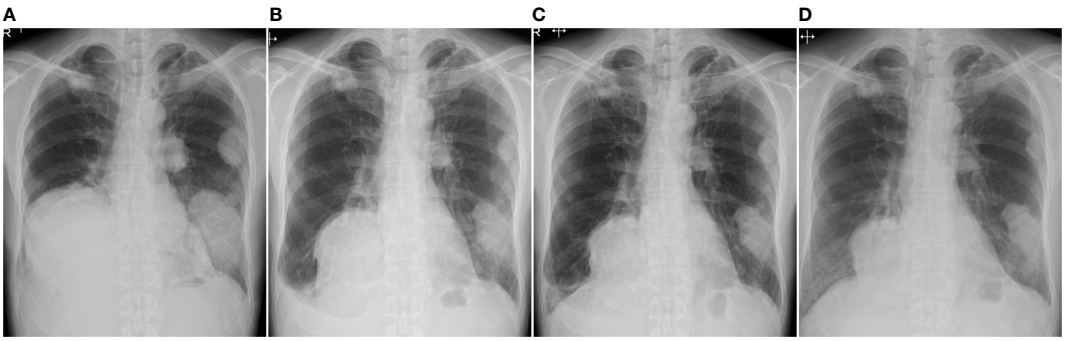

FIGURE 4
Radiography examination before treatment **(A)**, 1 month **(B)**, 3 months **(C)**, and 18 months **(D)** after the initial treatment of denosumab. The pulmonary lesions show response to the treatment of denosumab.

TABLE 1 Recent reports of systemic treatment of pulmonary metastasis of GCTB.

Author	N	Treatment	Malignant change	Response	Severe side effect
Gong T (29)	1	Denosumab	–	PD	–
		Denosumab + apatinib		PR	
Feng L (30)	1	Denosumab and radiotherapy	–	Denosumab: PD Radiotherapy: PR	–
Wang G (31)	1	Denosumab	–	PD	–
		Denosumab + sunitinib		PR	
Luo Y (32)	7	Denosumab	–	PR: 3 SD: 4	–
Sachan DK (33)	1	Chemotherapy and radiotherapy	–	CR	–
Yamagishi T (34)	1	Denosumab	–	PR	–
Wei F (35)	2	IFN-α	–	PR	leukocytopenia
		IFN-α	–	PR	leukocytopenia
Iwai T (36)	1	Pazopanib	+	PR	–
Kudawara I (37)	1	Denosumab	–	PR	–
Egbert RC (38)	1	Denosumab	–	PR	–
Present report	1	Denosumab	-	PR	-

CR, complete response; PR, partial response; SD, stable disease; PD, progressive disease.

treatment after achieving the stabilization of GCTB was 6 months. Thus, reducing the dose or extending the dosing interval as much as possible is desirable for patients who are unable to discontinue the medication.

4 Conclusions

In this case report, we present the pulmonary metastases from a GCTB mimicking malignancy. PET/CT revealed a high accumulation of ^{18}F-FDG in the lesions. A metastatic malignant tumor was suspected in this case; however, histological examination revealed a metastatic GCTB without malignant changes. Although the pulmonary nodules were unresectable, they were controlled with denosumab. Denosumab may be a treatment option for patients with unresectable GCTB metastases. Further studies on dose reduction or extension of the treatment interval of denosumab treatment are demanded.

Data availability statement

The original contributions presented in the study are included in the article/supplementary material. Further inquiries can be directed to the corresponding author.

Ethics statement

Ethical review and approval were not required for the study on human participants in accordance with the local legislation and institutional requirements. The patients/participants provided written informed consent to participate in this study. Written informed consent was obtained from the patients to publish any potentially identifiable images or data in this article.

Author contributions

The manuscript was drafted by ShM, NY, and HT. ShM, NY, KH, AT, KI, YT, SeM and YA examined and treated the patient. TN performed the histopathological assessment. NY, TN, and HT supervised this study. All authors contributed to the article and approved the submitted version.

Conflict of interest

The authors declare that the research was conducted in the absence of any commercial or financial relationships that could be construed as a potential conflict of interest.

Publisher's note

References

1. Puri A, Gulia A, Hegde P, Verma V, Rekhi B. Neoadjuvant denosumab: its role and results in operable cases of giant cell tumour of bone. *Bone Joint J* (2019) 101-B:170–7. doi: 10.1302/0301-620X.101B2.BJJ-2018-0907.R2

2. Tsukamoto S, Mavrogenis AF, Kido A, Errani C. Current Concepts in the Treatment of Giant Cell Tumors of Bone. *Cancers (Basel)* (2021) 13:3647. doi: 10.3390/cancers13153647

3. WHO Classification of Tumours Editorial Board. *WHO Classification of Tumours of Soft Tissue and Bone. 5th ed*. Lyon, France: IARC Press (2020).

4. Bullough BM. Malignancy in giant cell tumour. World Health Organization classification of tumours. In: *pathology and genetics of tumours of soft tissue and bone*. Lyon: International Agency for Research on Cancer (IARC (2002).

5. Thomas D, Henshaw R, Skubitz K, Chawla S, Staddon A, Blay J-Y, et al. Denosumab in patients with giant-cell tumour of bone: an open-label, phase 2 study. *Lancet Oncol* (2010) 11:275–80. doi: 10.1016/S1470-2045(10)70010-3

6. Fuller K, Wong B, Fox S, Choi Y, Chambers TJ. TRANCE is necessary and sufficient for osteoblast-mediated activation of bone resorption in osteoclasts. *J Exp Med* (1998) 188:997–1001. doi: 10.1084/jem.188.5.997

7. Huang L, Xu J, Wood DJ, Zheng MH. Gene expression of osteoprotegerin ligand, osteoprotegerin, and receptor activator of NF-kappaB in giant cell tumor of bone: possible involvement in tumor cell-induced osteoclast-like cell formation. *Am J Pathol* (2000) 156:761–7. doi: 10.1016/S0002-9440(10)64942-5

8. Lacey DL, Tan HL, Lu J, Kaufman S, Van G, Qiu W, et al. Osteoprotegerin ligand modulates murine osteoclast survival *in vitro* and *in vivo*. *Am J Pathol* (2000) 157:435–48. doi: 10.1016/S0002-9440(10)64556-7

9. Lacey DL, Timms E, Tan HL, Kelley MJ, Dunstan CR, Burgess T, et al. Osteoprotegerin ligand is a cytokine that regulates osteoclast differentiation and activation. *Cell* (1998) 93:165–76. doi: 10.1016/S0092-8674(00)81569-X

10. Tsukamoto S, Ciani G, Mavrogenis AF, Ferrari C, Akahane M, Tanaka Y, et al. Outcome of lung metastases due to bone giant cell tumor initially managed with observation. *J Orthop Surg Res* (2020) 15:510. doi: 10.1186/s13018-020-02038-1

11. Chawla S, Blay J-Y, Rutkowski P, Le Cesne A, Reichardt P, Gelderblom H, et al. Denosumab in patients with giant-cell tumour of bone: a multicentre, open-label, phase 2 study. *Lancet Oncol* (2019) 20:1719–29. doi: 10.1016/S1470-2045(19)30663-1

12. Palmerini E, Chawla NS, Ferrari S, Sudan M, Picci P, Marchesi E, et al. Denosumab in advanced/unresectable giant-cell tumour of bone (GCTB): For how long? *Eur J Cancer* (2017) 76:118–24. doi: 10.1016/j.ejca.2017.01.028

13. Bekker PJ, Holloway DL, Rasmussen AS, Murphy R, Martin SW, Leese PT, et al. A single-dose placebo-controlled study of AMG 162, a fully human monoclonal antibody to RANKL, in postmenopausal women. *J Bone Miner Res* (2004) 19:1059–66. doi: 10.1359/JBMR.040305

14. McClung MR, Lewiecki EM, Cohen SB, Bolognese MA, Woodson GC, Moffett AH, et al. Denosumab in postmenopausal women with low bone mineral density. *N Engl J Med* (2006) 354:821–31. doi: 10.1056/NEJMoa044459

15. Lipton A, Steger GG, Figueroa J, Alvarado C, Solal-Celigny P, Body JJ, et al. Randomized active-controlled phase II study of denosumab efficacy and safety in patients with breast cancer-related bone metastases. *J Clin Oncol* (2007) 25:4431–7. doi: 10.1200/JCO.2007.11.8604

16. Chawla S, Henshaw R, Seeger L, Choy E, Blay J-Y, Ferrari S, et al. Safety and efficacy of denosumab for adults and skeletally mature adolescents with giant cell tumour of bone: interim analysis of an open-label, parallel-group, phase 2 study. *Lancet Oncol* (2013) 14:901–8. doi: 10.1016/S1470-2045(13)70277-8

17. Liang H, Liu X, Yang Y, Guo W, Yang R, Tang X, et al. Ultra-Short Course of Neo-Adjuvant Denosumab for Nerve-Sparing Surgery for Giant Cell Tumor of Bone in Sacrum. *Spine (Phila Pa* (2022) 1976) 47:691–701. doi: 10.1097/BRS.0000000000004318

18. Traub F, Singh J, Dickson BC, Leung S, Mohankumar R, Blackstein ME, et al. Efficacy of denosumab in joint preservation for patients with giant cell tumour of the bone. *Eur J Cancer* (2016) 59:1–12. doi: 10.1016/j.ejca.2016.01.006

19. Muller DA, Beltrami G, Scoccianti G, Campanacci DA, Franchi A, Capanna R. Risks and benefits of combining denosumab and surgery in giant cell tumor of bone-a case series. *World J Surg Oncol* (2016) 14:281. doi: 10.1186/s12957-016-1034-y

20. Errani C, Tsukamoto S, Leone G, Righi A, Akahane M, Tanaka Y, et al. Denosumab may increase the risk of local recurrence in patients with giant-cell tumor of bone treated with curettage. *J Bone Joint Surg Am* (2018) 100:496–504. doi: 10.2106/JBJS.17.00057

21. Chinder PS, Hindiskere S, Doddarangappa S, Pal U. Evaluation of local recurrence in giant-cell tumor of bone treated by neoadjuvant denosumab. *Clin Orthop Surg* (2019) 11:352–60. doi: 10.4055/cios.2019.11.3.352

22. Hindiskere S, Errani C, Doddarangappa S, Ramaswamy V, Rai M, Chinder PS. Is a short-course of preoperative denosumab as effective as prolonged therapy for giant cell tumor of bone? *Clin Orthop Relat Res* (2020) 478:2522–33. doi: 10.1097/CORR.0000000000001285

23. Treffel M, Lardenois E, Larousserie F, Karanian M, Gomez-Brouchet A, Bouvier C, et al. Denosumab-treated giant cell tumors of bone: a clinicopathologic analysis of 35 cases from the french group of bone pathology. *Am J Surg Pathol* (2020) 44:1–10. doi: 10.1097/PAS.0000000000001388

24. Lewiecki EM. Clinical use of denosumab for the treatment for postmenopausal osteoporosis. *Curr Med Res Opin* (2010) 26:2807–12. doi: 10.1185/03007995.2010.533651

25. Branstetter DG, Nelson SD, Manivel JC, Blay JY, Chawla S, Thomas DM, et al. Denosumab induces tumor reduction and bone formation in patients with giant-cell tumor of bone. *Clin Cancer Res* (2012) 18:4415–24. doi: 10.1158/1078-0432.CCR-12-0578

26. Rekhi B, Verma V, Gulia A, Jambhekar NA, Desai S, Juvekar SL, et al. Clinicopathological features of a series of 27 cases of post-denosumab treated giant cell tumors of bones: a single institutional experience at a tertiary cancer referral centre, india. *Pathol Oncol Res* (2017) 23:157–64. doi: 10.1007/s12253-016-0123-0

27. Hoshi M, Takada J, Oebisu N, Hata K, Ieguchi M, Nakamura H. Overexpression of hexokinase-2 in giant cell tumor of bone is associated with false positive in bone tumor on FDG-PET/CT. *Arch Orthop Trauma Surg* (2012) 132:1561–8. doi: 10.1007/s00402-012-1588-2

28. Miwa S, Mochizuki T, Yamamoto N, Shirai T, Hayashi K, Takeuchi A, et al. Efficacy and limitations of f-18-fluoro-2-deoxy-d-glucose positron emission tomography to differentiate between malignant and benign bone and soft tissue tumors. *Anticancer Res* (2018) 38:4065–72. doi: 10.21873/anticanres.12696

29. Aoki J, Watanabe H, Shinozaki T, Takagishi K, Ishijima H, Oya N, et al. FDG PET of primary benign and malignant bone tumors: standardized uptake value in 52 lesions. *Radiology* (2001) 219:774–7. doi: 10.1148/radiology.219.3.r01ma08774

30. Zhang Y, Reeve IP, Lewis DH. A case of giant cell tumor of sacrum with unusual pulmonary metastases: CT and FDG PET findings. *Clin Nucl Med* (2012) 37:920–1. doi: 10.1097/RLU.0b013e31825b2441

31. Makis W, Alabed YZ, Nahal A, Novales-Diaz JA, Hickeson M. Giant cell tumor pulmonary metastases mimic primary malignant pulmonary nodules on (18)F-FDG PET/CT. *Nucl Med Mol Imag* (2012) 46:134–7. doi: 10.1007/s13139-012-0134-z

32. Eisenhauer EA, Therasse P, Bogaerts J, Schwartz LH, Sargent D, Ford R, et al. New response evaluation criteria in solid tumours: revised RECIST guideline (version 1.1). *Eur J Cancer* (2009) 45:228–47. doi: 10.1016/j.ejca.2008.10.026

33. Dominkus M, Ruggieri P, Bertoni F, Briccoli A, Picci P, Rocca M, et al. Histologically verified lung metastases in benign giant cell tumours–14 cases from a single institution. *Int Orthop* (2006) 30:499–504. doi: 10.1007/s00264-006-0204-x

34. Gupta R, Seethalakshmi V, Jambhekar NA, Prabhudesai S, Merchant N, Puri A, et al. Clinicopathologic profile of 470 giant cell tumors of bone from a cancer hospital in western India. *Ann Diagn Pathol* (2008) 12:239–48. doi: 10.1016/j.anndiagpath.2007.09.002

35. Siebenrock KA, Unni KK, Rock MG. Giant-cell tumour of bone metastasising to the lungs. *J Bone Joint Surg Br* (1998) 80-B:43–7. doi: 10.1302/0301-620X.80B1.0800043

36. Tubbs WS, Brown LR, Beabout JW, Rock MG, Unni KK. Benign giant-cell tumor of bone with pulmonary metastases: clinical findings and radiologic appearance of metastases in 13 cases. *AJR Am J Roentgenol* (1992) 158:331–4. doi: 10.2214/ajr.158.2.1729794

37. Rosario M, Kim HS, Yun JY, Han I. Surveillance for lung metastasis from giant cell tumor of bone. *J Surg Oncol* (2017) 116:907–13. doi: 10.1002/jso.24739

38. Katz E, Nyska M, Okon E, Zajicek G, Robin G. Growth rate analysis of lung metastases from histologically benign giant cell tumor of bone. *Cancer* (1987) 59:1831–6. doi: 10.1002/1097-0142(19870515)59:10<1831::AID-CNCR2820591025>3.0.CO;2-A

39. Chan CM, Adler Z, Reith JD, Gibbs CPJr. Risk factors for pulmonary metastases from giant cell tumor of bone. *J Bone Joint Surg Am* (2015) 97:420–8. doi: 10.2106/JBJS.N.00678

40. Hayashida K, Kawabata Y, Kato I, Kamiishi T, Matsuo K, Takeyama M, et al. Clinical and pathological analysis of giant cell tumor of bone with denosumab treatment and local recurrence. *J Orthop Sci* (2022) 27:215–21. doi: 10.1016/j.jos.2020.11.005

41. Hakozaki M, Tajino T, Yamada H, Hasegawa O, Tasaki K, Watanabe K, et al. Radiological and pathological characteristics of giant cell tumor of bone treated with denosumab. *Diagn Pathol* (2014) 9:111. doi: 10.1186/1746-1596-9-111

42. Engellau J, Seeger L, Grimer R, Henshaw R, Gelderblom H, Choy E, et al. Assessment of denosumab treatment effects and imaging response in patients with giant cell tumor of bone. *World J Surg Oncol* (2018) 16:191. doi: 10.1186/s12957-018-1478-3

43. Park HL, Yoo IR, Lee Y, Park SY, Jung CK. Giant cell tumor of the rib: two cases of F-18 FDG PET/CT findings. *Nucl Med Mol Imaging* (2017) 51:182–5. doi: 10.1007/s13139-016-0442-9

44. Selby L, Kukar M, Wang J, Beg M, Sullivan J. Pigmented villous nodular synovitis mimicking metastatic melanoma on PET-CT. *Int J Surg Case Rep* (2014) 5:231–3. doi: 10.1016/j.ijscr.2014.02.009

45. Hamada K, Tomita Y, Qiu Y, Zhang B, Ueda T, Myoui A, et al. 18F-FDG-PET of musculoskeletal tumors: a correlation with the expression of glucose transporter 1 and hexokinase II. *Ann Nucl Med* (2008) 22:699–705. doi: 10.1007/s12149-008-0173-9

46. Ong LC, Jin Y, Song IC, Yu S, Zhang K, Chow PK. 2-[18F]-2-deoxy-D-glucose (FDG) uptake in human tumor cells is related to the expression of GLUT-1 and hexokinase II. *Acta Radiol* (2008) 49:1145–53. doi: 10.1080/02841850802482486

47. Burke B, Giannoudis A, Corke KP, Gill D, Wells M, Ziegler-Heitbrock L, et al. Hypoxia-induced gene expression in human macrophages: implications for ischemic tissues and hypoxia-regulated gene therapy. *Am J Pathol* (2003) 163:1233–43. doi: 10.1016/S0002-9440(10)63483-9

48. Malide D, Davies-Hill TM, Levine M, Simpson IA. Distinct localization of GLUT-1, -3, and -5 in human monocyte-derived macrophages: effects of cell activation. *Am J Physiol* (1998) 274:E516–26. doi: 10.1152/ajpendo.1998.274.3.E516

49. Fu Y, Maianu L, Melbert BR, Garvey WT. Facilitative glucose transporter gene expression in human lymphocytes, monocytes, and macrophages: a role for GLUT isoforms 1, 3, and 5 in the immune response and foam cell formation. *Blood Cells Mol Dis* (2004) 32:182–90. doi: 10.1016/j.bcmd.2003.09.002

50. Pallas A, Hagge R, Borys D, Hunter J. Intense FDG uptake in an intra-articular localized giant-cell tumor of the tendon sheath (pigmented villonodular synovitis) mimics metastatic melanoma. *Radiol Case Rep* (2009) 4:343. doi: 10.2484/rcr.v4i4.343

51. Gong T, Luo Y, Wang Y, Zheng C, Fang J, Min L, et al. Multiple pulmonary metastases of recurrent giant cell tumor of bone with expression of VEGFR-2 successfully controlled by denosumab and apatinib: a case report and literature review. *Cancer Manag Res* (2021) 13:4447–54. doi: 10.2147/CMAR.S312846

52. Feng L, Ye T, Zhang J, Yuan S, Chen Y, Chen J. Stereotactic body radiotherapy for lung metastases in a patient with giant cell tumor of bone: a case report and literature review. *Ann Transl Med* (2022) 10:156. doi: 10.21037/atm-21-6575

53. Wang G, Jiang S, Li Z, Dong Y. Denosumab and Sunitinib in the treatment of giant-cell tumor of bone with pulmonary and bone metastases in an adolescent: A case report. *Med (Baltimore)* (2019) 98:e17778. doi: 10.1097/MD.0000000000017778

54. Luo Y, Tang F, Wang Y, Zhou Y, Min L, Zhang W, et al. Safety and efficacy of denosumab in the treatment of pulmonary metastatic giant cell tumor of bone. *Cancer Manag Res* (2018) 10:1901–6. doi: 10.2147/CMAR.S161871

55. Sachan DK, Bansal N, Gupta S, Kumar S. A rare case of giant cell tumour (GCT) of bone with lung metastases. *BMJ Case Rep* (2018) 2018:bcr2017221667. doi: 10.1136/bcr-2017-221667

56. Yamagishi T, Kawashima H, Ogose A, Sasaki T, Hotta T, Inagawa S, et al. Disappearance of giant cells and presence of newly formed bone in the pulmonary metastasis of a sacral giant-cell tumor following denosumab treatment: A case report. *Oncol Lett* (2016) 11:243–6. doi: 10.3892/ol.2015.3858

57. Wei F, Liu X, Liu Z, Jiang L, Dang G, Ma Q, et al. Interferon alfa-2b for recurrent and metastatic giant cell tumor of the spine: report of two cases. *Spine (Phila Pa 1976)* (2010) 35:E1418–22. doi: 10.1097/BRS.0b013e3181e7bf5a

58. Iwai T, Oebisu N, Hoshi M, Takada N, Nakamura H. Efficacy of Pazopanib in the Treatment of Metastatic Malignant Giant Cell Tumor of Soft Tissue: A Case Report. *Curr Oncol* (2022) 29:758–65. doi: 10.3390/curroncol29020064

59. Kudawara I, Kakunaga S, Takami K. Objective response of denosumab for multiple pulmonary metastases from giant cell tumor of bone: A case report and review of the literature. *Curr Problems Cancer: Case Rep* (2021) 3:100073. doi: 10.1016/j.cpccr.2021.100073

60. Egbert RC, Folsom R, Bell J, Rajani R. Denosumab Therapy for Giant Cell Tumor of Bone Pulmonary Metastasis. *Case Rep Orthop* (2017) 2017:2302597. doi: 10.1155/2017/2302597

61. Tanikawa M, Yamada H, Sakata T, Mase M. Dosing interval adjustment of denosumab for the treatment of giant cell tumor of the sphenoid bone: A case report. *Surg Neurol Int* (2020) 11:370. doi: 10.25259/SNI_439_2020

frontiers | Frontiers in Pharmacology

TYPE Original Research
PUBLISHED 17 August 2023
DOI 10.3389/fphar.2023.1246783

OPEN ACCESS

EDITED BY
Zhiyu Zhang,
Fourth Affiliated Hospital of China Medical University, China

REVIEWED BY
Changfeng Fu,
The First Hospital of Jilin University, China
Jiyu Han,
Tongji University, China

*CORRESPONDENCE
Jin-Song Wei,
WJS13652855121@outlook.com,
Jinsong.wei@gdmu.edu.cn

†These authors have contributed equally to this work and share first authorship

RECEIVED 24 June 2023
ACCEPTED 02 August 2023
PUBLISHED 17 August 2023

CITATION
Zhang W-L, Dai Z-W, Chen S-Y, Guo W-X, Wang Z-W and Wei J-S (2023), A novel poly(3-hydroxybutyrate-*co*-3-hydroxyvalerate) (PHBV)-PEG-melatonin composite scaffold enhances for inhibiting bone tumor recurrence and enhancing bone regeneration. *Front. Pharmacol.* 14:1246783. doi: 10.3389/fphar.2023.1246783

A novel poly(3-hydroxybutyrate-*co*-3-hydroxyvalerate) (PHBV)-PEG-melatonin composite scaffold enhances for inhibiting bone tumor recurrence and enhancing bone regeneration

Wei-Lin Zhang†, Zhi-Wen Dai†, Si-Yuan Chen, Wei-Xiong Guo, Zhong-Wei Wang and Jin-Song Wei*

Department of Spinal Degeneration and Deformity Surgery, Affiliated Hospital of Guangdong Medical University, Zhanjiang, China

Introduction: Postoperative comprehensive treatment has become increasingly important in recent years. This study was to repair tissue defects resulting from the removal of diseased tissue and to eliminate or inhibit the recurrence and metastasis of residual tumors under the condition of reducing the systemic side effects of chemotherapeutic drugs. To address these challenges, multifunctional scaffolds based local drug delivery systems will be a promising solution.

Methods: An optimal drug-loaded scaffold material PHBV-mPEG5k (PP5) was prepared, which is biocompatible, hydrophilic and biodegradable. Furthermore, this material showed to promote bone healing, and could be conveniently prepared into porous scaffold by freeze-drying the solution. By means of introducing melatonin (MT) into the porous surfaces, the MT loaded PP5 scaffold with desirable sustained release ability was successfully prepared. The effectiveness of the MT loaded PP5 scaffold in promoting bone repair and anti-tumor properties was evaluated through both *in vivo* and *in vitro* experiments.

Results and Discussion: The MT loaded PP5 scaffold is able to achieve the desired outcome of bone tissue repair and anti-bone tumor properties. Furthermore, our study demonstrates that the PP5 scaffold was able to enhance the anti-tumor effect of melatonin by improving cellular autophagy, which provided a therapeutic strategy for the comprehensive postoperative treatment of osteosarcoma.

KEYWORDS

PHBV, PEG, melatonin, scaffold, osteosarcoma, bone tissue regeneration

1 Introduction

Bone tumors, particularly osteosarcoma, have a higher incidence in adolescents. The current treatment for metastatic bone cancers involves the resection of tumor tissue, combined with chemotherapy and radiotherapy, unfortunately, this approach often results in bone defects (Ma et al., 2017). Therefore, there is a need for a multifunctional method that can eliminate residual cancer cells while repaire bone defects (Xue et al., 2020). Local drug delivery systems using multifunctional scaffolds can effectively address these challenges. Yang et al.

(2020) demonstrated the efficacy of a PDA-coated, DOX-loaded LHAp/PLGA fibrous scaffold, in achieving controlled drug release, inhibiting tumor cell growth and promoting the proliferation of normal cells during the early stages of treatment (Lu et al., 2021).

The copolymer of 3- hydroxybutyrate and 3-hydroxyvalerate (PHBV) is a piezoelectric a material that possesses extremely good biocompatibility has been used in tissue engineering and regenerative medicine for many years (Ye et al., 2018; Chen et al., 2021; Kaniuk,, Stachewicz, 2021). In addition to biocompatibility, the copolymer PHBV has excellent biodegradability. And the piezoelectric properties of PHBV result in a negatively charged surface potential on material's surface, which is similar to that of human bone. And recent studies have demonstrated the beneficial impact of negative potential on the surface of materials, particularly in terms of promoting mineralization and osteogenic differentiation of cells (Kang et al., 2013; Mihaila et al., 2014). As a result, PHBV has emerged as the most promising biopolymer for a variety of applications, particularly in bone tissue engineering where it has been extensively utilized (Huang et al., 2010; Jacob et al., 2018).

However, due to its hydrophobic characteristic, causing low cellular interaction and bioactivity, which limits the application of PHBV in bone regeneration. Polyethylene glycol (PEG) with biodegradable and biocompatible and commercially available in molecular weights ranging from 500 to 20,000 Da, which has been approved by the US Food and Drug Administration (FDA) for using in human body, is the most commonly used hydrophilic component of polymeric micelles. To make up the shortcomings of PHBV, a new block copolymer (PHBV-mPEG5K, PP5) was developed using mPEG with an average molecular weight of 5,000 and PHBV, the hydrophilicity, biocompatibility and biodegradability of PP5 were improved compare to PHBV, making it a promising candidate for constructing tissue engineering scaffold. Combining the above, PP5 was employed as a carrier for melatonin to repair bone defect and prevent tumor recurrence after osteosarcoma surgery.

Melatonin (N-acetyl-5-methoxy-tryptamine) plays a significant role in regulating the sleep-wake cycle, declining tumor progress and ameliorating immune system actions (Ekmekcioglu, 2006; Cheng et al., 2013). Some Studies revealed that melatonin can be effective against many types of tumors including Endometrial Cancer and osteosarcoma et al. (Dana et al., 2020; Yang et al., 2022). In addition, melatonin levels are related to bone metabolism which can prevent bone degradation and promote bone formation (Cutando et al., 2012). The results of studies indicate that melatonin may have anti-tumor properties by activating or inhibiting various mechanisms including apoptosis, anti-proliferative and anti-oxidant activities. Accumulating evidence studies has provided evidence of melatonin's anti-osteosarcoma properties, making it a promising candidate as an adjuvant agent in osteosarcoma treatment. Melatonin is a safe potential therapeutic agent for children and adolescents and has shown promise as an adjuvant in reinforcing the therapeutic effects of chemotherapies while also abolishing the unwanted consequence.

In this study, we present a new approach for MT delivery using a MT-loaded PP5 scaffold. The PP5 scaffold was prepared by modifying PHBV with mPEG5k and lyophilizing the solution. MT was then loaded onto the scaffold by dissolving it with GelMA and coating to the scaffold porous surfaces. GelMA has been broadly applied as biomaterials for bone tissue regeneration and other tissue repair owing to suitable biological properties and tunable physical characteristics (Sun et al., 2018). Especially, the source of GelMA is collagen, the major component of ECM, so there is much arginine-glycine-aspartic acid (RGD) sequences in GelMA that are favorable for cell adhesion, migration and growth (Liu and Chan-Park, 2010; Klotz et al., 2016). We characterized the chemical structure of PP5 and evaluated the drug release behavior, bioactivity to promote bone defect repair and ability for preventing bone tumor of the MT-loaded PP5 scaffold. Finally, the mechanism of the enhancement of MT's antitumor effect by PP5 scaffold was also revealed.

2 Methods and materials

2.1 The preparation of PHBV-mPEG5k (PP5) scaffold

To prepare PHBV-mPEG5k (PP5), mPEG-5k (Sigma, China) was dissolved in dry dichloromethane. The solution was then heated to 80°C under vacuum for 24 h and subsequently cooled to room temperature. The mPEG-5k solution was then added dropwise to the hexamethylene diisocyanate solution with stirring and the mixture was left to react in the dark at room temperature for 6 h to obtain mPEG5k-NCO. Next, PHBV (Tianan Biologic Material Ltd., China) was dissolved in dry dichloromethane and heated to 80°C under vacuum for 5 h and subsequently cooled to room temperature. The mPEG5k-NCO solution was then added dropwise to the PHBV solution and the mixture was left to react in the dark at room temperature for 3 days. The crude product was obtained by rotary evaporation to remove the dichloromethane. The resulting product was then purified by dissolving it in tetrahydrofuran and gradually adding distilled water with stirring. After filtration and washing with distilled water, the purified product was dried under vacuum to obtain PHBV-PEG5k (PP5).

For preparation of PP5 scaffold, PP5 was dissolved in deionized water and heated to 50°C for 24 h, until the polymer was completely dissolved, transferring the solution to 6 mm cell culture dish and stored at −20°C for 12 h. Finally, the solution was lyophilizated at −20°C, the scaffold was obtained.

2.2 Characterization of PHBV-PEG5k (PP5)

The Fourier transform infrared spectra of mPEG5k, PHBV and PP5 were recorded using a Perkin Elmer spectrophotometer (spectrum 2) through the solid-state KBr pellet method within the range of 4,000–400 cm^{-1}.

The ^{1}H-NMR of the polymer was recorded using FT-NMR JEOL AL 500 FT-NMR Proton nuclear magnetic resonance spectrometer in $CDCl_3$. Tetramethylsilane was used as an internal reference.

2.3 Melatonin loading on the scaffold

A series of GelMA (SunP Gel G1) gels with varying concentration (0.25% w/v, 0.5% w/v, 1% w/v, 1.5% w/v and 2% w/v) were prepared to find the optimal concentration for loading MT. A mixture of 0.05 gMT and different masses of GelMa were added to 10 mL Phosphate Buffer Saline (PBS), and stirred at 650 r/min for 2 h in a 40°C water bath until fully dissolved. Then the MT

solution was fully absorbed by PP5 scaffold and placed at room temperature (23–25°C) until it underwent liquid-solid conversion, resulting in the production of MT-loaded PP5 scaffold.

2.4 Determination of loading efficiency (LE) and loading capacity (LC)

To prepare the MT solution, a mixture of absolute ethanol and chloroform (V: V = 9:1) was used as the solvent. The maximum absorption peak was measured using an ultraviolet-visible spectrophotometer (Mettler Toledo, Switzerland) within a wavelength range of 200–350 nm. A standard curve was drawn by fitting the absorbance with the mass concentration of the MT solution at the wavelength of the maximum absorption peak (278 nm) using linear regression. Freeze-dried MT-loaded GelMa gel (50 mg) was dissolved in PBS (10 mL) and centrifuged at 12,000 rpm for 5 min. Then, 0.5 mL of the supernatant was diluted in PBS in a 25 mL volumetric flask and the absorbance value of the solution was measured at 278 nm. The mass of melatonin was calculated from the standard curve and the LE and LC was calculated by following formula: *In vitro* scaffold drug release study

$$LE = m_a/m_b \times 100\%; \quad LC = m_a/m_c \times 100\%$$

where m_a means the mass of melatonin in MT-loaded GelMA gel, m_b represents total mass of MT and m_c is the mass of GelMA in MT-loaded GelMA gel.

2.5 *In vitro* drug release behavior

Standard curve of MT was first drawn using PBS (pH = 7.4) as solvent under the wavelength of the maximum absorption peak (278 nm). MT-loaded GelMA (100 mg) was dissolved in PBS and placed in a dialysis bag. The dialysis bag was then placed in a beaker containing the same pH PBS buffer and was vibrated horizontally in a constant temperature shaker (37°C ± 0.5°C) with a vibration frequency of 50 times/min. The release liquid (5 mL) was replaced with same amounts of fresh PBS at selected time intervals. The absorbance value of the solution was measured at 278 nm and the drug release rate was calculated as follow:

$$R(\%) = \frac{\rho_n V + V_i \sum_i^{n-i} \rho i}{M_D} \times 100$$

where R means the cumulative drug release rate (%); *n* means the number of samplings. (%) represents the mass concentration (g/L) of the drug in the nth release. V represents the total volume of the release liquid. ρ_i represents the mass concentration (g/L) of the drug in the ith release, V_i represents the volume of the release liquid at the ith sampling and MD means the mass of drug loaded (g).

2.6 Biocompatibility tests

Human bone mesenchymal stem cells (hMSCs) were originally purchased from Cell Bank of Shanghai Institutes for Biological Sciences. The PHBV and PP5 scaffold were sterilized by ultraviolet irradiation for 30 min and then placed in a 48 well cell culture plate. The hMSCs were seed on both materials at a density of 5×10^4 cells/well, incubated at 37°C, 5% CO_2 atmosphere and 95% humidity for predetermined durations of 24 h, 48 h and 72 h. Then the materials with adhered cells were rinsed with PBS, stained with phalloidin and 4,6-Diamidino-2-phenylindole dihydrochloride (DAPI) for 30 s, and finally observed under inverted microscope.

In order to quantitatively evaluate the cell viability on both materials, CCK8 assay was used. Following incubation as described above, 10 ul CCK8 was added to each well and the plate was incubated in darkness at 37°C for 4 h, the absorbance (OD) values were measured at 450 nm (iMark, Bio-rad, USA).

2.7 Evaluation of osteogenic differentiation of PP5 scaffold *in vitro*

The mRNA expression of collagen I (COL I), Runt-related transcription factor 2 (Runx2), osteocalcin (OCN), osteoprotegerin (OPG) and alkaline phosphatase (ALP) were quantified to assess the osteogenic differentiation of different scaffolds by Real-Time PCR. hMSCs were adhered in 6-well plates and RNA were harvested after osteogenic induction for 7 days using TRIzol reagent (Invitrogen). Prime Script RT reagent kit (Takara, Shiga, Japan) was used for mRNA to be reversely transcribed into complementary DNA. ABI 7,900 was used for quantitative analysis of the reverse transcription reaction. The data were normalized to glyceraldehyde-3-phosphate dehydrogenase (GAPDH) expression and analyzed by the $2^{-\Delta\Delta CT}$ method.

Alizarin red S staining was used to evaluate the extracellular calcium deposition, revealing individual osteo-induction capacity of different scaffolds. HBMSCs were seeded into 24-transwell plates and co-cultured with PHBV or PP5 in osteogenic differentiation medium for 21 days. After 21 days, cells were washed twice with PBS and fixed with 4% paraformaldehyde for 15 min and then stained with Alizarin Red S (2% aqueous, Sigma) solution for 30 min.

2.8 *In vivo* bioactivity analysis

Femur defect models were established on sixteen 8-week-old male SD rats to examine the repair efficacy of the PP5 scaffolds. The femoral defects model was prepared according to previously described protocols (Chou et al., 2008). The experimental rats underwent general anesthesia with intraperitoneal injection of 50 mg/kg pentobarbital sodium All animals were cared and experiments were conducted in accordance with the National Institutes of Health Guide for the Care and Use of Laboratory Animals (2011 revision). The experimental protocol was approved by the Ethics Committee of Affiliated Hospital of Guangdong Medical University (No. PJKT 2022-046). All possible efforts were made to reduce the number of rats used and discomfort to the rats. Afterwards, the surgical sites were shaved and disinfected. A bone defect of approximately 4 mm in diameter and 5 mm in depth was created at the right femoral epicondyle using a slow-speed cylindrical burr. Subsequently, according to the type of scaffolds

implanted, the animals were randomly divided into two groups (8 rats per group): (1) no treatment (defect control), (2) PP5-scaffold. The post-operative pain was controlled by intramuscular injection of 5 mg/kg morphine every 4 h. Two months post-implantation, the rats were sacrificed and the femurs were extracted for micro-CT analysis. 3D bone reconstruction and quantitative analysis of bone regeneration were conducted using the system software. Bone volume/tissue volume (BV/TV) and bone mineral density (BMD) of each sample were analyzed and calculated. Afterwards, the collected femur samples were decalcified and prepared for hematoxylin-eosin (H&E) staining to visualize bone regeneration.

2.9 Evaluation of anti-tumor migration effect

Transwell system was used to analyze cell migration, cells were seeded in the top chambers of the transwell migration plates in DMEM containing 10% FBS. At 24 h after seeding, cells that migrated to the underside of the trans well were stained with 0.5% crystal violet for 5 min and imaged in ten random fields. To investigate the invasion and migration of cells in PP5 or MT-loaded PP5 scaffold, the cells (5×10^5) were injected to the scaffold with a designated site, and the cell migration away from the injection sites was monitored with a light microscope (Leica, Germany) and quantified using ImageJ.

2.10 Evaluration of anti-tumor performance *in vivo*

The protocols of use and care of the animals were reviewed and approved by Institutional Animal Care and Use Committee of Affiliated Hospital of Guangdong Medical University. 2.0×10^5 LM-8 (murine osteosarcoma cells) per mouse were injected subcutaneously into the leg of the nude mouse (6 week-old Balb/c, Vital River Laboratory Animal Technology Co. Ltd., Beijing, China). When the volume of the tumor grew to about 300 mm^3, the mice were randomly divided into three groups ($n = 4$). A small incision was made on the leg of the mouse and the functional cuboid scaffold (length: 8 mm, width: 2 mm, height: 2 mm) was implanted under the tumor. The first day of the treatment was regarded as Day 0. The weight of tumor was measured after 1 month. The tail vein injection was used for MT group treatment, and the dose of MT was consistent with that of MT + PP5 group.

2.11 Mechanism exploring about enhancement of anti-tumor effect by PP5

Western blotting was used to determine the protein expression level of LC3 II/LC3 I and P62/GAPDH.The cellular proteins were extract with by cell lysis buffer (Invitrogen, United States). Protein samples were separated on 10% SDS-PAGE, followed by transferred onto PVDF membranes (Millipore, United States). The membranes were blocked with 2% bovine serum albumin (BSA) in PBST for 1 h at room temperature, then the membranes were incubated with the primary antibodies and secondary antibodies for 1 h at 37°C. Finally, the membrane was observed by sensitive enhanced chemiluminescence (ECL) detection kit (Beyotime, China) and bands were detected by ChemiDoc Imaging Systems (Bio-Rad, United States).

The immunocytochemistry was performed on cells grown on 22 × 22 mm coverslips. Wash the cells with PBS for 3 × 5 min. Fix the cells on a coverslip and fix them with 3.7% formaldehyde in PBS for 5 min. Permeabilize cells with PBS containing 0.1% Triton X-100 for 3 min. Block with 7.5% BSA in PBS. Incubate with primary antibodies diluted in PBS containing 0.5% BSA. Wash the cells 3 times. Incubate with secondary antibodies for 1 h. Counterstain the nuclei with PBS containing 10 ng/mL Hoechst 33342 for 3 min. Fluorescence is observed under a microscope.

2.12 Statistical analysis

Statistical data analysis was performed with SPSS software. Data from at least three independent experiments were collected, analyzed, and expressed as mean ± standard deviation (SD). Results with p-values of < 0.05 were considered statistically significant.

3 Results

3.1 Synthesis and characterization of PP5

In order to overcome the limitations of PHBV, we opted to synthesize PP5 using PBHV and mPEG5k as the primary raw materials. The chemical structure of PP5 was confirmed through 1H NMR analysis as depicted in Figure 1, δ = 1.5–2.03, 2.32,4.0–4.19,4.32–4.47 ppm belongs to PHBV (a-g) while δ = 3.66 ppm was corresponded to mPEG5k, which confirmed that we graft mPEG5k to PHBV successfully (Park et al., 1998; Pasek-Allen et al., 2023). The structure of PEG5k, PHBV and PP5 were characterized by FT-IR (Figure 1). In the spectrum of mPEG5k, the absorption peak at approximately at 2,887 and 1,467 cm^{-1} respectively are associated with the stretching and bending vibration of methylene (Xiang et al., 2013). And the peaks also appear in spectrum of PP5, therefore, the FT-IR results confirm that PP5 has been produced.

3.2 Biocompatibility of PP5

We utilized the material-cell co-culture method to evaluate the cytotoxicity of PBHV and PP5 and determine their biocompatibility. Human bone marrow mesenchymal cells were co-cultured with the materials for 24, 48, and 72 h, and cell viability was assessed using the CCK8 assay kit. Our findings indicated that both materials displayed no-cytotoxicity and showed some pro-proliferative effect. Moreover, PP5 exhibited a more pronounced pro-proliferative effect compared to PHBV (Figure 2C). Cellular immunofluorescence staining for cytoskeletal proteins (β-tublin) was performed to evaluate cell spreading on the scaffold materials. Fluorescence analysis (Figure 2A) demonstrated that cells exhibited greater extensibility on PP5. In conclusion, the addition with mPEG5k resulted in the synthesis of PP5 biomaterials with improved hydrophilicity and biocompatibility.

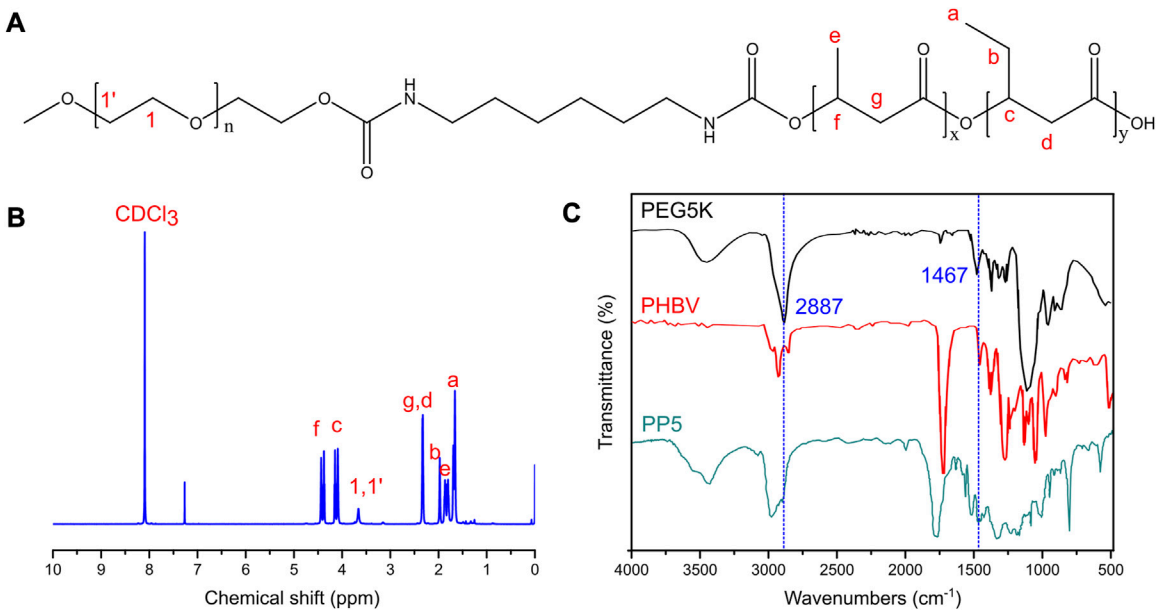

FIGURE 1
Characteristics of PP5 materials **(A)** The structural formula of PP5. **(B)** The NMR H1 profiles of PP5. **(C)** The FT-IR of PEG5K, PHBV and PP5.

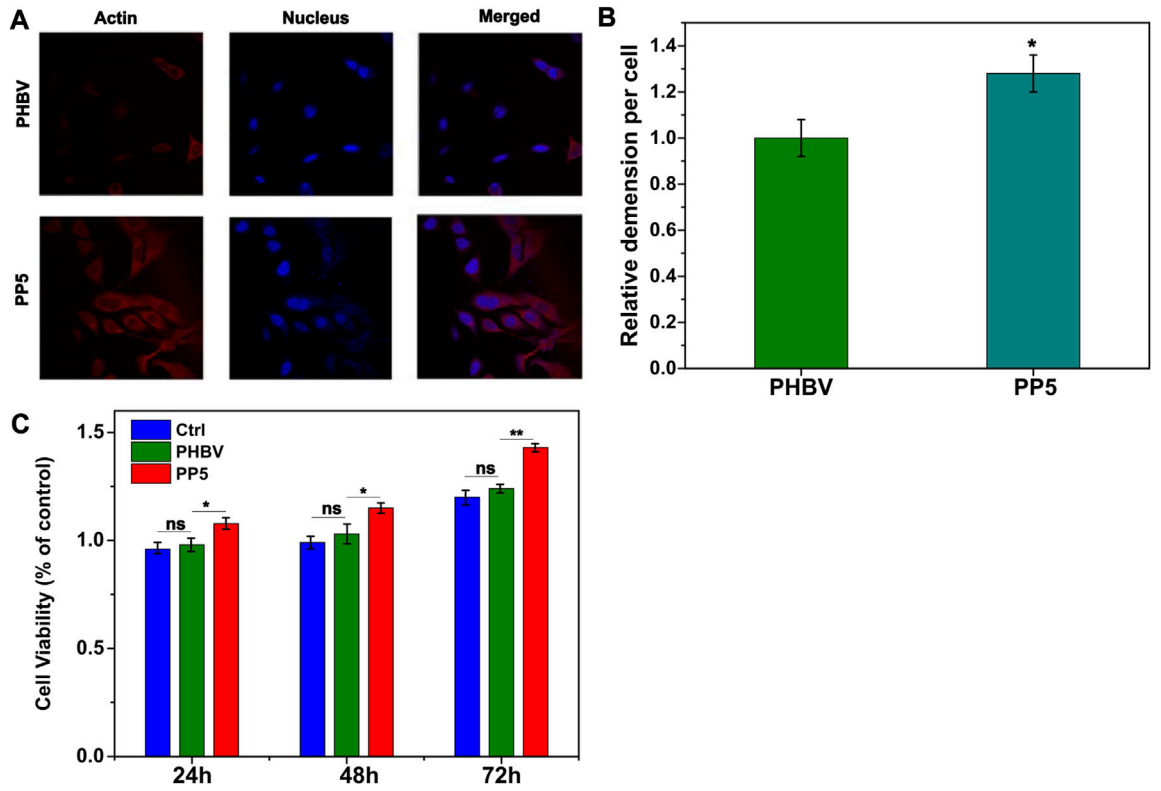

FIGURE 2
Biocompatibility of PP5 materials. **(A)** Fluorescence observation of cell ductility cocultured with PHBV and PP5 materials; **(B)** The proliferation of HBMSCs co-cultured with PBHV and PP5. **(C)** Cell viability at different exposure times (24 h, 48 h, and 72 h) cocultured with PHBV, PP5 materials and Ctrl.

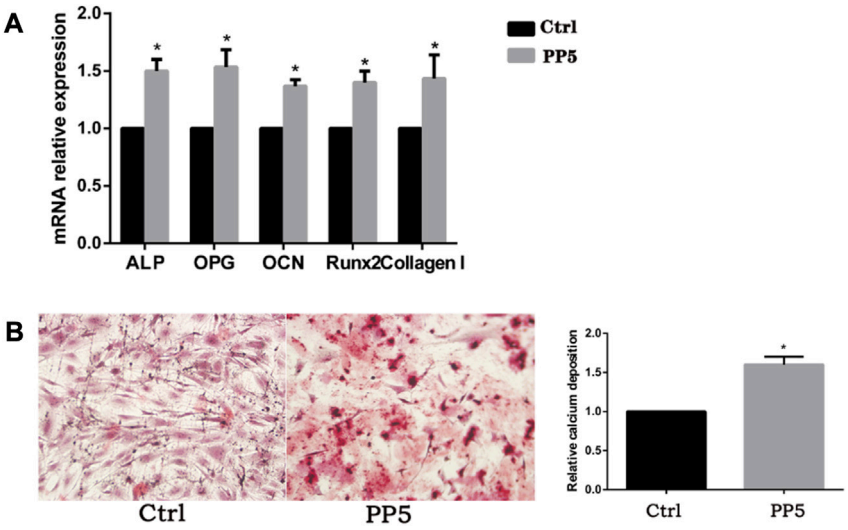

FIGURE 3
Pharmacokinetics of melatonin. **(A)** UV scanning spectrum of melatonin standard. **(B)** The standard curve of melatonin. **(C)** The drug loading efficiency of melatonin with different GelMA concentration. **(D)** The drug loading capacity of melatonin with different GelMA concentration. **(E)** The drug release rate of melatonin loaded GelMA.

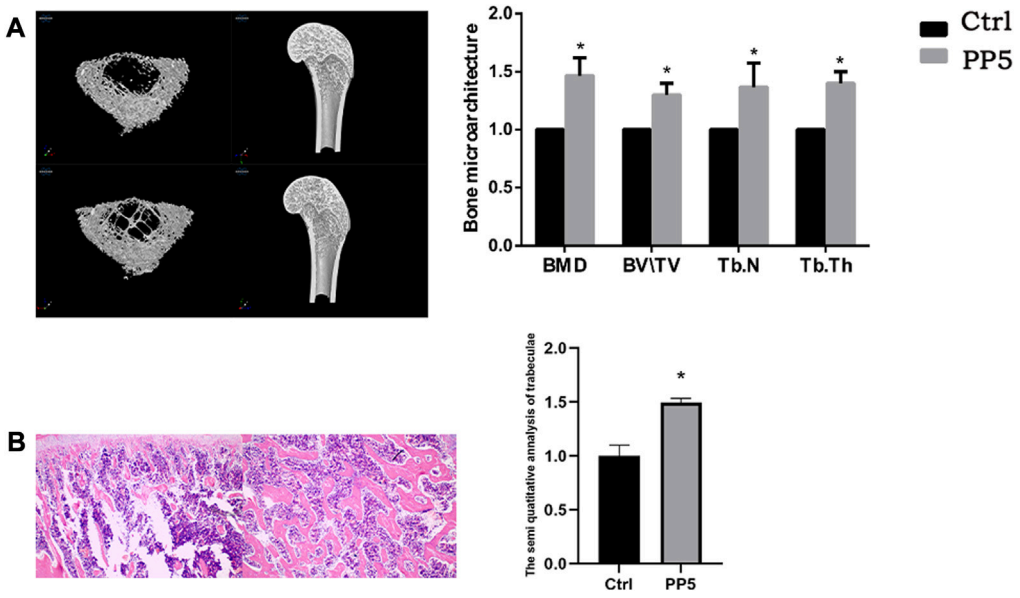

FIGURE 4
Assessment of *in vitro* osteogenic efficacy of PP5 **(A)** Relative osteogenesis-related gene expressions of the hMSCs cultured on PP5 for 7 days by real-time PCR. **(B)** Alizarin red staining of hMSCs cultured on PP5 and quantitative analysis by ImageJ.

3.3 Osteotropic effects of PP5 *in vivo* and *in vitro*

To further evaluate the osteogenic ability of PP5, we conducted both cellular and animal models to investigate the osteogenic effect of each material. We co-cultured both materials with cells and performed RT-PCR analysis of osteogenesis-related genes. (Figure 3A). The expression of osteogenesis-related genes such as ALP, OPG, OCN, Runx2, and Collagen I were significantly higher in the PP5 group compared to the PBHV group. In the alizarin red mineralized nodules staining assay, the PP5 group exhibited higher mineralized nodules compared with control group. For the *in vivo* study, we utilized a femoral defect model in SD rats, a small bone defect was artificially created in the lower femur of SD rats and then implanted with PBHV and PP5, respectively. After euthanasia at 8 weeks postoperatively, the specimens were taken for Micro-CT analysis and HE. As shown in Figure 4A, after data analysis

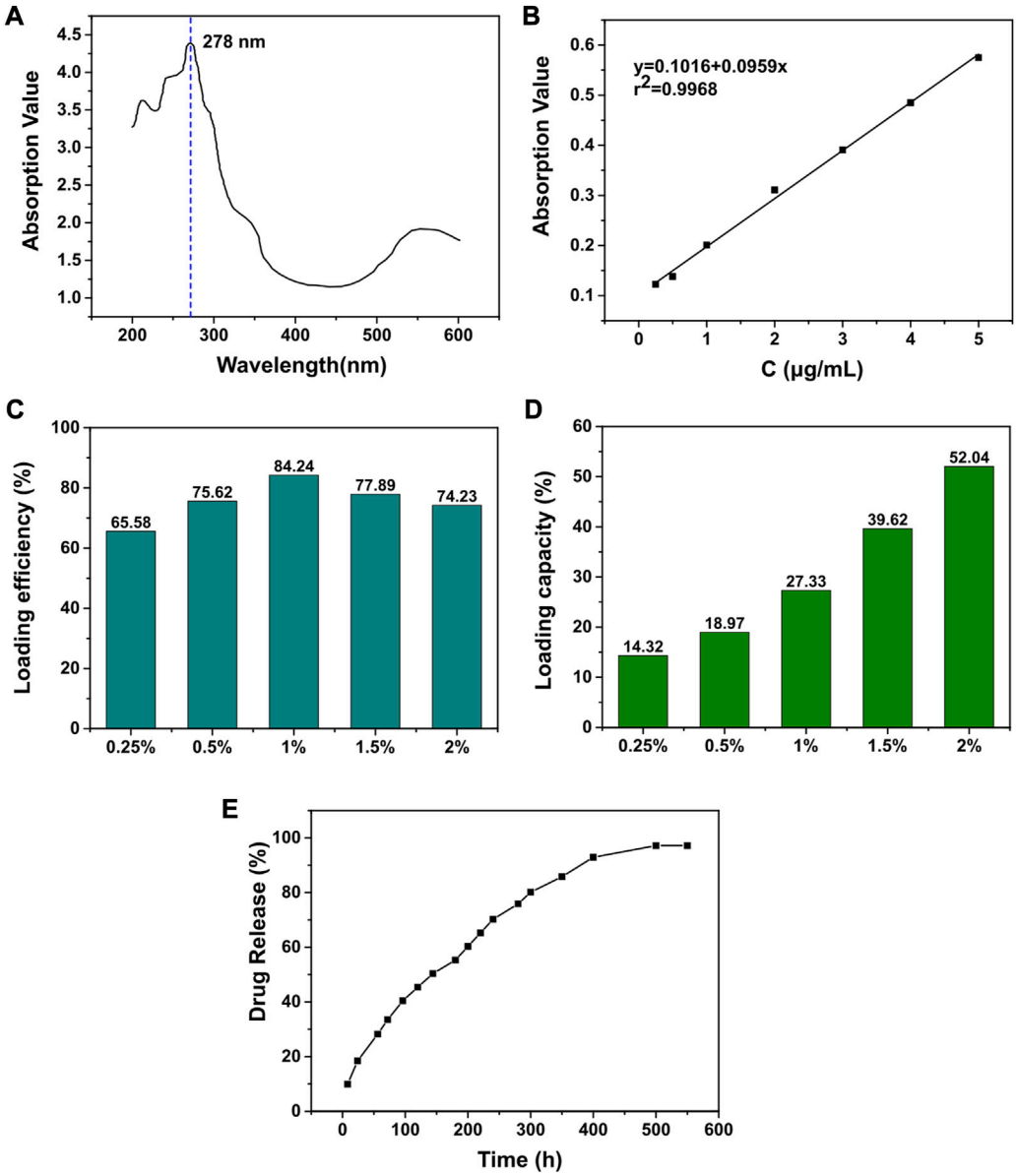

FIGURE 5
Assessing the *in vivo* osteotropic efficacy of PP5 **(A)** MicroCT evaluation of the effect of PP5 on bone microstructure. **(B)** HE staining to evaluate the promoting effect of PP5 on trabecular bone.

by specific software, the bone mineral density (BMD), bone volume fraction (BV/TV), bone trabecular number (Tb.N), and bone trabecular thickness (Tb.Th) were found to be statistically higher in the PP5 group compared to the PBHV group ($p < 0.05$). These differences were also observed in HE staining (Figure 4B). From the above, it can be concluded that PP5 has a significantly better bone healing promoting effect than PBHV.

3.4 Loading and release effects of melatonin on PP5

As a potential drug against bone tumors, we proposed to construct a local drug delivery system by loading melatonin to provide a new option for improving the quality of comprehensive management of bone tumors after surgery. Through GelMA, we successfully loaded melatonin on PP5 scaffold and performed release experiments. (Figure 5). The loading capacity increased with decreasing gel concentration, and the loading efficiency initially increased with the increasing concentration and reached a peak at the gel concentration of 1%, so the 1% gel concentration was used for subsequent experiments. In the drug release curve, the melatonin release process was able to sustain the release for more than 14 days without sudden mass release, and the release efficiency of MT was able to reach more than 97.1%. The result indicating that the MT loaded PP5 has the ability to achieve sustained and slow release of MT.

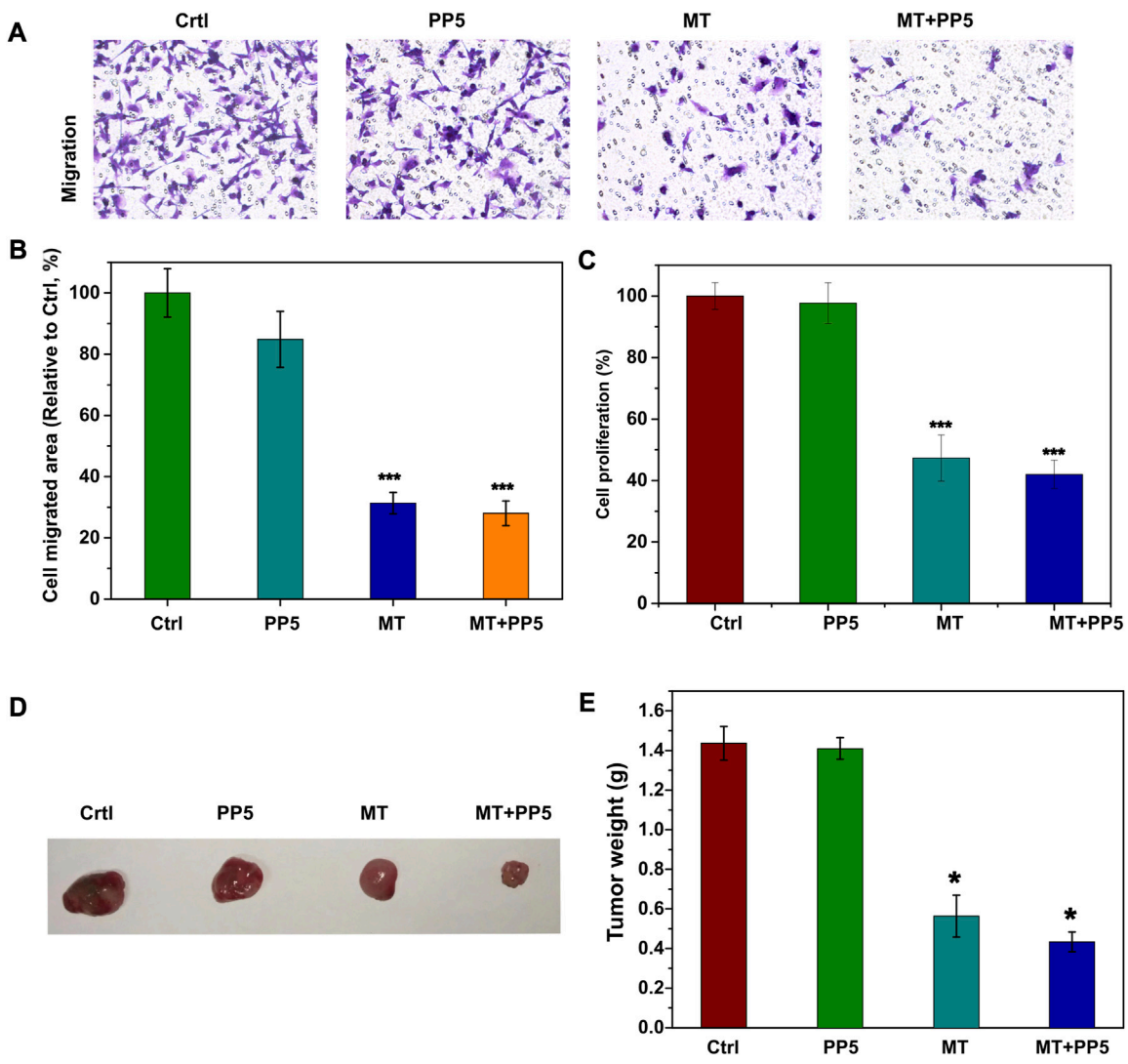

FIGURE 6
Anti-tumor effect of drug delivery system **(A)** Effect of MT + PP5 on MG63 cell migration *in vitro* and quantitative analysis by ImageJ **(B, C)** Estimation of MG63 cell proliferation on PP5 materials. **(D, E)** Evaluation of tumor suppressive effect of DDS by subcutaneous tumor model.

3.5 Antitumor capacity of melatonin-loaded drug delivery system (MT + PP5)

To evaluate the anti-tumor efficacy of the drug delivery system, we conducted both *in vitro* and *in vivo* experiments. Specifically, we treated tumor cells (MG-3) with two different scaffold and melatonin for a period of 24 h. We then performed cell transwell assays and cell proliferation assays (Figures 6A–C). Both the free melatonin group and MT + PP5 group exhibited anti-bone tumor abilities. In addition, the cell proliferation assay measured by the CCK8 kit also demonstrated inhibitory effects of the above two groups on the proliferation of MG63 cells. Interestingly, the MT + PP5 group showed stronger anti-tumor ability than the free MT group in both experiments.

In vivo experiments, we utilized a nude mouse allogeneic subcutaneous tumorigenesis model, once the subcutaneous tumor volume reached 300 mm^2 in nude mice, we implanted scaffold materials subcutaneously in the tumors, and the tumor specimens were euthanized and weighed after 14 days (Figure 6D). The tumors in the MT + PP5 group were significantly smaller than those in the other three groups.

3.6 Study on the mechanism of PP5 to enhance the anti-tumor effect of melatonin

To further explore the enhanced antitumor effect of melatonin, we examined the autophagic effect of melatonin on tumors. Western blotting and cellular immunofluorescence showed differential expression of markers associated with cellular autophagy (Figure 7A). The LC3B protein expression was upregulated in the MT group and MT + PP5 group, while P62 protein expression was decreased, with a greater difference observed in the MT + PP5 group. The difference in protein expressions was confirmed through cellular immunofluorescence (Figure 7B). Based on the results, it can be inferred that PP5 can enhance the anti-tumor effects of melatonin by promoting autophagy.

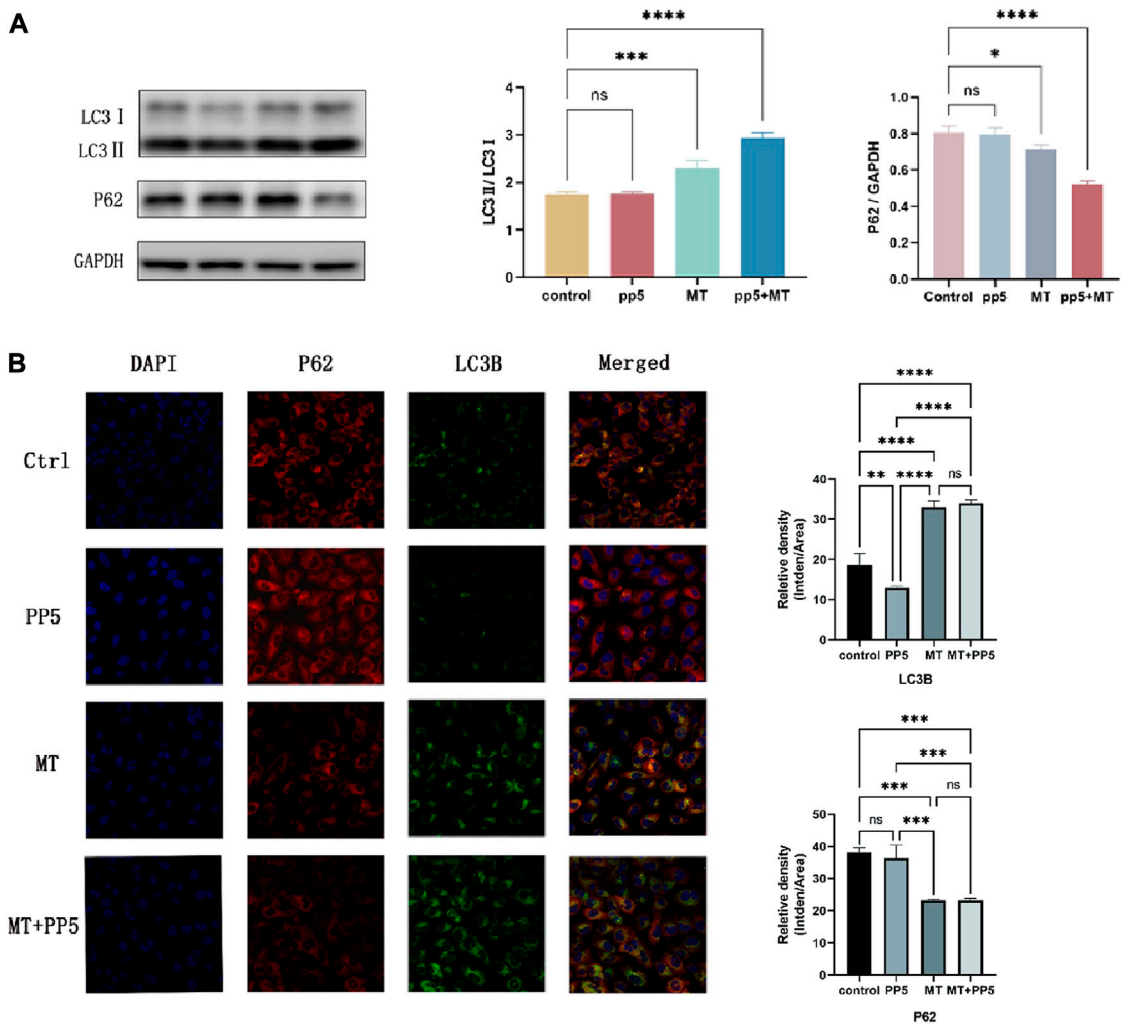

FIGURE 7
Effect of MT-loaded PP5 scaffold on cellular autophagy **(A)** LC3 and P62 protein expression bands and quantification results after co-culture of tumor cells (MG63) with PP5, MT + PP5, and free melatonin for 48 h, respectively. **(B)** Immunofluorescence staining and quantification of LC3 and P62 after co-culture of tumor cells (MG63) with PP5, MT + PP5, and free melatonin for 48 h, respectively.

4 Discussion

Currently, the clinical treatment of OS involves preoperative or neoadjuvant chemotherapy, surgical removal of primary and metastatic tumor sites, and post-operative chemotherapy. However, surgical resection often results in bone defects that require reconstruction using biomaterials. The biodegradable material poly (3-hydroxybutyrate-co-3-hydroxyvalerate) (PHBV) scaffold has good biodegradability, but its application in the biological field is limited due to poor biocompatibility. Further research is necessary to enhance these characteristics. Polyethylene glycol (PEG) is a faculty of water-soluble polymers with various molecular weights that possess beneficial properties such as protein resistance, low toxicity and immunogenicity. Due to their biocompatibility and minimal toxicity and good solubility in water or other common solvents, PEGs are often selected as drug carriers. In this study, we designed and evaluated PP5 scaffold for its potential to promote bone repair. Material characterization experiments were performed to determine the molecular structure of PP5, as shown in Figures 1A, B, δ = 1.5–2.03, 2.32, 4.0–4.19, 4.32–4.47 ppm belongs to PHBV (a-g) while δ = 3.66 ppm was correspond to mPEG in ^{1}H NMR spectrum suggest that we graft mPEG to PHBV successfully. (Park et al., 1998). And the result was also proved in FT-IR, the absorption peak at approximately at 2,887–1,467 cm^{-1} were associated with the stretching and bending vibration of methylene, the result was the same with reported work. In order to evaluate the bioactivity of PP5, the experiments *in vivo* and *in vitro* showed that PP5 exhibited superior biocompatibility and anti-tumor ability than PHBV, in Figure 2B, C, the cell dimension cultured on PP5 is about 1.35 times than PHBV, the cell viability is significantly more than PHBV and control group especially at 72 h. Also, the expression of ALP, OPG, OCN, Runx2 and Collagen I of PP5 group were significantly higher than Control group, indicated that PP5 scaffold could promote bone growth and might be a suitable option for bone tissue engineering; however, it cannot inhibit tumor metastasis.

At present, the clinical treatment mode of OS is utilizing combination of surgical intervention and chemo/radiotherapy. Inevitably, surgical resection can result in extensive bone defects and

leave behind residual neoplastic cells in the defect area, increasing the risk of local recurrence. However, the postsurgical chemo/radiotherapy still encounters some drawbacks, such as inefficient elimination of the residual cancer cells and severe side effects. Meanwhile, the extensive bone defect, the low immunity caused by chemo/radiotherapy, infection and poor blood supply can cause serious issues for defect healing. Melatonin, as a hormone naturally produced in the human body, has the natural advantages of good biocompatibility and high safety. Studies have shown that melatonin can inhibit tumor growth and metastasis. However, higher doses of melatonin are often necessary to achieve the desired effect of tumor suppression. In contrast to systemic high-dose melatonin, topical application of the drug not only achieves the necessary concentration for treatment, but also mitigates the adverse effects of systemic administration, this is particularly beneficial in adolescents, who are more sensitivity to melatonin.

In this study, we used hydrogel to load melatonin on PP5 scaffold. Our results suggested the cumulative release rate of melatonin has reached 96.3% at 10 h, while the drug release cycle of melatonin loaded GelMA can reach 14 days and there is no obvious burst release (Figure 2). Through anti-tumor experiments *in vivo* and *in vitro*, we found that MT-loaded PP5 scaffold has better anti-tumor effect than melatonin alone, the cell migration in transwell assay showed that the MG-3 cell was inhabited of in the MT and MT-loaded PP5 group in Figrue 6, more interestingly, the MT-loaded PP5 group has more effective anti-tumor ability, the weight of tumor in MT-loaded PP5 group was smaller than other two groups, in order to further analyze this phenomenon, we detected autophagy-related markers, including LC3 and P62. The result was shown in Figure 7, autophagy in MT + PP5 group exhibited stronger than that in MT group. Autophagy is a crucial and conserved cellular process that selectively targets abnormal organelles and proteins for lysosomal degradation. The role of autophagy in cancer is controversial. Autophagy can act as a cytoprotective response to chemotherapeutic drugs in cancer cells, and it can also promote metastasis by facilitating the mobility and anoikic resistance of tumor cells. However, several studies have shown that autophagy can induce autophagic cell death, inhibit cell proliferation, and degrade oncoproteins. This can suppress tumorigenesis, impede metastasis, and even enhance chemosensitivity. Several studies have shown that melatonin has antitumor effects, but the exact mechanism is still unknown. Our study found that melatonin induces enhanced autophagy in tumor cells and induces autophagic cell death, resulting in anti-tumorigenic and metastatic effects. The MT-loaded PP5 drug delivery system showed stronger autophagic effect, which seems to be attributed to the slow release of melatonin with local concentration above the therapeutic threshold, the MT group did have significant autophagic effect, but without sustain release ability, MT will be diffused and metabolized in a short time, so the autophagic effect is limited. However, the detailed mechanism needs to be further investigated.

5 Conclusion

In summary, a bifunctional scaffold which can inhibit bone tumor recurrence and enhance bone regeneration has been successfully developed by coating MT-loading GelMA on porous surfaces of freeze-dried PP5 prepared with PHBV and mPEG5k by a novel method. The introduction of mPEG5k significantly improves the bio-activity of PP5 scaffold, which leads to the great bone regeneration capacity. The GelMA coating realize long-acting and slowly release of MT from scaffold and efficiently improves the ant-tumor effect. This material meets the necessary requirements for promoting bone repair and eliminating residual tumor to prevent recurrence and metastasis. Therefore, it provides a promising option to improve the comprehensive treatment of bone tumors after surgery. Additionally, due to its excellent ability to promote bone regeneration, this approach is also suitable for treating bone defect diseases or other conditions that require bone implantation.

Data availability statement

The original contributions presented in the study are included in the article/Supplementary Material, further inquiries can be directed to the corresponding author.

Ethics statement

This study was reviewed and approved by the ethics committee of Affiliated Hospital of Guangdong Medical University. The study was conducted in accordance with the local legislation and institutional requirements.

Author contributions

J-SW and W-LZ contributed to the conception of the study. Z-WD, S-YC, and W-XG performed and visualized the experiment in silico. Z-WW contributed significantly to analysis and manuscript preparation. W-LZ and Z-WD performed the data analyses and wrote the manuscript. All authors contributed to the article and approved the submitted version.

Funding

This study was supported by Guangdong Natural Science Foundation (2021A1515010975).

Conflict of interest

The authors declare that the research was conducted in the absence of any commercial or financial relationships that could be construed as a potential conflict of interest.

Publisher's note

References

Chen, W., Li, Y., Huang, Y., Dai, Y., Xi, T., Zhou, Z., et al. (2021). Quercetin modified electrospun PHBV fibrous scaffold enhances cartilage regeneration. *J. Mater Sci. Mater Med.* 32, 92. doi:10.1007/s10856-021-06565-z

Cheng, Y., Cai, L., Jiang, P., Wang, J., Gao, C., Feng, H., et al. (2013). SIRT1 inhibition by melatonin exerts antitumor activity in human osteosarcoma cells. *Eur. J. Pharmacol.* 715, 219–229. doi:10.1016/j.ejphar.2013.05.017

Chou, A. J., Geller, D. S., and Gorlick, R. (2008). Therapy for osteosarcoma: where do we go from here? *Paediatr. Drugs* 10 (5), 315–327. doi:10.2165/00148581-200810050-00005

Cutando, A., López-Valverde, A., Arias-Santiago, S., Vicente, J. D. E., and Diego, R. G. D. E. (2012). Role of melatonin in cancer treatment. *Anticancer Res.* 32, 2747–2753.

Dana, P. M., Sadoughi, F., Mobini, M., Shafabakhsh, R., Chaichian, S., Moazzami, B., et al. (2020). Molecular and biological functions of melatonin in endometrial cancer. *Curr. Drug Targets* 21, 519–526. doi:10.2174/1389450120666190927123746

Ekmekcioglu, C. (2006). Melatonin receptors in humans: biological role and clinical relevance. *Biomed. Pharmacother.* 60, 97–108. doi:10.1016/j.biopha.2006.01.002

Huang, W., Shi, X., Ren, L., Du, C., and Wang, Y. (2010). PHBV microspheres--PLGA matrix composite scaffold for bone tissue engineering. *Biomaterials* 31, 4278–4285. doi:10.1016/j.biomaterials.2010.01.059

Jacob, J., More, N., Kalia, K., and Kapusetti, G. (2018). Piezoelectric smart biomaterials for bone and cartilage tissue engineering. *Inflamm. Regen.* 38, 2. doi:10.1186/s41232-018-0059-8

Kang, K. S., Hong, J. M., Kang, J. A., Rhie, J. W., Jeong, Y. H., and Cho, D. W. (2013). Regulation of osteogenic differentiation of human adipose-derived stem cells by controlling electromagnetic field conditions. *Exp. Mol. Med.* 45, e6. doi:10.1038/emm.2013.11

Kaniuk, Ł., and Stachewicz, U. (2021). Development and advantages of biodegradable PHA polymers based on electrospun PHBV fibers for tissue engineering and other biomedical applications. *ACS Biomater. Sci. Eng.* 7, 5339–5362. doi:10.1021/acsbiomaterials.1c00757

Klotz, B. J., Gawlitta, D., Rosenberg, A. J. W. P., Malda, J., and Melchels, F. P. W. (2016). Gelatin-methacryloyl hydrogels: towards biofabrication-based tissue repair. *Trends Biotechnol.* 34 (5), 394–407. doi:10.1016/j.tibtech.2016.01.002

Liu, Y., and Chan-Park, M. B. (2010). A biomimetic hydrogel based on methacrylated dextran-graft-lysine and gelatin for 3D smooth muscle cell culture. *Biomaterials* 31 (6), 1158–1170. doi:10.1016/j.biomaterials.2009.10.040

Lu, Y., Wan, Y., Gan, D., Zhang, Q., Luo, H., Deng, X., et al. (2021). Enwrapping polydopamine on doxorubicin-loaded lamellar hydroxyapatite/poly(lactic-co-glycolic acid) composite fibers for inhibiting bone tumor recurrence and enhancing bone regeneration. *ACS Appl. Bio Mater* 4, 6036–6045. doi:10.1021/acsabm.1c00297

Ma, R., Li, Q., Wang, L., Zhang, X., Fang, L., Luo, Z., et al. (2017). Mechanical properties and *in vivo* study of modified-hydroxyapatite/polyetheretherketone biocomposites. *Mater Sci. Eng. C Mater Biol. Appl.* 73, 429–439. doi:10.1016/j.msec.2016.12.076

Mihaila, S. M., Gaharwar, A. K., Reis, R. L., Khademhosseini, A., Marques, A. P., and Gomes, M. E. (2014). The osteogenic differentiation of SSEA-4 sub-population of human adipose derived stem cells using silicate nanoplatelets. *Biomaterials* 35, 9087–9099. doi:10.1016/j.biomaterials.2014.07.052

Park, J., Choi, W. M., Ha, C. S., Kim, W. H., and Cho, W. J. (1998). Synthesis and controlled photo- and biodegradabilities of poly[(hydroxybutyrate -Co-hydroxyvalerate)-G-styrene]. *Macromol. Symp.* 130, 53–69. doi:10.1002/masy.19981300106

Pasek-Allen, J. L., Wilharm, R. K., Bischof, J. C., and Pierre, V. C. (2023). NMR characterization of polyethylene glycol conjugates for nanoparticle functionalization. *ACS Omega* 8, 4331–4336. doi:10.1021/acsomega.2c07669

Sun, M. Y., SunWang, X. T. Z. Y., Guo, S. Y., Yu G, J., and Yang, H. Z. (2018). Synthesis and properties of gelatin methacryloyl (GelMA) hydrogels and their recent applications in load-bearing tissue. *Polymers* 10 (11), 1290. doi:10.3390/polym10111290

Xiang, H., Wang, S., Wang, R., Zhou, Z., Peng, C., and Zhu, M. (2013). Synthesis and characterization of an environmentally friendly PHBV/PEG copolymer network as a phase change material. *Sci. China Chem.* 56, 716–723. doi:10.1007/s11426-013-4837-5

Xue, Y., Niu, W., Wang, M., Chen, M., Guo, Y., and Lei, B. (2020). Engineering a biodegradable multifunctional antibacterial bioactive nanosystem for enhancing tumor photothermo-chemotherapy and bone regeneration. *ACS Nano* 14, 442–453. doi:10.1021/acsnano.9b06145

Yang, C., Blum, N. T., Lin, J., Qu, J., and Huang, P. (2020). Biomaterial scaffold-based local drug delivery systems for cancer immunotherapy. *Sci. Bull.* 65, 1489–1504. doi:10.1016/j.scib.2020.04.012

Yang, C., Kang, F., Huang, X., Zhang, W., Wang, S., Han, M., et al. (2022). Melatonin attenuates bone cancer pain via the SIRT1/HMGB1 pathway. *Neuropharmacology* 220, 109254. doi:10.1016/j.neuropharm.2022.109254

Ye, X., Li, L., Lin, Z., Yang, W., Duan, M., Chen, L., et al. (2018). Integrating 3D-printed PHBV/Calcium sulfate hemihydrate scaffold and chitosan hydrogel for enhanced osteogenic property. *Carbohydr. Polym.* 202, 106–114. doi:10.1016/j.carbpol.2018.08.117

frontiers | Frontiers in Pharmacology

TYPE Review
PUBLISHED 21 August 2023
DOI 10.3389/fphar.2023.1269224

OPEN ACCESS

EDITED BY
Duoyi Zhao,
Fourth Affiliated Hospital of China Medical University, China

REVIEWED BY
Weilin Zhang,
Affiliated Hospital of Guangdong Medical University, China
Changfeng Fu,
The First Hospital of Jilin University, China

*CORRESPONDENCE
Xiaojun Huang,
279325194@qq.com

RECEIVED 29 July 2023
ACCEPTED 09 August 2023
PUBLISHED 21 August 2023

CITATION
Zhang H, Luo P and Huang X (2023), Engineered nanomaterials enhance drug delivery strategies for the treatment of osteosarcoma.
Front. Pharmacol. 14:1269224.
doi: 10.3389/fphar.2023.1269224

Engineered nanomaterials enhance drug delivery strategies for the treatment of osteosarcoma

Haorui Zhang[1], Ping Luo[2] and Xiaojun Huang[1]*

[1]Department of Spine, Trauma Surgery, The First People's Hospital of Guangyuan, Guangyuan, China, [2]Science and Technology Education Section, The First People's Hospital of Guangyuan, Guangyuan, China

Osteosarcoma (OS) is the most common malignant bone tumor in adolescents, and the clinical treatment of OS mainly includes surgery, radiotherapy, and chemotherapy. However, the side effects of chemotherapy drugs are an issue that clinicians cannot ignore. Nanomedicine and drug delivery technologies play an important role in modern medicine. The development of nanomedicine has ushered in a new turning point in tumor treatment. With the emergence and development of nanoparticles, nanoparticle energy surfaces can be designed with different targeting effects. Not only that, nanoparticles have unique advantages in drug delivery. Nanoparticle delivery drugs can not only reduce the toxic side effects of chemotherapy drugs, but due to the enhanced permeability retention (EPR) properties of tumor cells, nanoparticles can survive longer in the tumor microenvironment and continuously release carriers to tumor cells. Preclinical studies have confirmed that nanoparticles can effectively delay tumor growth and improve the survival rate of OS patients. In this manuscript, we present the role of nanoparticles with different functions in the treatment of OS and look forward to the future treatment of improved nanoparticles in OS.

KEYWORDS

osteosarcoma, nanomaterials, drug delivery, chemotherapy, adverse reactions

1 Introduction

Osteosarcoma is the most common type of bone tumor in children and adolescents, accounting for about 60% of primary malignant bone tumors (Jemal et al., 2005). In children and adolescents, OS occurs in 2–3 per million people per year (Li et al., 2023). OS originates from osteoblasts responsible for bone growth, and osteoblasts damage important areas of bone, causing the bone to not repair itself (Shao et al., 2022). OS grows in a complex environment consisting of osteoblasts, osteoclasts, blood vessels, immune cells, and extracellular matrix (Alfranca et al., 2015). Imbalance in the balance between tumor parenchymal cells and non-tumor cell stromal cells is the basis for OS development and metastasis (Corre et al., 2020). Osteoclast-mediated osteolysis is the main cause of reduced bone fragility (Avnet et al., 2008). OS not only causes defects and damage to bone, affecting the functional integrity of bone but also brings serious accompanying symptoms to patients, manifested as unbearable bone pain, hypercalcemia, and pathological fractures (von Schacky et al., 2022). OS has a very high degree of malignancy, is prone to metastasis in the early stage, has strong drug resistance, and has a very poor prognosis. The lung is the most common site of metastasis in OS, up to 74% (Zhang et al., 2019). OS is the second leading cause of death among adolescent tumor-related diseases (Siclari and Qin, 2010). Over the past four decades, the incidence of bone tumors has stabilized, but the mortality rate of bone tumors in patients

with bone tumors has gradually increased due to their highly aggressive and metastatic nature (Zhu et al., 2022).

In recent years, the treatment of OS has been continuously explored and studied. However, treatment of OS is still quite limited (Sergi, 2021). Current conventional treatments for malignancy are chemotherapy, radiation therapy, and surgical resection (Wu et al., 2022a). Surgery can only remove the local tumor, but cannot cure the metastasis (Zhu et al., 2022). Chemotherapy is one of the most commonly used cancer treatments. However, due to drug resistance and tumor heterogeneity, likely, chemotherapy alone will not eliminate the tumor (Zhang et al., 2020). The commonly used clinical approach to malignant OS is neoadjuvant chemotherapy combined with surgery (Somaiah et al., 2022). Although this treatment modality has made good progress, survival for malignant OS has been significantly improved (Eaton et al., 2021). However, there are still some thorny problems, such as drug resistance, large side effects, and poor improvement in survival rates of metastatic patients. The treatment of malignant bone tumors is still a difficult problem to solve clinically. The key factors reducing the therapeutic effect of OS: 1) the resistance of OS cells to chemoradiotherapy; 2) Reducing the adverse reactions of chemotherapy drugs (Zhu et al., 2022).

With the development of nanomedicine, nanomaterials offer new opportunities to improve drug delivery and reduce their adverse effects (Xia et al., 2022a). Nanoexamples are widely used in the immunotherapy of tumors using their unique size, charge properties, and targeting properties (Wu et al., 2022a). The enhanced permeability retention (EPR) properties of tumor cells allow nanoparticles to remain in the tumor microenvironment for a long time (Morales-Orue et al., 2019). Nanoparticles encapsulate chemotherapy drugs, immune adjuvants, etc., which can achieve precise release of drugs and avoid drug decomposition and inactivity in blood vessels (Nguyen et al., 2020). Through reasonable design, the pharmacokinetics of nanoparticles can be improved, and their circulation time in the body can be enhanced to improve the therapeutic effect of OS (Yuan et al., 2023). The manuscript focuses on the application of nanoparticles with different functions in OS, and analyzes the prospect of nanoparticles in the treatment of OS.

2 pH-responsive nanoparticles

Surface charge plays an important role in signal transmission between nanoparticles and cells (Hu et al., 2020). The surface of tumor cells often exhibits negative electricity, which makes the positively charged nanoparticles have a strong attraction effect with it. However, the tumor microenvironment is often weakly acidic, which makes positively charged nanoparticles often less likely to come into direct contact with tumor cells. Acid-unstable acetal ligates exhibit ideal stability at physiological pH and exhibit instability under acidic conditions (Feng et al., 2020). Acetal linking enables nanoparticles to achieve pH transitions and deliver carriers to tumor cells. Cinnamaldehyde (CA) has been shown to have antibacterial, antioxidant, anti-inflammatory, hypoglycemic, and antitumor effects (Zong et al., 2022). CA has been reported to regulate the Wnt/β-catenin and phosphatidylinositol-3-kinase (PI3K)/AKT signaling pathways to inhibit the proliferation of OS cells and induce their apoptosis (Huang et al., 2020). However, the disadvantages of high toxicity and low solubility of CA limit its clinical application. Deng et al. (2023) made an amphiphilic CA prodrug from polyethylene glycol (mPEG), ethanol, and CA. Amphiphilic polymers can self-assemble into nano micelles in an aqueous solution with a diameter of 227 ± 16 nm and a zeta potential neutral at pH 7.4. Due to the protonation of ethanol, the surface charge of the nano micelles increases dramatically with the decrease in pH, and the zeta potential of the nano micelles becomes +6.25 mV at pH 7.9. This charge conversion facilitates the targeting of OS by nano micelles. *In vitro*, experiments have shown that nano micelles can release about 96% of CA in 5 h. Not only that, but nano micelles can also enhance the release of reactive oxygen species (ROS), promote apoptosis of OS cells and achieve powerful anti-tumor effects.

Mesoporous silica nanoparticles (MSNs) play an integral role in nanomedicine due to their excellent high drug delivery efficiency, controlled drug release and biocompatibility (Tarn et al., 2013). Polydopamine (PDA) surfaces are rich in bioactive groups, and pH response can be achieved by improving their surface groups. Photothermal therapy is an emerging way of tumor treatment, the main principle is to irradiate the photothermal agent at a specific wavelength, so that the photothermal agent heats up and kills tumor cells (Zhang et al., 2013). Shi et al. (2022) designed a nanoparticle with pH responsiveness and photothermal performance (MSN@QPC) using MSN, PDA, and quercetin (Qr). At the same time, collagen is added, so that the nanoparticles have a unique role in inducing extracellular matrix deposition and enhancing osteogenic activity. MSN@QPC can inhibit tumor growth and improve the efficacy of PTT. The diameter of the MSN@QPC is 80 nm and has a high specific surface area (Figure 1A). The drug load rate of MSN@QPC was 31.73%. Due to the addition of PDA, the release of Qr is delayed MSN@QPC, and *in vitro* tests, 55% of Qr can be released in 72 h MSN@QPC, thus achieving a long-term release effect. The released Qr can cause an increase in the temperature in the OS cells without causing an increase in the temperature of the surrounding tissues under ultraviolet light irradiation of 4 nm. In the case of light, MSN@QPC causes tumor cell death without causing normal cell death (Figure 1B). Not only that, but MSN@QPC also promotes extracellular matrix mineralization (Figure 1C). MSN@QPC *in vivo* has been shown to enhance the killing effect of tumors (Figures D–F).

Yang et al. (2018) used ZSM-5 zeolite loaded with doxorubicin to make ZSM-5/CS/DOX core-shell nanodisks with chitosan as the shell. The Si element released in ZSM-5 zeolite contributes to osteoblast differentiation by antagonizing NF-κB activation (Zhou et al., 2016). The ZSM-5/CS/DOX core-shell nanodisk has a diameter of 100 nm, a pore size of 3.75 nm, and a drug loading rate of 97.7%. Due to the positive charge on the surface of chitosan, ZSM-5/CS/DOX core-shell nanodisks are pH responsive. At pH 6, ZSM-5/CS/DOX core-shell nanodisks can release 58.7% of DOX. DOX enters the tumor nucleus and interferes with the DNA proliferation of osteosarcoma to achieve anti-tumor effects (Maiuri et al., 2007). ZSM-5/CS/DOX core-shell nanodisks have a stronger anti-tumor effect than pH 7.4 at pH 5. This feature is more conducive to the role of nanoparticles in the acidic tumor microenvironment. Not only that, compared with intravenous DOX, ZSM-5/CS/DOX core-shell nanodiscs release DOX in 24 h

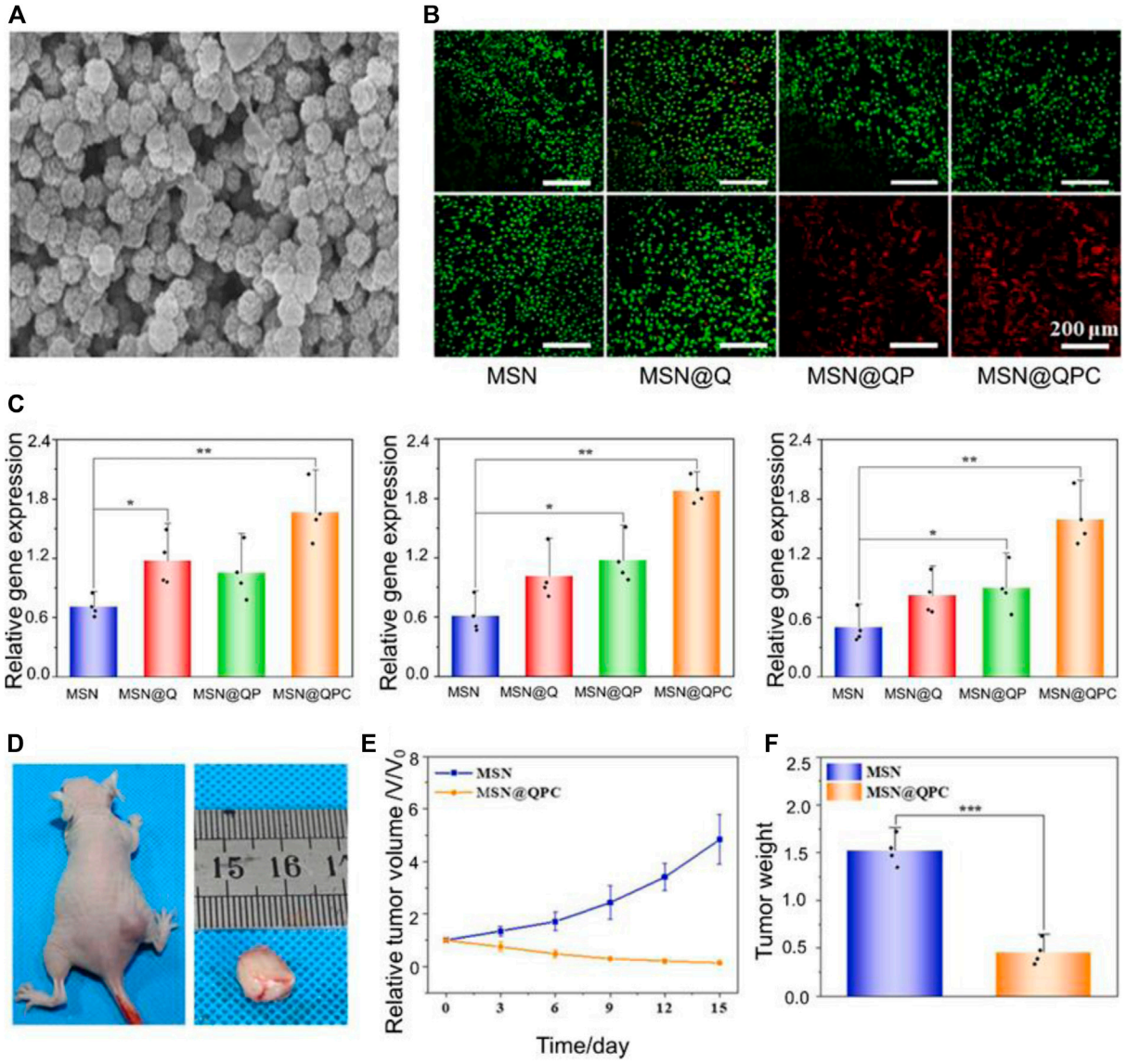

FIGURE 1
(A) Transmission electron microscopy image of MSN@QPC. **(B)** Cell Hoss staining: Causes more cell death (red: dead cells, green: live cells) in the case of MSN@QPC of light (bottom) than no light (top). **(C)** MSN@QPC Promotes extracellular matrix mineralization-related gene expression (CN, OPN, and RUNX2). **(D)** Tumor volume on day 15 of MSN@QPC treatment. **(E)** Relative tumor volume change. **(F)** Tumor weight on day 15. Reproduced with permission from (Shi et al., 2022).

in the body, which is high around the tumor and low in the heart. This phenomenon indicates that ZSM-5/CS/DOX core-shell nanodisks have a higher targeting effect and can reduce the cardiotoxicity of DOX.

3 ROS-responsive nanoparticles

It is well known that in a hypoxic environment of the tumor microenvironment, the increase in oxygen is not conducive to tumor cell growth (Xia et al., 2022a). Hypoxia-inducible factor-1α (HIF-1α) is a hypoxia-stable transcription factor that regulates the expression of multiple target genes involved in glycolysis, mitochondrial respiration, tumor metastasis, and chemotherapy resistance (Akman et al., 2021). Strategies to alleviate hypoxia and inhibit HIF-1α in the tumor microenvironment are an important way to treat tumors (Niu et al., 2021). ROS acts as a double-edged sword for tumor cells (Jia et al., 2022). ROS also has different effects on cells because of different concentrations. The cause of tumor cells is that genes are mutated in the process of cell division and proliferation, and ROS will promote this process. The cause of cell death is the damage to cellular DNA and proteins caused by high concentrations of ROS (Wang et al., 2020a; Zheng et al., 2023). Albendazole (ABZ) is a safe HIF-1α inhibitor with low toxicity that has been approved by the FDA (Pourgholami et al., 2010). However, the low bioavailability and low solubility of ABZ limit its clinical application (García et al., 2014). Poly(lactic-co-glycolic acid)-polyethylene glycol (PLGA-PEG) nanoparticles (NPs) have been

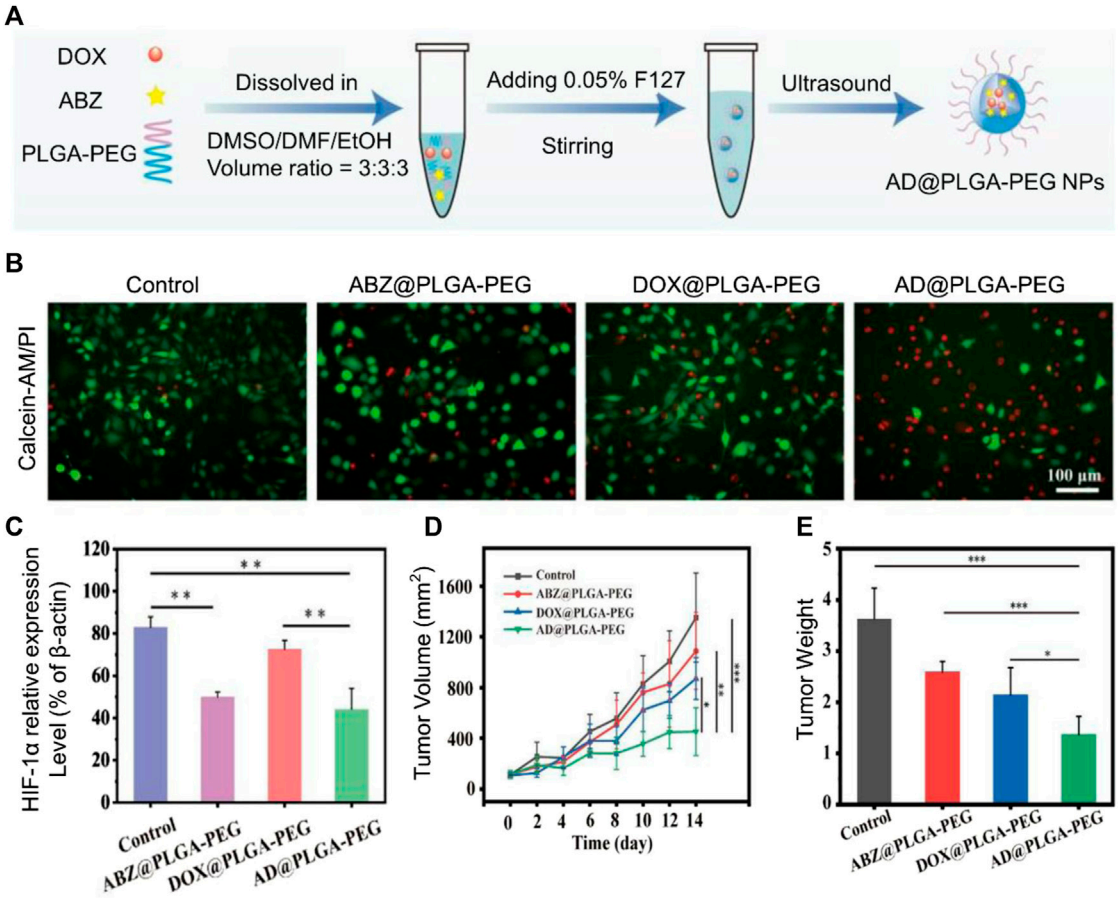

FIGURE 2
(A) AD@PLGA-PEG NPs production flowchart. **(B)** Antitumor activity of AD@PLGA-PEG NPs (red: dead cells, green: live cells). **(C)** Quantitative analysis of HIF-1α-related protein expression. **(D)** Tumor growth curve and tumor volume. **(E)** Tumor weights in different treatment groups. Reproduced with permission from (Zhao T.-T. et al., 2023a).

widely used in nanomedicine and regenerative medicine due to their biocompatibility (Xia et al., 2022b; Xia et al., 2023). Zhao et al. (2023a) fabricated AD@PLGA-PEG NPs with PLGA–PEG loads ABZ and DOX (ABZ and DOX molar ratio of 4:1) (Figure 2A). ABZ combined with DOX increases intracellular ROS and induces more tumor cell apoptosis compared to free DOX (Figure 2B) (Baldini et al., 1992). The particle size of AD@PLGA-PEG NP is about 140.51 ± 1.3 nm. When AD@PLGA-PEG NP is taken up by tumor cells, ABZ interferes with the mitochondrial respiratory chain, promotes oxidative stress, causes downregulation of HIF-related gene expression, and causes ROS production (Figure 2C). Compared with the control group, tumor volume was detected in tumor-bearing mice for 42 days (Figure 2D), the tumor size of the AD@PLGA-PEG NP group shrank threefold, and the tumor weight was also the lightest (Figure 2E). Not only that, AD@PLGA-PEG NP can also reduce the metastasis rate of OS.

Metal oxides are a material commonly used in biomedicine. Zirconia (ZrO2) has a strong ultraviolet absorption capacity and is widely used as a catalyst and photosensitizer (Zhang et al., 2021). Chianese et al. (2022) designed photoemissive ZrO2-acetylacetonate nanoparticles (ZrO2-acac NPs). Modifying hyaluronic acid on the surface of ZrO2-acac NPs can enhance the uptake of nanoparticles by tumor cells. ZrO2-acac NPs absorbed by tumor cells can release ZrO2, which can produce a large amount of ROS under light conditions, which in turn kills tumor cells. It was found that the particle size of ZrO2-acac NPs was 365 nm, and the loading rate of ZrO2 was 7.3% ± 0.1%. ZrO2-acac NPs and tumor cells were incubated for 48 h, and it was observed that ZrO2-acac NPs caused more tumor cell death than the control group. Zinc oxide nanoparticles (ZnO NPs) are widely used in the biomedical field, and their antibacterial, hemostatic, and other effects have been widely known (Shi et al., 2014). In recent years, the anti-tumor effect of ZnO NPs has gradually been well known. ZnO NPs have been reported to induce degradation of β-catenin mediated by HIF-1α/BNIP1/LC3B, triggering HIF-3 and Wnt pathway activation to inhibit OS cell metastasis (Zhang and Wang, 2020; He et al., 2023). Manganese dioxide (MnO2) can catalyze the decomposition of endogenous hydrogen peroxide in tumors to produce oxygen, thereby alleviating the hypoxic conditions of the tumor microenvironment (Liu et al., 2020). Phytic acid (PA) is a natural compound extracted from plants with certain antitumor activity, antioxidant, chelating agent and good bone targeting ability (Chen et al., 2018). Ju et al. (2023) made MnO2@PA NPs by modifying MnO2 NPs with PA. MnO2@PA NPs have a particle size of 111.1 ± 1.9 nm. *In vivo*, experiments confirmed

that mice treated with MnO2@PA NPs had significantly smaller tumor volumes than controls within 16 days.

4 Mitochondrial autophagy nanoparticles

Autophagy is a highly conserved process in cellular catabolism. The effect of autophagy on cells is bidirectional, with proper levels of autophagy protecting cells from damage, while excessive or reduced autophagy can trigger apoptosis (Chen et al., 2015). Mitochondria, as the main site of adenosine triphosphate (ATP) supply, are the main source of cellular energy (Duan and Fang, 2016). Automitochondrial phagogy helps cells remove aging proteins and maintain the stability of mitochondrial structure and function. However, pathological mitochondrial autophagy can lead to structural disturbances of cells, and abnormal cell metabolism leads to cell death (Wang et al., 2020b). Exogenous induction of intracellular mitophagy to promote tumor cell necrosis has attracted attention in recent years (Sun et al., 2021). Hydroxyapatite nanoparticles (HANPs) can promote autophagy of tumor cells to cause anti-tumor activity (Li et al., 2020). This mitophagy is often associated with calcium levels within tumor cells. Calcium ions as a second signal, and its disorder can lead to the imbalance of cellular metabolism (Yin et al., 2021). Not only that, HANPs also promote bone regeneration. Wu et al. (2022b) designed HANPs of different sizes to assess the antitumor activity of HANPs. Studies have shown that HANPs can cause upregulation of mitochondrial apoptosis-related genes (p53, Bcl-2 and caspase proteins). The anti-inflammatory and antitumor properties of gallic acid (GA) have been widely demonstrated (Zamudio-Cuevas et al., 2021). GA has been reported to inhibit highly expressed heat shock proteins in tumor cells, affecting ATP production (Ding et al., 2022). Liu et al. (2023) coordinated metal ions (Fe and Mn) with GA to make nanoparticles that can release GA and metal ions on demand. The average size of FeGA and MnGA is 105.7 and 164.2 nm, respectively. Fe and Mn catalyze the Fenton reaction in cancer cells, leading to organelle damage. FeGA and MnGA cause changes in mitochondrial membrane potential (MMP), and a large amount of ROS enters tumor cells to cause mitochondrial dysfunction. Studies have shown that metallo-gallic acid nanoparticles first upregulate the mitochondrial apoptosis-related gene, Bax, thereby activating caspase-3 by upregulated intracellular ROS. In tumor-bearing mice, MnGA was enriched at the tumor site, with a targeting efficiency of 39.8% at 14 h, and no obvious tissue damage occurred in the heart, liver, spleen, lung, and kidney. This indicates that the amount of metal-GA nanoparticles recruited at the tumor site is greatly increased without causing significant adverse effects.

Exosomes (EVs) are a heterogeneous population of membrane vesicles secreted by all living cells. EVs represent a new form of cell-to-cell communication that promotes cell proliferation, and differentiation, and inhibits apoptosis and inflammation to mediate tissue repair by delivering the proteins, RNA, and lipids it carries to target cells (Xia et al., 2022c). Rifampicin (RIF) binds to the β subunit of RNA polymerase to achieve its antibacterial effect (Maggi et al., 2009). RIF is known for being a traditional anti-TB drug. It has been found that RIF can cause mitochondrial lysis, induce apoptosis and cell cycle arrest, and achieve its anti-tumor effect (Mieras et al., 2016). Chen et al. (2022) isolated bone marrow-derived mesenchymal stem cells by ultracentrifugation to generate EVs for RIF delivery to make EXO-RIFs. The particle size of EXO-RIF is 65–225 nm, and the drug release rate of EXO-RIF is found to be significantly higher at pH 4.5 than at pH 7.4. Since the membrane structure of EV is similar to that of tumor cells, it is conducive to the uptake of EXO-RIF by tumor cells. In tumor-bearing mice, the EXO-RIF treatment group showed decreased Ki67 expression, elevated c-caspase-3 and Bax, and low Bcl-2 expression compared to RIF treatment. Not only that, the ALT, AST, BUN, CR, CK, and CK-MB levels in the EXO-RIF treatment group were lower than in the RIF group. This result shows that EXO-RIF greatly reduces the systemic toxicity of RIF.

5 Nanoparticles induce bone regeneration

The destruction of bone by OS is one of the factors that cannot be ignored. Whether it is the damage to the bone by surgery or the damage to the bone by the OS itself, it brings serious harm to the patient. Not only that, but chemotherapy drugs can also cause damage to the bone microenvironment, destroying bone stability (Lamora et al., 2016). Being able to cause bone remodeling during the treatment of OS is considered a better strategy. miR-29b is a non-coding small RNA that regulates gene expression and has been shown *in vivo* experiments to inhibit proliferation and migration and induce apoptosis in OS cells (Chen et al., 2017). miR-29b can also significantly inhibit BCL-2 expression and upregulate Bax expression, promoting tumor cell expression. Poly β aminoester (pBAE) nanoparticles have repeating ester groups, are capable of degradation in water, and have low toxicity and high biocompatibility (Dosta et al., 2021). Freeman et al. (2023) developed a pBAE nanoparticle delivery vehicle for delivery of miR-29b to OS cells and surrounding stromal cells. Subsequently, Fiona et al. developed HA hydrogels for the sustained release of bone morphogenetic protein-2 (BMP-2) and pBAE nanoparticles. BMP-2 is a strong inducer of bone remodeling and promotes bone regeneration (Xia et al., 2022d). *In vitro*, experiments have shown that the HA hydrogel system can continuously release 18% of pBAE nanoparticles within 100 days and 42% of BMP-2 within 33 days. The pBAE nanoparticles are 151 ± 2 nm with a surface charge of 5.6 ± 3.5 mV. The released miR-29b inhibited tumor cell growth, and in tumor-bearing mice, pBAE nanoparticles reduced tumor volume by 15% within 45 days of treatment compared to the control group. Not only that, BAM-2 released by the HA hydrogel system can promote bone regeneration, and osteolysis is reduced by an average of 29% compared to the control group. Most importantly, HA hydrogel systems can greatly extend the continuous release capacity of pBAE nanoparticles.

Ma et al. (2022) developed a fabricating groovelike micro-nanostructures (Fs-BP) using black phosphorus (BP) nanosheets for the delivery of DOX and PDA (Fs-BP-DOX@PDA) (Figure 3). PDA can enhance photothermal therapy of OS under near-infrared (NIR) mediation. The micro-nano layered structure of Fs-BP-DOX@PDA provides a strong surface area for bone regeneration. Fs-BP-DOX@PDA has load ratios of 93.2% and 35.2% for DOX and

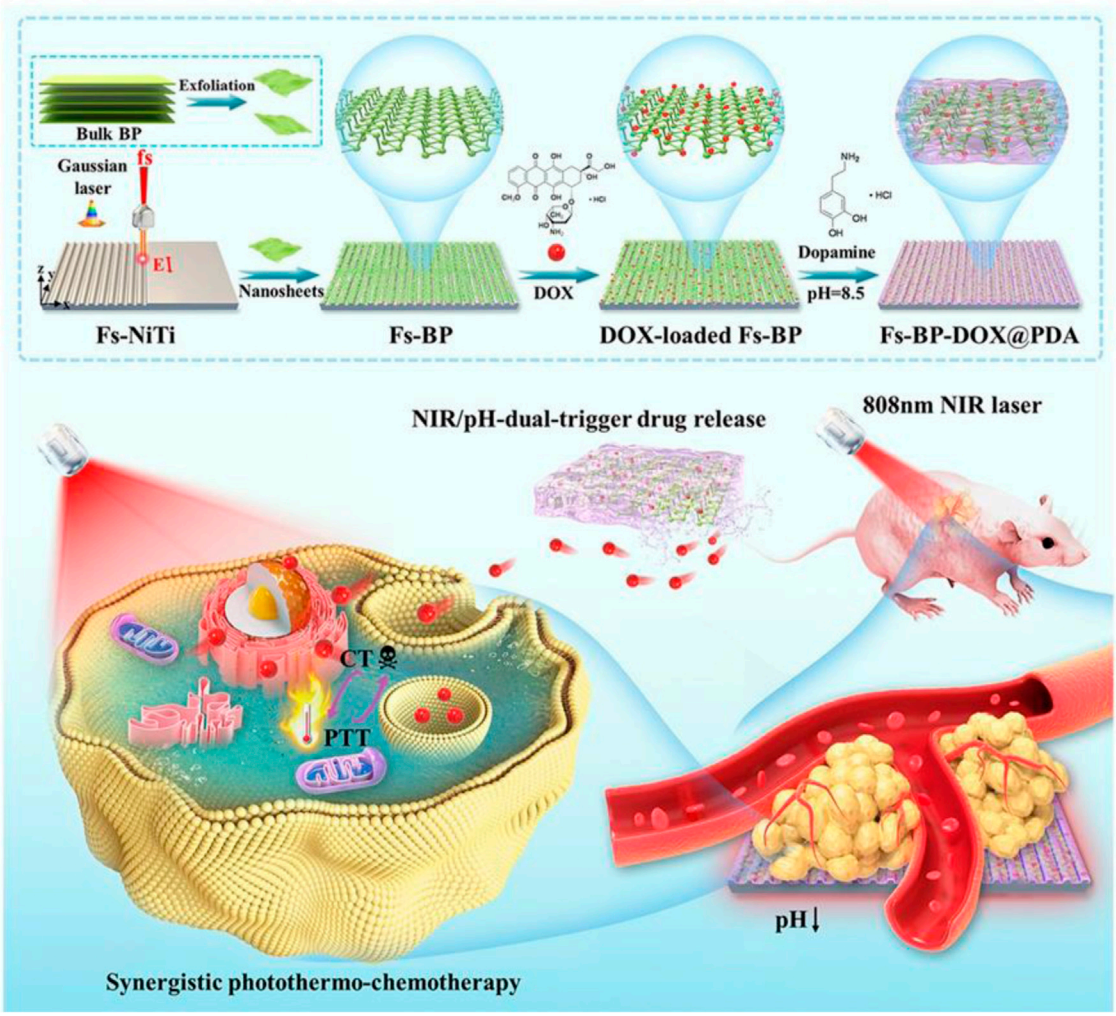

FIGURE 3
Schematic illustration of the design and fabrication strategy of the versatile multiscale therapeutic platform. Reproduced with permission from (Ma et al., 2022).

PDA, respectively. Fs-BP-DOX@PDA has higher photothermal conversion and stability under NIR. In tumor-bearing mice, Fs-BP-DOX@PDA was able to virtually eliminate tumor cells on day 14 and increase the survival rate of tumor-bearing mice to 60% after 100 days of treatment. What's more, Fs-BP-DOX@PDA is able to release phosphate ions, which form calcium phosphate deposition with calcium ions around bone to promote osteoblast mineralization. FS-BP-DOX@PDA also has unique antibacterial properties, with clearances of 99.2% and 99.6% against *Staphylococcus aureus* and *Pseudomonas aeruginosa*, respectively. Fs-BP-DOX@PDA avoids poor bone repair due to bacterial infection.

Curcumin (CM) is a polyphenolic compound extracted from plants, and its anti-tumor properties are well known (Saleh et al., 2019; Lu et al., 2023). The low solubility and bioavailability of CM limit its clinical application. Silkfibroin (SF) has been well known in recent years for tumor treatment and bone regeneration (Asadpour et al., 2020). Han et al. (2023) developed SF/HA scaffolds using supercritical carbon dioxide (SC-CO2) technology, filling PDA-coated CM-loaded chitosan nanoparticles on SF/HA scaffolds to make CM-PDA/SF/nHA nanofibrous scaffolds. The average particle size of 204.7 nm for nanoparticles. The porosity of the stent is 77.3%. Large porosity and compressive strength can meet the conditions for bone regeneration. SF/HA stent is able to continuously release CM and SF around the tumor, and in the presence of PDA, can enhance photothermal therapy. In mice, CM-PDA/SF/nHA nanofibrous scaffolds were detected to cause an increase in alkaline phosphatase, an early marker of bone differentiation, at 40 days.

6 Nanoparticles for delivery strategies

Nanoparticles are widely used in nanomedicine because of their precise delivery and slow release of carriers. The surface of the nanoparticle can be modified with different groups to set up nanoparticles with different functions (Hoang et al., 2022). Nano-loaded drugs can reduce the toxic side effects of the drug itself and achieve precise release of the tumor site (Iinuma et al., 2002).

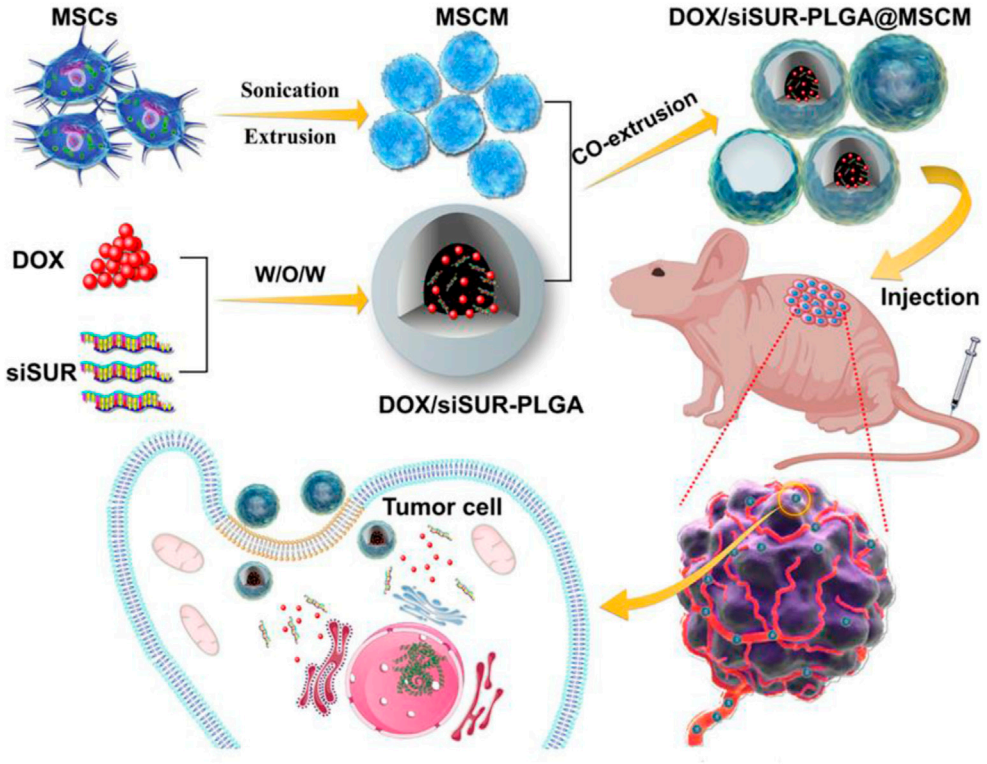

FIGURE 4
Mesenchymal stem cell membrane-camouflaged nanoparticles coloaded with DOX and survivin siRNA for osteosarcoma treatment. Reproduced with permission from (Zhao J. et al., 2023b).

Cisplatin (CDDP) is one of the commonly used chemotherapy drugs for OS, and its mechanism of action is to bind to DNA, destroy DNA and inhibit tumor cell mitosis (Dasari and Bernard Tchounwou, 2014; Xiang et al., 2023). However, CDDP has strong neurotoxicity and gastrointestinal reactions (Isakoff et al., 2015). Nanoliposomes are highly biocompatible drug-loading carriers. Alendronate can inhibit osteoclast activity and is considered a bone targeting vehicle (Fisher et al., 1999). Alendronate bindronate specifically binds to hydroxyapatite in the bone system for bone targeting. Zhong et al. (2023) made LCA NPs with sodium alendronate attached to liposomes loaded with CDDP. The particle size of LCA NPs is 144.4 ± 20.23 nm. *In vitro*, experiments have shown that LCA NPs can kill 99% of tumor cells. The encapsulation of nanoliposomes alleviates the systemic toxic side effects of CDDP. Wei et al. (2019) demonstrated anti-tumor effects *in vitro* with bone marrow-derived EVs-loaded DOX. The DOX-loaded EVs have a particle size of 152.7 nm. The vesicle structure of EVs allows them to easily bind to tumor cell membranes and release DOX into tumor cells. The encapsulation efficiency of the drug is about 7%, and the release of Exo-Dox after 60 h is about 36%. Compared to free Dox, Exo-Dox can kill OS cells more efficiently and exhibits lower cytotoxicity in cardiomyocytes. Ginsenosides can inhibit the growth of cancer cells, induce apoptosis of tumor cells and improve immunity (Han et al., 2006). However, ginsenosides have low bioavailability and are difficult to absorb by the body (Hasegawa et al., 1996). Fu et al. (2022) modified tumor cell membrane-camouflaged nanoparticles with alendronate sodium for delivery of MnO2 and ginsenosides. The particle size of the nanoparticles is 141.5 nm, and the nanoparticle seeds have good bone targeting ability due to the addition of sodium alendronate. MnO2 can promote the breakdown of H2O2 in the body and enhance tumor killing. The nanoparticles enhance immune cell infiltration and improve mouse survival up to 55 days.

Mesenchymal stem cells have unique tumor homing and migration effects and can be used for tumor targeting (Chen and Liu, 2016). Zhao et al. (2023b) used solvent evaporation to load DOX and siRNA into MSCMs-modified PLGAs to make DOX/siRNA-PLGA@MSCM NPs (Figure 4). The encapsulation rate and drug load of DOX/siRNA-PLGA@MSCM NPs were 53.10% ± 1.45% and 53.94 ± 2.31, respectively. *In vitro* experiments showed that DOX/siRNA-PLGA@MSCM NPs could be endocytosed by tumor cells within 3 h, and the cumulative release of DOX within 48 h was 26.67%. After 48 h of mouse tail vein injection of DOX/siRNA-PLGA@MSCM NPs, DOX/siRNA-PLGA@MSCM NPs were mainly deposited at the tumor site. This suggests that DOX/siRNA-PLGA@MSCM NPs have a strong ability to target tumor cells. The antitumor activity of DOX/siRNA-PLGA@MSCM NPs was detected in tumor-bearing mice, and DOX/siRNA-PLGA@MSCM NPs could promote apoptosis of tumor cells and reduce the metastasis

rate of tumors. Not only that but DOX/siRNA-PLGA@MSCM NPs also greatly reduced the adverse events of cardiotoxicity and bone marrow suppression of DOX. Zoledronic acid (ZOL) has a significant effect in promoting apoptosis of tumor cells, inhibiting angiogenesis and metastasis, and is a bisphosphonate for the prevention and treatment of metastatic bone disease (Nadar et al., 2017; Wang et al., 2020c). Xu et al. (2022) used HA and PEG to synthesize nanoparticles to deliver ZOL to make HA-PEG-N-HA-ZOL NP. HA-PEG-NHA-ZOL NP has a particle size of 159 ± 2.3 nm.

HA-PEG-NHA-ZOL NP could increase the expression level of Bcl-2-associated X protein (BAX), indicating that HA-PG-NHA-ZOL NP could promote apoptosis in tumor cells. HA-PEG-NHA-ZOL NP was shown in mice to reduce the expression of tumor cells Ki-67 and inhibit tumor cell proliferation. In mice for 5 days, HA-PEG-NHA-ZOL NP did not cause lung, liver, spleen, kidney and other functions. AbouAitah et al. (2022) developed an example of a core-shell nanoparticle that uses mesoporous silica nanoparticles (MSN) loaded colchicine (CL) to make nanoparticle shells, and chitosan-curcumin mixtures to make nanoparticle nuclei. The high surface area, large size, and large pore structure of MSN favor its use as a carrier-loaded drug (AbouAitah et al., 2020). *In vivo* experimental results show that core-shell nanoparticles can improve the anti-cancer treatment efficiency of CL while reducing its toxicity to normal cells.

7 Conclusion

OS is highly malignant, highly aggressive and metastatic. Although chemotherapy improves survival in OS. However, the side effects of chemotherapy drugs and drug resistance in OS remain treatment challenges. Preclinical studies have demonstrated that nanoparticles are effective in delaying the growth of OS and improving the survival rate of OS patients. In recent years, several nanocarrier-based drug delivery systems have been explored to target and treat OS. Although the nano-delivery system has made breakthroughs in the treatment of OS, improving the survival rate of OS mice. However, most of the current research is limited to *in vitro* cell experiments and animal experiments, which is still far from clinical application. Appropriate nanoparticles need to meet the following conditions: 1) Nanoparticles can effectively target OS cells; 2) Nanoparticles are able to accumulate and release payloads in OS cells; 3) Nanoparticles are reduced in other organs (heart, liver, kidney, etc.) that are aggregated to reduce systemic complications 4) Nanoparticles have good biosafety and bioavailability. Based on the current research base, we believe that the treatment of OS by nanoparticles will achieve good clinical results.

Author contributions

HZ: Writing–original draft. PL: Writing–original draft. XH. Writing–review and editing.

Funding

The author(s) declare that no financial support was received for the research, authorship, and/or publication of this article.

Acknowledgments

We would like to express our appreciation to everyone who was involved in the drafting and preparation of the manuscript.

Conflict of interest

The authors declare that the research was conducted in the absence of any commercial or financial relationships that could be construed as a potential conflict of interest.

Publisher's note

References

AbouAitah, K., Hassan, H. A., Swiderska-Sroda, A., Gohar, L., Shaker, O. G., Wojnarowicz, J., et al. (2020). Targeted nano-drug delivery of colchicine against colon cancer cells by means of mesoporous silica nanoparticles. *Cancers* 12, 144. doi:10.3390/cancers12010144

AbouAitah, K., Soliman, A. A. F., Swiderska-Sroda, A., Nassrallah, A., Smalc-Koziorowska, J., Gierlotka, S., et al. (2022). Co-delivery system of curcumin and colchicine using functionalized mesoporous silica nanoparticles promotes anticancer and apoptosis effects. *Pharmaceutics* 14, 2770. doi:10.3390/pharmaceutics14122770

Jemal, A., Murray, T., Ward, E., Samuels, A., Tiwari, R. C., Ghafoor, A., et al. (2005). Cancer statistics, *CA a cancer J. Clin.* 55 10–30. doi:10.3322/canjclin.55.1.10

Akman, M., Belisario, D. C., Salaroglio, I. C., Kopecka, J., Donadelli, M., De Smaele, E., et al. (2021). Hypoxia, endoplasmic reticulum stress and chemoresistance: dangerous liaisons. *J. Exp. Clin. Cancer Res.* 40, 28. doi:10.1186/s13046-020-01824-3

Alfranca, A., Martinez-Cruzado, L., Tornin, J., Abarrategi, A., Amaral, T., de Alava, E., et al. (2015). Bone microenvironment signals in osteosarcoma development. *Cell. Mol. Life Sci.* 72, 3097–3113. doi:10.1007/s00018-015-1918-y

Asadpour, S., Kargozar, S., Moradi, L., Ai, A., Nosrati, H., and Ai, J. (2020). Natural biomacromolecule based composite scaffolds from silk fibroin, gelatin and chitosan toward tissue engineering applications. *Int. J. Biol. Macromol.* 154, 1285–1294. doi:10.1016/j.ijbiomac.2019.11.003

Avnet, S., Longhi, A., Salerno, M., Halleen, J. M., Perut, F., Granchi, D., et al. (2008). Increased osteoclast activity is associated with aggressiveness of osteosarcoma. *Int. J. Oncol.* 33, 1231–1238. doi:10.3892/ijo_00000113

Baldini, N., Scotlandi, K., Serra, M., Kusuzaki, K., Shikita, T., Manara, M. C., et al. (1992). Adriamycin binding assay: A valuable chemosensitivity test in human osteosarcoma. *J. Cancer Res. Clin. Oncol.* 119, 121–126. doi:10.1007/BF01209668

Chen, F. M., and Liu, X. (2016). Advancing biomaterials of human origin for tissue engineering. *Prog. Polym. Sci.* 53, 86–168. doi:10.1016/j.progpolymsci.2015.02.004

Chen, H. X., Xu, X. X., Tan, B. Z., Zhang, Z., and Zhou, X. D. (2017). MicroRNA-29b inhibits angiogenesis by targeting VEGFA through the MAPK/ERK and PI3K/akt signaling pathways in endometrial carcinoma. *Cell. physiology Biochem. Int. J. Exp. Cell. physiology, Biochem. Pharmacol.* 41, 933–946. doi:10.1159/000460510

Chen, J.-W., Ni, B.-B., Zheng, X.-F., Li, B., Jiang, S.-D., and Jiang, L.-S. (2015). Hypoxia facilitates the survival of nucleus pulposus cells in serum deprivation by down-regulating excessive autophagy through restricting ROS generation. *Int. J. Biochem. Cell. Biol.* 59, 1–10. doi:10.1016/j.biocel.2014.11.009

Chen, K., Zhang, S., Li, A., Tang, X., Li, L., and Guo, L. (2018). Bioinspired interfacial chelating-like reinforcement strategy toward mechanically enhanced lamellar materials. *ACS Nano* 12, 4269–4279. doi:10.1021/acsnano.7b08671

Chen, W., Lin, W., Yu, N., Zhang, L., Wu, Z., Chen, Y., et al. (2022). Activation of dynamin-related protein 1 and induction of mitochondrial apoptosis by exosome-rifampicin nanoparticles exerts anti-osteosarcoma effect. *Int. J. nanomedicine* 17, 5431–5446. doi:10.2147/IJN.S379917

Chianese, G., Fasolino, I., Tramontano, C., De Stefano, L., Imparato, C., Aronne, A., et al. (2022). ROS-generating hyaluronic acid-modified zirconium dioxide-acetylacetonate nanoparticles as a theranostic platform for the treatment of osteosarcoma. *Nanomater. (Basel, Switz.* 13, 54. doi:10.3390/nano13010054

Corre, I., Verrecchia, F., Crenn, V., Redini, F., and Trichet, V. (2020). The osteosarcoma microenvironment: A complex but targetable ecosystem. *Cells* 9, 976. doi:10.3390/cells9040976

Dasari, S., and Bernard Tchounwou, P. (2014). Cisplatin in cancer therapy: molecular mechanisms of action. *Eur. J. Pharmacol.* 740, 364–378. doi:10.1016/j.ejphar.2014.07.025

Deng, J., Liu, S., Li, G., Zheng, Y., Zhang, W., Lin, J., et al. (2023). pH-sensitive charge-conversion cinnamaldehyde polymeric prodrug micelles for effective targeted chemotherapy of osteosarcoma *in vitro*. *Front. Chem.* 11, 1190596. doi:10.3389/fchem.2023.1190596

Ding, X.-L., Liu, M.-D., Cheng, Q., Guo, W.-H., Niu, M.-T., Huang, Q.-X., et al. (2022). Multifunctional liquid metal-based nanoparticles with glycolysis and mitochondrial metabolism inhibition for tumor photothermal therapy. *Biomaterials* 281, 121369. doi:10.1016/j.biomaterials.2022.121369

Dosta, P., Tamargo, I., Ramos, V., Kumar, S., Kang, D. W., Borrós, S., et al. (2021). Delivery of anti-microRNA-712 to inflamed endothelial cells using poly(β-amino ester) nanoparticles conjugated with VCAM-1 targeting peptide. *Adv. Healthc. Mater.* 10, e2001894. doi:10.1002/adhm.202001894

Duan, Y., and Fang, H. (2016). RecQL4 regulates autophagy and apoptosis in U2OS cells. *Biochem. Cell. Biol.* 94, 551–559. doi:10.1139/bcb-2016-0005

Eaton, B. R., Schwarz, R., Vatner, R., Yeh, B., Claude, L., Indelicato, D. J., et al. (2021). Osteosarcoma. *Pediatr. Blood Cancer* 68, e28352. doi:10.1002/pbc.28352

Feng, Z., Guo, J., Liu, X., Song, H., Zhang, C., Huang, P., et al. (2020). Cascade of reactive oxygen species generation by polyprodrug for combinational photodynamic therapy. *Biomaterials* 255, 120210. doi:10.1016/j.biomaterials.2020.120210

Fisher, J. E., Rogers, M. J., Halasy, J. M., Luckman, S. P., Hughes, D. E., Masarachia, P. J., et al. (1999). Alendronate mechanism of action: geranylgeraniol, an intermediate in the mevalonate pathway, prevents inhibition of osteoclast formation, bone resorption, and kinase activation *in vitro*. *Proc. Natl. Acad. Sci.* 96, 133–138. doi:10.1073/pnas.96.1.133

Freeman, F. E., Dosta, P., Shanley, L. C., Ramirez Tamez, N., Riojas Javelly, C. J., Mahon, O. R., et al. (2023). Localized nanoparticle-mediated delivery of miR-29b normalizes the dysregulation of bone homeostasis caused by osteosarcoma whilst simultaneously inhibiting tumor growth. *Adv. Mater.* 35, 2207877. doi:10.1002/adma.202207877

Fu, L., Zhang, W., Zhou, X., Fu, J., and He, C. (2022). Tumor cell membrane-camouflaged responsive nanoparticles enable MRI-guided immuno-chemodynamic therapy of orthotopic osteosarcoma. *Bioact. Mater.* 17, 221–233. doi:10.1016/j.bioactmat.2022.01.035

García, A., Leonardi, D., Salazar, M. O., and Lamas, M. C. (2014). Modified β-cyclodextrin inclusion complex to improve the physicochemical properties of albendazole. complete *in vitro* evaluation and characterization. *PloS one* 9, e88234. doi:10.1371/journal.pone.0088234

Han, J. Y., Kwon, Y. S., Yang, D. C., Jung, Y. R., and Choi, Y. E. (2006). Expression and RNA interference-induced silencing of the dammarenediol synthase gene in Panax ginseng. *Plant & Cell. physiology* 47, 1653–1662. doi:10.1093/pcp/pcl032

Han, R., Min, Y., Li, G., Chen, S., Xie, M., and Zhao, Z. (2023). Supercritical CO(2)-assisted fabrication of CM-PDA/SF/nHA nanofibrous scaffolds for bone regeneration and chemo-photothermal therapy against osteosarcoma. *Biomaterials Sci.* 11, 5218–5231. doi:10.1039/d3bm00532a

Hasegawa, H., Sung, J. H., Matsumiya, S., and Uchiyama, M. (1996). Main ginseng saponin metabolites formed by intestinal bacteria. *Planta medica*. 62, 453–457. doi:10.1055/s-2006-957938

He, G., Nie, J. J., Liu, X., Ding, Z., Luo, P., Liu, Y., et al. (2023). Zinc oxide nanoparticles inhibit osteosarcoma metastasis by downregulating β-catenin via HIF-1α/BNIP3/LC3B-mediated mitophagy pathway. *Bioact. Mater.* 19, 690–702. doi:10.1016/j.bioactmat.2022.05.006

Hoang, K. N. L., McClain, S. M., Meyer, S. M., Jalomo, C. A., Forney, N. B., and Murphy, C. J. (2022). Site-selective modification of metallic nanoparticles. *Chem. Commun. Camb. Engl.* 58, 9728–9741. doi:10.1039/d2cc03603g

Hu, D., Deng, Y., Jia, F., Jin, Q., and Ji, J. (2020). Surface charge switchable supramolecular nanocarriers for nitric oxide synergistic photodynamic eradication of biofilms. *ACS Nano* 14, 347–359. doi:10.1021/acsnano.9b05493

Huang, Y., Chen, J., Yang, S., Tan, T., Wang, N., Wang, Y., et al. (2020). Cinnamaldehyde inhibits the function of osteosarcoma by suppressing the wnt/β-catenin and PI3K/akt signaling pathways. *Drug Des. Dev. Ther.* 14, 4625–4637. doi:10.2147/DDDT.S277160

Iinuma, H., Maruyama, K., Okinaga, K., Sasaki, K., Sekine, T., Ishida, O., et al. (2002). Intracellular targeting therapy of cisplatin-encapsulated transferrin-polyethylene glycol liposome on peritoneal dissemination of gastric cancer. *Int. J. Cancer* 99, 130–137. doi:10.1002/ijc.10242

Isakoff, M. S., Bielack, S. S., Meltzer, P., and Gorlick, R. (2015). Osteosarcoma: current treatment and a collaborative pathway to success. *J. Clin. Oncol.* 33, 3029–3035. doi:10.1200/JCO.2014.59.4895

Jia, F., Liu, Y., Dou, X., Du, C., Mao, T., and Liu, X. (2022). Liensinine inhibits osteosarcoma growth by ROS-mediated suppression of the JAK2/STAT3 signaling pathway. *Oxidative Med. Cell. Longev.* 2022, 8245614. doi:10.1155/2022/8245614

Ju, Q., Huang, R., Hu, R., Fan, J., Zhang, D., Ding, J., et al. (2023). Phytic acid-modified manganese dioxide nanoparticles oligomer for magnetic resonance imaging and targeting therapy of osteosarcoma. *Drug Deliv.* 30, 2181743. doi:10.1080/10717544.2023.2181743

Lamora, A., Talbot, J., Mullard, M., Brounais-Le Royer, B., Redini, F., and Verrecchia, F. (2016). TGF-B signaling in bone remodeling and osteosarcoma progression. *J. Clin. Med.* 5, 96. doi:10.3390/jcm5110096

Li, S., Zhang, H., Liu, J., and Shang, G. (2023). Targeted therapy for osteosarcoma: A review. *J. Cancer Res. Clin. Oncol.* 149, 6785–6797. doi:10.1007/s00432-023-04614-4

Li, X., Wang, Y., Chen, Y., Zhou, P., Wei, K., Wang, H., et al. (2020). Hierarchically constructed selenium-doped bone-mimetic nanoparticles promote ROS-mediated autophagy and apoptosis for bone tumor inhibition. *Biomaterials* 257, 120253. doi:10.1016/j.biomaterials.2020.120253

Liu, J., Zhang, W., Kumar, A., Rong, X., Yang, W., Chen, H., et al. (2020). Acridine orange encapsulated mesoporous manganese dioxide nanoparticles to enhance radiotherapy. *Bioconjugate Chem.* 31, 82–92. doi:10.1021/acs.bioconjchem.9b00751

Liu, K., Zhang, L., Lu, H., Wen, Y., Bi, B., Wang, G., et al. (2023). Enhanced mild-temperature photothermal therapy by pyroptosis-boosted ATP deprivation with biodegradable nanoformulation. *J. nanobiotechnology* 21, 64. doi:10.1186/s12951-023-01818-1

Lu, K. H., Lu, P. W., Lin, C. W., and Yang, S. F. (2023). Curcumin in human osteosarcoma: from analogs to carriers. *Drug Discov. today* 28, 103437. doi:10.1016/j.drudis.2022.103437

Ma, Y., Jiang, L., Hu, J., Zhu, E., and Zhang, N. (2022). Developing a versatile multiscale therapeutic platform for osteosarcoma synergistic photothermo-chemotherapy with effective osteogenicity and antibacterial capability. *ACS Appl. Mater. Interfaces* 14, 44065–44083. doi:10.1021/acsami.2c10772

Maggi, N., Pasqualucci, C. R., Ballotta, R., and Sensi, P. (2009). Rifampicin: A new orally active rifamycin. *Chemotherapia* 11, 285–292. doi:10.1159/000220462

Maiuri, M. C., Zalckvar, E., Kimchi, A., and Kroemer, G. (2007). Self-eating and self-killing: crosstalk between autophagy and apoptosis. *Nat. Rev. Mol. Cell. Biol.* 8, 741–752. doi:10.1038/nrm2239

Mieras, L., Anthony, R., van Brakel, W., Bratschi, M. W., van den Broek, J., Cambau, E., et al. (2016). Negligible risk of inducing resistance in *Mycobacterium tuberculosis* with single-dose rifampicin as post-exposure prophylaxis for leprosy. *Infect. Dis. Poverty* 5, 46. doi:10.1186/s40249-016-0140-y

Morales-Orue, I., Chicas-Sett, R., and Lara, P. C. (2019). Nanoparticles as a promising method to enhance the abscopal effect in the era of new targeted therapies. *Rep. Pract. Oncol. Radiotherapy* 24, 86–91. doi:10.1016/j.rpor.2018.11.001

Nadar, R. A., Margiotta, N., Iafisco, M., van den Beucken, J. J. J. P., Boerman, O. C., and Leeuwenburgh, S. C. G. (2017). Bisphosphonate-Functionalized imaging agents, anti-tumor agents and nanocarriers for treatment of bone cancer. *Adv. Healthc. Mater.* 6, 1601119. doi:10.1002/adhm.201601119

Nguyen, T. L., Cha, B. G., Choi, Y., Im, J., and Kim, J. (2020). Injectable dual-scale mesoporous silica cancer vaccine enabling efficient delivery of antigen/adjuvant-loaded nanoparticles to dendritic cells recruited in local macroporous scaffold. *Biomaterials* 239, 119859. doi:10.1016/j.biomaterials.2020.119859

Niu, G., Zhou, M., Wang, F., Yang, J., Huang, J., and Zhu, Z. (2021). Marein ameliorates Ang II/hypoxia-induced abnormal glucolipid metabolism by modulating the HIF -1α/PPARα/γ pathway in H9c2 cells. *Drug Dev. Res.* 82, 523–532. doi:10.1002/ddr.21770

Pourgholami, M. H., Khachigian, L. M., Fahmy, R. G., Badar, S., Wang, L., Chu, S. W. L., et al. (2010). Albendazole inhibits endothelial cell migration, tube formation, vasopermeability, VEGF receptor-2 expression and suppresses retinal neovascularization in ROP model of angiogenesis. *Biochem. Biophysical Res. Commun.* 397, 729–734. doi:10.1016/j.bbrc.2010.06.019

Saleh, T., Soudi, T., and Shojaosadati, S. A. (2019). Aptamer functionalized curcumin-loaded human serum albumin (HSA) nanoparticles for targeted delivery to HER-2

positive breast cancer cells. *Int. J. Biol. Macromol.* 130, 109–116. doi:10.1016/j.ijbiomac.2019.02.129

Sergi, C. M. (2021). Targeting the 'garbage-bin' to fight cancer: HDAC6 inhibitor WT161 has an anti-tumor effect on osteosarcoma and synergistically interacts with 5-FU. *Biosci. Rep.* 41. doi:10.1042/BSR20210952

Shao, R., Wang, Y., Li, L., Dong, Y., Zhao, J., and Liang, W. (2022). Bone tumors effective therapy through functionalized hydrogels: current developments and future expectations. *Drug Deliv.* 29, 1631–1647. doi:10.1080/10717544.2022.2075983

Shi, L. E., Li, Z. H., Zheng, W., Zhao, Y. F., Jin, Y. F., and Tang, Z. X. (2014). Synthesis, antibacterial activity, antibacterial mechanism and food applications of ZnO nanoparticles: A review. *Food Addit. Contam. Part A, Chem. analysis, control, Expo. risk Assess.* 31, 173–186. doi:10.1080/19440049.2013.865147

Shi, Q., Lu, Y., Zhang, G., Yang, X., Li, R., Zhang, G., et al. (2022). Multifunctional mesoporous silica nanoparticles for pH-response and photothermy enhanced osteosarcoma therapy. *Colloids Surfaces B Biointerfaces* 217, 112615. doi:10.1016/j.colsurfb.2022.112615

Siclari, V. A., and Qin, L. (2010). Targeting the osteosarcoma cancer stem cell. *J. Orthop. Surg. Res.* 5, 78. doi:10.1186/1749-799X-5-78

Somaiah, N., Conley, A. P., Parra, E. R., Lin, H., Amini, B., Solis Soto, L., et al. (2022). Durvalumab plus tremelimumab in advanced or metastatic soft tissue and bone sarcomas: A single-centre phase 2 trial. *Lancet. Oncol.* 23, 1156–1166. doi:10.1016/s1470-2045(22)00392-8

Sun, K., Jing, X., Guo, J., Yao, X., and Guo, F. (2021). Mitophagy in degenerative joint diseases. *Autophagy* 17, 2082–2092. doi:10.1080/15548627.2020.1822097

Tarn, D., Ashley, C. E., Xue, M., Carnes, E. C., Zink, J. I., and Brinker, C. J. (2013). Mesoporous silica nanoparticle nanocarriers: biofunctionality and biocompatibility. *Accounts Chem. Res.* 46, 792–801. doi:10.1021/ar3000986

von Schacky, C. E., Wilhelm, N. J., Schäfer, V. S., Leonhardt, Y., Jung, M., Jungmann, P. M., et al. (2022). Development and evaluation of machine learning models based on X-ray radiomics for the classification and differentiation of malignant and benign bone tumors. *Eur. Radiol.* 32, 6247–6257. doi:10.1007/s00330-022-08764-w

Wang, L., Fang, D., Xu, J., and Luo, R. (2020c). Various pathways of zoledronic acid against osteoclasts and bone cancer metastasis: A brief review. *BMC Cancer* 20, 1059. doi:10.1186/s12885-020-07568-9

Wang, S., Deng, Z., Ma, Y., Jin, J., Qi, F., Li, S., et al. (2020b). The role of autophagy and mitophagy in bone metabolic disorders. *Int. J. Biol. Sci.* 16, 2675–2691. doi:10.7150/ijbs.46627

Wang, S., Li, H., Chen, S., Wang, Z., Yao, Y., Chen, T., et al. (2020a). Andrographolide induces apoptosis in human osteosarcoma cells via the ROS/JNK pathway. *Int. J. Oncol.* 56, 1417–1428. doi:10.3892/ijo.2020.5032

Wei, H., Chen, J., Wang, S., Fu, F., Zhu, X., Wu, C., et al. (2019). A nanodrug consisting of doxorubicin and exosome derived from mesenchymal stem cells for osteosarcoma treatment *in vitro*. *Int. J. nanomedicine* 14, 8603–8610. doi:10.2147/IJN.S218988

Wu, H., Liu, S., Chen, S., Hua, Y., Li, X., Zeng, Q., et al. (2022b). A selective reduction of osteosarcoma by mitochondrial apoptosis using hydroxyapatite nanoparticles. *Int. J. nanomedicine* 17, 3691–3710. doi:10.2147/IJN.S375950

Wu, W., Guo, H., Jing, D., Zhang, Z., Zhang, Z., Pu, F., et al. (2022a). Targeted delivery of PD-L1-derived phosphorylation-mimicking peptides by engineered biomimetic nanovesicles to enhance osteosarcoma treatment. *Adv. Healthc. Mater.* 11, e2200955. doi:10.1002/adhm.202200955

Xia, Y., Wang, H., Li, Y., and Fu, C. (2022d). *Engineered bone cement trigger bone defect regeneration*, 9.

Xia, Y., Wang, H., Yang, R., Hou, Y., Li, Y., Zhu, J., et al. (2023). Biomaterials delivery strategies to repair degenerated intervertebral discs by regulating the inflammatory microenvironment. *Front. Immunol.* 14, 1051606. doi:10.3389/fimmu.2023.1051606

Xia, Y., Yang, R., Hou, Y., Wang, H., Li, Y., Zhu, J., et al. (2022c). Application of mesenchymal stem cell-derived exosomes from different sources in intervertebral disc degeneration. *Front. Bioeng. Biotechnol.* 10, 1019437. doi:10.3389/fbioe.2022.1019437

Xia, Y., Yang, R., Wang, H., Hou, Y., Li, Y., Zhu, J., et al. (2022b). Biomaterials delivery strategies to repair spinal cord injury by modulating macrophage phenotypes. *J. tissue Eng.* 13, 20417314221143059. doi:10.1177/20417314221143059

Xia, Y., Yang, R., Zhu, J., Wang, H., Li, Y., Fan, J., et al. (2022a). Engineered nanomaterials trigger abscopal effect in immunotherapy of metastatic cancers. *Front. Bioeng. Biotechnol.* 10, 890257. doi:10.3389/fbioe.2022.890257

Xiang, D., Han, X., Li, J., Zhang, J., Xiao, H., Li, T., et al. (2023). Combination of Ido inhibitors and platinum(IV) prodrugs reverses low immune responses to enhance cancer chemotherapy and immunotherapy for osteosarcoma. *Mater. today Bio* 20, 100675. doi:10.1016/j.mtbio.2023.100675

Xu, Y., Qi, J., Sun, W., Zhong, W., and Wu, H. (2022). Therapeutic effects of zoledronic acid-loaded hyaluronic acid/polyethylene glycol/nano-hydroxyapatite nanoparticles on osteosarcoma. *Front. Bioeng. Biotechnol.* 10, 897641. doi:10.3389/fbioe.2022.897641

Yang, F., Wen, X., Ke, Q.-F., Xie, X.-T., and Guo, Y.-P. (2018). pH-responsive mesoporous ZSM-5 zeolites/chitosan core-shell nanodisks loaded with doxorubicin against osteosarcoma. *Mater. Sci. Eng. C* 85, 142–153. doi:10.1016/j.msec.2017.12.024

Yin, Y., Jiang, T., Hao, Y., Zhang, J., Li, W., Hao, Y., et al. (2021). Cascade catalytic nanoplatform based on ions interference strategy for calcium overload therapy and ferroptosis. *Int. J. Pharm.* 606, 120937. doi:10.1016/j.ijpharm.2021.120937

Yuan, P., Min, Y., and Zhao, Z. (2023). Multifunctional nanoparticles for the treatment and diagnosis of osteosarcoma. *Biomater. Adv.* 151, 213466. doi:10.1016/j.bioadv.2023.213466

Zamudio-Cuevas, Y., Andonegui-Elguera, M. A., Aparicio-Juárez, A., Aguillón-Solís, E., Martínez-Flores, K., Ruvalcaba-Paredes, E., et al. (2021). The enzymatic poly(gallic acid) reduces pro-inflammatory cytokines *in vitro*, a potential application in inflammatory diseases. *Inflammation* 44, 174–185. doi:10.1007/s10753-020-01319-5

Zhang, C., Guo, X., Xu, Y., Han, X., Cai, J., Wang, X., et al. (2019). Lung metastases at the initial diagnosis of high-grade osteosarcoma: prevalence, risk factors and prognostic factors. A large population-based cohort study. *Sao Paulo Med. J. = Revista paulista de Med.* 137, 423–429. doi:10.1590/1516-3180.2018.0381120619

Zhang, M., Zhang, F., Liu, T., Shao, P., Duan, L., Yan, J., et al. (2020). <p>Polydopamine nanoparticles camouflaged by stem cell membranes for synergistic chemo-photothermal therapy of malignant bone tumors</p>. *Int. J. nanomedicine* 15, 10183–10197. doi:10.2147/ijn.s282931

Zhang, W., Wang, Z., Huang, J., and Jiang, Y. (2021). Zirconia-based solid acid catalysts for biomass conversion. *Energy & Fuels* 35, 9209–9227. doi:10.1021/acs.energyfuels.1c00709

Zhang, Y., and Wang, X. (2020). Targeting the Wnt/β-catenin signaling pathway in cancer. *J. Hematol. Oncol.* 13, 165. doi:10.1186/s13045-020-00990-3

Zhang, Z., Wang, J., and Chen, C. (2013). Near-infrared light-mediated nanoplatforms for cancer thermo-chemotherapy and optical imaging. *Adv. Mater.* 25, 3869–3880. doi:10.1002/adma.201301890

Zhao, J., Mu, X., Hou, X., Zhang, X., Li, P., and Jiang, J. (2023b). Synergistic treatment of osteosarcoma with biomimetic nanoparticles transporting doxorubicin and siRNA. *Front. Oncol.* 13, 1111855. doi:10.3389/fonc.2023.1111855

Zhao, T.-T., Zhou, T.-J., Zhang, C., Liu, Y.-X., Wang, W.-J., Li, C., et al. (2023a). Hypoxia inhibitor combined with chemotherapeutic agents for antitumor and antimetastatic efficacy against osteosarcoma. *Mol. Pharm.* 20, 2612–2623. doi:10.1021/acs.molpharmaceut.3c00068

Zheng, G. Z., Zhang, Q. H., Chang, B., Xie, P., Liao, H., Du, S. X., et al. (2023). Dioscin induces osteosarcoma cell apoptosis by upregulating ROS-mediated P38 MAPK signaling. *Drug Dev. Res.* 84, 25–35. doi:10.1002/ddr.22009

Zhong, J., Wen, W., Wang, J., Zhang, M., Jia, Y., Ma, X., et al. (2023). Bone-Targeted dual functional lipid-coated drug delivery system for osteosarcoma therapy. *Pharm. Res.* 40, 231–243. doi:10.1007/s11095-022-03430-8

Zhou, X., Moussa, F. M., Mankoci, S., Ustriyana, P., Zhang, N., Abdelmagid, S., et al. (2016). Orthosilicic acid, Si(OH)4, stimulates osteoblast differentiation *in vitro* by upregulating miR-146a to antagonize NF-κB activation. *Acta Biomater.* 39, 192–202. doi:10.1016/j.actbio.2016.05.007

Zhu, P., Li, T., Li, Q., Gu, Y., Shu, Y., Hu, K., et al. (2022). Mechanism and role of endoplasmic reticulum stress in osteosarcoma. *Biomolecules* 12, 1882. doi:10.3390/biom12121882

Zong, Q., Li, J., Xiao, X., Du, X., and Yuan, Y. (2022). Self-amplified chain-shattering cinnamaldehyde-based poly(thioacetal) boosts cancer chemo-immunotherapy. *Acta Biomater.* 154, 97–107. doi:10.1016/j.actbio.2022.09.066

frontiers | Frontiers in Pharmacology

TYPE Review
PUBLISHED 21 September 2023
DOI 10.3389/fphar.2023.1271321

OPEN ACCESS

EDITED BY
Duoyi Zhao,
Fourth Affiliated Hospital of China Medical University, China

REVIEWED BY
Wei Zhao,
China Medical University, China
Daqian Wan,
Tongji University, China

*CORRESPONDENCE
Changfeng Fu,
fucf@jlu.edu.cn

RECEIVED 02 August 2023
ACCEPTED 12 September 2023
PUBLISHED 21 September 2023

CITATION
Zhu J, Fan J, Xia Y, Wang H, Li Y, Feng Z and Fu C (2023), Potential targets and applications of nanodrug targeting myeloid cells in osteosarcoma for the enhancement of immunotherapy. *Front. Pharmacol.* 14:1271321. doi: 10.3389/fphar.2023.1271321

Potential targets and applications of nanodrug targeting myeloid cells in osteosarcoma for the enhancement of immunotherapy

Jianshu Zhu[1], Jiawei Fan[2], Yuanliang Xia[3], Hengyi Wang[1], Yuehong Li[1], Zijia Feng[1] and Changfeng Fu[1]*

[1]Department of Spine Surgery, The First Hospital of Jilin University, Changchun, China, [2]Department of Gastroenterology, The First Hospital of Jilin University, Changchun, China, [3]Department of Cardiac Surgery, The First Hospital of Jilin University, Changchun, China

Targeted immunotherapies have emerged as a transformative approach in cancer treatment, offering enhanced specificity to tumor cells, and minimizing damage to healthy tissues. The targeted treatment of the tumor immune system has become clinically applicable, demonstrating significant anti-tumor activity in both early and late-stage malignancies, subsequently enhancing long-term survival rates. The most frequent and significant targeted therapies for the tumor immune system are executed through the utilization of checkpoint inhibitor antibodies and chimeric antigen receptor T cell treatment. However, when using immunotherapeutic drugs or combined treatments for solid tumors like osteosarcoma, challenges arise due to limited efficacy or the induction of severe cytotoxicity. Utilizing nanoparticle drug delivery systems to target tumor-associated macrophages and bone marrow-derived suppressor cells is a promising and attractive immunotherapeutic approach. This is because these bone marrow cells often exert immunosuppressive effects in the tumor microenvironment, promoting tumor progression, metastasis, and the development of drug resistance. Moreover, given the propensity of myeloid cells to engulf nanoparticles and microparticles, they are logical therapeutic targets. Therefore, we have discussed the mechanisms of nanomedicine-based enhancement of immune therapy through targeting myeloid cells in osteosarcoma, and how the related therapeutic strategies well adapt to immunotherapy from perspectives such as promoting immunogenic cell death with nanoparticles, regulating the proportion of various cellular subgroups in tumor-associated macrophages, interaction with myeloid cell receptor ligands, activating immunostimulatory signaling pathways, altering myeloid cell epigenetics, and modulating the intensity of immunostimulation. We also explored the clinical implementations of immunotherapy grounded on nanomedicine.

KEYWORDS

nanomedicine systems, myeloid cells, immunotherapy, tumor immune microenvironment, osteosarcoma

1 Introduction

Osteosarcoma (OS) is a specific type of malignant bone tumor that is particularly concerning in the medical community because it often affects adolescents and young adults. Like other types of malignant tumors, one of the challenges in treating osteosarcoma is chemotherapy resistance. This resistance implies that conventional chemotherapy methods have limited effectiveness against osteosarcoma (Ritter and Bielack, 2010; Gill and Gorlick, 2021). Efforts are being made to identify specific molecular targets and promising innovative approaches in OS treatment (Chen et al., 2021; Wei and Yang, 2023). Osteosarcoma cells genetically differ from their normal counterparts, and tumor-associated antigens (TAAs) often have poor immunogenicity due to immune editing (Meltzer and Helman, 2021). The tumor continuously interacts with the host immune system, ultimately escaping immune surveillance. The tumor microenvironment consists of a complex system made up of tumor cells and the surrounding cells, molecules, and extracellular matrix. Within this microenvironment, interactions between tumor cells and the immunosuppressive cells and matrix cells in the tumor microenvironment form a network of immunosuppressive pathways, simultaneously inhibiting the activation of immune defense (Kansara et al., 2014; Isakoff et al., 2015). Therefore, treatments targeting immune mechanisms, such as immunotherapies, are especially significant. Checkpoint blockade is an immunotherapeutic approach. Under normal circumstances, these immune checkpoints help protect the body's normal cells from attack (Wei et al., 2017; Guan et al., 2022). However, cancer cells might exploit these immune checkpoints to evade surveillance by the immune system (Postow et al., 2018; Kalbasi and Ribas, 2020). Consequently, by inhibiting certain signals, the ability of immune cells to combat tumor cells is enhanced (Anwar et al., 2020). The key to successful immunotherapy is overcoming local immune suppression in the tumor microenvironment and activating mechanisms leading to tumor eradication (Li et al., 2023). Chimeric Antigen Receptor (CAR) T-cell therapy is another cutting-edge technique in which T cells are genetically engineered to recognize and attack "chimeric" cells carrying specific tumor antigens (Porter et al., 2011; June and Sadelain, 2018). Once these T cells are redirected and proliferated, they are reinfused into the patient, exerting their immunotherapeutic effects against cancer cells (Grupp et al., 2013; Yu et al., 2019). This method has demonstrated significant efficacy in the treatment of hematologic malignancies (Larson and Maus, 2021; Amini et al., 2022). However, so far, treatment of more common sarcomas such as osteosarcoma and solid epithelial cancers typically has not made a significant impact (Depil et al., 2020; Maalej et al., 2023).

But successfully activating myeloid cells to elicit anti-tumor immune responses poses several challenges, including 1) the heterogeneous nature of myeloid cell populations within the tumor microenvironment, 2) the potential for tumor-induced myeloid cell immunosuppression, and 3) the complexities associated with modulating myeloid cell functions without adversely affecting other crucial physiological processes. The intersection between nanomedicine and cancer immunotherapy is becoming the focal point of frontier developments in cancer treatment, with profound therapeutic prospects. Nanodrugs, as the core carrier of this interdisciplinary field, bring revolutionary possibilities for cancer immunotherapy (Lakshmanan et al., 2021). In cancer immunotherapy, the emergence of nanodrugs offers a more precise and targeted approach. Nanodrugs can effectively improve drug delivery, increasing its concentration in tumor cells while reducing toxicity to normal cells (Fang et al., 2018; Fang et al., 2023). An increasing number of preclinical and clinical data indicate that combining nanodrugs with immunotherapy can enhance therapeutic effects by activating immune responses in the tumor microenvironment (Duan et al., 2019a; Liu and Sun, 2021). When targeting cancer cells, nanodrugs generally aim to induce immunogenic cell death, triggering the release of tumor antigens and danger-associated molecular patterns, such as calreticulin translocation, high mobility group box 1 protein, and adenosine triphosphate, capable of inducing immune responses to eliminate tumor cells (Kepp et al., 2021; Fu et al., 2022). In this process, the release of high mobility group box 1 protein (HMGB1) plays a key role, as it can serve as an alarm signal, promoting antigen presentation processes and inducing a stronger immune response (Inoue and Tani, 2014; Stagg et al., 2023). Nanodrugs targeting the tumor immune microenvironment enhance cancer immunotherapy by inhibiting immune suppressive cells (such as M2-like tumor-associated macrophages) and reducing the expression of immune suppressive molecules (such as transforming growth factor β) (Binnemars-Postma et al., 2017; Baig et al., 2020) Moreover, myeloid cells, like M2-like tumor-associated macrophages, are essential components of the tumor immune microenvironment playing an immunosuppressive role, often expressing factors that inhibit immune responses, such as transforming growth factor β (TGF-β). Nanodrugs can target these immunosuppressive myeloid cells, thereby modulating the tumor immune microenvironment (van der Meel et al., 2013; Jin et al., 2018).

In this review, we discuss the mechanisms of preclinical model immunotherapies based on nanomedicine that enhance the therapeutic effect of the immune system by targeting myeloid cells. We focus on strategies established in nanomedicine that complement those established in genetic engineering and molecular biology, potential therapeutic targets, and applications of nanodrugs targeting myeloid cells, particularly tumor-associated macrophages, in osteosarcoma to strengthen immunotherapy. However, due to the heterogeneity of different tumors and individuals, nanoplatform delivery systems may not be effective for all types of tumors. Lastly, we provide our views on the anticipated challenges and future directions of nanomedicine in the era of immunotherapy.

2 Mechanism of action of nanomedicine targeting myeloid cells

Nanomedicine provides new mechanisms of action for immunotherapy, including promoting immunogenic cell death, regulating the proportion of different cell subgroups in the myeloid cells, presenting immune-stimulating ligands to immune cells, activating immune-stimulating signal transduction pathways, delivering nucleic acids to cells, changing epigenetics, and controlling the intensity of immune stimulation (Yang et al., 2021) In this section, we briefly introduce the mechanisms of nanomedicines targeting myeloid cells and their potential role in osteosarcoma treatment. As illustrated in Figure 1, Mechanism of Action of Nanoparticles Targeting Bone Marrow Cells in the Modulation of Immunotherapy.

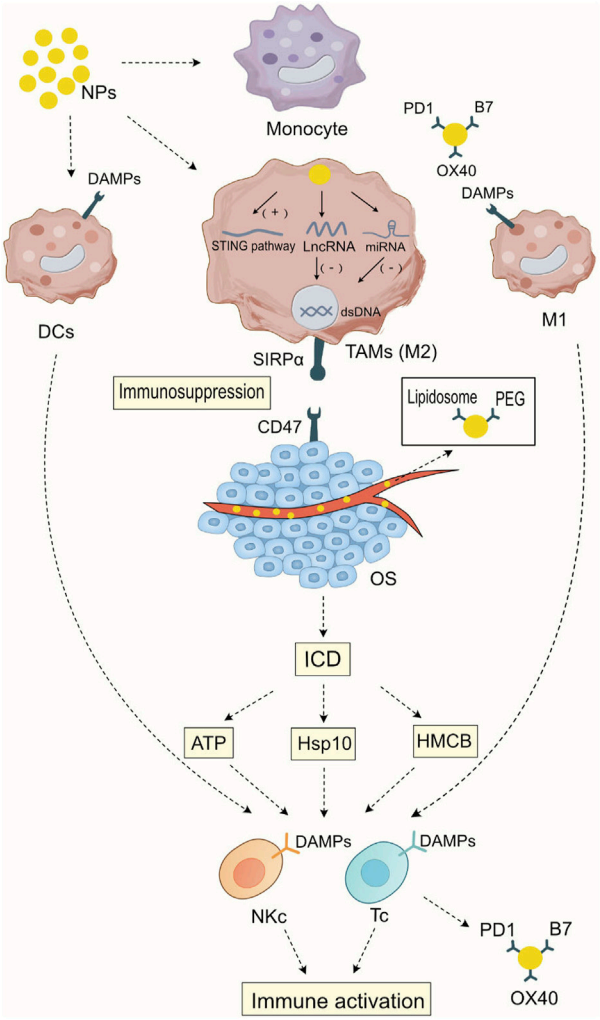

FIGURE 1
Mechanism of Action of Nanoparticles Targeting Bone Marrow Cells in the Modulation of Immunotherapy After being phagocytosed by myeloid cells, nanoparticles can activate the STING signaling pathway in tumor-associated macrophages, thereby initiating cellular immunity. At the same time, they can release the carried LncRNA or miRNA to silence specific gene expressions, leading to a transformation in the macrophage subtype. Nanoparticles carrying specific ligands such as PD1, B7, and OX40 can bind to specific ligands on dendritic cells and M1-type macrophages, enhancing the antigen presentation ability of dendritic cells and M1-type macrophages and strengthening the specific immunity against tumor cells. Nanoparticles carrying chemotherapy drugs have a direct cytotoxic effect on tumor tissues, promoting immunogenic cell death (ICD) and thus enhancing the direct cytotoxic effects of T cells and NK cells on tumor cells. In addition, during blood transport, nanoparticles wrap Lipidosomes and PEG to reduce cytotoxic side effects on normal tissues, enhancing the specificity of immunotherapy.

2.1 Abnormal phagocytic function of M1 macrophages and immune-inflammatory injury promote immunogenic cell death

The event of tumor cell death that encourages anti-tumor immune responses is known as Immunogenic Cell Death (ICD) (Yu et al., 2023). ICD is a unique form of cell death. ICD releases certain molecules, which in turn activate the immune system (Duan et al., 2019a). In the treatment of osteosarcoma, ICD is employed to activate the immune system, assisting the body in recognizing and eradicating osteosarcoma cells (Figure 2A).

ICD reveals that when tumor cells die, they release damage-associated molecular patterns (DAMPs), which in turn activate reactive immune cells, assisting the body's immune system in recognizing and eliminating remaining cancer cells, such as ATP and high mobility group box 1 (HMGB1), as well as the surface exposure of calreticulin and heat shock protein 90 (HSP90) (Krysko et al., 2012; Ahmed and Tait, 2020). However, conventional cancer ablation treatments like chemotherapy or ionizing radiation exhibit different capacities to induce ICD, and their immunoenhancing effects may be counterbalanced by their toxicity to responsive immune cells (Adkins et al., 2014; Yan et al., 2020). Against this backdrop, nanodrugs promote the release of tumor antigens and DAMPs, allowing antigen-presenting cells to capture and present them to $CD8^+$ T cells, leading to the activation of $CD8^+$ T cells and enhancing their specific cytotoxic effects against cancer cells. Additionally, other myeloid cells, especially dendritic cells, also play a pivotal role during the ICD process. These cells can further enhance the activation and proliferation of T cells. Specifically, the increased expression of surface molecule $CD80^+$ in myeloid cells further strengthens the immune response (Krysko et al., 2013).

Nanomaterial-induced ICD is also employed to boost combination therapies, either by co-encapsulating various drugs into the same particle to assure co-delivery to target cells or by inducing prominent ICD in tumors via combination treatment-loaded particles that result from the amalgamation of drugs with synergistic action patterns (Mishchenko et al., 2019). Additionally, emerging therapeutic approaches also harness external energy sources, such as light or heat, to interact with nanoparticles, thereby enhancing their therapeutic effects. For instance, nanoparticles can be designed to be sensitive to specific wavelengths of light or temperatures, synergistically producing ICD-inducing effects, thereby amplifying the exposure of calreticulin on the surface of tumor cells and the infiltration of immune cells (Guo et al., 2022).

2.2 Adjustment of the ratio of different cell subgroups within tumor-associated macrophages

By regulating strategies that transform TAMs from an M2 phenotype to an M1 phenotype, researchers aim to reshape the tumor microenvironment and promote anti-tumor immune responses. The latest developments in macrophage immunotherapy focus on strategies to reeducate TAMs from M2 to M1 phenotypes. Tumor-associated macrophages (TAMs) are defined as M2-type and are considered an important cellular subset in the tumor microenvironment that exerts immunosuppressive effects (Chen et al., 2019a). TAMs participate in various processes of tumor progression through the expression of cytokines, chemokines, growth factors, proteolytic enzymes, etc., thereby enhancing tumor cell proliferation, angiogenesis, and immune suppression, supporting invasion and metastasis (Pathria et al., 2019).

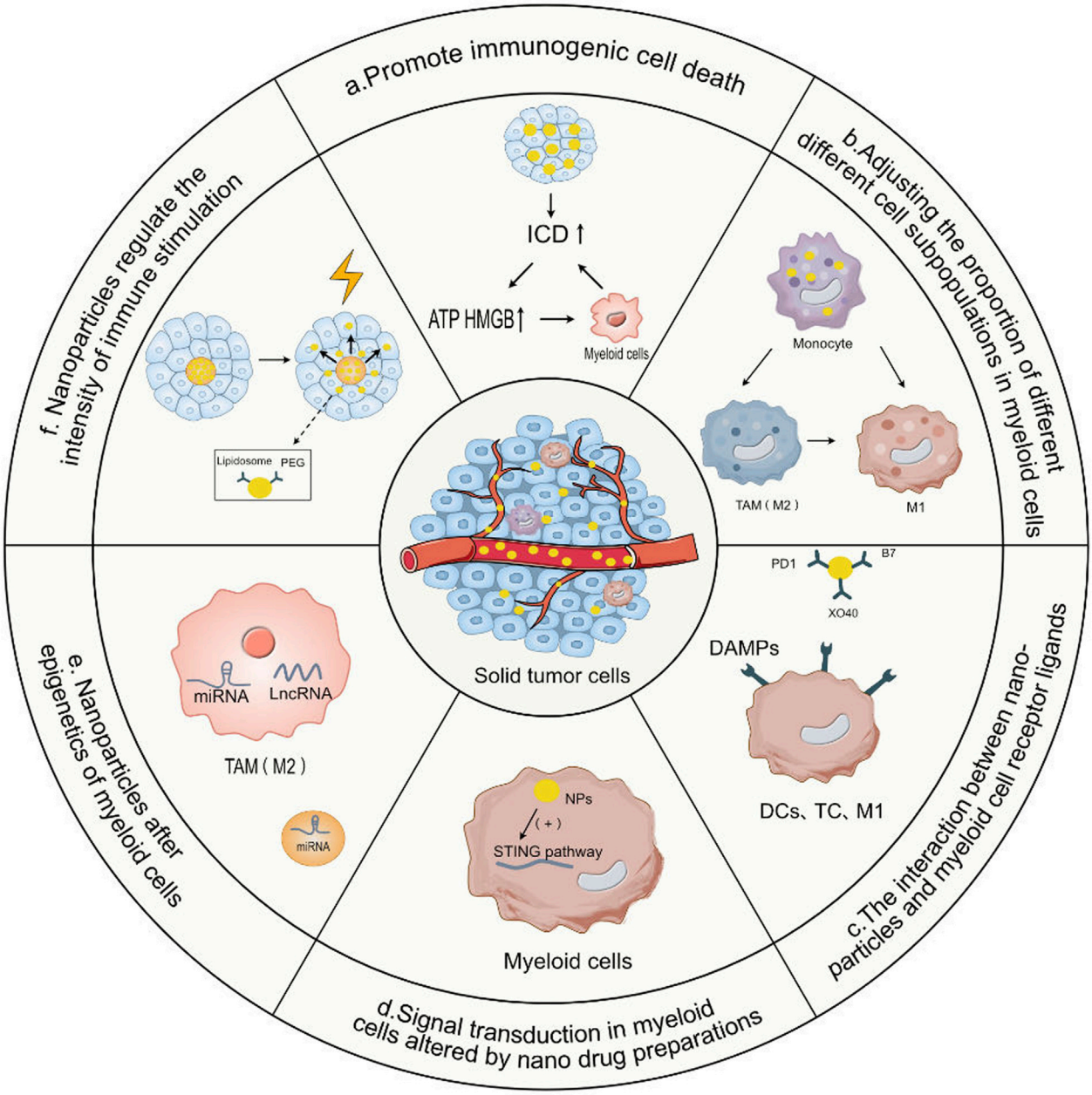

FIGURE 2
The mode of action of nanoparticles targeting myeloid cells in regulating immunotherapy. **(A)** Promote immunogenic cell death. Nanoparticles promote the release of ATP and High Mobility Group Box 1 (HMGB1) by promoting tumor immunogenic cell death (ICD), thereby activating the uptake of tumor antigens by antigen-presenting cells in myeloid cells and their subsequent activation, thereby enhancing the direct killing effect of T cells and NK cells on tumor cells. **(B)** Adjusting the proportion of different cell subpopulations in myeloid cells. By targeting myeloid cells with a nanodrug system and then adjusting the proportion of different subgroups of tumor-associated macrophages, the effects of T cell immunotherapy can be enhanced by depleting the M2 macrophage subpopulation and MDSCs in TAMs. **(C)** The interaction between nanoparticles and myeloid cell receptor ligands. Nanoparticles provide a series of ligands or release cytokines, co-stimulatory signals DAMPs provided by myeloid antigen-presenting cells to T cells and natural killer cells (NK), receptor-ligand interactions, activating dendritic cells (DCs), T cells and natural killer cells (NKC). **(D)** Signal transduction in myeloid cells altered by nano drug preparations. Nanodrug formulations can directly deliver drugs to myeloid cells, changing the signal transduction of myeloid cells and enhancing their anti-tumor activity. **(E)** Nanoparticles Alter Epigenetics of Myeloid Cells. Nanoparticles carrying miRNA are internalized in myeloid cells such as M2 TAMs and solid tumor cells, and siRNA is released, leading to effective gene silencing. **(F)** Nanoparticles regulate the intensity of immune stimulation. Nanodrug formulations can be designed to interact with external energy sources such as light or heat, thereby precisely controlling the timing of drug release and the intensity of myeloid cell immune stimulation, or controlling their bioactivity through liposomes, the delivery of prodrugs hidden by Polyethylene Glycol (PEG) chains.

Utilizing the nanodrug system to target myeloid cells and then regulate the proportion of different subgroups of tumor-associated macrophages is a clinically attractive method because myeloid cells usually act as myeloid-derived suppressor cells (MDSCs) or TAMs with inhibitory effects, and they are reasonable therapeutic targets due to their tendency to phagocytize nanoparticles and

microparticles (Zhu et al., 2020; Zhao et al., 2022). In mouse tumor models, intravenously administered nanoparticles easily accumulate in TAMs, and studies show that myeloid cells absorb ten times more nanoparticles than tumor cells (Kwong et al., 2013) Therefore, recent preclinical studies have tried to utilize this effect to eliminate the subgroup of myeloid cells that play an immune suppression role in the tumor immune microenvironment. Furthermore, M2 macrophages can inhibit $CD8^+$ T cells to support tumor survival (Zhao et al., 2022). Therefore, T cell therapy can be enhanced by depleting MDSCs.

Another promising immunotherapeutic strategy to reduce inhibitory myeloid cells is to switch the phenotype that promotes anti-tumor immunity through reprogramming TAM (Li et al., 2021). The reversal of TAMs releases cytokines and gradually inhibits tumor angiogenesis, allowing for the remodeling of the tumor microenvironment (Figure 2B). Activated M1 macrophages are not only effector cells in innate immunity but also antigen-presenting cells that deliver processed antigens to T cells via MHC class II molecules, thereby promoting adaptive immune responses (Han et al., 2021). $CD47^+$ is a protein expressed on the surface of cancer cells. It binds with the signal-regulatory protein α (SIRPα) on macrophages, producing a "don't eat me" signal, which prevents the phagocytic activity of the macrophages. Blocking the CD47-SIRPα signaling axis and promoting repolarization from M2 to M1 in the tumor microenvironment can significantly prevent the local recurrence and distant metastasis of malignant tumors (Rao et al., 2020).

Furthermore, the latest findings in the field of immunometabolism indicate that macrophages, based on their polarization state, such as M1 macrophages mainly relying on glycolysis for energy and M2 macrophages primarily utilizing fatty acid oxidation and the TCA cycle for energy, display different metabolic characteristics among different macrophage subgroups (Ramesh et al., 2022). Therefore, these metabolic products are essential drivers of cellular signal transduction.

2.3 Interaction between nanoparticles and ligands of myeloid cell receptors

There are many key immune regulatory receptors involved in anti-tumor immunity, especially the co-stimulatory signals presented by myeloid antigen presenting cells to T cells and natural killer (NK) cells, involving cell-cell contacts and receptor-ligand interactions. The size and properties of nanoparticles enable them to serve as a carrier for antibodies and other therapeutic drugs, specifically delivering them to cancer cells (Irvine and Dane, 2020; Zhao et al., 2022). The interaction of nanoparticles with myeloid cell receptor ligands combines nanodrugs with immunotherapy, aiming to enhance the cancer immune response by enhancing key steps in the immune response cascade (Chaib et al., 2020).

The use of nanoparticles can optimize this process and enhance the immune response to cancer in several stages: nanoparticles can more specifically deliver drugs to cancer cells by loading ligands (such as antibodies or small molecules) onto nanoparticles, thus enhancing antigen release (Ifergan and Miller, 2020). Myeloid cells initiate immune responses by taking up and processing antigens. Nanoparticles can be designed to carry specific ligands or release specific signaling molecules that can stimulate myeloid cells, such as macrophages and dendritic cells, to more effectively take up and process antigens (Zhu et al., 2023). Myeloid cells play a pivotal role in T cell activation. This is achieved by presenting antigen fragments through their major histocompatibility complex (MHC) surfaces. Nanoparticles can be designed to enhance this process (Figure 2C), for example, by providing stimulating signals or directly presenting antigen fragments, DCs enhance tumor antigen presentation, leading to an increase in $CD8^+$ T cell tumor infiltration, to more effectively activate T cells (Tuettenberg et al., 2016). Upon activation, the immune system's key players, namely, Natural Killer (NK) cells and T cells, possess the capability to identify and subsequently eliminate cancer cells that express specific antigens. Nanoparticles carry specific ligands, and release signals that stimulate NK cells, and T cells, thereby enhancing their killing ability against cancer cells (Amoozgar and Goldberg, 2015).

In these processes, the interaction of nanoparticles with myeloid cell receptor ligands is crucial. Appropriate ligand design can make nanoparticles more targeted and more effectively activate the immune response. Overall, through these mechanisms, the combination of nanoparticles and immunotherapy can effectively enhance the immune response to cancer.

2.4 Activating the signal transduction pathway for immune stimulation

Nanodrug formulations can deliver drugs directly to myeloid cells, and nanodrug formulations play an important role in altering immune therapeutic drug-mediated myeloid cell signaling, thereby enhancing the anti-tumor activity of myeloid cells (Garner and de Visser, 2020). Nanodrug formulations can change immune therapeutic drug-mediated signal transduction, these drugs target cell signal transduction pathways in various ways to enhance their anti-tumor activity (Kumar et al., 2023).

Nanodrug formulations can provide multiple nanodrug formulations that can change immune therapeutic drug-mediated signal transduction (Figure 2D), these drugs target cell signal transduction pathways in various ways to enhance their anti-tumor activity (Darling et al., 2020; Xia et al., 2022). One of the main applications of nanomaterials in medicine is to promote intracellular drug delivery. Nanomaterials as alternatives to natural viruses have been widely studied to promote the entry of other drugs into the cytoplasm to change the signal transduction of myeloid cells (Fiering, 2017). Cancer immunonanodrugs mainly target TAM by blocking M2-type TAM survival or affecting its signal cascade, limit the recruitment of M2-type macrophages to tumors, and re-induce tumor-promoting M2-type TAM to anti-tumor M1-like phenotype, thereby enhancing the anti-tumor function of myeloid cells or inhibiting the immune-suppressive function of M2-type tumor-associated macrophages (Ovais et al., 2019). In addition, nanodrug formulations can be designed to have an impact on specific signaling pathways. For example, the key role of the stimulant of interferon genes (STING) pathway in anti-tumor immunity is by regulating the receptors or other signaling molecules on the surface of myeloid cells, thereby changing the signal transduction inside the cells, and further affecting the activity of

myeloid cells (Luo et al., 2017). This is particularly important for manipulating the role of myeloid cells in immune responses.

2.5 Alteration of myeloid cell epigenetics by nanoparticles

Progress in the nanomedicine realm over the past years has laid the groundwork for the development of siRNA-based drugs as another category of personalized cancer immunonanodrugs (Zins and Abraham, 2020). Small interfering RNA (siRNA) therapies for cancer are increasingly becoming the focus of research interest (Huang et al., 2023).

Various microRNAs (miRNAs) disseminated by exosomes from tumors participate in intercellular communication (Hosseini et al., 2021). Nanoparticles often act as carriers for siRNA, similar to exosomes. siRNA primarily functions to reduce the expression of specific mRNA through the RNA interference (RNAi) mechanism, thereby inhibiting the production of corresponding proteins and altering the epigenetic state of myeloid cells (Xin et al., 2017; Kara et al., 2022). Furthermore, nanoparticles are readily internalized by phagocytic cells, enabling penetration into cells and potential interactions with biological macromolecules such as DNA and proteins (Ashrafizadeh et al., 2022). Nanoparticles carrying miRNAs exhibit high accumulation in myeloid cells and tumor tissues due to prolonged blood circulation and increased pH sensitivity. The current strategy involves both active and passive targeting, where nanoparticles carrying small interfering RNA (siRNA) are internalized into M2 TAMs (Tumor-Associated Macrophages) and solid tumor cells (Kanasty et al., 2013; Zhu and Palli, 2020) (Figure 2E). As the charge reversal occurs in the microenvironment where nanoparticles reside, nanoparticles exhibit effective endosome/lysosome escape and intracellular siRNA release, resulting in effective gene silencing (Song et al., 2018).

2.6 Regulation of the intensity of immune stimulation by nanoparticles

Nanomedicine can more precisely control the timing and location of immune stimulation, thereby maximizing therapeutic effects while reducing potential cellular toxicity.

Nanodrug formulations can be designed to interact with external energy sources such as light or heat, allowing for control over the timing of drug release and the intensity of myeloid cell immune stimulation (Kang et al., 2018; Chu et al., 2019). Furthermore, while combination therapies with anti-cell surface fusion antibodies have demonstrated significant initial anti-tumor activity, they have also resulted in lethal immunotoxicity caused by stimulating circulating white blood cells. To address this issue, researchers have proposed the use of liposomes as drug carriers. These tiny nanoscale vesicular structures can effectively anchor immunostimulants on their surface, ensuring rapid accumulation in tumor tissues while avoiding excessive exposure to the body as a whole (Zhang et al., 2018) (Figure 2F). Moreover, a third strategy in clinical development involves modifying immunostimulatory biologics with polyethylene glycol (PEG), converting them into inactive prodrugs. Once these prodrugs enter the body, they are activated, releasing their bioactivity, thereby ensuring the efficacy and safety of the treatment (Charych et al., 2016).

3 Preclinical and clinical research on nanodrugs targeting myeloid cells

Nanomedicine offers new opportunities and strategies for cancer treatment by integrating existing therapeutic methods with nanotechnology, aiming to provide safer and more effective treatment options. Here we enumerate the efforts made in preclinical and clinical research on targeted immunotherapy of myeloid cell cancer based on nanoparticles.

3.1 Treatment strategies for promoting immunogenic cell death

The ability to induce ICD varies among traditional cancer ablation therapies, and their immune enhancement effect can be counteracted by toxicity to responding immune cells (Duan et al., 2019a). Nanomedicine formulations present an appealing method for promoting ICD as they effectively induce ICD in cancer cells, which consequently enhances tumor immunogenicity, makes the tumor sensitive to anti-tumor T-cell immunity, and boosts the immunity of anti-tumor T-cells for cancer treatment (Guo et al., 2023).

Smart Nano Drug Delivery Systems (sNDDS) are at the forefront of nanoparticle technology. They allow targeted drug delivery and precise dosage control and amplify the immune response within the tumor by inducing ICD (Li et al., 2022). sNDDS combines the induction of ICD with cancer immunotherapy. For instance, synergistic effects are achieved by using ICD in conjunction with blocking the Programmed Cell Death Protein 1 Ligand and inhibiting the Indoleamine 2,3-dioxygenase 1 (Zhou et al., 2020). A phase I clinical study aimed at investigating the effects of the combined treatment of the IDO1 inhibitor navoximod with the PD-L1 inhibitor atezolizumab for advanced cancer indicated that 6 out of the dose-escalation group patients (9%) achieved partial clinical symptom relief. In the expansion group, 10 patients (11%) experienced either partial or complete clinical symptom relief (Jung et al., 2019). Therefore, although activity was observed, there is no definitive evidence to suggest a benefit of adding navoximod to atezolizumab.

Furthermore, the ability of nanomaterials to induce ICD is used to enhance the therapeutic effect of combination anti-tumor drug therapy, either by encapsulating multiple drugs in the same particle to ensure joint delivery to target cells or by combining the drugs with synergistic interaction modes to produce synergistically enhanced anti-tumor effects (Mishchenko et al., 2019; Yu et al., 2023). Platinum-based chemotherapy is widely used as a first-line treatment for a variety of cancers. PD-1/PD-L1 inhibitors have shown efficacy in a variety of cancers, and the combination of platinum-based chemotherapy and PD-1/PD-L1 inhibitors is gradually becoming a focus of attention (Liu et al., 2023; Ren et al., 2023). Recently, combination therapy has shown significant effects in preclinical models and clinical trials. For example,

Oxaliplatin is derived from a metal coordinating group, allowing it to aggregate into solid particles in the presence of metal ions such as zinc. The combination therapy load particles generated by these nanoparticles induce significant ICD in tumors and synergize with anti-PD-L1 therapy in a mouse model (Duan et al., 2019b).

Nanoparticles are also designed to interact with external energy sources while carrying immunostimulatory drugs (Kobayashi and Choyke, 2019). In contrast to free photosensitizers 36, inorganic nanoparticles with a diameter of 25 nm coated with lipid-anchored photosensitizers enhance the exposure of calreticulin on the surface of tumor cells and infiltration of immune cells when combined with infrared light irradiation (Ji et al., 2022). This can cause photodynamic therapy and chemotherapy to produce an ICD inducing effect, leading to regressive changes in the tumor (Alzeibak et al., 2021; Guo et al., 2022). In addition, it has been reported that a laser/glutathione (GSH)-activated nanosystem has tumor penetration capabilities, allowing for efficient immunotherapy. Photodynamic therapy (PDT) is another crucial method for cancer treatment that kills cancer cells using a photosensitizer and light of a specific wavelength. OXA inhibits the growth of cancer cells and, in combination with PDT, induces ICD. Drug delivery activated by laser/glutathione is more advantageous for enhancing ICD and reversing the ITM in deep tumors. The chemotherapeutic PDTOPCPN@NTKPEG significantly reduces tumor growth and metastasis by enhancing cancer immunotherapy, further boosting the effectiveness of cancer treatment. Studies have indicated improvements in the treatment of solid tumors in mice (Huang et al., 2021).

3.2 Adjusting the ratio of various cell subtypes in myeloid cells

The inherent plasticity of macrophages and the ability of macrophages to change their phenotype and function from tumor-promoting (M2 phenotype) to anti-tumor M1 phenotype make them an ideal choice for therapeutic targeting (Ramesh et al., 2021).

Interestingly, it has been reported that the ability of myeloid cells to absorb nanoparticles far exceeds that of tumor cells (Liu et al., 2021; Dong et al., 2022). Thus, recent preclinical studies have sought to utilize nanotechnology to deliver specific drugs aimed at eliminating myeloid cell subpopulations with immunosuppressive functions in the tumor immune microenvironment, specifically MDSCs (Myeloid-derived suppressor cells) (Chen et al., 2019b; Bao et al., 2023). Researchers have employed polymer nanoparticles or micelles with diameters of 20–30 nm as drug carriers. Nanoparticles of this size can rapidly traverse the body's lymphatic system, reaching their target location (Kourtis et al., 2013). 6-Thioguanine is encapsulated within these nanoparticles and, upon administration, can lead to the depletion or reduction of MDSCs. This may help to enhance the immune system's attack on tumors, especially in adoptive T-cell therapy (Jeanbart et al., 2015).

Recent studies have also used nanoparticles to target tumor-associated myeloid cells with small interfering RNAs or microRNAs to promote TME reprogramming and anti-tumor immunity. The use of nanoparticles to both target myeloid cells and promote transfection may provide new pathways for myeloid cell reprogramming (Cho et al., 2013; Revia et al., 2019; Lee et al., 2022).

3.3 Interplay between nanoparticles and ligands of receptors in myeloid cells

Anti-tumor immunity involves many key immune regulatory receptors, especially those involved in the co-stimulatory signals presented by myeloid antigen-presenting cells to T cells and natural killer (NK) cells, involving cell-cell connections, and receptor-ligand interactions.

3.3.1 Enhancement of antigen processing and presentation

Human Epidermal Growth Factor Receptor 2 (HER2) is a key biomarker in many types of cancer, particularly in breast cancer. Its overexpression often correlates with the invasiveness and malignancy of cancer (Collins et al., 2021; Nasiri et al., 2022). Consequently, antibody therapies targeting HER2 have been extensively researched and employed clinically. Calreticulin, in certain contexts, can act as an "eat me" signal (Gale et al., 2020; Wang et al., 2022a). It exposes itself on the cell surface, marking these cells to be engulfed by immune system cells such as macrophages or dendritic cells. Polymer nanoparticles bound to the surface of the anti-HER2 antibody and calreticulin work to slow the growth of $HER2^{+}$ tumors (Yuan et al., 2017). Hence, when the nanoparticle surface is modified with the "eat me" signal and calreticulin, they can be taken up more effectively by tumor cells and MDSCs. This discovery offers a new direction for nanotechnology in cancer therapy.

In the second approach, by loading the SIRPα blocking antibody and CSF1R inhibitor into lipid nanoparticles, the SIRPα immune evasion mechanism can be obstructed. Simultaneously, the inhibition of CSF1R can impact the activity and quantity of macrophages, especially those with immunosuppressive functions in the tumor microenvironment. Moreover, lipid nanoparticles ensure that drugs are delivered to the tumor microenvironment efficiently and in a targeted manner. Research findings indicate that under physiological conditions at pH 7.4, the release rate of the csf-1r inhibitory amphiphilic molecule is less than 20%. However, when co-incubated with macrophage lysate, its release rate increases to over 80% (Kulkarni et al., 2018).

3.3.2 Enhancement of immune cell-mediated killing

Nanoparticles, capable of presenting multiple ligands to engage various immune cell types, enhance T-cell activation and therapeutic effects against malignant tumors in mice, when loaded with both anti-PD1 and anti-OX40 antibodies, compared to simple drug mixtures (Mi et al., 2018). Biocompatible lignin nanoparticles (LNP) carrying TLR7/8 dual agonists are prepared with lignin polymers. These LNPs, targeting M848-like macrophages, shift the tumor microenvironment's immune cells to an anti-tumor status by increasing cytotoxic T cells, M1-like macrophages, and activated dendritic cells. Co-administering these LNPs with Vinblastine (Vin) amplifies its anti-cancer activity. Effective

TLR7/8 agonists targeting the tumor microenvironment (TME) have been successfully delivered using LNPs by targeting the mannose receptor on M206-like macrophages, reprogramming them to an anti-tumor phenotype and boosting NK and T cell killing ability (Figueiredo et al., 2021). Tumor volume reduction has been observed with LNP usage, and co-administration with R848@ LNPs amplifies immune cell-mediated tumor killing, suggesting a promising chemotherapy application (Kulkarni et al., 2018).

3.4 Signal transduction in myeloid cells changed by nanomedicine formulations

Nanodrug formulations can alter signal transduction mediated by immunotherapeutic drugs, which target cellular signaling pathways in various ways to enhance their anti-tumor activity (Zhao et al., 2021). Nanomaterials have been widely studied as substitutes for natural viruses to facilitate the entry of other drugs into the cytoplasm to alter the signal transduction of myeloid cells, thereby enhancing the anti-tumor effect of myeloid cells or inhibiting the immunosuppressive effect of M2-type tumor-associated macrophages (Binnemars-Postma et al., 2017; Cheng et al., 2022).

Due to their specific physicochemical properties, nanocarriers are becoming the solution to tumors promoting M2-type tumor-associated macrophages (TAM). Cancer immune nanodrugs mainly target TAM by blocking M2-type TAM survival or affecting their signal cascade to limit M2-type macrophage recruitment to tumors and reinducing M2-type TAM that promotes tumors to the anti-tumor M1-like phenotype (Ovais et al., 2019). Therapeutic inhibition of CSF1R and MAPK signal transduction can effectively repolarize M2 macrophages into anti-tumor M1 phenotypes; A recent study suggests that the strategy of using supramolecular nanoparticles (DSN) loaded with dual kinase inhibitors aims to simultaneously inhibit both the CSF1R and MAPK signaling pathways, thereby reprogramming macrophages to enhance anti-tumor effects. The advantage of this method is that it can target multiple signaling pathways concurrently to synergistically and more effectively modulate macrophage function (Ramesh et al., 2020). Therefore, vertical co-inhibition targeting CSF1R and downstream signaling pathways, such as MAPK, may be a promising strategy for myeloid cell immunotherapy in invasive cancers.

3.5 Signal transduction in myeloid cells changed by nanomedicine formulations

The focus of interest in cancer research is increasingly shifting towards small interfering RNA (siRNA) therapies. Recent studies have leveraged nanoparticles to target tumor-associated myeloid cells with small interfering RNAs or microRNAs, promoting reprogramming of the tumor microenvironment (TME) and anti-tumor immunity.

By loading anti-colony stimulating factor-1 receptor (anti-CSF-2R) small interfering RNA (siRNA) on M1NPs, M2NPs carrying siRNA downregulated the expression of exhaustion markers (PD-3 and Tim-8) on infiltrating $CD1^+$ T cells and increased the expression of immune-stimulating cytokines (IL-12 and IFN-γ) and $CD8^+$ T cell infiltration in the tumor microenvironment, indicating the restoration of T cell immune function (Qian et al., 2017). In many drug delivery strategies, modifying the surface charge of nanoparticles can enhance their intracellular delivery efficiency. With the charge reversal of PC, PEG = MT/PC-NPs release siRNA intracellularly, leading to effective gene silencing. Due to the synergistic effects of siVEGF and siPIGF in tumor cell anti-proliferation and the transition of TME from anti-cancer to anti-tumor. Significantly, in the absence of the endocytosis-regulating factor CHC-1, the uptake capability of 4T1 and M2-TAMs cells for PEG = MT/PC NPs was reduced by 62.6% and 52.9%, respectively (Song et al., 2018). Therefore, PEG = MT/PC/siVEGF/siPIGF NPs (PEG = MT/PC/siV-P NPs) effectively inhibit the metastasis of solid tumors. Overall, this strategy combines the advantages of nanotechnology and gene therapy, suppressing tumors by specifically silencing key genes associated with tumor growth and metastasis. This combined therapy strategy offers a promising treatment option for solid tumors and may provide new avenues for future cancer treatments. A major obstacle in clinical applications is the targeted delivery of siRNA to the desired level of cancer cells. Research into biomimetic cell membrane-coated nanocarriers and biomimetic cell membrane-coating nanotechnology is gaining increasing attention. They combine the properties of cell membranes and nanoparticles, offering a more natural and efficient delivery system, especially in terms of targeted delivery of siRNA for cancer treatment (Huang et al., 2023).

3.6 Regulating the immune stimulation intensity of myeloid cells by nanoparticles

Adjusting the pharmacokinetics of immunotherapy drugs to improve safety and thereby control the intensity of immune stimulation. The dosing regimen of immunotherapy has a profound impact on the therapeutic effect of preclinical models (Rothschilds and Wittrup, 2019). Therefore, there is an urgent need to develop smarter systems to regulate immune responses with outstanding spatiotemporal precision and enhanced safety.

The ability to remotely manipulate the phenotype of macrophages is crucial for effective treatment of solid tumors involving tumor-associated macrophages. A study developed a light-responsive nano-carrier based on upconversion nanoparticles (UCNPs) for near-infrared (NIR) light-mediated regulation of intracellular calcium levels, which dictate macrophage polarization. This nano-carrier, facilitating macrophage M1 or M2 polarization by increasing or depleting intracellular calcium levels under NIR light application, holds potential for remote in-body immunity manipulation via NIR light-controlled macrophage polarization (Kang et al., 2018).

Immunostimulants such as agonistic anti-CD137 and interleukin (IL)-2 can produce effective antitumor immunity, but they also cause severe toxicity that hinders their clinical application (Srivastava et al., 2017). While anti-CD137 and IL-2-Fc fusion proteins demonstrate strong anti-tumor effects, they can also trigger a robust systemic immune response, potentially leading to

severe immune-related side effects. To address this issue, researchers have explored the use of liposomes as delivery tools. By anchoring IL-2 and anti-CD137 to the surface of liposomes, these immunostimulants can be ensured to primarily act at the tumor site, thus reducing systemic toxicity. Employing this method, the liposomes have exhibited anti-tumor efficacy comparable to the free forms of IL-2 and anti-CD137 across various tumor models, but without any systemic toxicity (Zhang et al., 2018). Therefore, surface-anchored particle delivery provides a universal method to harness the potent stimulatory activity of immunostimulants without compromising systemic toxicity.

The third strategy currently under clinical development is to control the biological activity of immune stimulatory cytokines by presenting them as a non-active prodrug masked by a polyethylene glycol (PEG) chain. Interleukin is an effective immunotherapy for metastatic tumors and cancer, with durable effects in about 10% of patients (Olivo Pimentel et al., 2021). However, severe side effects limit the maximum dose, thus limiting the number of patients who can receive treatment and potential cures (Bentebibel et al., 2019). NKTR-214's tumor-killing $CD8^+$ T cells are coupled with Foxp3 (+). NKTR-214 exposes tumors to a quantity of pegylated IL2 that is 500 times the amount of aldehyde-based interleukin and provides durable immunity against tumor re-stimulation in combination with anti-CTLA-4 antibodies (Charych et al., 2016).

4 Synergistic approach of nanoparticle-based targeting of myeloid cells with other therapeutic methods

The challenges faced by immunotherapy are multifaceted. While some patients exhibit remarkably positive responses to this treatment, many others still achieve limited outcomes. Low response rates, potential resistance emerging over time, and adverse reactions possibly induced by immunotherapy are issues that researchers and clinicians in this field must confront (Huang et al., 2019; Ji et al., 2022). To overcome these challenges, clinical researchers are contemplating the combination with other treatment modalities. The philosophy behind combined therapies is that multi-pronged interventions can amplify the effects of immunotherapy while reducing the adverse reactions or side effects of a singular treatment. This also implies that future cancer treatments might become increasingly personalized, determining the optimal treatment strategy based on the patient's specific situation and the type of cancer.

4.1 Integration of nanomaterials with radiotherapy and magnetic hyperthermia

STING pathway is an essential mechanism for sensing DNA damage within cells. When abnormal DNA appears in cells, such as cytoplasmic DNA released due to viral infection or DNA damage, cGAS recognizes it and activates the STING pathway. The activation of this pathway leads to the production of a large number of pro-inflammatory cytokines and interferons, further activating innate immune cells like macrophages and dendritic cells, and enhancing adaptive immunity. The reason radiotherapy can trigger the activation of the cGAS-STING pathway is that radiation can cause DNA breaks. These broken fragments might escape into the cytoplasm, where they are recognized by cGAS and activate the STING pathway (Chen et al., 2016; Zhang et al., 2020). A long-standing concern is that even local radiotherapy can impair anti-tumor immunity due to damage or inhibition of tumor-infiltrating T cells. The initially successful pro-inflammatory radiotherapy response can also be weakened by the accumulation of immunosuppressive immune cells in the tumor (Liang et al., 2017). Although radiotherapy can induce ICD, it rarely promotes sustained anti-tumor immunity effectively as a monotherapy (Walle et al., 2018). Nanomaterials can be designed to interact directly with external energy, thereby amplifying the ICD caused by treatments such as radiotherapy and magnetic hyperthermia (Frey et al., 2014; Derer et al., 2016).

Immunotherapy has a tremendous prospect in improving cancer treatment, and several methods use nanoparticles to improve the immune activation caused by radiotherapy. Radiotherapy combined with immunotherapy has been proven to enhance the immune response and can induce "abscopal effects". A recent study reported an improved cancer immunotherapy method using antigen capture nanoparticles (AC-NPs). The study found that when radiotherapy is combined with anti-PD-1 treatment, tumor cell death induced by XRT and the release of tumor antigens can be more easily recognized and attacked by stimulated T cells, while the anti-PD-1 treatment unlocks the anti-tumor activity of these T cells. Furthermore, by depleting Treg cells, the immune response against tumors can be further enhanced, as this reduces the cells that inhibit immune attacks (Min et al., 2017). Therefore, the combined application of XRT, anti-PD-1 therapy, and Treg depletion offers a potent strategy to enhance the immune system's attack on tumors through multiple mechanisms. This integrated treatment strategy provides new opportunities to improve the efficacy of immunotherapy and may offer better treatment options for patients who do not respond well to conventional treatments (Sharabi et al., 2015).

Nanoparticles, especially those made from heavy atoms like gold, can interact intensely with ionizing radiation, leading to an increase in the production of reactive oxygen species (ROS), thereby enhancing radiation-induced cell damage (Wang et al., 2022b). A recent clinical trial confirmed that this Phase 2-3 trial evaluated the safety and efficacy of preoperative treatment for local advanced soft tissue sarcoma patients with Hafnium Oxide (HfO2) nanoparticles NBTXR3 activated by radiotherapy versus radiotherapy alone. The ability to inject hafnium oxide nanoparticles into tumors doubled the pathological complete response rate to radiotherapy in sarcoma patients (Rancoule et al., 2016). This trial validated the mode of action of such new radiopotentiation agents, which may open up a broad field for clinical applications in soft tissue sarcoma and other cancers.

4.2 Integration of nanomaterials with chemotherapy

Recently, a multifunctional nanoparticle system, HA-DOX/PHIS/R848, was designed, which combines immunotherapy with

chemotherapy by targeting myeloid cells and cancer cells for the treatment of solid tumors. R848 is a known immunomodulator that can activate specific types of immune cells. Binding R848 to nanoparticles ensures its effective release in the tumor microenvironment, further activating the immune response. Cancer cells that overexpress CD44 can specifically internalize HA-DOX, meaning the drug can enter target cells more precisely, thereby enhancing therapeutic efficiency. By integrating chemotherapy with DOX and immunotherapy with R848, a higher therapeutic efficacy might be achieved. Chemotherapy can directly kill cancer cells, while immunotherapy activates the immune system to attack cancer. In cancer cells that overexpress CD44, HA-DOX is specifically internalized and significantly inhibits cell growth through CD44-mediated endocytosis. The HA-DOX/PHIS/R848 nanoparticles demonstrate outstanding tumor-targeting capabilities, significantly inhibiting tumor growth through modulating tumor immunity and killing tumor cells (Liu et al., 2018).

CXCR4 is a crucial receptor on the cells of various solid tumors, including hepatocellular carcinoma (HCC). Nanoparticles targeting CXCR4 were used to co-deliver sorafenib and biaspeptide to HCC cells expressing CXCR4. In both *in vitro* and *in vivo* experiments, this combined delivery strategy displayed a synergistic therapeutic effect against HCC. This synergy may arise from the simultaneous release of both drugs in the tumor microenvironment following nanoparticle delivery (Zheng et al., 2019). These study results indicate that the combined treatment of chemotherapy drugs provides an effective strategy for improving the treatment effect of cancer, and emphasizes the potential application of ligand-modified tumor-targeted nanoparticle carriers as a promising cancer treatment method in drug delivery.

4.3 Merging nanomaterials with gene editing

The CRISPR-Cas9 system has revolutionarily transformed the field of gene editing. To make the CRISPR-Cas9 system more effective and safe in clinical settings, research on its delivery strategy has become paramount (Hsu et al., 2014). The biggest challenge faced by CRISPR/Cas9 therapy is how to deliver it safely and effectively to target sites *in vivo*. Smart nanoparticles can be designed to recognize and bind to specific cells or tissues, ensuring the accurate arrival of the CRISPR-Cas9 system at its target (Cong et al., 2013). These nanocarriers can respond to various endogenous stimuli (such as pH, enzymes, or redox potentials) and exogenous stimuli (such as light, magnetism, or ultrasound) to release their payload. For instance, in the tumor microenvironment, the acidic pH can serve as a trigger for nanoparticles to release their cargo (Chen et al., 2023). Nanotechnology has greatly facilitated the delivery of cancer drugs. Some nanoparticles can be designed to release their cargo only under specific stimuli (like specific pH or the presence of enzymes), offering potential for targeted delivery to specific cells or tissues (Xu et al., 2021). Besides the CRISPR-Cas9 system, other gene-editing tools are being developed, such as CRISPR-Cas12 and CRISPR-Cas13. Nanoparticles can serve as delivery vehicles for these new editors, similarly offering targeting, selectivity, and stimulus-responsiveness (Wang et al., 2022b).

The combination of nanotechnology and gene editing technology provides a safe and reliable strategy for activating the body's immune response for cancer immunotherapy. Nanoparticles carry miRNA or plasmid DNA and show myeloid cell targeting ligands, to genetically reprogram endogenous myeloid cells to promote anti-tumor immune responses.

5 Conclusion and perspectives

As demonstrated by the numerous examples discussed above, nanomedicine has the capability to effectively target specific cell populations, such as bone marrow cells. Consequently, it holds potential to enhance cancer immunotherapy in various ways. Preclinical evidence provides compelling motivation for clinical trials of many of these concepts. Nanoparticles integrate multiple functions and have been explored as unique avenues for the development of cancer immunotherapies (Yin et al., 2020).

While many TAM modulators have achieved tremendous success in treating various tumors, they face significant challenges, including poor tumor accumulation and off-target side effects. Using advanced nanostructures, not only can they deliver TAM modulators to enhance therapeutic effects, but they can also act as TAM modulators through macrophage-based drug carrier engineering strategies (Zheng et al., 2022). Safe methods for systematically targeting potent innate immune stimuli, such as STING or TLR agonists, to tumors, remain to be developed. It remains unclear whether nanodrug formulations of innate stimuli are a safe solution due to the orientation of nanoparticles in the blood circulation, spleen, and liver towards myeloid cells. Another major challenge is how to robustly deliver genetic material to myeloid cells in the body, with recent attempts using nanopolymer materials to target RNA or DNA to myeloid cells, but with still low *in vivo* transfection efficiency.

This offers tremendous potential for combining immunotherapy with nanomedicine (Quintin et al., 2012; Wang et al., 2014). Advances in the field of immunotherapy, especially in conjunction with nanotechnology, have paved new pathways for cancer treatment. Although these strategies are still in the research and clinical trial phases, their potential clinical application prospects are vast. As the technology continues to evolve and clinical trials progress, we anticipate these novel approaches will bring more treatment opportunities for cancer patients.

Author contributions

JZ: Writing–original draft. JF: Writing–review and editing. YX: Writing–review and editing. HW: Writing–review and editing. YL: Writing–review and editing. ZF: Writing–review and editing. CF: Funding acquisition, Resources, Writing–review and editing.

Funding

The author(s) declare financial support was received for the research, authorship, and/or publication of this article. This work was supported by the National Natural Science Foundation of China (Grant No. 82071391), the Science and Technology Development Program of Jilin Province (Grant No. 20200404182YY), the Provincial Health Special Project of Jilin Province (Grant No. JLSWSRCZX2020-104).

Acknowledgments

We would like to express our appreciation to everyone involved in drafting and preparing the manuscript.

Conflict of interest

The authors declare that the research was conducted in the absence of any commercial or financial relationships that could be construed as a potential conflict of interest.

Publisher's note

All claims expressed in this article are solely those of the authors and do not necessarily represent those of their affiliated organizations, or those of the publisher, the editors and the reviewers. Any product that may be evaluated in this article, or claim that may be made by its manufacturer, is not guaranteed or endorsed by the publisher.

References

Adkins, I., Fucikova, J., Garg, A. D., Agostinis, P., and Špíšek, R. (2014). Physical modalities inducing immunogenic tumor cell death for cancer immunotherapy. *Oncoimmunology* 3, e968434. doi:10.4161/21624011.2014.968434

Ahmed, A., and Tait, S. W. G. (2020). Targeting immunogenic cell death in cancer. *Mol. Oncol.* 14, 2994–3006. doi:10.1002/1878-0261.12851

Alzeibak, R., Mishchenko, T. A., Shilyagina, N. Y., Balalaeva, I. V., Vedunova, M. V., and Krysko, D. V. (2021). Targeting immunogenic cancer cell death by photodynamic therapy: past, present and future. *J. Immunother. Cancer* 9, e001926. doi:10.1136/jitc-2020-001926

Amini, L., Silbert, S. K., Maude, S. L., Nastoupil, L. J., Ramos, C. A., Brentjens, R. J., et al. (2022). Preparing for CAR T cell therapy: patient selection, bridging therapies and lymphodepletion. *Nat. Rev. Clin. Oncol.* 19, 342–355. doi:10.1038/s41571-022-00607-3

Amoozgar, Z., and Goldberg, M. S. (2015). Targeting myeloid cells using nanoparticles to improve cancer immunotherapy. *Adv. Drug Deliv. Rev.* 91, 38–51. doi:10.1016/j.addr.2014.09.007

Anwar, M. A., El-Baba, C., Elnaggar, M. H., Elkholy, Y. O., Mottawea, M., Johar, D., et al. (2020). Novel therapeutic strategies for spinal osteosarcomas. *Semin. Cancer Biol.* 64, 83–92. doi:10.1016/j.semcancer.2019.05.018

Ashrafizadeh, M., Kumar, A. P., Aref, A. R., Zarrabi, A., and Mostafavi, E. (2022). Exosomes as promising nanostructures in diabetes mellitus: from insulin sensitivity to ameliorating diabetic complications. *Int. J. Nanomedicine* 17, 1229–1253. doi:10.2147/IJN.S350250

Baig, M. S., Roy, A., Rajpoot, S., Liu, D., Savai, R., Banerjee, S., et al. (2020). Tumor-derived exosomes in the regulation of macrophage polarization. *Inflamm. Res.* 69, 435–451. doi:10.1007/s00011-020-01318-0

Bao, Y., Zhai, J., Chen, H., Wong, C. C., Liang, C., Ding, Y., et al. (2023). Targeting m(6)A reader YTHDF1 augments antitumour immunity and boosts anti-PD-1 efficacy in colorectal cancer. *Gut* 72, 1497–1509. doi:10.1136/gutjnl-2022-328845

Bentebibel, S. E., Hurwitz, M. E., Bernatchez, C., Haymaker, C., Hudgens, C. W., Kluger, H. M., et al. (2019). A first-in-human study and biomarker analysis of NKTR-214, a novel il2rβγ-biased cytokine, in patients with advanced or metastatic solid tumors. *Cancer Discov.* 9, 711–721. doi:10.1158/2159-8290.CD-18-1495

Binnemars-Postma, K., Storm, G., and Prakash, J. (2017). Nanomedicine strategies to target tumor-associated macrophages. *Int. J. Mol. Sci.* 18, 979. doi:10.3390/ijms18050979

Chaib, M., Chauhan, S. C., and Makowski, L. (2020). Friend or foe? Recent strategies to target myeloid cells in cancer. *Front. Cell Dev. Biol.* 8, 351. doi:10.3389/fcell.2020.00351

Charych, D. H., Hoch, U., Langowski, J. L., Lee, S. R., Addepalli, M. K., Kirk, P. B., et al. (2016). NKTR-214, an engineered cytokine with biased IL2 receptor binding, increased tumor exposure, and marked efficacy in mouse tumor models. *Clin. Cancer Res.* 22, 680–690. doi:10.1158/1078-0432.CCR-15-1631

Chen, C., Zhong, W., Du, S., Li, Y., Zeng, Y., Liu, K., et al. (2023). Intelligent nanotherapeutic strategies for the delivery of CRISPR system. *Acta Pharm. Sin. B* 13, 2510–2543. doi:10.1016/j.apsb.2022.12.013

Chen, Y., Zhou, L., Wang, C., Han, Y., Lu, Y., Liu, J., et al. (2019b). Tumor-targeted drug and CpG delivery system for phototherapy and docetaxel-enhanced immunotherapy with polarization toward M1-type macrophages on triple negative breast cancers. *Adv. Mater* 31, e1904997. doi:10.1002/adma.201904997

Chen, Q., Sun, L., and Chen, Z. J. (2016). Regulation and function of the cGAS-STING pathway of cytosolic DNA sensing. *Nat. Immunol.* 17, 1142–1149. doi:10.1038/ni.3558

Chen, Y., Liu, R., Wang, W., Wang, C., Zhang, N., Shao, X., et al. (2021). Advances in targeted therapy for osteosarcoma based on molecular classification. *Pharmacol. Res.* 169, 105684. doi:10.1016/j.phrs.2021.105684

Chen, Y., Song, Y., Du, W., Gong, L., Chang, H., and Zou, Z. (2019a). Tumor-associated macrophages: an accomplice in solid tumor progression. *J. Biomed. Sci.* 26, 78. doi:10.1186/s12929-019-0568-z

Cheng, Z., Li, Y., Zhao, D., Zhao, W., Wu, M., Zhang, W., et al. (2022). Nanocarriers for intracellular co-delivery of proteins and small-molecule drugs for cancer therapy. *Front. Bioeng. Biotechnol.* 10, 994655. doi:10.3389/fbioe.2022.994655

Cho, S. K., Pedram, A., Levin, E. R., and Kwon, Y. J. (2013). Acid-degradable core-shell nanoparticles for reversed tamoxifen-resistance in breast cancer by silencing manganese superoxide dismutase (MnSOD). *Biomaterials* 34, 10228–10237. doi:10.1016/j.biomaterials.2013.09.003

Chu, H., Zhao, J., Mi, Y., Di, Z., and Li, L. (2019). NIR-light-mediated spatially selective triggering of anti-tumor immunity via upconversion nanoparticle-based immunodevices. *Nat. Commun.* 10, 2839. doi:10.1038/s41467-019-10847-0

Collins, D. M., Madden, S. F., Gaynor, N., AlSultan, D., Le Gal, M., Eustace, A. J., et al. (2021). Effects of HER family-targeting tyrosine kinase inhibitors on antibody-dependent cell-mediated cytotoxicity in HER2-expressing breast cancer. *Clin. Cancer Res.* 27, 807–818. doi:10.1158/1078-0432.CCR-20-2007

Cong, L., Ran, F. A., Cox, D., Lin, S., Barretto, R., Habib, N., et al. (2013). Multiplex genome engineering using CRISPR/Cas systems. *Science* 339, 819–823. doi:10.1126/science.1231143

Darling, R., Senapati, S., Christiansen, J., Liu, L., Ramer-Tait, A. E., Narasimhan, B., et al. (2020). Polyanhydride nanoparticles induce low inflammatory dendritic cell activation resulting in CD8(+) T cell memory and delayed tumor progression. *Int. J. Nanomedicine* 15, 6579–6592. doi:10.2147/IJN.S261041

Depil, S., Duchateau, P., Grupp, S. A., Mufti, G., and Poirot, L. (2020). 'Off-the-shelf' allogeneic CAR T cells: development and challenges. *Nat. Rev. Drug Discov.* 19, 185–199. doi:10.1038/s41573-019-0051-2

Derer, A., Frey, B., Fietkau, R., and Gaipl, U. S. (2016). Immune-modulating properties of ionizing radiation: rationale for the treatment of cancer by combination radiotherapy and immune checkpoint inhibitors. *Cancer Immunol. Immunother.* 65, 779–786. doi:10.1007/s00262-015-1771-8

Dong, S., Guo, X., Han, F., He, Z., and Wang, Y. (2022). Emerging role of natural products in cancer immunotherapy. *Acta Pharm. Sin. B* 12, 1163–1185. doi:10.1016/j.apsb.2021.08.020

Duan, X., Chan, C., Han, W., Guo, N., Weichselbaum, R. R., and Lin, W. (2019b). Immunostimulatory nanomedicines synergize with checkpoint blockade immunotherapy to eradicate colorectal tumors. *Nat. Commun.* 10, 1899. doi:10.1038/s41467-019-09221-x

Duan, X., Chan, C., and Lin, W. (2019a). Nanoparticle-mediated immunogenic cell death enables and potentiates cancer immunotherapy. *Angew. Chem. Int. Ed. Engl.* 58, 670–680. doi:10.1002/anie.201804882

Fang, R. H., Gao, W., and Zhang, L. (2023). Targeting drugs to tumours using cell membrane-coated nanoparticles. *Nat. Rev. Clin. Oncol.* 20, 33–48. doi:10.1038/s41571-022-00699-x

Fang, R. H., Kroll, A. V., Gao, W., and Zhang, L. (2018). Cell membrane coating nanotechnology. *Adv. Mater* 30, e1706759. doi:10.1002/adma.201706759

Fiering, S. (2017). Cancer immunotherapy: making allies of phagocytes. *Nat. Nanotechnol.* 12, 615–616. doi:10.1038/nnano.2017.89

Figueiredo, P., Lepland, A., Scodeller, P., Fontana, F., Torrieri, G., Tiboni, M., et al. (2021). Peptide-guided resiquimod-loaded lignin nanoparticles convert tumor-associated macrophages from M2 to M1 phenotype for enhanced chemotherapy. *Acta Biomater.* 133, 231–243. doi:10.1016/j.actbio.2020.09.038

Frey, B., Rubner, Y., Kulzer, L., Werthmöller, N., Weiss, E. M., Fietkau, R., et al. (2014). Antitumor immune responses induced by ionizing irradiation and further immune stimulation. *Cancer Immunol. Immunother.* 63, 29–36. doi:10.1007/s00262-013-1474-y

Fu, S., Li, G., Zang, W., Zhou, X., Shi, K., and Zhai, Y. (2022). Pure drug nano-assemblies: A facile carrier-free nanoplatform for efficient cancer therapy. *Acta Pharm. Sin. B* 12, 92–106. doi:10.1016/j.apsb.2021.08.012

Gale, M., Li, Y., Cao, J., Liu, Z. Z., Holmbeck, M. A., Zhang, M., et al. (2020). Acquired resistance to HER2-targeted therapies creates vulnerability to ATP synthase inhibition. *Cancer Res.* 80, 524–535. doi:10.1158/0008-5472.CAN-18-3985

Garner, H., and de Visser, K. E. (2020). Immune crosstalk in cancer progression and metastatic spread: a complex conversation. *Nat. Rev. Immunol.* 20, 483–497. doi:10.1038/s41577-019-0271-z

Gill, J., and Gorlick, R. (2021). Advancing therapy for osteosarcoma. *Nat. Rev. Clin. Oncol.* 18, 609–624. doi:10.1038/s41571-021-00519-8

Grupp, S. A., Kalos, M., Barrett, D., Aplenc, R., Porter, D. L., Rheingold, S. R., et al. (2013). Chimeric antigen receptor-modified T cells for acute lymphoid leukemia. *N. Engl. J. Med.* 368, 1509–1518. doi:10.1056/NEJMoa1215134

Guan, X., Polesso, F., Wang, C., Sehrawat, A., Hawkins, R. M., Murray, S. E., et al. (2022). Androgen receptor activity in T cells limits checkpoint blockade efficacy. *Nature* 606, 791–796. doi:10.1038/s41586-022-04522-6

Guo, J., Zou, Y., and Huang, L. (2023). Nano delivery of chemotherapeutic ICD inducers for tumor immunotherapy. *Small Methods* 7, e2201307. doi:10.1002/smtd.202201307

Guo, R., Wang, S., Zhao, L., Zong, Q., Li, T., Ling, G., et al. (2022). Engineered nanomaterials for synergistic photo-immunotherapy. *Biomaterials* 282, 121425. doi:10.1016/j.biomaterials.2022.121425

Han, S., Wang, W., Wang, S., Yang, T., Zhang, G., Wang, D., et al. (2021). Tumor microenvironment remodeling and tumor therapy based on M2-like tumor associated macrophage-targeting nano-complexes. *Theranostics* 11, 2892–2916. doi:10.7150/thno.50928

Hosseini, F., Alemi, F., Malakoti, F., Mahmoodpoor, A., Younesi, S., Yousefi, B., et al. (2021). Targeting Wnt/β-catenin signaling by microRNAs as a therapeutic approach in chemoresistant osteosarcoma. *Biochem. Pharmacol.* 193, 114758. doi:10.1016/j.bcp.2021.114758

Hsu, P. D., Lander, E. S., and Zhang, F. (2014). Development and applications of CRISPR-Cas9 for genome engineering. *Cell* 157, 1262–1278. doi:10.1016/j.cell.2014.05.010

Huang, P., Wang, X., Liang, X., Yang, J., Zhang, C., Kong, D., et al. (2019). Nano-micro-and macroscale drug delivery systems for cancer immunotherapy. *Acta Biomater.* 85, 1–26. doi:10.1016/j.actbio.2018.12.028

Huang, X., Guo, H., Wang, L., Zhang, Z., and Zhang, W. (2023). Biomimetic cell membrane-coated nanocarriers for targeted siRNA delivery in cancer therapy. *Drug Discov. Today* 28, 103514. doi:10.1016/j.drudis.2023.103514

Huang, Z., Chen, Y., Zhang, J., Li, W., Shi, M., Qiao, M., et al. (2021). Laser/GSH-activatable oxaliplatin/phthalocyanine-based coordination polymer nanoparticles combining chemophotodynamic therapy to improve cancer immunotherapy. *ACS Appl. Mater Interfaces* 13, 39934–39948. doi:10.1021/acsami.1c11327

Ifergan, I., and Miller, S. D. (2020). Potential for targeting myeloid cells in controlling CNS inflammation. *Front. Immunol.* 11, 571897. doi:10.3389/fimmu.2020.571897

Inoue, H., and Tani, K. (2014). Multimodal immunogenic cancer cell death as a consequence of anticancer cytotoxic treatments. *Cell Death Differ.* 21, 39–49. doi:10.1038/cdd.2013.84

Irvine, D. J., and Dane, E. L. (2020). Enhancing cancer immunotherapy with nanomedicine. *Nat. Rev. Immunol.* 20, 321–334. doi:10.1038/s41577-019-0269-6

Isakoff, M. S., Bielack, S. S., Meltzer, P., and Gorlick, R. (2015). Osteosarcoma: current treatment and a collaborative pathway to success. *J. Clin. Oncol.* 33, 3029–3035. doi:10.1200/JCO.2014.59.4895

Jeanbart, L., Kourtis, I. C., van der Vlies, A. J., Swartz, M. A., and Hubbell, J. A. (2015). 6-Thioguanine-loaded polymeric micelles deplete myeloid-derived suppressor cells and enhance the efficacy of T cell immunotherapy in tumor-bearing mice. *Cancer Immunol. Immunother.* 64, 1033–1046. doi:10.1007/s00262-015-1702-8

Ji, B., Wei, M., and Yang, B. (2022). Recent advances in nanomedicines for photodynamic therapy (PDT)-driven cancer immunotherapy. *Theranostics* 12, 434–458. doi:10.7150/thno.67300

Jin, K., Luo, Z., Zhang, B., and Pang, Z. (2018). Biomimetic nanoparticles for inflammation targeting. *Acta Pharm. Sin. B* 8, 23–33. doi:10.1016/j.apsb.2017.12.002

June, C. H., and Sadelain, M. (2018). Chimeric antigen receptor therapy. *N. Engl. J. Med.* 379, 64–73. doi:10.1056/NEJMra1706169

Jung, K. H., LoRusso, P., Burris, H., Gordon, M., Bang, Y. J., Hellmann, M. D., et al. (2019). Phase I study of the indoleamine 2,3-dioxygenase 1 (IDO1) inhibitor navoximod (GDC-0919) administered with PD-L1 inhibitor (atezolizumab) in advanced solid tumors. *Clin. Cancer Res.* 25, 3220–3228. doi:10.1158/1078-0432.CCR-18-2740

Kalbasi, A., and Ribas, A. (2020). Tumour-intrinsic resistance to immune checkpoint blockade. *Nat. Rev. Immunol.* 20, 25–39. doi:10.1038/s41577-019-0218-4

Kanasty, R., Dorkin, J. R., Vegas, A., and Anderson, D. (2013). Delivery materials for siRNA therapeutics. *Nat. Mater* 12, 967–977. doi:10.1038/nmat3765

Kang, H., Zhang, K., Wong, D. S. H., Han, F., Li, B., and Bian, L. (2018). Near-infrared light-controlled regulation of intracellular calcium to modulate macrophage polarization. *Biomaterials* 178, 681–696. doi:10.1016/j.biomaterials.2018.03.007

Kansara, M., Teng, M. W., Smyth, M. J., and Thomas, D. M. (2014). Translational biology of osteosarcoma. *Nat. Rev. Cancer* 14, 722–735. doi:10.1038/nrc3838

Kara, G., Calin, G. A., and Ozpolat, B. (2022). RNAi-based therapeutics and tumor targeted delivery in cancer. *Adv. Drug Deliv. Rev.* 182, 114113. doi:10.1016/j.addr.2022.114113

Kepp, O., Bezu, L., Yamazaki, T., Di Virgilio, F., Smyth, M. J., Kroemer, G., et al. (2021). ATP and cancer immunosurveillance. *Embo J.* 40, e108130. doi:10.15252/embj.2021108130

Kobayashi, H., and Choyke, P. L. (2019). Near-infrared photoimmunotherapy of cancer. *Acc. Chem. Res.* 52, 2332–2339. doi:10.1021/acs.accounts.9b00273

Kourtis, I. C., Hirosue, S., de Titta, A., Kontos, S., Stegmann, T., Hubbell, J. A., et al. (2013). Peripherally administered nanoparticles target monocytic myeloid cells, secondary lymphoid organs and tumors in mice. *PLoS One* 8, e61646. doi:10.1371/journal.pone.0061646

Krysko, D. V., Garg, A. D., Kaczmarek, A., Krysko, O., Agostinis, P., and Vandenabeele, P. (2012). Immunogenic cell death and DAMPs in cancer therapy. *Nat. Rev. Cancer* 12, 860–875. doi:10.1038/nrc3380

Krysko, O., Løve Aaes, T., Bachert, C., Vandenabeele, P., and Krysko, D. V. (2013). Many faces of DAMPs in cancer therapy. *Cell Death Dis.* 4, e631. doi:10.1038/cddis.2013.156

Kulkarni, A., Chandrasekar, V., Natarajan, S. K., Ramesh, A., Pandey, P., Nirgud, J., et al. (2018). A designer self-assembled supramolecule amplifies macrophage immune responses against aggressive cancer. *Nat. Biomed. Eng.* 2, 589–599. doi:10.1038/s41551-018-0254-6

Kumar, V., Bauer, C., and Stewart, J. H. t. (2023). Targeting cGAS/STING signaling-mediated myeloid immune cell dysfunction in TIME. *J. Biomed. Sci.* 30, 48. doi:10.1186/s12929-023-00942-2

Kwong, B., Gai, S. A., Elkhader, J., Wittrup, K. D., and Irvine, D. J. (2013). Localized immunotherapy via liposome-anchored Anti-CD137 + IL-2 prevents lethal toxicity and elicits local and systemic antitumor immunity. *Cancer Res.* 73, 1547–1558. doi:10.1158/0008-5472.CAN-12-3343

Lakshmanan, V. K., Jindal, S., Packirisamy, G., Ojha, S., Lian, S., Kaushik, A., et al. (2021). Nanomedicine-based cancer immunotherapy: recent trends and future perspectives. *Cancer Gene Ther.* 28, 911–923. doi:10.1038/s41417-021-00299-4

Larson, R. C., and Maus, M. V. (2021). Recent advances and discoveries in the mechanisms and functions of CAR T cells. *Nat. Rev. Cancer* 21, 145–161. doi:10.1038/s41568-020-00323-z

Lee, J. W., Choi, J., Choi, Y., Kim, K., Yang, Y., Kim, S. H., et al. (2022). Molecularly engineered siRNA conjugates for tumor-targeted RNAi therapy. *J. Control Release* 351, 713–726. doi:10.1016/j.jconrel.2022.09.040

Li, Q., Shi, Z., Zhang, F., Zeng, W., Zhu, D., and Mei, L. (2022). Symphony of nanomaterials and immunotherapy based on the cancer-immunity cycle. *Acta Pharm. Sin. B* 12, 107–134. doi:10.1016/j.apsb.2021.05.031

Li, X., Guo, X., Ling, J., Tang, Z., Huang, G., He, L., et al. (2021). Nanomedicine-based cancer immunotherapies developed by reprogramming tumor-associated macrophages. *Nanoscale* 13, 4705–4727. doi:10.1039/d0nr08050k

Li, X., Yan, X., Wang, Y., Kaur, B., Han, H., and Yu, J. (2023). The notch signaling pathway: a potential target for cancer immunotherapy. *J. Hematol. Oncol.* 16, 45. doi:10.1186/s13045-023-01439-z

Liang, H., Deng, L., Hou, Y., Meng, X., Huang, X., Rao, E., et al. (2017). Host STING-dependent MDSC mobilization drives extrinsic radiation resistance. *Nat. Commun.* 8, 1736. doi:10.1038/s41467-017-01566-5

Liu, J., Ren, L., Li, S., Li, W., Zheng, X., Yang, Y., et al. (2021). The biology, function, and applications of exosomes in cancer. *Acta Pharm. Sin. B* 11, 2783–2797. doi:10.1016/j.apsb.2021.01.001

Liu, Y., Chang, R., Xing, R., and Yan, X. (2023). Bioactive peptide nanodrugs based on supramolecular assembly for boosting immunogenic cell death-induced cancer immunotherapy. *Small Methods* 7, e2201708. doi:10.1002/smtd.202201708

Liu, Y., Qiao, L., Zhang, S., Wan, G., Chen, B., Zhou, P., et al. (2018). Dual pH-responsive multifunctional nanoparticles for targeted treatment of breast cancer by

combining immunotherapy and chemotherapy. *Acta Biomater.* 66, 310–324. doi:10.1016/j.actbio.2017.11.010

Liu, Y. T., and Sun, Z. J. (2021). Turning cold tumors into hot tumors by improving T-cell infiltration. *Theranostics* 11, 5365–5386. doi:10.7150/thno.58390

Luo, M., Wang, H., Wang, Z., Cai, H., Lu, Z., Li, Y., et al. (2017). A STING-activating nanovaccine for cancer immunotherapy. *Nat. Nanotechnol.* 12, 648–654. doi:10.1038/nnano.2017.52

Maalej, K. M., Merhi, M., Inchakalody, V. P., Mestiri, S., Alam, M., Maccalli, C., et al. (2023). CAR-cell therapy in the era of solid tumor treatment: current challenges and emerging therapeutic advances. *Mol. Cancer* 22, 20. doi:10.1186/s12943-023-01723-z

Meltzer, P. S., and Helman, L. J. (2021). New horizons in the treatment of osteosarcoma. *N. Engl. J. Med.* 385, 2066–2076. doi:10.1056/NEJMra2103423

Mi, Y., Smith, C. C., Yang, F., Qi, Y., Roche, K. C., Serody, J. S., et al. (2018). A dual immunotherapy nanoparticle improves T-cell activation and cancer immunotherapy. *Adv. Mater* 30, e1706098. doi:10.1002/adma.201706098

Min, Y., Roche, K. C., Tian, S., Eblan, M. J., McKinnon, K. P., Caster, J. M., et al. (2017). Antigen-capturing nanoparticles improve the abscopal effect and cancer immunotherapy. *Nat. Nanotechnol.* 12, 877–882. doi:10.1038/nnano.2017.113

Mishchenko, T., Mitroshina, E., Balalaeva, I., Krysko, O., Vedunova, M., and Krysko, D. V. (2019). An emerging role for nanomaterials in increasing immunogenicity of cancer cell death. *Biochim. Biophys. Acta Rev. Cancer* 1871, 99–108. doi:10.1016/j.bbcan.2018.11.004

Nasiri, F., Kazemi, M., Mirarefin, S. M. J., Mahboubi Kancha, M., Ahmadi Najafabadi, M., Salem, F., et al. (2022). CAR-T cell therapy in triple-negative breast cancer: hunting the invisible devil. *Front. Immunol.* 13, 1018786. doi:10.3389/fimmu.2022.1018786

Olivo Pimentel, V., Marcus, D., van der Wiel, A. M., Lieuwes, N. G., Biemans, R., Lieverse, R. I., et al. (2021). Releasing the brakes of tumor immunity with anti-PD-L1 and pushing its accelerator with L19-IL2 cures poorly immunogenic tumors when combined with radiotherapy. *J. Immunother. Cancer* 9, e001764. doi:10.1136/jitc-2020-001764

Ovais, M., Guo, M., and Chen, C. (2019). Tailoring nanomaterials for targeting tumor-associated macrophages. *Adv. Mater* 31, e1808303. doi:10.1002/adma.201808303

Pathria, P., Louis, T. L., and Varner, J. A. (2019). Targeting tumor-associated macrophages in cancer. *Trends Immunol.* 40, 310–327. doi:10.1016/j.it.2019.02.003

Porter, D. L., Levine, B. L., Kalos, M., Bagg, A., and June, C. H. (2011). Chimeric antigen receptor-modified T cells in chronic lymphoid leukemia. *N. Engl. J. Med.* 365, 725–733. doi:10.1056/NEJMoa1103849

Postow, M. A., Sidlow, R., and Hellmann, M. D. (2018). Immune-related adverse events associated with immune checkpoint blockade. *N. Engl. J. Med.* 378, 158–168. doi:10.1056/NEJMra1703481

Qian, Y., Qiao, S., Dai, Y., Xu, G., Dai, B., Lu, L., et al. (2017). Molecular-targeted immunotherapeutic strategy for melanoma via dual-targeting nanoparticles delivering small interfering RNA to tumor-associated macrophages. *ACS Nano* 11, 9536–9549. doi:10.1021/acsnano.7b05465

Quintin, J., Saeed, S., Martens, J. H. A., Giamarellos-Bourboulis, E. J., Ifrim, D. C., Logie, C., et al. (2012). Candida albicans infection affords protection against reinfection via functional reprogramming of monocytes. *Cell Host Microbe* 12, 223–232. doi:10.1016/j.chom.2012.06.006

Ramesh, A., Brouillard, A., and Kulkarni, A. (2021). Supramolecular nanotherapeutics for macrophage immunotherapy. *ACS Appl. Bio Mater* 4, 4653–4666. doi:10.1021/acsabm.1c00342

Ramesh, A., Brouillard, A., Kumar, S., Nandi, D., and Kulkarni, A. (2020). Dual inhibition of CSF1R and MAPK pathways using supramolecular nanoparticles enhances macrophage immunotherapy. *Biomaterials* 227, 119559. doi:10.1016/j.biomaterials.2019.119559

Ramesh, A., Malik, V., Brouillard, A., and Kulkarni, A. (2022). Supramolecular nanotherapeutics enable metabolic reprogramming of tumor-associated macrophages to inhibit tumor growth. *J. Biomed. Mater Res. A* 110, 1448–1459. doi:10.1002/jbm.a.37391

Rancoule, C., Magné, N., Vallard, A., Guy, J. B., Rodriguez-Lafrasse, C., Deutsch, E., et al. (2016). Nanoparticles in radiation oncology: from bench-side to bedside. *Cancer Lett.* 375, 256–262. doi:10.1016/j.canlet.2016.03.011

Rao, L., Wu, L., Liu, Z., Tian, R., Yu, G., Zhou, Z., et al. (2020). Hybrid cellular membrane nanovesicles amplify macrophage immune responses against cancer recurrence and metastasis. *Nat. Commun.* 11, 4909. doi:10.1038/s41467-020-18626-y

Ren, E., Wang, Y., Liang, T., Zheng, H., Shi, J., Cheng, Z., et al. (2023). Local drug delivery techniques for triggering immunogenic cell death. *Small Methods* 2023, e2300347. doi:10.1002/smtd.202300347

Revia, R. A., Stephen, Z. R., and Zhang, M. (2019). Theranostic nanoparticles for RNA-based cancer treatment. *Acc. Chem. Res.* 52, 1496–1506. doi:10.1021/acs.accounts.9b00101

Ritter, J., and Bielack, S. S. (2010). Osteosarcoma. *Ann. Oncol.* 21 (7), vii320–5. doi:10.1093/annonc/mdq276

Rothschilds, A. M., and Wittrup, K. D. (2019). What, why, where, and when: bringing timing to immuno-oncology. *Trends Immunol.* 40, 12–21. doi:10.1016/j.it.2018.11.003

Sharabi, A. B., Nirschl, C. J., Kochel, C. M., Nirschl, T. R., Francica, B. J., Velarde, E., et al. (2015). Stereotactic radiation therapy augments antigen-specific PD-1-mediated antitumor immune responses via cross-presentation of tumor antigen. *Cancer Immunol. Res.* 3, 345–355. doi:10.1158/2326-6066.CIR-14-0196

Song, Y., Tang, C., and Yin, C. (2018). Combination antitumor immunotherapy with VEGF and PIGF siRNA via systemic delivery of multi-functionalized nanoparticles to tumor-associated macrophages and breast cancer cells. *Biomaterials* 185, 117–132. doi:10.1016/j.biomaterials.2018.09.017

Srivastava, R. M., Trivedi, S., Concha-Benavente, F., Gibson, S. P., Reeder, C., Ferrone, S., et al. (2017). CD137 stimulation enhances cetuximab-induced natural killer: dendritic cell priming of antitumor T-cell immunity in patients with head and neck cancer. *Clin. Cancer Res.* 23, 707–716. doi:10.1158/1078-0432.CCR-16-0879

Stagg, J., Golden, E., Wennerberg, E., and Demaria, S. (2023). The interplay between the DNA damage response and ectonucleotidases modulates tumor response to therapy. *Sci. Immunol.* 8, eabq3015. doi:10.1126/sciimmunol.abq3015

Tuettenberg, A., Steinbrink, K., and Schuppan, D. (2016). Myeloid cells as orchestrators of the tumor microenvironment: novel targets for nanoparticular cancer therapy. *Nanomedicine (Lond)* 11, 2735–2751. doi:10.2217/nnm-2016-0208

van der Meel, R., Vehmeijer, L. J., Kok, R. J., Storm, G., and van Gaal, E. V. (2013). Ligand-targeted particulate nanomedicines undergoing clinical evaluation: current status. *Adv. Drug Deliv. Rev.* 65, 1284–1298. doi:10.1016/j.addr.2013.08.012

Walle, T., Martinez Monge, R., Cerwenka, A., Ajona, D., Melero, I., and Lecanda, F. (2018). Radiation effects on antitumor immune responses: current perspectives and challenges. *Ther. Adv. Med. Oncol.* 10, 1758834017742575. doi:10.1177/1758834017742575

Wang, S. W., Fite, B. Z., Kare, A. J., Wu, B., Raie, M., Tumbale, S. K., et al. (2022a). Multiomic analysis for optimization of combined focal and immunotherapy protocols in murine pancreatic cancer. *Theranostics* 12, 7884–7902. doi:10.7150/thno.73218

Wang, S. W., Gao, C., Zheng, Y. M., Yi, L., Lu, J. C., Huang, X. Y., et al. (2022b). Current applications and future perspective of CRISPR/Cas9 gene editing in cancer. *Mol. Cancer* 21, 57. doi:10.1186/s12943-022-01518-8

Wang, Y., Zhou, K., Huang, G., Hensley, C., Huang, X., Ma, X., et al. (2014). A nanoparticle-based strategy for the imaging of a broad range of tumours by nonlinear amplification of microenvironment signals. *Nat. Mater* 13, 204–212. doi:10.1038/nmat3819

Wei, S. C., Levine, J. H., Cogdill, A. P., Zhao, Y., Anang, N. A. S., Andrews, M. C., et al. (2017). Distinct cellular mechanisms underlie anti-CTLA-4 and anti-PD-1 checkpoint blockade. *Cell* 170, 1120–1133. doi:10.1016/j.cell.2017.07.024

Wei, X., and Yang, M. (2023). Cell- and subcellular organelle-targeting nanoparticle-mediated breast cancer therapy. *Front. Pharmacol.* 14, 1180794. doi:10.3389/fphar.2023.1180794

Xia, Y., Yang, R., Wang, H., Hou, Y., Li, Y., Zhu, J., et al. (2022). Biomaterials delivery strategies to repair spinal cord injury by modulating macrophage phenotypes. *J. Tissue Eng.* 13, 20417314221143059. doi:10.1177/20417314221143059

Xin, Y., Huang, M., Guo, W. W., Huang, Q., Zhang, L. Z., and Jiang, G. (2017). Nano-based delivery of RNAi in cancer therapy. *Mol. Cancer* 16, 134. doi:10.1186/s12943-017-0683-y

Xu, X., Liu, C., Wang, Y., Koivisto, O., Zhou, J., Shu, Y., et al. (2021). Nanotechnology-based delivery of CRISPR/Cas9 for cancer treatment. *Adv. Drug Deliv. Rev.* 176, 113891. doi:10.1016/j.addr.2021.113891

Yan, W., Lang, T., Qi, X., and Li, Y. (2020). Engineering immunogenic cell death with nanosized drug delivery systems improving cancer immunotherapy. *Curr. Opin. Biotechnol.* 66, 36–43. doi:10.1016/j.copbio.2020.06.007

Yang, M., Li, J., Gu, P., and Fan, X. (2021). The application of nanoparticles in cancer immunotherapy: targeting tumor microenvironment. *Bioact. Mater* 6, 1973–1987. doi:10.1016/j.bioactmat.2020.12.010

Yin, W. M., Li, Y. W., Gu, Y. Q., and Luo, M. (2020). Nanoengineered targeting strategy for cancer immunotherapy. *Acta Pharmacol. Sin.* 41, 902–910. doi:10.1038/s41401-020-0417-3

Yu, S., Xiao, H., Ma, L., Zhang, J., and Zhang, J. (2023). Reinforcing the immunogenic cell death to enhance cancer immunotherapy efficacy. *Biochim. Biophys. Acta Rev. Cancer* 1878, 188946. doi:10.1016/j.bbcan.2023.188946

Yu, S., Yi, M., Qin, S., and Wu, K. (2019). Next generation chimeric antigen receptor T cells: safety strategies to overcome toxicity. *Mol. Cancer* 18, 125. doi:10.1186/s12943-019-1057-4

Yuan, H., Jiang, W., von Roemeling, C. A., Qie, Y., Liu, X., Chen, Y., et al. (2017). Multivalent bi-specific nanobioconjugate engager for targeted cancer immunotherapy. *Nat. Nanotechnol.* 12, 763–769. doi:10.1038/nnano.2017.69

Zhang, X., Bai, X. C., and Chen, Z. J. (2020). Structures and mechanisms in the cGAS-STING innate immunity pathway. *Immunity* 53, 43–53. doi:10.1016/j.immuni.2020.05.013

Zhang, Y., Li, N., Suh, H., and Irvine, D. J. (2018). Nanoparticle anchoring targets immune agonists to tumors enabling anti-cancer immunity without systemic toxicity. *Nat. Commun.* 9, 6. doi:10.1038/s41467-017-02251-3

Zhao, C., Pang, X., Yang, Z., Wang, S., Deng, H., and Chen, X. (2022). Nanomaterials targeting tumor associated macrophages for cancer immunotherapy. *J. Control Release* 341, 272–284. doi:10.1016/j.jconrel.2021.11.028

Zhao, D., Huang, X., Zhang, Z., Ding, J., Cui, Y., and Chen, X. (2021). Engineered nanomedicines for tumor vasculature blockade therapy. *Wiley Interdiscip. Rev. Nanomed Nanobiotechnol* 13, e1691. doi:10.1002/wnan.1691

Zheng, N., Liu, W., Li, B., Nie, H., Liu, J., Cheng, Y., et al. (2019). Co-delivery of sorafenib and metapristone encapsulated by CXCR4-targeted PLGA-PEG nanoparticles overcomes hepatocellular carcinoma resistance to sorafenib. *J. Exp. Clin. Cancer Res.* 38, 232. doi:10.1186/s13046-019-1216-x

Zheng, Y., Han, Y., Sun, Q., and Li, Z. (2022). Harnessing anti-tumor and tumor-tropism functions of macrophages via nanotechnology for tumor immunotherapy. *Explor. (Beijing)* 2, 20210166. doi:10.1002/EXP.20210166

Zhou, L., Zhang, P., Wang, H., Wang, D., and Li, Y. (2020). Smart nanosized drug delivery systems inducing immunogenic cell death for combination with cancer immunotherapy. *Acc. Chem. Res.* 53, 1761–1772. doi:10.1021/acs.accounts.0c00254

Zhu, J., Fan, J., Xia, Y., Wang, H., Li, Y., Feng, Z., et al. (2023). Potential therapeutic targets of macrophages in inhibiting immune damage and fibrotic processes in musculoskeletal diseases. *Front. Immunol.* 14, 1219487. doi:10.3389/fimmu.2023.1219487

Zhu, K. Y., and Palli, S. R. (2020). Mechanisms, applications, and challenges of insect RNA interference. *Annu. Rev. Entomol.* 65, 293–311. doi:10.1146/annurev-ento-011019-025224

Zhu, Y., Yu, X., Thamphiwatana, S. D., Zheng, Y., and Pang, Z. (2020). Nanomedicines modulating tumor immunosuppressive cells to enhance cancer immunotherapy. *Acta Pharm. Sin. B* 10, 2054–2074. doi:10.1016/j.apsb.2020.08.010

Zins, K., and Abraham, D. (2020). Cancer immunotherapy: ttargeting tumor-associated macrophages by gene silencing. *Methods Mol. Biol.* 2115, 289–325. doi:10.1007/978-1-0716-0290-4_17

frontiers | Frontiers in Pharmacology

TYPE Review
PUBLISHED 03 October 2023
DOI 10.3389/fphar.2023.1284406

OPEN ACCESS

EDITED BY
Duoyi Zhao,
Fourth Affiliated Hospital of China Medical University, China

REVIEWED BY
Ke Li,
Yangzhou University, China
Zhiping Qi,
Jilin University, China

*CORRESPONDENCE
Jianping Wang,
2411247949@qq.com

RECEIVED 28 August 2023
ACCEPTED 25 September 2023
PUBLISHED 03 October 2023

CITATION
Hou Y, Wang J and Wang J (2023), Engineered biomaterial delivery strategies are used to reduce cardiotoxicity in osteosarcoma. *Front. Pharmacol.* 14:1284406. doi: 10.3389/fphar.2023.1284406

Engineered biomaterial delivery strategies are used to reduce cardiotoxicity in osteosarcoma

Yulin Hou, Jie Wang and Jianping Wang*

Department of Cardiology, Guangyuan Central Hospital, Guangyuan, China

Osteosarcoma (OS) is the most common malignant bone tumor in children and adolescents. Chemotherapy drugs play an integral role in OS treatment. Preoperative neoadjuvant chemotherapy and postoperative conventional adjuvant chemotherapy improve survival in patients with OS. However, the toxic side effects of chemotherapy drugs are unavoidable. Cardiotoxicity is one of the common side effects of chemotherapy drugs that cannot be ignored. Chemotherapy drugs affect the destruction of mitochondrial autophagy and mitochondria-associated proteins to cause a decrease in cardiac ejection fraction and cardiomyocyte necrosis, which in turn causes heart failure and irreversible cardiomyopathy. Biomaterials play an important role in nanomedicine. Biomaterials act as carriers to deliver chemotherapy drugs precisely around tumor cells and continuously release carriers around the tumor. It not only promotes anti-tumor effects but also reduces the cardiotoxicity of chemotherapy drugs. In this paper, we first introduce the mechanism by which chemotherapy drugs commonly used in OS cause cardiotoxicity. Subsequently, we introduce biomaterials for reducing cardiotoxicity in OS chemotherapy. Finally, we prospect biomaterial delivery strategies to reduce cardiotoxicity in OS.

KEYWORDS

Osteosarcoma, cardiotoxicity, biomaterials, drug delivery, chemotherapy

1 Introduction

Osteosarcoma (OS) is the most common malignancy in children and adolescents, accounting for 0.2 percent of all malignancies (Rossi and Del Fattore, 2023). In the US, approximately 4.4 patients per million children and adolescents have OS (Longhi et al., 2006). OS originates from mesenchymal stem cells and occurs in the long diaphyseal epiphysis in children and adolescents, more commonly in the distal femur, proximal tibia, and humerus (Brown et al., 2018; Dong et al., 2022). OS is highly aggressive and often causes pathological fractures and excruciating pain (Franchi, 2012). The prognosis of OS is poor because of its early metastasis and high drug resistance, and the lung is the most common metastatic organ for OS (Farnood et al., 2023). Although surgery and chemotherapy respond well to most malignancies, long-term survival in osteosarcoma is less than 30 percent (Luetke et al., 2014). The rarity of OS and the lack of reliable markers make OS difficult to diagnose and detect early (Beird et al., 2022). The high mortality rate of OS not only brings a heavy financial burden to the patient's family but also brings great challenges to clinicians.

Surgical resection is usually an effective means of early OS treatment. Amputation is usually the classic treatment for OS, and although it can cure early OS, it can seriously affect the quality of life (Zhang et al., 2022). Neoadjuvant chemotherapy prior to surgical resection

and adjuvant chemotherapy after surgery are usually essential (Khadembaschi et al., 2022a). Neoadjuvant chemotherapy reduces the volume of the primary tumor of OS, reduces the rate of OS metastasis, and increases the limb salvage rate of OS (Khadembaschi et al., 2022b). OS without metastasis has a 5-year survival rate of 70 percent (Bielack et al., 2010). Despite new advances in neoadjuvant chemotherapy, effective treatment of OS has not improved (Panez-Toro et al., 2023). This may be related to the fact that OS is resistant to chemotherapy. For chemotherapy-resistant metastatic patients, radiation therapy is another palliative option for prolonging the patient's life (Ren et al., 2019). Unfortunately, OS cells are not sensitive to radiation therapy, which only prolongs OS survival by 6 months (Ren et al., 2019). Treatment of cases of unresectable metastatic or recurrent OS relies primarily on chemotherapy (Strauss et al., 2021). However, chemotherapy drugs have poor targeting (Panez-Toro et al., 2023). For children and adolescents, timely chemotherapy drugs can target tumor cells, but the side effects of chemotherapy drugs, especially cardiotoxicity, are still a big blow (Heng et al., 2020).

Biomaterials are widely used in various fields of nanomedicine and regenerative medicine because of their biohistocompatibility, targeting, and degradability (Quadros et al., 2021). Over the past few years, a variety of biomaterials have been developed for chemotherapy of malignancies (Xia et al., 2022a). Biomaterials have been developed to encapsulate various chemotherapy drugs and efficiently deliver them to tumor tissue, reducing off-target side effects and side effects of chemotherapy drugs (Zhang et al., 2022). In this article, we first introduce chemotherapy drugs applied to osteosarcoma. Second, we describe the mechanism of cardiotoxicity of chemotherapy drugs. Finally, we summarize and prospect biomaterials for reducing the cardiotoxicity of chemotherapy drugs in the treatment of osteosarcoma.

2 Cardiotoxicity of first-line chemotherapy drugs for osteosarcoma

2.1 Doxorubicin

Doxorubicin (DOX) is an anthracycline chemotherapy drug used in solid tumors and hematologic malignancies. DOX is widely used and is one of the most commonly used chemotherapy drugs for intermediate and advanced tumors (Chatterjee et al., 2021). DOX plays an important role in cancers such as breast cancer (BC), hematologic tumors, and OS (Rawat et al., 2021). The main mechanism of action of DOX is to inhibit DNA replication and topoisomerase II (Top2) activity of tumor cells, resulting in DNA double-strand breaks that affect the proliferation ability of tumor cells (Corremans et al., 2019). DOX not only has a killing effect on tumor cells, but also has toxic side effects on normal tissue cell fluid, DOX is mainly manifested as nephrotoxicity, hair loss, liver toxicity, chemotherapy brain and bone marrow suppression, and other toxic side effects (Du et al., 2021). But what is more serious about DOX is its toxicity to the heart. Due to its dose-dependent nature, the clinical use of DOX is hampered by life-threatening cardiotoxicity, including cardiac dilation and heart failure (Wu et al., 2023). Studies have shown that DOX induces chronic heart failure beyond its cumulative dose (700 mg/m in adults and 300 mg/m in children) (Xu et al., 2020). Approximately 30 percent of patients develop acute cardiotoxicity following DOX administration, with ST-segment changes, tachycardia, and premature ventricular beats (Ahmad et al., 2022). Most of the symptoms of acute cardiotoxicity can be reversed, and once acute cardiotoxicity persists, it will induce chronic toxicity to the heart. Chronic cardiotoxicity occurs mainly weeks or even months after DOX administration, and the main symptoms are irreversible cardiomyopathy and even congestive heart failure (Koleini et al., 2019). The specific molecular mechanism of DOX cardiotoxicity remains unknown (Feng and Wu, 2023). Studies have shown that the cardiotoxicity of DOX is primarily associated with the destruction of mitochondrial autophagy and mitochondria-associated proteins (Wang et al., 2019). Mitochondrial damage affects mitochondrial substrate metabolism, mitochondrial respiratory chain, and myocardial ATP storage and utilization in tumor cells (Ling et al., 2022). Mechanisms such as oxidative stress, inflammation, iron diesis, imbalanced calcium balance, apoptosis, and autophagy are all implicated in the cardiotoxicity of DOX (Chen et al., 2022).

2.2 Platinum-based chemotherapy drugs

Platinum-based chemotherapy is one of the first-line treatments for solid tumors (Weiss and Christian, 1993). The most commonly used platinum chemotherapy drugs in clinical practice are cisplatin, carboplatin and oxaliplatin. Cisplatin is the more commonly used platinum-based chemotherapy agent in the treatment of OS than other platinum-based chemotherapy drugs (Qi et al., 2019). Cisplatin, also known as cis-diamine dichloroplatin, mainly binds to the N7 position on the purine ring and causes DNA damage to tumor cells by blocking cell division leading to apoptosis (Minerva et al., 2023). After DNA damage, tumors lose their ability to proliferate, thereby inducing oxidative stress, upregulating p53, mitogen-activated protein kinase (MAPK) and Jun N-terminal kinase (JNK) or Akt pathways, and inducing apoptosis (Gupta and Nebreda, 2015). Cisplatin also has a killing effect on normal tissue cells, mainly including hepatotoxicity, cardiotoxicity, neurotoxicity, *etc.* (Zhu et al., 2022). Cardiotoxicity with cisplatin alone has been reported to be rare (Jakubowski and Kemeny, 1988). Between 1980 and 2017, only five clinical studies reported cardiotoxicity from cisplatin (Hu et al., 2018). Cisplatin has relatively early cardiotoxic effects, mainly causing arrhythmias leading to ECG changes and chronic heart failure (Fukuhara et al., 2014). Yang et al. reported a decrease in left ventricular ejection fraction (LVEF) from 70% to 48% in a 53-year-old woman with cervical cancer after 3 weeks of cisplatin application (Hu et al., 2018). Although cisplatin alone has not been reported to cause cardiotoxicity, we cannot ignore this problem. The mechanism of cisplatin's cardiotoxicity remains unknown. Most current views support that cisplatin promotes cardiomyocyte apoptosis by upregulating ROS and mitochondrial DNA disruption leading to mitochondrial dysfunction (Ma et al., 2020).

2.3 Methotrexate

Methotrexate is a folate analog that inhibits the activity of dihydrofolate reductase by competing with substrates, resulting in defects in purine and pyrimidine synthesis (Bidaki et al., 2017). Decreased purine and pyrimidine synthesis inhibit tumor cell proliferation, and as a result, methotrexate is also used as an antineoplastic drug (Malaviya, 2016). Methotrexate is mostly used in rheumatoid arthritis and rarely as an antitumor treatment alone (Zhao et al., 2022). Methotrexate is often used in combination with other chemotherapy drugs for antitumor therapy. For example, fluorouracil, doxorubicin, and methotrexate are used for gastric cancer, cyclophosphamide, methotrexate, and 5-fluoropyrimidine are used for advanced breast cancer, and methotrexate, vinblastine, doxorubicin, and cyclophosphamide are used for bladder cancer (Walling, 2006). The chemotherapy regimen in OS is methotrexate-DOX-cisplatin (Smrke et al., 2021). Methotrexate is excreted primarily through the kidneys, and nephrotoxicity is caused by methotrexate crystals in the tubular lumen, leading to tubular toxicity leading to acute kidney injury (Christensen et al., 2012). Methotrexate reduces inflammation, improves cardiovascular risk factors, reduces mortality, and generally has a protective effect on the heart (Bălănescu et al., 2019). However, high doses of methotrexate are toxic to the heart. Shah et al. reported a decrease in ejection fraction and an acute decline in biventricular function in a 54-year-old man with systemic sclerosis after taking methotrexate (Shah et al., 2022). The mechanism of action of methotrexate inducing cardiotoxicity is still very clear. Methotrexate-induced cardiac damage manifests as distortion of normal cardiac tissue structure, significant oxidative and nitrosizing stress, along with decreased glutathione concentration and decreased superoxide dismutase activity, which in turn affects myocardial function (Perez-Verdia et al., 2005; Al-Taher et al., 2020).

2.4 Ifosfamide/ifosfamide

Cyclophosphamide is an alkylating agent and immunosuppressant that is widely used in antitumor, organ transplantation, and anti-graft rejection reactions (Song et al., 2016). Cyclophosphamide is primarily used in combination chemotherapy regimens for lymphoma, leukemia, breast, lung, and neuroblastoma (Emadi et al., 2009; Iqubal et al., 2019). Cyclophosphamide binds to guanine residues of tumor cell DNA and causes tumor death (Veal et al., 2016). The pharmacological effects of cyclophosphamide depend on the metabolism of the drug, the dose administered, and the timing of administration (Huyan et al., 2011). The cardiotoxicity of cyclophosphamide is one of the important factors limiting its wide clinical application. Although the mechanism of cyclophosphamide cardiotoxicity has not been completely cleared, the current general consensus is mainly in the following aspects. Cyclophosphamide induces oxygen radical production and inflammation in cardiomyocytes, and its metabolites also reduce the production of endothelial nitric oxide synthase phosphorylation (Iqubal et al., 2019). Cyclophosphamide also induces activation of the p53 and p38 mitogen-activating protein kinase pathways, leading to cardiac apoptosis, inflammation, and hypertrophy (DeJarnett et al., 2014).

Ifosfamide is more commonly used in chemotherapy for OS than cyclophosphamide (Spalato and Italiano, 2021). Similar to cyclophosphamide, ifosfamide is a cell-cycle, nonspecific antineoplastic agent that can be hydrolyzed by phosphoramidase to phosphamide mustard in humans for antitumor effects (Palmerini et al., 2020). The most common adverse effect of ifosfamide is central system toxicity, which occurs in nearly 20 percent of patients with severe hallucinations, confusion, or episodes of drowsiness and coma called ifosfamide encephalopathy (Lee Brink et al., 2020; Ilyas et al., 2021). The toxic effects of ifosfamide on the heart are also not fully understood. Similar to cyclophosphamide, ifosfamide induces oxygen radical production and inflammation in cardiomyocytes, inducing apoptosis in cardiomyocytes (Savani and Skubitz, 2019). Chemotherapy regimens of doxorubicin, cisplatin, ifosfamide, and/or high-dose methotrexate are considered first-line chemotherapy agents for OS (Marec-Berard et al., 2020). However, the cardiotoxicity of chemotherapy drugs is inevitable, and the development of biomaterials to deliver chemotherapy drugs to reduce cardiotoxicity is the development trend of OS therapy.

3 Biomaterials reduce cardiotoxicity of OS chemotherapy

3.1 Extracellular vesicles

Extracellular vesicles (EVs) are vesicle-like structures with a diameter of 30–150 nm produced by living cells (Lee and Kim, 2021). As an emerging mode of intercellular communication, EVs can deliver RNA, proteins, and other carriers to target cells, thereby regulating the proliferation and differentiation of target cells and affecting the structure and function of target cells (Chang et al., 2021). The advantage of EVs as delivery vehicles is that they can fuse membranes with target cells without destroying the carrier five, thereby releasing the carrier into the target cell (Xia et al., 2022b). EVs produced by cells from different sources have cell-homing effects at different locations in the body (Wiklander et al., 2015). This property makes EVs uniquely targeted. Chemical modifications also give EVs more precise targeting ability, and EVs have more systemic toxic side effects than other biological materials. Wei et al. used bone marrow-derived EVs to deliver DOX (EVs-Dox) to reduce the cardiotoxicity of DOX in OS therapy (Wei et al., 2022). The EVs loaded with DOX have a diameter of 178.1 nm. EVs-Dox is more toxic to tumor cells than DOX and much less toxic to cardiomyocytes than DOX. EVs-DOX can target OS cells *in vivo*, effectively inhibiting the proliferation and migration of OS cells. At 12 h *in vivo*, the concentration of EVs-DOX in cardiomyocytes was much lower than in the DOX group. This is mainly due to the fact that Evs can express SDF-1 protein, and the interaction of Stromal cell-derived factor-1 (SDF-1) and C-X-C motif chemokine receptor 4 (CXCR4) induces DOX-loaded EVs to tend to osteosarcoma sites, reducing the accumulation of cardiomyocytes and reducing the cardiotoxicity of DOX.

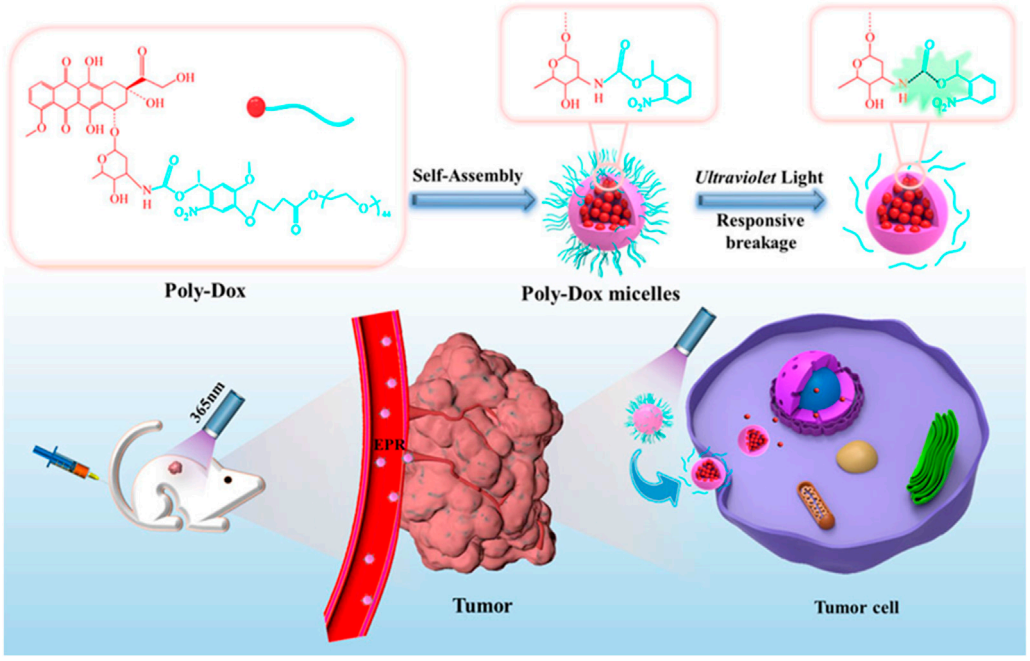

FIGURE 1
Schematic illustration of the self-assembly and responsive breakage of Poly-Dox micelles, and the process of tumor therapy. DOX self-assembles into photoresponsive polymeric micelles. After tail vein injection in mice, polymeric micelles can aggregate around tumor cells due to the EPR effect. Increase the concentration of DOX in tumor cells to achieve anti-tumor effect. Reproduced with permission from (Chen et al., 2021).

3.2 Liposomes

The FDA-approved DOX liposomal preparation, Caelyx, is significantly less cardiotoxic and well tolerated (De Sanctis et al., 2015). DOX liposomes reduce the expression of P-glycoprotein, which is the main mediator of DOX cardiotoxicity. OS also expresses CD44 receptors. Gazzano et al. made HA-Lsdox by coupling DOX liposomes with hyaluronic acid (HA) (Gazzano et al., 2019). HA is a donor to CD44, and the high expression of CD44 in OS makes it an ideal target to increase HA-Lsdox delivery to tumors. HA-Lsdox has a size range of 190 nm–204 nm and effectively releases DOX *in vivo* to promote apoptosis of tumor cells. HA-Lsdox can also promote sulfation and ubiquitination of P-glycoprotein, reducing the cardiotoxic effect of DOX. Nanomicelles can enhance the enhanced permeability and retention (EPR) effect of tumor cells, and the inert groups on the surface of nanomicelles can effectively reduce the uptake of drugs by other normal tissue cells, thereby effectively reducing the side effects of drugs (Riley et al., 2019). Chen et al. synthesized a photoresponsive DOX conjugated polymer (Poly-Dox-M) (Figure 1) (Chen et al., 2021). Nanomicelles indicate cross-linked polyethylene glycol (PEG), which is stable *in vivo* after self-assembly into Poly-Dox-M due to the inert nature of PEG. Poly-Dox-M has a diameter of 27 nm and a drug loading rate of 13.62%. The surface-inert PEG is decomposed by amide bond destruction after several minutes of UV irradiation, promoting the release of DOX by Poly-Dox-M. *In vivo*, experiments have shown that Poly-Dox-M accumulates in large numbers of tumor cells compared to DOX, while the heart, spleen, liver, lungs, and kidneys are very small. As a result, Poly-Dox-M reduces the toxic side effects caused by DOX. This may be due to the lack of ultraviolet light exposure to vital organs, and Poly-Dox-M cannot break down the DOX that releases its load, thus reducing the visceral toxicity of DOX. The cardiotoxic effects of DOX liposomes in reducing DOX have been clinically proven. Huang et al. demonstrated that ifosfamide combined with DOX liposomes for OS treatment can reduce cardiotoxicity compared with ifosfamide plus DOX (Huang et al., 2022). Yang et al. demonstrated that PEG-DOX clinically reduces the cardiotoxicity of DOX (Yang et al., 2020).

3.3 Nanoparticles

Wang et al. made PCP-PEG-ALD nanoparticles from aldehyde rubicin (ALD), positively charged proteins (PCP), and PEG (Wang et al., 2021). The solubility of ALD is extremely low, and poor bioavailability limits its clinical use (Gong et al., 2018). PCP-PEG-ALD nanoparticles have good biocompatibility. PCP-PEG-ALD nanoparticles have a diameter of 200 nm, which has a hihg encapsulation rate for ALD and can deliver ALDto tumor cells. PCP-PEG-ALD nanoparticles can kill tumor cells (survival rate 29%) without causing damage to normal cells (survival rate 95%). Compared with DOX-induced focal necrosis of cardiomyocytes, PCP-PEG-ALD nanoparticles only cause mild symptoms of myocardial stromal adiposia. Feng et al. used the principle that redox-sensitive nanoparticles containing disulfide bonds were used to respond to the redox potential of tumor cells, and coupled bone-targeted partial alendronate (ALN) with the CD44 ligand hyaluronic acid (HA) to form functionalized liposomes (ALN-HA-SS-L-L) for DOX delivery (Figure 2) (Feng et al., 2019). ALN-HA-SS-L-L is able to target bone tumors *in vivo*

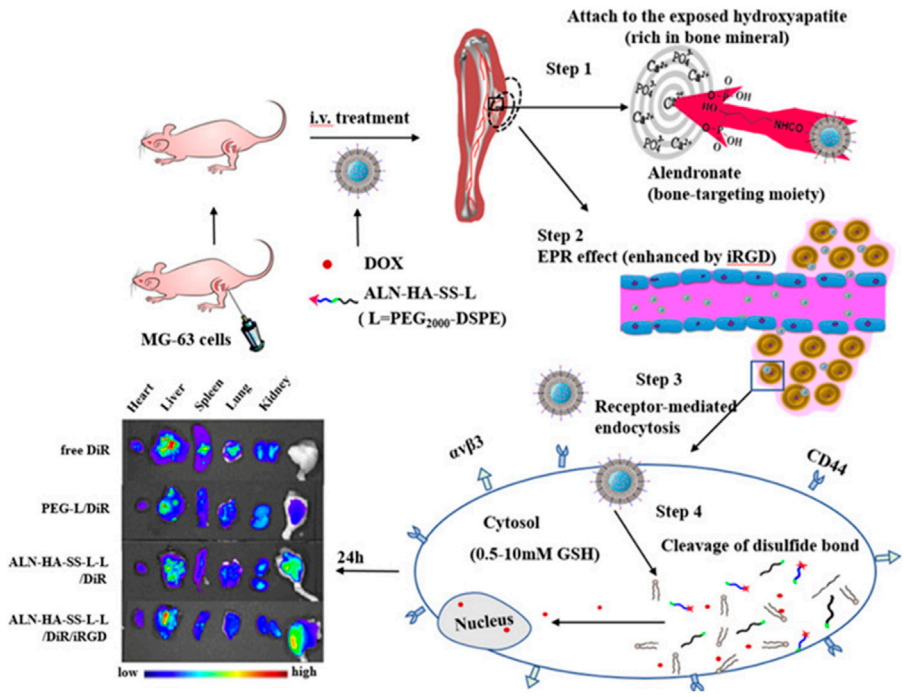

FIGURE 2
Alendronate (ALN) is coupled to the CD44 ligand hyaluronic acid (HA). The ALN-HA conjugate was conjugated to DSPE-PEG 2000–COOH to obtain functionalized lipid ALN-HA-SS-L by a bioreducible disulfide bonder (–SS–), which was inserted into a preformed liposome loaded with doxorubicin (DOX). ALN-HA-SS-L-L/DOX is significantly more cytotoxic to human OS MG-63 cells with high and rapid cell uptake. The antitumor effects of various liposomes are the same as those shown by *in vivo*/*ex vivo* imaging. In the *in situ* OS nude mouse model, ALN-HA-SS-L-L/DOX showed significant tumor growth inhibition and prolonged survival. Reproduced with permission from (Feng et al., 2019).

and break disulfide bonds within tumor cells to release DOX to achieve anti-tumor effects. ALN-HA-SS-L-L released 3% and 72% of DOX in the first 6 h and 23 h, respectively. *In vivo* experiments, free DOX treatment was confirmed to cause severe cardiotoxicity and liver and kidney damage, while ALN-HA-SS-L-L/DOX treatment reduced cardiotoxicity and inhibited lung metastases.

3.4 Hydrogels

Hydrogels are plastic, adherent, biocompatible, and biodegradable and widely used in tissue engineering and nanomedicine (Liang et al., 2023). Topical delivery systems for hydrogel drugs are able to deliver anticancer drugs directly to the target, reducing the toxic effects of chemotherapy drugs (Yoo et al., 2018). β-cyclodextrin (β-CD) can be used as a nanoscale drug carrier for anticancer drugs, enhancing the water solubility of drugs (Li et al., 2015). Sun et al. made DOX, cisplatin-loaded β-CD into nanoscale HP-β-CD drug-delivery hydrogels for combination chemotherapy for OS (Yoon et al., 2019). HP-β-CD hydrogels continuously release DOX and cisplatin for anti-tumor effects. *In vitro* experiments have confirmed that HP-β-CD hydrogel can reduce the proliferation rate of tumor cells. HP-β-CD hydrogel can reduce tumor volume *in vivo* for 4 weeks. Cao et al. used a hydrogel-microsphere (Gel-Mps) complex composed of collagenase (Col) and PLGA microspheres (Mps) to carry pioglitazone (Pio) and Dox to achieve combined chemotherapy for OS (Cao et al., 2023). Gel-MPS has a highly biodegradable, extremely efficient, and low-toxicity sustained drug release effect, showing an effective inhibitory effect on tumor proliferation. The average size of Mps is 3.97μm, and the load ratios of Dox and Pio are 3.79% and 13.69%, respectively. *In vitro* experiments, Gel-Mps was able to achieve sustained release of Dox and Pio within 20 days. *In vivo* experiments have shown that Gel-Mps can reduce the migration and proliferation of tumor cells. The Pio released by Gel-Mps can also reduce the expression of P-glycoprotein, and reduce cardiotoxicity and resistance to chemotherapy drugs.

3.5 Polymer brackets

OS often leads to increased destruction, often resulting in bone non-regeneration and severe pain (Whelan and Davis, 2018). Bioscaffolds can provide support around OS, providing a foundation for bone regeneration. He used poly(-lactide-collective) and polyethylene glycol (PEG) to make bioscaffolds for loading DOX (Figure 3) (He et al., 2022). The average diameter of the biological scaffold was (0.86 ± 0.03) mm and the length was (4.22 ± 0.26) mm, and the loading ratio of DOX was 78.0% ± 6.32%. *In vitro* experiments showed that the polymeric scaffold released about 26.4% of DOX within 2 hours, and was able to release all DOX within 15 days. Compared with DOX, DOX in stents can achieve *in situ* release around the tumor, reduce DOX accumulation in the heart, and reduce cardiotoxicity. Polymethyl methacrylate (PMMA) is a bone substitute with excellent formability, high mechanical strength, and appropriate biocompatibility (van Vugt et al., 2019). PMMA can release heat,

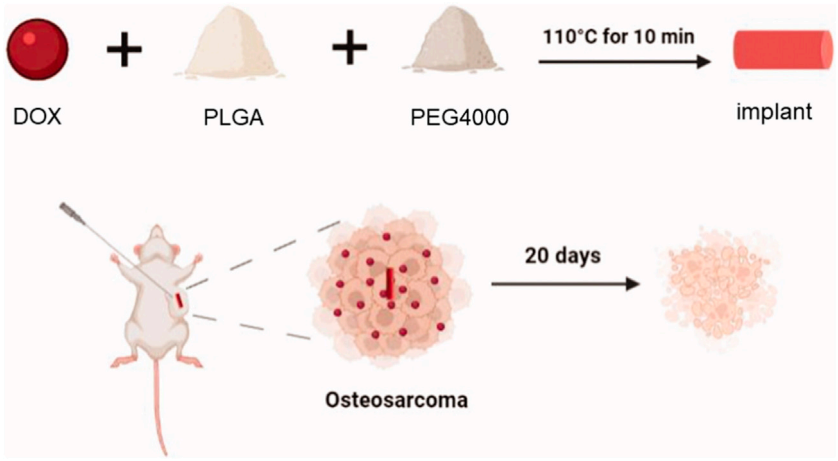

FIGURE 3
The schematic illustration of the DOX-loaded implant for intratumoral chemotherapy. Preparation of the DOX-loaded implant. DOX, PLGA, PEG are made of degradable polymer scaffolds, and polymer scaffolds can continuously release DOX into the tumor to achieve anti-tumor effects. After 20 days, tumor cells were observed to shrink. Reproduced with permission from (He et al., 2022).

causing thermal necrosis of tumor cells, resulting in local antitumor effects (Gaston et al., 2011). However, the thermal effects of PMMA often cause normal cell necrosis, and cement leakage also limits the widespread use of PMMA cement (Dolan et al., 2012). Wang et al. used carboxymethylcellulose (CMC) to increase the porosity of PMMA cement for enhanced cisplatin delivery (Wang et al., 2022). The addition of CMC reduces the compressive strength of PMMA. Bone cement has a porosity of 30–40 μm and a cisplatin loading rate of 16.6% ± 1.1%. Bone cement continuously releases cisplatin within 14 days to achieve the chemotherapy effect of bone cement.

4 Conclusion and outlook

As one of the most important organs of the human body, the role of the heart cannot be ignored. Although the cardiotoxicity of chemotherapy drugs is not fully understood, it has been agreed that they affect the ejection fraction of the heart and cardiomyocyte function, and thus cause heart failure and cardiomyocyte death by inhibiting mitochondrial activity. Although chemotherapy drugs have achieved good results in the treatment of advanced tumors, the adverse effects of chemotherapy drugs are often unbearable and painful for patients. Chemotherapy drugs kill tumor cells as well as normal tissue cells. This is a puzzle that clinicians cannot solve. How to reduce the toxicity of chemotherapy drugs remains a difficult problem for clinicians. The emergence of biomaterials has made great strides in tissue engineering and nanomedicine. Biomaterial delivery strategies have made major breakthroughs in bone regeneration, anti-tumor, tissue repair, and regenerative medicine. Nanoparticles, hydrogels, scaffolds, *etc.*, based on PLGA, PEG, chitosan, gelatin, alginate, bioactive glass, *etc.*, have been designed for anti-tumor treatment, and their effects have been confirmed in preclinical studies. Although biomaterial delivery strategies have achieved good results in preclinical studies, few have been truly applied clinically. At present, albumin paclitaxel chemotherapy drugs are widely used in clinical practice as a mature chemotherapy drug. However, other nanomaterials for delivery are still only in their initial stages. Preclinical research still needs to address the biological activity of biomaterials *in vivo* meet the persistence of antitumor therapy and reduce the side effects of chemotherapy drugs. Future research still needs to further develop biomaterials to reduce the cardiotoxicity of chemotherapy drugs. Based on the results achieved in current preclinical studies, we believe that sooner or later the toxic effects of biomaterials in reducing the toxicity of chemotherapy drugs will be applied to the clinic on a large scale.

Author contributions

YH: Writing–original draft. JeW: Writing–review and editing. JaW: Writing–review and editing.

Funding

The author(s) declare financial support was received for the research, authorship, and/or publication of this article.

Acknowledgments

We would like to express our appreciation to everyone who was involved in the drafting and preparation of the manuscript.

Conflict of interest

The authors declare that the research was conducted in the absence of any commercial or financial relationships that could be construed as a potential conflict of interest.

Publisher's note

References

Ahmad, N., Ullah, A., Chu, P., Tian, W., Tang, Z., and Sun, Z. (2022). Doxorubicin induced cardio toxicity through sirtuins mediated mitochondrial disruption. *Chemico-biological Interact.* 365, 110028. doi:10.1016/j.cbi.2022.110028

Al-Taher, A. Y., Morsy, M. A., Rifaai, R. A., Zenhom, N. M., and Abdel-Gaber, S. A. (2020). Paeonol attenuates methotrexate-induced cardiac toxicity in rats by inhibiting oxidative stress and suppressing TLR4-induced NF-κB inflammatory pathway. *Mediat. Inflamm.* 2020, 8641026. doi:10.1155/2020/8641026

Bălănescu, A. R., Bojincă, V. C., Bojincă, M., Donisan, T., and Bălănescu, S. M. (2019). Cardiovascular effects of methotrexate in immune-mediated inflammatory diseases. *Exp. Ther. Med.* 17, 1024–1029. doi:10.3892/etm.2018.6992

Beird, H. C., Bielack, S. S., Flanagan, A. M., Gill, J., Heymann, D., Janeway, K. A., et al. (2022). Osteosarcoma. *Nat. Rev. Dis. Prim.* 8, 77. doi:10.1038/s41572-022-00409-y

Bidaki, R., Kian, M., Owliaey, H., Babaei Zarch, M., and Feysal, M. (2017). Accidental chronic poisoning with methotrexate; report of two cases. *Emerg. (Tehran, Iran.* 5, e67.

Bielack, S., Jürgens, H., Jundt, G., Kevric, M., Kühne, T., Reichardt, P., et al. (2010). "Osteosarcoma: The COSS experience," in *Pediatric and adolescent osteosarcoma*. Editors N. Jaffe, O. S. Bruland, and S. Bielack (Boston, MA, USA: Springer US), 289–308.

Brown, H. K., Schiavone, K., Gouin, F., Heymann, M.-F., and Heymann, D. (2018). Biology of bone sarcomas and new therapeutic developments. *Calcif. Tissue Int.* 102, 174–195. doi:10.1007/s00223-017-0372-2

Cao, J., Du, X., Zhao, H., Zhu, C., Li, C., Zhang, X., et al. (2023). Sequentially degradable hydrogel-microsphere loaded with doxorubicin and pioglitazone synergistically inhibits cancer stemness of osteosarcoma. *Biomed. Pharmacother.* 165, 115096. doi:10.1016/j.biopha.2023.115096

Chang, W.-H., Cerione, R. A., and Antonyak, M. A. (2021). "Extracellular vesicles and their roles in cancer progression," in *Cancer cell signaling: Methods and protocols*. Editor M. Robles-Flores (New York, NY, USA: Springer US), 143–170.

Chatterjee, S., Hofer, T., Costa, A., Lu, D., Batkai, S., Gupta, S. K., et al. (2021). Telomerase therapy attenuates cardiotoxic effects of doxorubicin. *Mol. Ther. J. Am. Soc. Gene Ther.* 29, 1395–1410. doi:10.1016/j.ymthe.2020.12.035

Chen, J., Qian, C., Ren, P., Yu, H., Kong, X., Huang, C., et al. (2021). Light-responsive micelles loaded with doxorubicin for osteosarcoma suppression. *Front. Pharmacol.* 12, 679610. doi:10.3389/fphar.2021.679610

Chen, Y., Shi, S., and Dai, Y. (2022). Research progress of therapeutic drugs for doxorubicin-induced cardiomyopathy. *Biomed. Pharmacother.* 156, 113903. doi:10.1016/j.biopha.2022.113903

Christensen, A. M., Pauley, J. L., Molinelli, A. R., Panetta, J. C., Ward, D. A., Stewart, C. F., et al. (2012). Resumption of high-dose methotrexate after acute kidney injury and glucarpidase use in pediatric oncology patients. *Cancer* 118, 4321–4330. doi:10.1002/cncr.27378

Corremans, R., Adão, R., De Keulenaer, G. W., Leite-Moreira, A. F., and Brás-Silva, C. (2019). Update on pathophysiology and preventive strategies of anthracycline-induced cardiotoxicity. *Clin. Exp. Pharmacol. Physiology* 46, 204–215. doi:10.1111/1440-1681.13036

De Sanctis, R., Bertuzzi, A., Basso, U., Comandone, A., Marchetti, S., Marrari, A., et al. (2015). Non-pegylated liposomal doxorubicin plus ifosfamide in metastatic soft tissue sarcoma: Results from a phase-II trial. *Anticancer Res.* 35, 543–547.

DeJarnett, N., Conklin, D. J., Riggs, D. W., Myers, J. A., O'Toole, T. E., Hamzeh, I., et al. (2014). Acrolein exposure is associated with increased cardiovascular disease risk. *J. Am. Heart Assoc.* 3, e000934. doi:10.1161/JAHA.114.000934

Dolan, E. B., Haugh, M. G., Tallon, D., Casey, C., and McNamara, L. M. (2012). Heat-shock-induced cellular responses to temperature elevations occurring during orthopaedic cutting. *J. R. Soc. Interface* 9, 3503–3513. doi:10.1098/rsif.2012.0520

Dong, Z., Liao, Z., He, Y., Wu, C., Meng, Z., Qin, B., et al. (2022). Advances in the biological functions and mechanisms of miRNAs in the development of osteosarcoma. *Technol. Cancer Res. Treat.* 21, 15330338221117386. doi:10.1177/15330338221117386

Du, J., Zhang, A., Li, J., Liu, X., Wu, S., Wang, B., et al. (2021). Doxorubicin-induced cognitive impairment: The mechanistic insights. *Front. Oncol.* 11, 673340. doi:10.3389/fonc.2021.673340

Emadi, A., Jones, R. J., and Brodsky, R. A. (2009). Cyclophosphamide and cancer: Golden anniversary. *Nat. Rev. Clin. Oncol.* 6, 638–647. doi:10.1038/nrclinonc.2009.146

Farnood, P. R., Pazhooh, R. D., Asemi, Z., and Yousefi, B. (2023). Targeting signaling pathway by curcumin in osteosarcoma. *Curr. Mol. Pharmacol.* 16, 71–82. doi:10.2174/1874467215666220408104341

Feng, J., and Wu, Y. (2023). Endothelial-to-Mesenchymal transition: Potential target of doxorubicin-induced cardiotoxicity. *Am. J. Cardiovasc. drugs drugs, devices, other interventions* 23, 231–246. doi:10.1007/s40256-023-00573-w

Feng, S., Wu, Z.-X., Zhao, Z., Liu, J., Sun, K., Guo, C., et al. (2019). Engineering of bone- and CD44-dual-targeting redox-sensitive liposomes for the treatment of orthotopic osteosarcoma. *ACS Appl. Mater. interfaces* 11, 7357–7368. doi:10.1021/acsami.8b18820

Franchi, A. (2012). Epidemiology and classification of bone tumors. *official J. Italian Soc. Osteoporos. Mineral Metabolism, Skeletal Dis.* 9, 92–95.

Fukuhara, H., Yagi, M., Ando, K., and Tomita, Y. (2014). Long-term administration of single-agent carboplatin (auc 4) for advanced testicular seminoma safely achieved complete response in an 80-year-old man with chronic heart failure: A case report. *Can. Urological Assoc. J. = J. de l'Association des urologues du Can.* 8, E931–E933. doi:10.5489/cuaj.2089

Gaston, C. L., Bhumbra, R., Watanuki, M., Abudu, A. T., Carter, S. R., Jeys, L. M., et al. (2011). Does the addition of cement improve the rate of local recurrence after curettage of giant cell tumours in bone? The journal of bone and joint surgery. *Br. volume* 93, 1665–1669. doi:10.1302/0301-620X.93B12.27663

Gazzano, E., Buondonno, I., Marengo, A., Rolando, B., Chegaev, K., Kopecka, J., et al. (2019). Hyaluronated liposomes containing H2S-releasing doxorubicin are effective against P-glycoprotein-positive/doxorubicin-resistant osteosarcoma cells and xenografts. *Cancer Lett.* 456, 29–39. doi:10.1016/j.canlet.2019.04.029

Gong, J., Yan, J., Forscher, C., and Hendifar, A. (2018). Aldoxorubicin: A tumor-targeted doxorubicin conjugate for relapsed or refractory soft tissue sarcomas. *Drug Des. Dev. Ther.* 12, 777–786. doi:10.2147/DDDT.S140638

Gupta, J., and Nebreda, A. R. (2015). Roles of p38α mitogen-activated protein kinase in mouse models of inflammatory diseases and cancer. *FEBS J.* 282, 1841–1857. doi:10.1111/febs.13250

He, P., Xu, S., Guo, Z., Yuan, P., Liu, Y., Chen, Y., et al. (2022). Pharmacodynamics and pharmacokinetics of PLGA-based doxorubicin-loaded implants for tumor therapy. *Drug Deliv.* 29, 478–488. doi:10.1080/10717544.2022.2032878

Heng, M., Gupta, A., Chung, P. W., Healey, J. H., Vaynrub, M., Rose, P. S., et al. (2020). The role of chemotherapy and radiotherapy in localized extraskeletal osteosarcoma. *Eur. J. cancer* 125, 130–141. doi:10.1016/j.ejca.2019.07.029

Hu, Y., Sun, B., Zhao, B., Mei, D., Gu, Q., and Tian, Z. (2018). Cisplatin-induced cardiotoxicity with midrange ejection fraction: A case report and review of the literature. *Medicine* 97, e13807. doi:10.1097/MD.0000000000013807

Huang, G., Hua, S., Liu, H., Zhou, H., Chen, X., Wang, Z., et al. (2022). Efficacy of ifosfamide combined with liposome doxorubicin on osteosarcoma and its effects on serum IL-10, TNF-α, and IFN-γ in patients with osteosarcoma. *Am. J. Transl. Res.* 14, 1288–1296.

Huyan, X. H., Lin, Y. P., Gao, T., Chen, R. Y., and Fan, Y. M. (2011). Immunosuppressive effect of cyclophosphamide on white blood cells and lymphocyte subpopulations from peripheral blood of Balb/c mice. *Int. Immunopharmacol.* 11, 1293–1297. doi:10.1016/j.intimp.2011.04.011

Ilyas, S., Tabasum, R., Iftikhar, A., Nazir, M., Hussain, A., Hussain, A., et al. (2021). Effect of Berberis vulgaris L. root extract on ifosfamide-induced *in vivo* toxicity and *in vitro* cytotoxicity. *Sci. Rep.* 11, 1708. doi:10.1038/s41598-020-80579-5

Iqubal, A., Iqubal, M. K., Sharma, S., Ansari, M. A., Najmi, A. K., Ali, S. M., et al. (2019). Molecular mechanism involved in cyclophosphamide-induced cardiotoxicity: Old drug with a new vision. *Life Sci.* 218, 112–131. doi:10.1016/j.lfs.2018.12.018

Jakubowski, A. A., and Kemeny, N. (1988). Hypotension as a manifestation of cardiotoxicity in three patients receiving cisplatin and 5-fluorouracil. *Cancer* 62, 266–269. doi:10.1002/1097-0142(19880715)62:2<266::aid-cncr2820620207>3.0.co;2-y

Khadembaschi, D., Jafri, M., Praveen, P., Parmar, S., and Breik, O. (2022a). Does neoadjuvant chemotherapy provide a survival benefit in maxillofacial osteosarcoma: A systematic review and pooled analysis. *Oral Oncol.* 135, 106133. doi:10.1016/j.oraloncology.2022.106133

Khadembaschi, D., Jafri, M., Praveen, P., Parmar, S., and Breik, O. (2022b). Does neoadjuvant chemotherapy provide a survival benefit in maxillofacial osteosarcoma: A systematic review and pooled analysis. *Oral Oncol.* 135, 106133. doi:10.1016/j.oraloncology.2022.106133

Koleini, N., Nickel, B. E., Edel, A. L., Fandrich, R. R., Ravandi, A., and Kardami, E. (2019). Oxidized phospholipids in Doxorubicin-induced cardiotoxicity. *Chemico-biological Interact.* 303, 35–39. doi:10.1016/j.cbi.2019.01.032

Lee Brink, A., Bowe, C., and Dains, J. E. (2020). Risk factors for ifosfamide-related encephalopathy in adult cancer patients: An integrative review. *J. Adv. Pract. Oncol.* 11, 368–380. doi:10.6004/jadpro.2020.11.4.4

Lee, J. Y., and Kim, H. S. (2021). Extracellular vesicles in regenerative medicine: Potentials and challenges. *Tissue Eng. Regen. Med.* 18, 479–484. doi:10.1007/s13770-021-00365-w

Li, S., Sun, W., Wang, H., Zuo, D., Hua, Y., and Cai, Z. (2015). Research progress on the multidrug resistance mechanisms of osteosarcoma chemotherapy and reversal. *Tumor Biol.* 36, 1329–1338. doi:10.1007/s13277-015-3181-0

Liang, J., Wang, Z., Poot, A. A., Grijpma, D. W., Dijkstra, P. J., and Wang, R. (2023). Enzymatic post-crosslinking of printed hydrogels of methacrylated gelatin and tyramine-conjugated 8-arm poly(ethylene glycol) to prepare interpenetrating 3D network structures. *Int. J. bioprinting* 9, 750. doi:10.18063/ijb.750

Ling, G., Wang, X., Tan, N., Cao, J., Li, W., Zhang, Y., et al. (2022). Mechanisms and drug intervention for doxorubicin-induced cardiotoxicity based on mitochondrial bioenergetics. *Oxidative Med. Cell. Longev.* 2022, 7176282. doi:10.1155/2022/7176282

Longhi, A., Errani, C., De Paolis, M., Mercuri, M., and Bacci, G. (2006). Primary bone osteosarcoma in the pediatric age: State of the art. *Cancer Treat. Rev.* 32, 423–436. doi:10.1016/j.ctrv.2006.05.005

Luetke, A., Meyers, P. A., Lewis, I., and Juergens, H. (2014). Osteosarcoma treatment - where do we stand? A state of the art review. *Cancer Treat. Rev.* 40, 523–532. doi:10.1016/j.ctrv.2013.11.006

Ma, W., Wei, S., Zhang, B., and Li, W. (2020). Molecular mechanisms of cardiomyocyte death in drug-induced cardiotoxicity. *Front. Cell Dev. Biol.* 8, 434. doi:10.3389/fcell.2020.00434

Malaviya, A. N. (2016). Landmark papers on the discovery of methotrexate for the treatment of rheumatoid arthritis and other systemic inflammatory rheumatic diseases: A fascinating story. *Int. J. rheumatic Dis.* 19, 844–851. doi:10.1111/1756-185X.12862

Marec-Berard, P., Laurence, V., Occean, B. V., Ray-Coquard, I., Linassier, C., Corradini, N., et al. (2020). Methotrexate-etoposide-ifosfamide compared with doxorubicin-cisplatin-ifosfamide chemotherapy in osteosarcoma treatment, patients aged 18-25 years. *J. Adolesc. young adult Oncol.* 9, 172–182. doi:10.1089/jayao.2019.0085

Minerva, A. B., Verma, S., Chander, G., Jamwal, R. S., Sharma, B., et al. (2023). Cisplatin-based combination therapy for cancer. *J. Cancer Res. Ther.* 19, 530–536. doi:10.4103/jcrt.jcrt_792_22

Palmerini, E., Setola, E., Grignani, G., D'Ambrosio, L., Comandone, A., Righi, A., et al. (2020). High dose ifosfamide in relapsed and unresectable high-grade osteosarcoma patients: A retrospective series. *Cells* 9, 2389. doi:10.3390/cells9112389

Panez-Toro, I., Muñoz-García, J., Vargas-Franco, J. W., Renodon-Cornière, A., Heymann, M. F., Lézot, F., et al. (2023). Advances in osteosarcoma. *Curr. Osteoporos. Rep.* 21, 330–343. doi:10.1007/s11914-023-00803-9

Perez-Verdia, A., Angulo, F., Hardwicke, F. L., and Nugent, K. M. (2005). Acute cardiac toxicity associated with high-dose intravenous methotrexate therapy: Case report and review of the literature. *Pharmacother. J. Hum. Pharmacol. Drug Ther.* 25, 1271–1276. doi:10.1592/phco.2005.25.9.1271

Qi, L., Luo, Q., Zhang, Y., Jia, F., Zhao, Y., and Wang, F. (2019). Advances in toxicological research of the anticancer drug cisplatin. *Chem. Res. Toxicol.* 32, 1469–1486. doi:10.1021/acs.chemrestox.9b00204

Quadros, M., Momin, M., and Verma, G. (2021). Design strategies and evolving role of biomaterial assisted treatment of osteosarcoma. *Mater. Sci. Eng. C* 121, 111875. doi:10.1016/j.msec.2021.111875

Rawat, P. S., Jaiswal, A., Khurana, A., Bhatti, J. S., and Navik, U. (2021). Doxorubicin-induced cardiotoxicity: An update on the molecular mechanism and novel therapeutic strategies for effective management. *Biomed. Pharmacother.* 139, 111708. doi:10.1016/j.biopha.2021.111708

Ren, T., Zheng, B., Huang, Y., Wang, S., Bao, X., Liu, K., et al. (2019). Osteosarcoma cell intrinsic PD-L2 signals promote invasion and metastasis via the RhoA-ROCK-LIMK2 and autophagy pathways. *Cell death Dis.* 10, 261. doi:10.1038/s41419-019-1497-1

Riley, R. S., June, C. H., Langer, R., and Mitchell, M. J. (2019). Delivery technologies for cancer immunotherapy. *Nat. Rev. Drug Discov.* 18, 175–196. doi:10.1038/s41573-018-0006-z

Rossi, M., and Del Fattore, A. (2023). Molecular and translational research on bone tumors. *Int. J. Mol. Sci.* 24, 1946. doi:10.3390/ijms24031946

Savani, M., and Skubitz, K. M. (2019). Long-term outcome after doxorubicin and ifosfamide overdose in a patient with osteosarcoma and BARD1 mutation. *J. Pediatr. hematology/oncology* 41, e94–e96. doi:10.1097/MPH.0000000000001264

Shah, S., Haeger-Overstreet, K., and Flynn, B. (2022). Methotrexate-induced acute cardiotoxicity requiring veno-arterial extracorporeal membrane oxygenation support: A case report. *J. Med. case Rep.* 16, 447. doi:10.1186/s13256-022-03644-9

Smrke, A., Anderson, P. M., Gulia, A., Gennatas, S., Huang, P. H., and Jones, R. L. (2021). Future directions in the treatment of osteosarcoma. *Cells* 10, 172. doi:10.3390/cells10010172

Song, Y., Zhang, C., Wang, C., Zhao, L., Wang, Z., Dai, Z., et al. (2016). Ferulic acid against cyclophosphamide-induced heart toxicity in mice by inhibiting NF-κB pathway. *eCAM* 2016, 1261270. doi:10.1155/2016/1261270

Spalato, M., and Italiano, A. (2021). The safety of current pharmacotherapeutic strategies for osteosarcoma. *Expert Opin. drug Saf.* 20, 427–438. doi:10.1080/14740338.2021.1881060

Strauss, S. J., Frezza, A. M., Abecassis, N., Bajpai, J., Bauer, S., Biagini, R., et al. (2021). Bone sarcomas: ESMO-EURACAN-GENTURIS-ERN PaedCan clinical practice guideline for diagnosis, treatment and follow-up. *Ann. Oncol. official J. Eur. Soc. Med. Oncol.* 32, 1520–1536. doi:10.1016/j.annonc.2021.08.1995

van Vugt, T. A. G., Arts, J. J., and Geurts, J. A. P. (2019). Antibiotic-loaded polymethylmethacrylate beads and spacers in treatment of orthopedic infections and the role of biofilm formation. *Front. Microbiol.* 10, 1626. doi:10.3389/fmicb.2019.01626

Veal, G. J., Cole, M., Chinnaswamy, G., Sludden, J., Jamieson, D., Errington, J., et al. (2016). Cyclophosphamide pharmacokinetics and pharmacogenetics in children with B-cell non-Hodgkin's lymphoma. *Eur. J. cancer* 55, 56–64. doi:10.1016/j.ejca.2015.12.007

Walling, J. (2006). From methotrexate to pemetrexed and beyond. A review of the pharmacodynamic and clinical properties of antifolates. *Investig. new drugs* 24, 37–77. doi:10.1007/s10637-005-4541-1

Wang, P., Wang, L., Lu, J., Hu, Y., Wang, Q., Li, Z., et al. (2019). SESN2 protects against doxorubicin-induced cardiomyopathy via rescuing mitophagy and improving mitochondrial function. *J. Mol. Cell. Cardiol.* 133, 125–137. doi:10.1016/j.yjmcc.2019.06.005

Wang, S., Li, B., Zhang, H., Chen, J., Sun, X., Xu, J., et al. (2021). Improving bioavailability of hydrophobic prodrugs through supramolecular nanocarriers based on recombinant proteins for osteosarcoma treatment. *Angew. Chem. Int. Ed.* 60, 11252–11256. doi:10.1002/anie.202101938

Wang, Z., Nogueira, L. P., Haugen, H. J., Van Der Geest, I. C., de Almeida Rodrigues, P. C., Janssen, D., et al. (2022). Dual-functional porous and cisplatin-loaded polymethylmethacrylate cement for reconstruction of load-bearing bone defect kills bone tumor cells. *Bioact. Mater.* 15, 120–130. doi:10.1016/j.bioactmat.2021.12.023

Wei, H., Chen, F., Chen, J., Lin, H., Wang, S., Wang, Y., et al. (2022). Mesenchymal stem cell derived exosomes as nanodrug carrier of doxorubicin for targeted osteosarcoma therapy via SDF1-CXCR4 Axis. *Int. J. nanomedicine* 17, 3483–3495. doi:10.2147/IJN.S372851

Weiss, R. B., and Christian, M. C. (1993). New cisplatin analogues in development. A review. *A Rev. Drugs* 46, 360–377. doi:10.2165/00003495-199346030-00003

Whelan, J. S., and Davis, L. E. (2018). Osteosarcoma, chondrosarcoma, and chordoma. *J. Clin. Oncol. official J. Am. Soc. Clin. Oncol.* 36, 188–193. doi:10.1200/JCO.2017.75.1743

Wiklander, O. P., Nordin, J. Z., O'Loughlin, A., Gustafsson, Y., Corso, G., Mäger, I., et al. (2015). Extracellular vesicle *in vivo* biodistribution is determined by cell source, route of administration and targeting. *J. Extracell. vesicles* 4, 26316. doi:10.3402/jev.v4.26316

Wu, L., Wang, L., Du, Y., Zhang, Y., and Ren, J. (2023). Mitochondrial quality control mechanisms as therapeutic targets in doxorubicin-induced cardiotoxicity. *Trends Pharmacol. Sci.* 44, 34–49. doi:10.1016/j.tips.2022.10.003

Xia, Y., Yang, R., Hou, Y., Wang, H., Li, Y., Zhu, J., et al. (2022b). Application of mesenchymal stem cell-derived exosomes from different sources in intervertebral disc degeneration. *Front. Bioeng. Biotechnol.* 10, 1019437. doi:10.3389/fbioe.2022.1019437

Xia, Y., Yang, R., Zhu, J., Wang, H., Li, Y., Fan, J., et al. (2022a). Engineered nanomaterials trigger abscopal effect in immunotherapy of metastatic cancers. *Front. Bioeng. Biotechnol.* 10, 890257. doi:10.3389/fbioe.2022.890257

Xu, S., Wang, Y., Yu, M., Wang, D., Liang, Y., Chen, Y., et al. (2020). LongShengZhi capsule inhibits doxorubicin-induced heart failure by anti-oxidative stress. *Biomed. Pharmacother.* 123, 109803. doi:10.1016/j.biopha.2019.109803

Yang, Y. K., Xu, H. R., Huang, Z., Li, Y., and Niu, X. H. (2020). Effectiveness and safety of polyethylene glycol liposome doxorubicin in the treatment of osteosarcoma. *Zhonghua zhong liu za zhi Chin. J. Oncol.* 42, 692–696. doi:10.3760/cma.j.cn112152-20190510-00300

Yoo, Y., Yoon, S. J., Kim, S. Y., Lee, D. W., Um, S., Hyun, H., et al. (2018). A local drug delivery system based on visible light-cured glycol chitosan and doxorubicin·hydrochloride for thyroid cancer treatment *in vitro* and *in vivo*. *Drug Deliv.* 25, 1664–1671. doi:10.1080/10717544.2018.1507058

Yoon, S. J., Moon, Y. J., Chun, H. J., and Yang, D. H. (2019). Doxorubicin·Hydrochloride/Cisplatin-Loaded hydrogel/nanosized (2-hydroxypropyl)-beta-cyclodextrin local drug-delivery system for osteosarcoma treatment *in vivo*. *Nanomater. (Basel, Switz.* 9, 1652. doi:10.3390/nano9121652

Zhang, H., Zhu, J., Fang, T., Li, M., Chen, G., and Chen, Q. (2022b). Supramolecular biomaterials for enhanced cancer immunotherapy. *J. Mater. Chem.* 10, 7183–7193. doi:10.1039/d2tb00048b

Zhang, Z., Tan, X., Jiang, Z., Wang, H., and Yuan, H. (2022a). Immune checkpoint inhibitors in osteosarcoma: A hopeful and challenging future. *Front. Pharmacol.* 13, 1031527. doi:10.3389/fphar.2022.1031527

Zhao, Z., Hua, Z., Luo, X., Li, Y., Yu, L., Li, M., et al. (2022). Application and pharmacological mechanism of methotrexate in rheumatoid arthritis. *Biomed. Pharmacother. = Biomedecine Pharmacother.* 150, 113074. doi:10.1016/j.biopha.2022.113074

Zhu, Y., Hu, Y., Tang, C., Guan, X., and Zhang, W. (2022). Platinum-based systematic therapy in triple-negative breast cancer. *Biochimica biophysica acta. Rev. cancer* 1877, 188678. doi:10.1016/j.bbcan.2022.188678

frontiers | Frontiers in Oncology

TYPE Original Research
PUBLISHED 16 November 2023
DOI 10.3389/fonc.2023.1227789

OPEN ACCESS

EDITED BY
Zhiyu Zhang,
Fourth Affiliated Hospital of China Medical University, China

REVIEWED BY
Hao Wu,
Chinese Academy of Sciences (CAS), China
Min Xie,
Ningbo Women and Children's Hospital, China

*CORRESPONDENCE
Shen Jun
sj@njmu.edu.cn
Zou Tian-Ming
zoutianming0@163.com
Shen Cong
congshen@njmu.edu.cn

†These authors have contributed equally to this work

RECEIVED 23 May 2023
ACCEPTED 31 October 2023
PUBLISHED 16 November 2023

CITATION
Chen-Xi G, Jin-Fu X, An-Quan H, Xiao Y, Ying-Hui W, Suo-Yuan L, Cong S, Tian-Ming Z and Jun S (2023) Long non-coding RNA PRR7-AS1 promotes osteosarcoma progression via binding RNF2 to transcriptionally suppress MTUS1. *Front. Oncol.* 13:1227789. doi: 10.3389/fonc.2023.1227789

Long non-coding RNA PRR7-AS1 promotes osteosarcoma progression via binding RNF2 to transcriptionally suppress MTUS1

Gu Chen-Xi[1†], Xu Jin-Fu[2†], Huang An-Quan[1†], Yu Xiao[1†], Wu Ying-Hui[1], Li Suo-Yuan[1], Shen Cong[3*], Zou Tian-Ming[1*] and Shen Jun[1*]

[1]Department of Orthopedic Surgery, The Affiliated Suzhou Hospital of Nanjing Medical University, Suzhou Municipal Hospital, Gusu School, Nanjing Medical University, Suzhou, China, [2]State Key Laboratory of Reproductive Medicine, Department of Histology and Embryology, Nanjing Medical University, Nanjing, China, [3]State Key Laboratory of Reproductive Medicine, Center for Reproduction and Genetics, The Affiliated Suzhou Hospital of Nanjing Medical University, Suzhou Municipal Hospital, Gusu School, Nanjing Medical University, Suzhou, China

Introduction: Osteosarcoma is a common bone malignant tumor in adolescents with high mortality and poor prognosis. At present, the progress of osteosarcoma and effective treatment strategies are not clear. This study provides a new potential target for the progression and treatment of osteosarcoma.

Methods: The relationship between lncRNA PRR7-AS1 and osteosarcoma was analyzed using the osteosarcoma databases and clinical sample testing. Cell function assays and tumor lung metastasis were employed to study the effects of PRR7-AS1 on tumorigenesis *in vivo* and *in vitro*. Potential downstream RNF2 of PRR7-AS1 was identified and explored using RNA pulldown and RIP. The GTRD and KnockTF database were used to predict the downstream target gene, MTUS1, and ChIP-qPCR experiments were used to verify the working mechanismy. Rescue experiments were utilized to confirm the role of MTUS1 in the pathway.

Results: Deep mining of osteosarcoma databases combined with clinical sample testing revealed a positive correlation between lncRNA PRR7-AS1 and osteosarcoma progression. Knockdown of PRR7-AS1 inhibited osteosarcoma cell proliferation and metastasis in vitro and in vivo. Mechanistically, RNA pulldown and RIP revealed that PRR7-AS1 may bind RNF2 to play a cancer-promoting role. ChIP-qPCR experiments were utilized to validate the working mechanism of the downstream target gene MTUS1. RNF2 inhibited the transcription of MTUS1 through histone H2A lysine 119 monoubiquitin. Rescue experiments confirmed MTUS1 as a downstream direct target of PRR7-AS1 and RNF2.

Discussion: We identified lncRNA PRR7-AS1 as an important oncogene in osteosarcoma progression, indicating that it may be a potential target for diagnosis and prognosis of osteosarcoma.

KEYWORDS

LncRNA PRR7-AS1, RNF2, osteosarcoma, histone modification, MTUS1 LncRNA PRR7-AS1, MTUS1

1 Introduction

Osteosarcoma (OS) is a common malignant bone tumor that mainly affects adolescents or children under the age of 20 years (1). OS accounts for approximately 5% of pediatric tumors, and it is a highly malignant tumor in children (2). OS has poor prognosis, and lung metastasis usually occurs within months. It has been reported that the survival of OS patients after amputation ranges from 5 to 20% (3). At present, surgery combined with neoadjuvant radiotherapy and chemotherapy is preferred to treat OS (4). Early diagnosis and timely treatment significantly improve the survival of OS (5). Therefore, it is urgent to elucidate the pathogenesis of OS and to identify more effective therapeutic targets to improve the prognosis of OS.

Long non-coding RNAs (lncRNAs) are non-coding RNAs exceeding 200 bp in length. LncRNAs are unable to directly encode proteins, but they are vital regulators in biological activities via interacting with proteins, DNA and RNA (6). Serving as oncogenes or tumor suppressor genes (7), lncRNAs have been highlighted for their involvement in the development of cancer, including prostate, breast, lung and liver cancers, through chromatin modification, transcriptional regulation and post-transcriptional regulation (8–10). Ding et al. (11) demonstrated that lncRNA CRNDE stimulates the growth of OS through the Wnt/β-catenin signaling pathway. Through downregulating microRNA-765, LINC00511 promotes the proliferation and migration of OS cells (12). Thus, the specific role of lncRNAs in the development of OS and the underlying mechanism should be further explored.

A novel oncogene PRR7-AS1 has been reported that is highly expressed in colorectal cancer (13) and hepatocellular cancer (14). In this study, we showed that lncRNA PRR7-AS1 was upregulated in OS tissues through bioinformatics analysis. The upregulation of PRR7-AS1 was further validated in clinical samples. Subsequently, *in vitro* and *in vivo* experiments demonstrated that PRR7-AS1 promoted the proliferation and migration of OS through binding RNF2, which further inhibited the transcription of the downstream target, MTUS1. The present study identified the oncogenic role of PRR7-AS1 in OS, suggesting its potential application in the clinical treatment of OS.

2 Materials and methods

2.1 Bioinformatics analysis

The GSE126209 dataset, contains RNA sequencing data from OS and normal tissues, was downloaded from Gene Expression Omnibus (GEO, https://www.ncbi.nlm.nih.gov/geo/). The FPKM values were transformed into TPM values and normalized by $\log_2$ (value+1) to further analysis. Afterwards, paired differential expression was analyzed using the R package limma and volcanic maps were draw by ggplot2 ($|FC| > 1$, and adj.p < 0.05).

Clinical and gene expression data of OS patients were obtained from the Tumor Alterations Relevant for Genomics-driven Therapy (TARGET) database. Patient samples (n=85) were divided into high and low groups based on the median of expression values, and survival curves were plotted by the "survival" package in R.

Putative RNF2 targets were predicted using the Gene Transcription Regulation Database (GTRD, http://gtrd.biouml.org) and the KnockTF Database (http://www.licpathway.net/KnockTF/index.php).

2.2 Sample collection

OS and adjacent non-tumoral bone tissues were collected from patients who were surgically treated at the Suzhou Municipal Hospital of Nanjing Medical University. Clinical samples were surgically collected, immediately fixed, dehydrated and embedded in paraffin. Written informed consent was obtained prior to sample collection, and this study was approved by the Ethics Committee of Suzhou Municipal Hospital.

2.3 Fluorescence *in situ* hybridization analysis

A specific FISH probe targeting PRR7-AS1 was designed and synthesized by Ribobio Biotechnology (Guangzhou, China). The hybridization was performed in OS tissue and paired adjacent non-tumoral tissues as previously reported (15). All images were analyzed on a confocal laser scanning microscope (LSM 810, Carl Zeiss, Oberkochen, Germany) (16).

2.4 Cell culture

The human osteosarcoma cell lines, 143B and U2OS, were obtained from the Institute of Biochemistry and Cell Biology of the Chinese Academy of Sciences (Shanghai, China). U2OS cells were cultured in Dulbecco's modified Eagle's medium (DMEM) (Gibco, NY, USA) supplemented with 10% fetal bovine serum (FBS) (ExCell Bio, New Zealand) and 1% penicillin/streptomycin (NCM Biotech, Suzhou, China), and 143B cells were cultured in Eagle's Minimum Essential Medium (EMEM) (Gibco) supplemented with 82% minimal essential medium (MEM), 15% FBS, 1% GlutaMAX, 1% sodium pyruvate and 1% penicillin/streptomycin. Cells were cultured in a humidified incubator with 5% CO2 and 95% air at 37°C.

2.5 Cell transfection

The small interfering RNAs (siRNAs) targeting PRR7-AS1, RNF2, MTUS1 and negative control and pcDNA3.1-PRR7-AS1

Abbreviations: OS, Osteosarcoma; lncRNA, long non-coding RNAs; PVT1, plasmacytoma variant translocation 1; RNF2, ring finger protein 2; MTUS1, microtubule associated scaffold protein 1; H2AK119ub, histone H2A lysine 119 monoubiquitin.

were designed by GenePharma (Shanghai, China) and transfected into cells using Lipofectamine 2000 (Invitrogen, USA) as described previously (17). After 48 h, cells were collected for subsequent experiments. The siRNA sequences used in the present study were shown on Table S1.

2.6 RNA extraction and real-time quantitative PCR

Total RNA was extracted from cells using the RNA isolater Total RNA Extraction Reagent (Vazyme, Nanjing, China), which was reverse transcribed into cDNA using the HiScript III RT SuperMix for qPCR (+gDNA wiper) kit (R323-01, Vazyme) as described previously (18, 19). RT-qPCR was performed using SYBR qPCR SuperMix Plus (Novoprotein Scientific Inc., Shanghai, China) and an Applied Biosystems 7500 Real Time PCR System. The primers were shown on Table S2.

2.7 Western blot

Osteosarcoma cells transfected with si-NC/si-PRR7-AS1 were lysed using a radioimmunoprecipitation assay (RIPA, Beyotime, Nantong, China) containing 1% protease inhibitor phenylmethylsulfonyl fluoride (PMSF) (17). After quantified using a bicinchoninic acid (Beyotime) kit, the protein samples were separated by SDS-PAGE (sodium dodecyl sulfate-polyacrylamide gel electrophoresis) and transferred onto polyvinylidene difluoride (PVDF) membranes. The membranes were blocked with 5% skim milk, and then incubated with the anti-RNF2 antibody (Proteintech, Wuhan, Hubei, China) and anti-Tubulin (Beyotime) at 4°C overnight. Secondary antibodies combined with horseradish peroxidase at room temperature were incubated and band signals were visualized by an enhanced chemiluminescent substrate and quantified by Image-Pro Plus (Media Cybernetics, San Diego, CA, USA).

2.8 Cell proliferation and migration assay

Cell Counting Kit-8 (CCK8) assay: cells were seeded into 96-well plate with 2.5×10^3 cells/well. CCK8 (Beyotime) was added into each well at 0, 24, 36, 72, 96 h. Cell viability was detected by measuring the optical density at 450 nm (OD450) using a microplate reader (Bio-Rad Model 680, Richmond, CA, USA).

Colony formation assay: cells were seeded into six-well plate with 1.0×10^3 cells/well and cultured for 14 days. Fresh medium was replaced every 5 days. After 14 days, culture medium was removed, and cells were fixed with methanol and stained with 0.1% crystal violet (Beyotime). Visible colonies were imaged and counted.

Transwell assay: transwell chambers (8 μm pore size; Millipore, Billerica, MA, USA) were added into 24-well plate. Cells at a density of 2.5×10^4 cells/well in 300 μl of serum-free medium were seeded in the upper chamber, and 700 μl of medium containing 10% FBS was added in the bottom chamber. After incubation for 48 h at 37°C, the cells migrated to the bottom were fixed with methanol and stained with 0.1% crystal violet. Finally, five randomly selected fields per sample were imaged using a light microscope for counting migratory cells.

2.9 *In vivo* assay

Four-week-old athymic BALB/c nude mice were habituated in a specific pathogen-free (SPF) environment. Animal experiments were approved by the Ethics Committee of Animal Experiments of Nanjing Medical University. Briefly, 100 μl of suspended 143B cells transfected with sh-PRR7-AS1 or sh-NC at 3×10^7 cells were subcutaneously injected into the mouse axillary region (17). Tumor growth was regularly recorded. After 2 weeks, mice were sacrificed, and OS tissues were collected. The tumor volume was calculated using the following formula: tumor volume (mm^3) = 0.5 × length (mm) × width^2 (mm^2).

For the *in vivo* cell metastasis assay, 100 μl of suspended 143B cells transfected with sh-PRR7-AS1 or sh-NC at 6×10^7 cells was injected into the mouse tail vein. After 2 months, mice were sacrificed, and lung tissues were collected. The number of metastatic lesions in the lung was counted.

Tumor tissues and lung metastasis lesions collected from mice were fixed with 4% paraformaldehyde and dehydrated in gradient concentrations of ethanol. After permeabilization in xylene, sections were embedded in paraffin, sliced into 5-μm-thick sections, deparaffinized with xylene and rehydrated in gradient concentrations of ethanol. Lung metastasis sections were stained with hematoxylin and eosin (H&E) for pathological examination.

2.10 Immunofluorescence

After deparaffinization and rehydration of paraffin-embedded tissues, antigen retrieval was performed by boiling samples in 10 mM sodium citrate buffer (pH 6.0). The sections were blocked with 1% bovine serum albumin (BSA) in PBS and incubated with primary antibodies, and the sections were then incubated with secondary antibodies. Cell nuclei were stained with DAPI (Beyotime), and images were acquired using a Zeiss laser confocal microscope (LSM 810) as previously described (20, 21). The following antibodies were used: mouse monoclonal anti-Ki67 antibody (Abcam, ab238020, 1:100), mouse monoclonal anti-E-cadherin antibody (Abcam, ab231303, 1:100), mouse monoclonal anti-N-cadherin antibody (Abcam, ab76057, 1:100) and mouse monoclonal anti-vimentin antibody (Abcam, ab20346, 1:100).

Isolated and cultured cells were fixed with 4% paraformaldehyde for 20 min. Next, the cells were treated with 0.2% triton for 20 min and blocked with 1% BSA in PBS. Then the slides containing target cells were incubated with primary and Alexa-Fluor secondary antibodies (Thermo Scientific, Waltham, USA) orderly. In addition, the cells were stained with DAPI and observed under a fluorescence microscope. Sections were analyzed under a confocal laser-scanning microscope.

2.11 RNA pull-down

PRR7-AS1 was transcribed using the Ribo™ RNAmax-T7 Biotin Labeling Transcription Kit (Ambio Life). The kit used the Biotin RNA Labeling Mix as a substrate and utilized a DNA template containing the T7 promoter to synthesize RNA complementary to the antisense strand in the DNA template starting downstream of the T7 promoter. Then PRR7-AS1 was purified with the RNeasy Plus Mini Kit (Qiagen) and treated with RNase-free DNase I (Qiagen). Subsequently, transcribed PRR7-AS1 was biotin-labeled with the Biotin RNA Labeling Mix (Ambio Life). RNA pull-down was then performed by PierceTM Magnetic RNA-Protein Pull-Down Kit according to the manufacturer's instructions (Thermo Scientific Pierce) and as previously described (22). The RNA-protein complexes were then subjected to mass spectrometry analysis, as previously described (23–25).

2.12 Chromatin immunoprecipitation-qPCR

ChIP was performed using the EZ-Magna ChIPTM A/G Chromatin Immunoprecipitation Kit (Millipore) as previously described (26). Briefly, transfected OS cells were lysed in 1% methanol and sonicated, which resulted in 500-bp DNA fragments. Cell lysate was incubated with the anti-RNF2 antibody, anti-H2AK119Ub antibody and anti-IgG. The chromatin supernatant was then incubated in 20 μl of protein A/G MagBeads at 4°C overnight. The protein-DNA complex was eluted and purified, and the obtained DNA samples were subjected to RT-qPCR. The primers used for ChIP-qPCR were follows:

MTUS1-F, 5'-AGACTGCGAATCAGCCCTTC-3'
MTUS1-R, 5'-TGCAGAATTATCAGGGCGGAA-3'

2.13 RNA immunoprecipitation

RIP was performed using the Magna RIPTM RNA-Binding Protein Immunoprecipitation Kit (Millipore) as previously described (16). Briefly, OS cells were lysed in RIP lysis buffer, and 100 μl of cell lysate was incubated with the anti-RNF2 antibody and anti-IgG. A protein–RNA complex was captured and digested with 0.5 mg/ml proteinase K containing 0.1% SDS. The magnetic beads were repeatedly washed with RIP washing buffer to remove non-specific adsorption. Finally, the extracted RNA was subjected to RT-qPCR.

2.14 Statistical analysis

All data are expressed as mean ± standard deviation ($\bar{x} \pm s$). GraphPad Prism 9.0 (GraphPad Software, CA, USA) was used for statistical analyses. Differences between two groups were compared by Student's t–test, and those among three or more groups were compared by one–way analysis of variance (ANOVA). Overall survival was estimated by the Kaplan–Meier method, and the log-rank test was employed to evaluate differences. $P<0.05$ was considered as statistically significant.

3 Results

3.1 PRR7-AS1 is upregulated in OS tissues and predicts poor prognosis

A total 19 lncRNAs were differentially expressed in osteosarcoma tissues (n=5) compared with paired normal tissues based on the GEO database (GSE126209) ($|FC| > 1.0$ and adj.$p < 0.01$) (Figure 1A), and 2 of them (PVT1 and PRR7-AS1) had a significant effect on the overall survival of OS patients (n=85) based on the TARGET database (Figure S1). It has been found that PVT1 (plasmacytoma variant translocation 1) could promote human OS malignant biological behaviors (27), but the role of PRR7-AS1 in osteosarcoma remains unknown.

PRR7-AS1 was significantly upregulated in OS tissues (n=5) (Figure 1B), and high PRR7-AS1 expression was associated with poor prognosis in OS patients (Figure 1C). Afterwards, the FISH assay verified the overexpression of PRR7-AS1 in OS tissues compared to non-tumor samples (Figures 1C, D), and it also demonstrated that PRR7-AS1 was mostly expressed in the nucleus (Figures 1C–F). These results suggested that PRR7-AS1 is upregulated in OS and mainly involved in functional regulation in the nucleus.

3.2 PRR7–AS1 promotes the proliferation and migration of OS *in vitro*

The transfection efficiency of si-PRR7-AS1 were verified by RT-qPCR (Figure 2A). Both CCK8 and colony formation assays found that knockdown of PRR7-AS1 significantly inhibited the proliferative capacity of 143B and U2OS cells (Figures 2B–E). In addition, transwell assays revealed a lower migration capacity of OS cells transfected with si-PRR7-AS1 than si-NC (Figures 2F, G). These findings indicated that PRR7-AS1 promotes the proliferation and migration of OS cells *in vitro*.

3.3 PRR7–AS1 promotes tumor growth and metastasis of OS *in vivo*

A xenograft model in nude mice was established to explore the *in vivo* function of PRR7-AS1. During the experimental period, tumor growth was significantly lower in the sh-PRR7-AS1 group compared to the controls. After 2 weeks, mice were sacrificed, and OS tissues were collected. Compared to the control group, both the volume and weight of OS tissues were significantly lower in the sh-PRR7-AS1 group than empty vector group (Figures 3A–C). In addition, the lower Ki-67-positive cells was shown in the sh-PRR7-AS1 group too (Figures 3D, E).

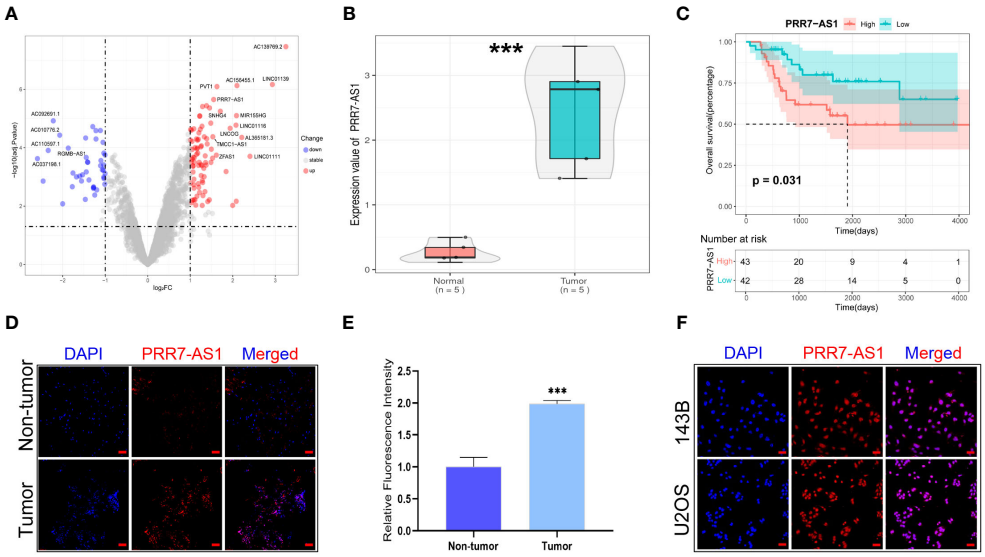

FIGURE 1
Relative PRR7-AS1 expression in osteosarcoma (OS) tissues and cell lines as well as its clinical significance. **(A)** Paired differentially expressed lncRNAs in OC and normal tissues based on GEO datasets (n=5) showed by volcanic map. **(B)** Relative expression of PRR7-AS1 in OC and normal tissues, n = 5. ***P < 0.001. **(C)** Kaplan–Meier curves for overall survival in OS patients (n=85). **(D)** A FISH assay was used to examine the expression and location of lncRNA PRR7-AS1 in OS tissues and paired non-tumor tissues. scale bars: 50 mm. **(E)** Statistical data are shown. **(F)** A FISH assay was used to examine the location of PRR7-AS1 in 143B and U2OS, scale bars: 50 mm. ***P < 0.001.

We established an OS lung metastasis model in nude mice through injecting 143B cells into the mouse tail vein as previously reported (28). Compared to the controls, the number of lung metastases was significantly lower in nude mice injected with 143B cells transfected with sh-PRR7-AS1 (Figures 3F, G). The same results were obtained with H&E staining (Figure 3H). Furthermore, increased E-cadherin as well as decreased N-cadherin and vimentin expression were obviously in the sh-PRR7-AS1 group (Figure 3I–L).

Collectively, these findings demonstrated that PRR7-AS1 promotes the proliferation and metastasis of OS cells *in vivo*.

3.4 PRR7–AS1 interacts with RNF2 in OS cells

To further explore the molecular mechanism underlying the carcinogenic activity of PRR7-AS1 in OS, an RNA pull-down LC-MS/MS assay was performed to identify potential proteins that interact with lncRNA PRR7-AS1 in OS cells (Figure 4A).

According to the label-free quantitation (LFQ) method, proteomic analysis identified 18 overlapping proteins from three independent RNA pull-down experiments (Figure 4B; Table S3). Figure 4C shows the top 10 proteins listed from high to low. Among them, RNF2 (ring finger protein 2) caught our attentions. As a member of the polycomb group (PcG), RNF2 is widely involved in tumor development through epigenetic regulation (29). RNA pull-down and RIP experiments in 143B and U2OS cells further confirmed the interaction between PRR7-AS1 and RNF2 (Figures 4D–F). Strikingly, it was noticed that RNF2 expression levels remained unaltered after knockdown of PRR7-AS1 compared to control (Figures 4G, H). These findings suggest that PRR7-AS1 only binds RNF2, but does not affect its expression.

3.5 RNF2 is involved in gene regulation and promotes the proliferation and migration of OS *in vitro*

We selected U2OS cells for western blotting and immunofluorescence experiments of RNF2. The protein expression of RNF2 was significantly reduced after knockdown of RNF2 (Figures 5A, B). Immunofluorescence analysis showed that RNF2 protein was primarily localized in the nucleus rather than the cytoplasm and could be significantly knocked down (Figures 5C, D), which further verified that RNF2 protein was involved in gene regulation. To explore the oncogenic features of RNF2 in OS, we synthesized two RNF2 siRNAs and verified their transfection efficiency (Figure 5E). Knockdown of RNF2 significantly reduced cell viability and the number of colonies in 143B and U2OS cells, indicating inhibition of proliferation (Figures 5F–I). Moreover, the number of migratory cells was reduced in OS cells transfected with si-RNF2 compared to si-NC (Figures 5J, K). Therefore, these findings suggested that RNF2 facilitates the proliferation and migration of OS cells *in vitro*.

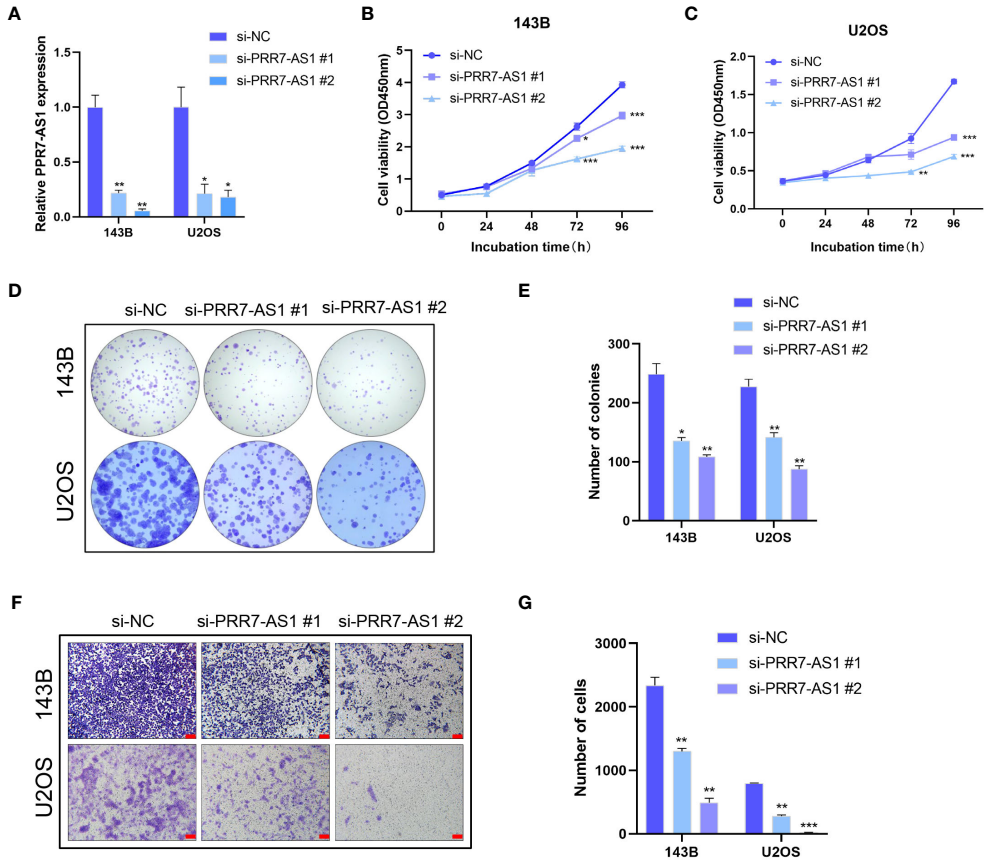

FIGURE 2
Effects of PRR7-AS1 on OS cells proliferation and migration capacity in vitro. **(A)** Relative PRR7-AS1 expression in 143B and U2OS cells transfected with negative control siRNA (si-NC) or siRNAs targeting PRR7-AS1 (si-PRR7-AS1 #1 and #2) for 48 h (n = 3 for each group). **(B, C)** Cell viability was assessed using a CCK8 assay in 143B and U2OS cells transfected with si-NC or si-PRR7-AS1 (n = 6 for each group). *P < 0.05, **P < 0.01 and ***P < 0.001. **(D, E)** Colony formation assays were performed to determine the proliferative ability of si-PRR7-AS1-transfected 143B and U2OS cells (n = 3 for each group). *P < 0.05, **P < 0.01. **(F, G)** Transwell assays were performed to investigate the migration capacity of 143B and U2OS cells after PRR7-AS1 knockdown for 48 h (n = 3 for each group). Scale bar= 100 mm. **P < 0.01, ***P < 0.001.

3.6 "PRR7-AS1-RNF2" inhibits the transcription of MTUS1 through histone H2A lysine 119 monoubiquitin

It has been reported that RNF2 contributes to inhibit gene transcription as a component of the polycomb repressive complex 1 (PRC1) (30). The KnockTF database predicted a total of 14,096 differentially expressed genes after knockdown of RNF2, and 2,778 genes were upregulated (|FC| >1.5). Through screening the ChIP-Seq datasets extracted from the publicly available Sequence Read Archive (SRA), GEO and ENCODE databases by GTRD, a total of 11,407 genes were identified to bind the RNF2 transcription factor, including 23,655 binding peaks. Venn diagram analysis yielded 272 candidate genes that not only bound to RNF2 but also were regulated by RNF2 (Figure 6A). Five of the target genes have been previously reported to have an oncogenic effect on OS cells (Figure 6B). RT-qPCR were performed to further confirm the regulatory effect of RNF2 on these target genes. MTUS1 (microtubule associated scaffold protein 1) was significantly upregulated in both 143B and U2OS cells after knockdown of RNF2 (Figures 6C, D). Therefore, RNF2 might target MTUS1 in OS cells.

RNF2 exerts its biological function in silencing target genes through histone H2A lysine 119 monoubiquitin (H2AK119ub) (31). The RNF2-binding region predicted by the GTRD falls from -2000 to +100 bp of the MTUS1 transcription start point, which is its promoter region (Figure 6E). ChIP-qPCR results showed that RNF2 was significantly recruited in this region (Figures 6F, G). Moreover, MTUS1 mRNA expression was upregulated after PRR7-AS1 silencing in 143B and U2OS (Figure 6H). Knockdown of PRR7-AS1 reduced the recruitment of H2AK119ub to the MTUS1 promoter (Figures 6I, J). Taken together, these findings demonstrated that PRR7-AS1 is required for RNF2 to inhibit the transcription of MTUS1 through H2AK119ub. Furthermore, it is obvious that overexpressing PRR7-AS1 decreased the MTUS1 mRNA level and knockdown of RNF2 reverses this decrease (Figure 6K). This finding demonstrated that PRR7-AS1 inhibit the expression of MTUS1 dependent on RNF2.

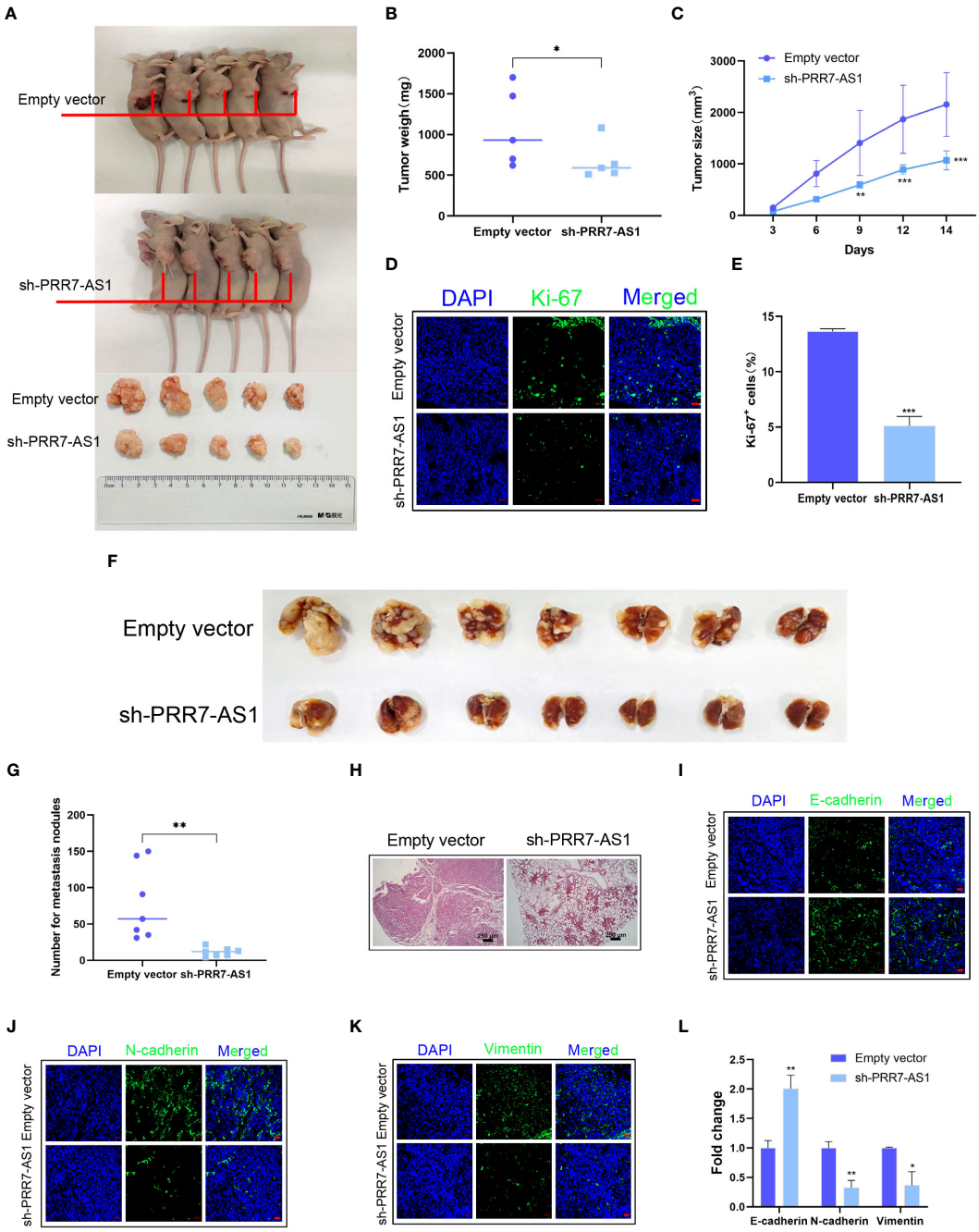

FIGURE 3
Effects of PRR7-AS1 on OS tumorigenesis and metastasis in vivo. 143B cells stably expressing shPRR7-AS1 or empty vector (control) were injected into nude mice (n=5). **(A)** Tumors were isolated from the nude mice and photographed, and tumor weights were measured **(B)**. *P < 0.05 **(C)** Tumor volumes were calculated every 3 days after injection. **P < 0.01, ***P < 0.001. **(D, E)** Immunostaining for the Ki-67+ cells in tumor sections (n = 3 for each group). Scale bar = 50 mm. ***P < 0.001. **(F)** 143B cells were transfected with sh-PRR7-AS1 or empty vector for 48 h and injected into the tail vein of nude mice (n = 7). After 2 months, lung tissues were removed and photographed. **(G)** The number of lung nodules was counted. **(H)** H&E staining of mouse lung tissues. **P < 0.01. **(I–K)** Immunofluorescence staining of E-cadherin, Ncadherin and vimentin, bar = 50 mm. **(L)** Quantification of **(D–F)**. *P < 0.05, **P < 0.01.

3.7 "PRR7-AS1-RNF2" promotes the cell proliferation and migration depend on MTUS1 in OS cells

MTUS1 is a tumor suppressor gene that has been validated to inhibit the proliferation and migration of OS cells. The transfection efficiency of si-MTUS1 were verified by RT-qPRCR (Figure 7A), si-MTUS1 2# was used in the following experiments. 143B and U2OS cells were co-transfected with si-MTUS1 and si-PRR7-AS1/si-RNF2. Interestingly, the proliferative and migration capacities of co-transfected cells were significantly higher than those only transfected with si-PRR7-AS1 or si-RNF2 (Figures 7B–G). These

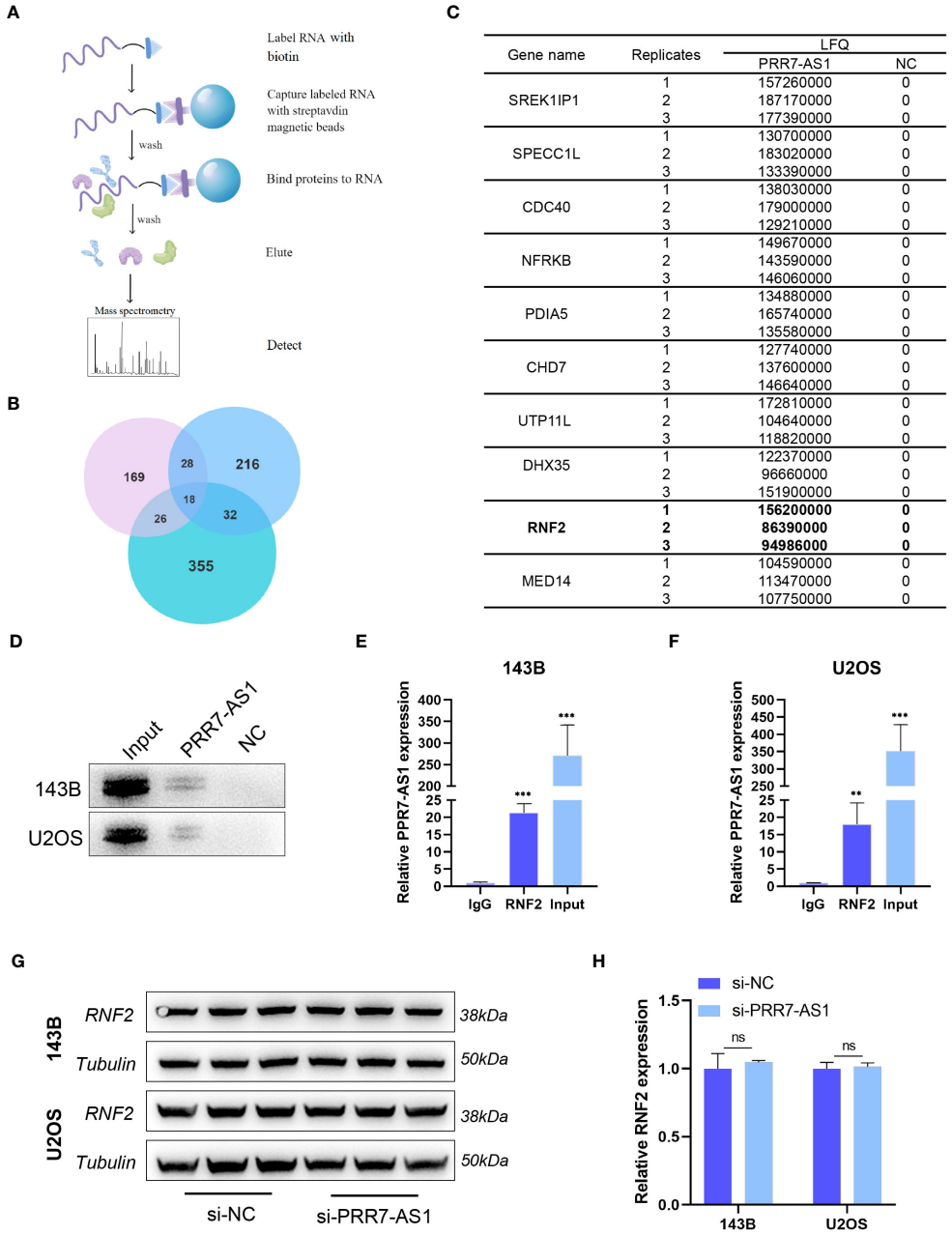

Gene name	Replicates	LFQ	
		PRR7-AS1	NC
SREK1IP1	1	157260000	0
	2	187170000	0
	3	177390000	0
SPECC1L	1	130700000	0
	2	183020000	0
	3	133390000	0
CDC40	1	138030000	0
	2	179000000	0
	3	129210000	0
NFRKB	1	149670000	0
	2	143590000	0
	3	146060000	0
PDIA5	1	134880000	0
	2	165740000	0
	3	135580000	0
CHD7	1	127740000	0
	2	137600000	0
	3	146640000	0
UTP11L	1	172810000	0
	2	104640000	0
	3	118820000	0
DHX35	1	122370000	0
	2	96660000	0
	3	151900000	0
RNF2	**1**	**156200000**	**0**
	2	**86390000**	**0**
	3	**94986000**	**0**
MED14	1	104590000	0
	2	113470000	0
	3	107750000	0

FIGURE 4
PRR7-AS1 interacts with RNF2. **(A)** Flow chart of the RNA pull-down assays. **(B)** Venn diagrams of proteins identified by mass spectrometry from three independent RNA pull-down assays. **(C)** The list of top 10 proteins. **(D)** Biotinylated PRR7-AS1 RNAs were incubated with 143B or U2OS cell lysates. The RNA–protein complexes were subjected to western blot analysis with an anti-RNF2 antibody. The antisense strand of PRR7-AS1 was used as the negative control. **(E, F)** RNA immunoprecipitation (RIP) assays for PRR7-AS1 binding to RNF2 in 143B and U2OS cells lysates. Rabbit IgG was included as the negative control for immunoprecipitation (n = 3). **P < 0.01 and ***P < 0.001. **(G)** The protein level of RNF2 were detected in 143B and U2OS transfected with si-NC and si-PRR7-AS1 using western blotting (n = 3). **(H)** Quantification of **(G)**. ns, not statistically significant.

findings indicated that knockdown of MTUS1 reverses the inhibited proliferation and migration of OS cells caused by knockdown of PRR7-AS1 and RNF2.

4 Discussion

OS is a common malignant tumor that mainly occurs in children and adolescents (32), and it is characterized by rapid progression, high metastasis rate and high mortality. At present, the precise pathogenesis of OS has not been fully elucidated. Surgery combined with adjuvant chemoradiotherapy is the main treatment of OS. Because early diagnosis is of significance to improve the prognosis, it is urgent to identify effective biomarkers for the diagnosis and management of OS. LncRNAs have been suggested to have clinical potential, and they are involved in cancer development (11, 12). In the present study, we first identified that PRR7-AS1 was upregulated in OS tissues, and high expression of

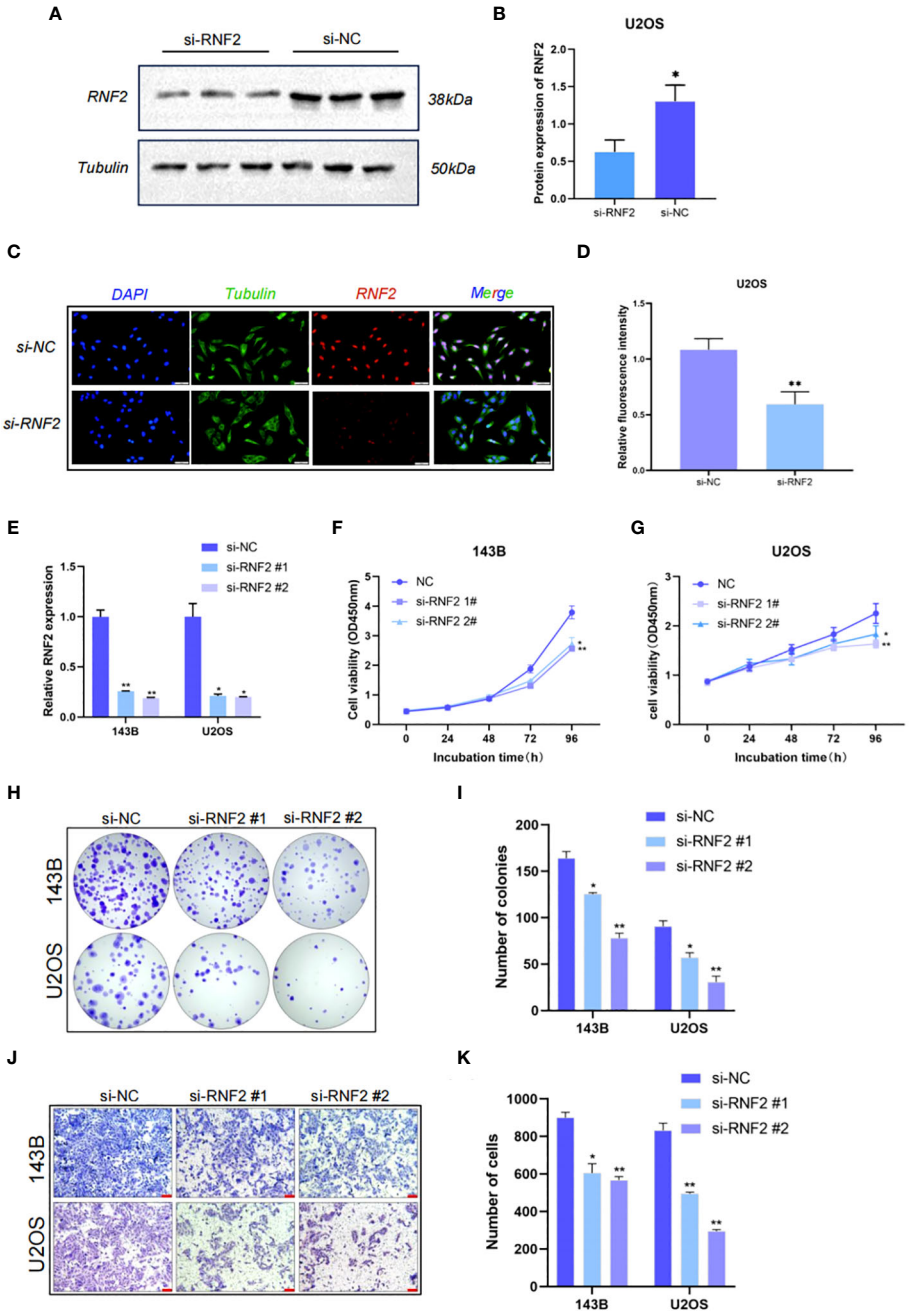

FIGURE 5
RNF2 is involved in gene regulation and promotes the proliferation and migration of OS in vitro. **(A)** Western blot analysis of RNF2 protein after the treatment with si-RNF2 or si-NC. Beta-tubulin protein was used as an internal control. **(B)** Quantification of RNF2 protein levels in **(A)**, n = 3. *P < 0.05. **(C)** Immunostaining of RNF2 in U2OS treated with si-NC or si-RNF2. RNF2 marker proteins are labeled in red, Tubulin marker proteins are labeled in green and nucleus are labeled in blue. **(D)** Quantitative immunofluorescence of RNF2 marker proteins in **(C)**, n = 3. **P < 0.01. **(E)** RT-qPCR analysis was used to detect the relative RNF2 mRNA expression levels after transfection with si-RNF2 (n = 3). *P < 0.05, **P < 0.01. **(F–K)** CCK8 (n = 6) **(F, G)**, colony formation (n = 3) **(H, I)** and transwell (n = 3, scale bar = 100 mm) **(J, K)** assays were used to assess the proliferative and migration capacity of 143B and U2OS cells transfected with si-NC or si-RNF2. *P < 0.05, **P < 0.01.

PRR7-AS1 indicated a poorer prognosis in OS through bioinformatics analysis. Subsequently, loss-function-assays demonstrated lncRNA PRR7-AS1 is a vital oncogene involved in the development of OS.

The biological functions of lncRNAs are diverse and complex with the involvement of multiple mechanisms, and lncRNAs regulate signaling pathways and serve as molecular decoys, guiding molecules and structural scaffolds (33, 34). In the present study, RNA pull-down was performed to search for proteins that interact with RPP7-AS1. Among them, increasing evidence has shown that RNF2 contributes to influence clinical characteristics of many types of cancers, including hepatocellular carcinoma,

10.3389/fonc.2023.1227789

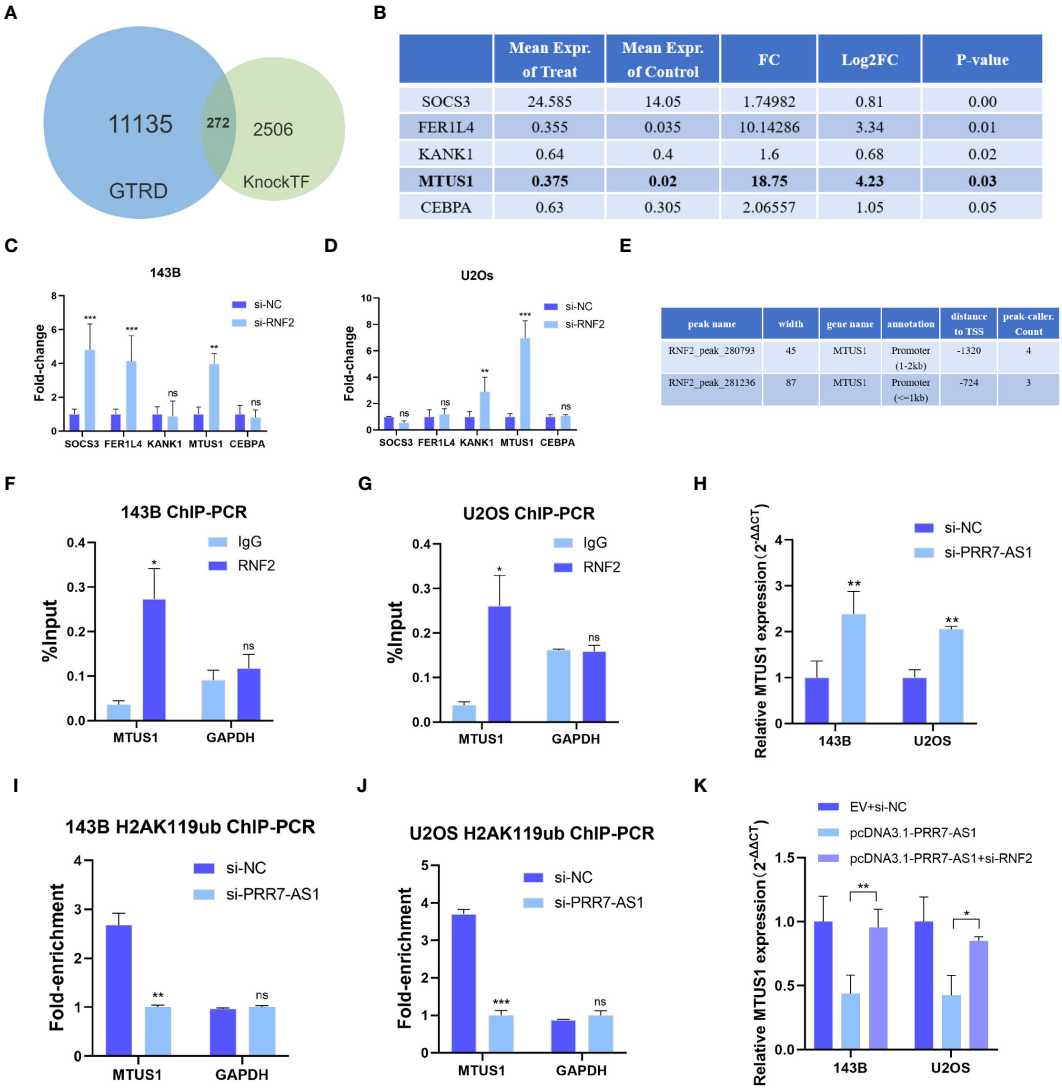

	Mean Expr. of Treat	Mean Expr. of Control	FC	Log2FC	P-value
SOCS3	24.585	14.05	1.74982	0.81	0.00
FER1L4	0.355	0.035	10.14286	3.34	0.01
KANK1	0.64	0.4	1.6	0.68	0.02
MTUS1	**0.375**	**0.02**	**18.75**	**4.23**	**0.03**
CEBPA	0.63	0.305	2.06557	1.05	0.05

peak name	width	gene name	annotation	distance to TSS	peak-caller. Count
RNF2_peak_280793	45	MTUS1	Promoter (1-2kb)	-1320	4
RNF2_peak_281236	87	MTUS1	Promoter (<=1kb)	-724	3

FIGURE 6
RNF2 inhibits the transcription of MTUS1. **(A)** Venn diagram analysis of putative RNF2 targets from the GTRD and KnockTF database. **(B)** Gene list of selected RNF2 targets (data from KnockTF). **(C, D)** RT-qPCR analysis was used to assess the mRNA levels of candidate genes after RNF2 knockdown in OS cells. **P < 0.01, ***P < 0.001. ns, not statistically significant. **(E)** Putative binding peaks of RNF2 on MTUS1 (data from GTRD). **(F, G)** ChIP-qPCR of RNF2-associated DNA sequences from the RNF2- binding region of the MTUS1 promoter in OS cells. The GAPDH gene was used as a negative control. **(H)** RT-qPCR analysis was used to assess the mRNA levels of MTUS1 after PRR7-AS1 knockdown in OS cells. **(I, J)** ChIP-PCR of H2AK119ub-associated DNA sequences in the putative RNF2- binding region of the MTUS1 promoter in OS cells treated with si-NC and si-PRR7-AS1. The GAPDH gene was used as a negative control. **(K)** Relative MTUS1 mRNA level was tested in 143B and U2OS transfected with EV + si-NC, pcDNA3.1-PRR7-AS1, and pcDNA3.1-PRR7-AS1 + si-RNF2 via RTqPCR (n = 3). *P < 0.05, **P < 0.01 and ***P < 0.001. ns, not statistically significant.

melanoma, prostate cancer, breast cancer, pancreatic cancer, gastric cancer and bladder urothelial carcinoma (29, 35, 36). RNA-pulldown-western-blot and RIP-PCR were verified this interaction. Through Western blot analysis, we suggest that PRR7-AS1 does not affect the expression of RNF2, which is likely to recruit RNF2 to their target sites. In addition, immunofluorescence analysis confirmed that RNF2 proteins were mainly localized in the nucleus, suggesting that RNF2 appears to be involved in gene regulation in OS cells.

The loss-function-assay has confirmed that RNF2 promoted the proliferation and migration of OS cells. We hypothesized that RNF2 forms a protein complex with PRR7-AS1, which further localizes to a specific DNA sequence to regulate the transcription of downstream genes. We next searched for downstream targets of RNF2 using the GTRD and KnockTF database. Through collecting uniformly processed ChIP-seq data from the SRA, GEO and ENCODE databases, GTRD identifies transcription factor binding sites (TFBS) and their motifs via peak calling. KnockTF is a comprehensive human gene expression profile database with TF knockdown/knockout (KnockTF), which provides a human gene expression profile dataset associated with TF knockdown/knockout and annotates TFs and their target genes in tissues or cells. Because the RNF2 oncogene exerts the inhibitory effect on gene transcription through H2AK119ub (37, 38), a total of 272 candidate genes who upregulated after RNF2 knockdown were identified.

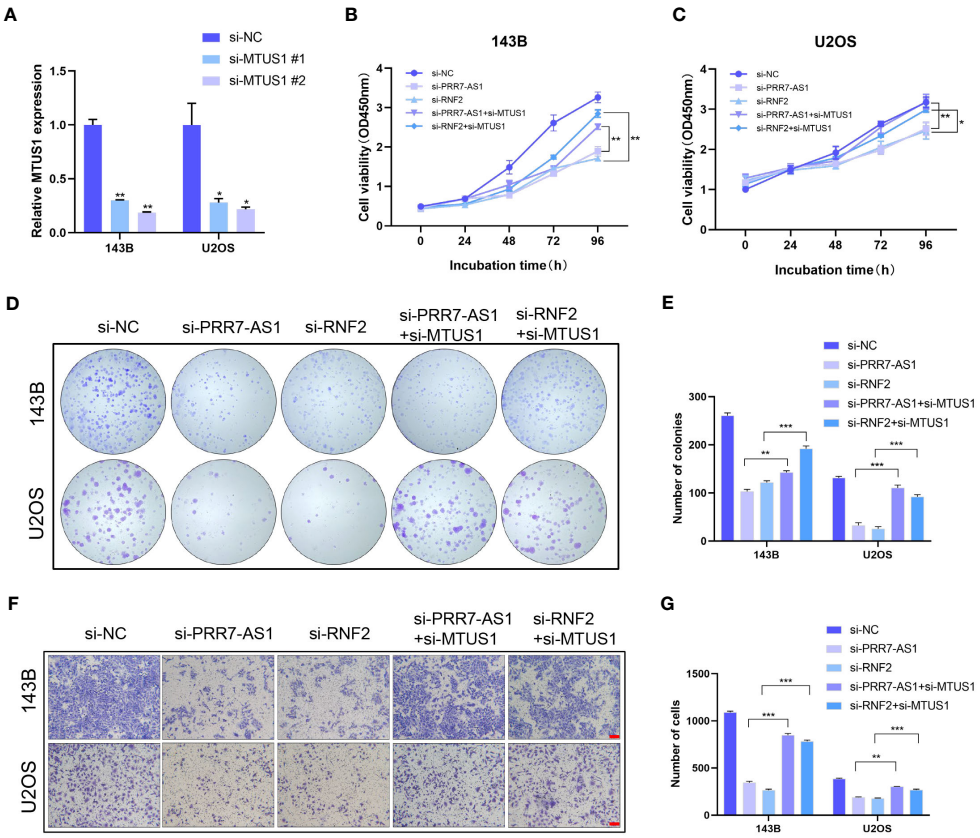

FIGURE 7
Knockdown of MTUS1 reverses the regulatory effect of PRR7-AS1 and RNF2 on OS cell behaviors. **(A)** Relative expression levels of MTUS1 in 143B and U2OS cells transfected with si-NC, si-MTUS1 were detected by RT-qPCR. *P < 0.05, **P < 0.01. **(B–E)** After co-transfection with si-MTUS1 and si-PRR7-AS1 or si-RNF2 for 48 h, the proliferative ability of OS cells was detected using CCK8 assays (n = 6) and colony formation assay (n = 3). *P < 0.05, **P < 0.01 and ***P < 0.001. **(F)** The cell migration in 143B and U2OS cells was detected by Transwell assays, n = 3, scale bar = 100 mm. **(G)** Quantification of **(F)**. **P < 0.01, ***P < 0.001.

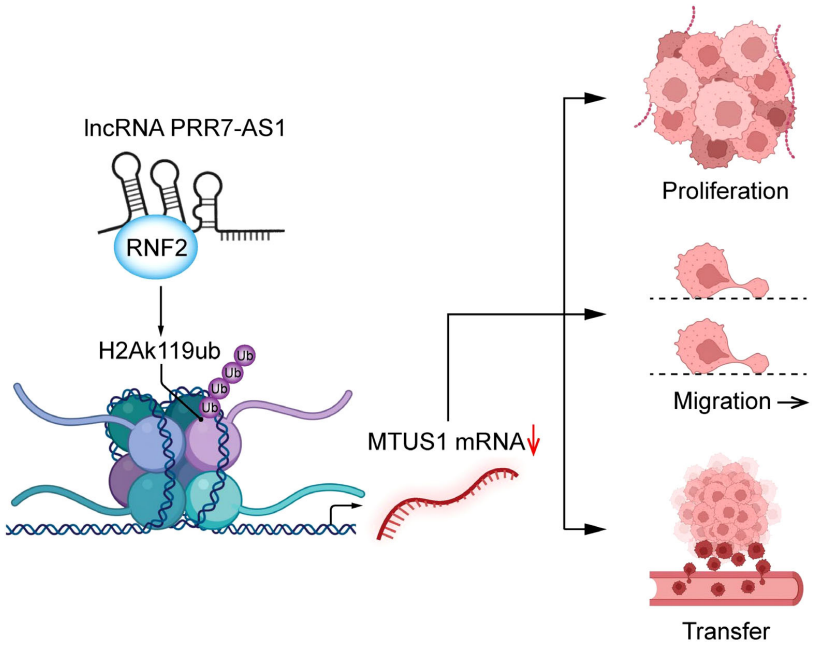

FIGURE 8
Schematic diagram of lncRNA PRR7-AS1 functions to promote tumor proliferation, migration and metastasis in OS cells.

Based on these findings and a literature review, MTUS1 was selected as the potential downstream target of RNF2, which has been demonstrated to be a tumor suppressor gene. MTUS1 is located on the human chromosome antisense strand 8p22, and it encodes a protein containing a C-terminal domain that interacts with the angiotensin II (AT2) receptor (39). Abnormally expressed MTUS1 is closely linked with colorectal cancer and prostate cancer (40, 41). In addition, MTUS1 promotes the development of OS through regulating the ERK/EMT signaling pathway (42). Knockdown of either PRR7-AS1 or RNF2 in OS cells significantly upregulated MTUS1, which indicated an inhibitory effect of the protein complex formed by PRR7-AS1 and RNF2 on the downstream target. In addition, knockdown of PRR7-AS1 significantly reduced the enrichment of H2AK119ub, suggesting that through binding RNF2, PRR7-AS1 induces the binding of RNF2 in the promoter region of the MTUS1 downstream gene, thus triggering the monoubiquitin of H2AK119 and inhibiting the transcription of MTUS1. Vitally, the capacity of RNF2 to bind and suppress the transcription of MTUS1 depended on PRR7-AS1, and PRR7-AS1 suppress the transcription of MTUS1 through targeting RNF2. Furthermore, this study revealed that knockdown of MTUS1 reversed the regulatory effect of PRR7-AS1 and RNF2 on OS cells behaviors, validating the anti-cancer role of MTUS1 in OS.

Taken together, our findings demonstrated that PRR7-AS1 is upregulated in OS tissues and is closely linked with the survival and prognosis of OS patients. PRR7-AS1 promotes the proliferation and migration of OS cells by binding RNF2, thereby inhibiting the transcription of MTUS1 through H2AK119ub (Figure 8). In summary, the PRR7-AS1/RNF2/MTUS1 axis promotes proliferation and migration of OS cells. Therefore, our study provides a novel biomarker that may be utilized in a lncRNA-guided therapeutic strategy for OS.

Data availability statement

The datasets presented in this study can be found in online repositories. The names of the repository/repositories and accession number(s) can be found in the article/Supplementary Material.

Ethics statement

The studies involving humans were approved by Ethics Committee of Suzhou Municipal Hospital. The studies were conducted in accordance with the local legislation and institutional requirements. The participants provided their written informed consent to participate in this study. The animal study was approved by Ethics Committee of Animal Experiments of Nanjing Medical University. The study was conducted in accordance with the local legislation and institutional requirements.

Author contributions

GC-X: Investigation, Data curation, Writing – original draft, Formal analysis. XJ-F: Investigation, Validation, Visualization. HA-Q: Investigation, Data curation, Methodology. YX: Investigation, Data curation, Writing – review & editing. WY-H: Investigation, Data curation. LS-Y: Investigation. SC: Supervision, Project administration. ZT-M: Supervision, Project administration, Funding acquisition. SJ: Conceptualization, Funding acquisition. All authors contributed to the article and approved the submitted version.

Funding

The author(s) declare that financial support was received for the research, authorship, and/or publication of this article. Grants from grants from the Gusu Health Talent Project of Suzhou (GSWS2020056), the "333" Talent Project of Jiangsu (BRA2017057) funded by the Jiangsu province government and the Key Disease Diagnosis and Treatment Technology Special Project of Suzhou, China (LCZX201910).

Conflict of interest

The authors declare that the research was conducted in the absence of any commercial or financial relationships that could be construed as a potential conflict of interest.

Publisher's note

Supplementary material

The Supplementary Material for this article can be found online at: https://www.frontiersin.org/articles/10.3389/fonc.2023.1227789/full#supplementary-material

SUPPLEMENTARY FIGURE 1
Kaplan–Meier curves of differentially expressed lncRNAs.

References

1. Kelleher FC, O'Sullivan H. Monocytes, macrophages, and osteoclasts in osteosarcoma. *J Adolesc Young Adult Oncol* (2017) 6(3):396–405. doi: 10.1089/jayao.2016.0078

2. Miller KD, Fidler-Benaoudia M, Keegan TH, Hipp HS, Jemal A, Siegel RL. Cancer statistics for adolescents and young adults, 2020. *CA Cancer J Clin* (2020) 70(6):443–59. doi: 10.3322/caac.21637

3. Zhang Y, Zhang L, Zhang G, Li S, Duan J, Cheng J, et al. Osteosarcoma metastasis: prospective role of ezrin. *Tumour Biol* (2014) 35(6):5055–9. doi: 10.1007/s13277-014-1799-y

4. Meazza C, Scanagatta P. Metastatic osteosarcoma: a challenging multidisciplinary treatment. *Expert Rev Anticancer Ther* (2016) 16(5):543–56. doi: 10.1586/14737140.2016.1168697

5. Yang C, Tian Y, Zhao F, Chen Z, Su P, Li Y, et al. Bone microenvironment and osteosarcoma metastasis. *Int J Mol Sci* (2020) 21(19):6985. doi: 10.3390/ijms21196985

6. Quinn JJ, Chang HY. Unique features of long non-coding RNA biogenesis and function. *Nat Rev Genet* (2016) 17(1):47–62. doi: 10.1038/nrg.2015.10

7. Bhan A, Soleimani M, Mandal SS. Long noncoding RNA and cancer: A new paradigm. *Cancer Res* (2017) 77(15):3965–81. doi: 10.1158/0008-5472.CAN-16-2634

8. Yang L, Peng X, Li Y, Zhang X, Ma Y, Wu C, et al. Long non-coding RNA HOTAIR promotes exosome secretion by regulating RAB35 and SNAP23 in hepatocellular carcinoma. *Mol Cancer* (2019) 18(1):78. doi: 10.1186/s12943-019-0990-6

9. Bhan A, Hussain I, Ansari KI, Kasiri S, Bashyal A, Mandal SS. Antisense transcript long noncoding RNA (lncRNA) HOTAIR is transcriptionally induced by estradiol. *J Mol Biol* (2013) 425(19):3707–22. doi: 10.1016/j.jmb.2013.01.022

10. Moiola CP, De Luca P, Zalazar F, Cotignola J, Rodríguez-Seguí SA, Gardner K, et al. Prostate tumor growth is impaired by CtBP1 depletion in high-fat diet-fed mice. *Clin Cancer Res* (2014) 20(15):4086–95. doi: 10.1158/1078-0432.CCR-14-0322

11. Ding Q, Mo F, Cai X, Zhang W, Wang J, Yang S, et al. LncRNA CRNDE is activated by SP1 and promotes osteosarcoma proliferation, invasion, and epithelial-mesenchymal transition via Wnt/β-catenin signaling pathway. *J Cell Biochem* (2020) 121(5-6):3358–71. doi: 10.1002/jcb.29607

12. Yan L, Wu X, Liu Y, Xian W. LncRNA Linc00511 promotes osteosarcoma cell proliferation and migration through sponging miR-765. *J Cell Biochem* (2018) 120 (5):7248–56. doi: 10.1002/jcb.27999

13. Lu Y, Wang W, Liu Z, Ma J, Zhou X, Fu W. Long non-coding RNA profile study identifies a metabolism-related signature for colorectal cancer. *Mol Med* (2021) 27 (1):83. doi: 10.1186/s10020-021-00343-x

14. Lu Y, Chen S, Wang Q, Zhang J, Pei X. PRR7-AS1 correlates with immune cell infiltration and is a diagnostic and prognostic marker for hepatocellular carcinoma. *J Oncol* (2022) 2022:1939368. doi: 10.1155/2022/1939368

15. Cai J, Chen Z, Wang J, Wang J, Chen X, Liang L, et al. circHECTD1 facilitates glutaminolysis to promote gastric cancer progression by targeting miR-1256 and activating beta-catenin/c-Myc signaling. *Cell Death Dis* (2019) 10(8):576. doi: 10.1038/s41419-019-1814-8

16. Zhou J-Y, Liu J-Y, Tao Y, Chen C, Liu S-L. LINC01526 promotes proliferation and metastasis of gastric cancer by interacting with TARBP2 to induce GNG7 mRNA decay. *Cancers (Basel)* (2022) 14(19):4940. doi: 10.3390/cancers14194940

17. Wang Q, Wu Y, Lin M, Wang G, Liu J, Xie M, et al. BMI1 promotes osteosarcoma proliferation and metastasis by repressing the transcription of SIK1. *Cancer Cell Int* (2022) 22(1):136. doi: 10.1186/s12935-022-02552-8

18. Gao T, Lin M, Shao B, Zhou Q, Wang Y, Chen X, et al. BMI1 promotes steroidogenesis through maintaining redox homeostasis in mouse MLTC-1 and primary Leydig cells. *Cell Cycle* (2020) 19(15):1884–98. doi: 10.1080/15384101.2020.1779471

19. Zhao D, Shen C, Gao T, Li H, Guo Y, Li F, et al. Myotubularin related protein 7 is essential for the spermatogonial stem cell homeostasis via PI3K/AKT signaling. *Cell Cycle* (2019) 18(20):2800–13. doi: 10.1080/15384101.2019.1661174

20. Zhang K, Xu J, Ding Y, Shen C, Lin M, Dai X, et al. BMI1 promotes spermatogonia proliferation through epigenetic repression of Ptprm. *Biochem Biophys Res Commun* (2021) 583:169–77. doi: 10.1016/j.bbrc.2021.10.074

21. Zheng B, Yu J, Guo Y, Gao T, Shen C, Zhang X, et al. Cellular nucleic acid-binding protein is vital to testis development and spermatogenesis in mice. *Reproduction* (2018) 156(1):59–69. doi: 10.1530/REP-17-0666

22. Zhou J, Li J, Qian C, Qiu F, Shen Q, Tong R, et al. LINC00624/TEX10/NF-kappaB axis promotes proliferation and migration of human prostate cancer cells. *Biochem Biophys Res Commun* (2022) 601:1–8. doi: 10.1016/j.bbrc.2022.02.078

23. Liu Y, Yu X, Huang A, Zhang X, Wang Y, Geng W, et al. INTS7-ABCD3 interaction stimulates the proliferation and osteoblastic differentiation of mouse bone marrow mesenchymal stem cells by suppressing oxidative stress. *Front Physiol* (2021) 12:758607. doi: 10.3389/fphys.2021.758607

24. Zheng B, Zhao D, Zhang P, Shen C, Guo Y, Zhou T, et al. Quantitative proteomics reveals the essential roles of stromal interaction molecule 1 (STIM1) in the testicular cord formation in mouse testis. *Mol Cell Proteomics* (2015) 14(10):2682–91. doi: 10.1074/mcp.M115.049569

25. Zhou Q, Guo Y, Zheng B, Shao B, Jiang M, Wang G, et al. Establishment of a proteome profile and identification of molecular markers for mouse spermatogonial stem cells. *J Cell Mol Med* (2015) 19(3):521–34. doi: 10.1111/jcmm.12407

26. Yu J, Wu Y, Li H, Zhou H, Shen C, Gao T, et al. BMI1 drives steroidogenesis through epigenetically repressing the p38 MAPK pathway. *Front Cell Dev Biol* (2021) 9:665089. doi: 10.3389/fcell.2021.665089

27. Wu T, Ji Z, Lin H, Wei B, Xie G, Ji G, et al. Noncoding RNA PVT1 in osteosarcoma: The roles of lncRNA PVT1 and circPVT1. *Cell Death Discovery* (2022) 8 (1):456. doi: 10.1038/s41420-022-01192-1

28. Xie M, Ma T, Xue J, Ma H, Sun M, Zhang Z, et al. The long intergenic non-protein coding RNA 707 promotes proliferation and metastasis of gastric cancer by interacting with mRNA stabilizing protein HuR. . *Cancer Lett* (2019) 443:67–79. doi: 10.1016/j.canlet.2018.11.032

29. Rai K, Akdemir KC, Kwong LN, Fiziev P, Wu CJ, Keung EZ, et al. Dual roles of RNF2 in melanoma progression. *Cancer Discovery* (2015) 5(12):1314–27. doi: 10.1158/2159-8290.CD-15-0493

30. Morey L, Santanach A, Blanco E, Aloia L, Nora EP, Bruneau BG, et al. Polycomb regulates mesoderm cell fate-specification in embryonic stem cells through activation and repression mechanisms. *Cell Stem Cell* (2015) 17(3):300–15. doi: 10.1016/j.stem.2015.08.009

31. Wang H, Wang L, Erdjument-Bromage H, Vidal M, Tempst P, Jones RS, et al. Role of histone H2A ubiquitination in Polycomb silencing. *Nature* (2004) 431 (7010):873–8. doi: 10.1038/nature02985

32. Gu Q, Luo Y, Chen C, Jiang D, Huang Q, Wang X. GREM1 overexpression inhibits proliferation, migration and angiogenesis of osteosarcoma. *Exp Cell Res* (2019) 384(1):111619. doi: 10.1016/j.yexcr.2019.111619

33. Cao L, Zhang P, Li J, Wu M. LAST, a c-Myc-inducible long noncoding RNA, cooperates with CNBP to promote CCND1 mRNA stability in human cells. *Elife* (2017) 6:e30433. doi: 10.7554/eLife.30433

34. Wang KC, Chang HY. Molecular mechanisms of long noncoding RNAs. *Mol Cell* (2011) 43(6):904–14. doi: 10.1016/j.molcel.2011.08.018

35. Chen Y, Cao XY, Li YN, Qiu YY, Li YN, Li W, et al. Reversal of cisplatin resistance by microRNA-139-5p-independent RNF2 downregulation and MAPK inhibition in ovarian cancer. *Am J Physiol Cell Physiol* (2018) 315(2):C225–C35. doi: 10.1152/ajpcell.00283.2017

36. Bosch A, Panoutsopoulou K, Corominas JM, Gimeno R, Moreno-Bueno G, Martín-Caballero J, et al. The Polycomb group protein RING1B is overexpressed in ductal breast carcinoma and is required to sustain FAK steady state levels in breast cancer epithelial cells. *Oncotarget* (2014) 5(8):2065–76. doi: 10.18632/oncotarget.1779

37. Chan HL, Beckedorff F, Zhang Y, Garcia-Huidobro J, Jiang H, Colaprico A, et al. Polycomb complexes associate with enhancers and promote oncogenic transcriptional programs in cancer through multiple mechanisms. *Nat Commun* (2018) 9(1):3377. doi: 10.1038/s41467-018-05728-x

38. Liu H, Xing R, Ou Z, Zhao J, Hong G, Zhao TJ, et al. G-protein-coupled receptor GPR17 inhibits glioma development by increasing polycomb repressive complex 1-mediated ROS production. *Cell Death Dis* (2021) 12(6):610. doi: 10.1038/s41419-021-03897-0

39. Di Benedetto M, Bieche I, Deshayes F, Vacher S, Nouet S, Collura V, et al. Structural organization and expression of human MTUS1, a candidate 8p22 tumor suppressor gene encoding a family of angiotensin II AT2 receptor-interacting proteins. *ATIP. Gene* (2006) 380(2):127–36. doi: 10.1016/j.gene.2006.05.021

40. Zuern C, Heimrich J, Kaufmann R, Richter KK, Settmacher U, Wanner C, et al. Down-regulation of MTUS1 in human colon tumors. *Oncol Rep* (2010) 23(1):183–9. doi: 10.3892/or_00000621

41. Louis SN, Chow L, Rezmann L, Krezel MA, Catt KJ, Tikellis C, et al. Expression and function of ATIP/MTUS1 in human prostate cancer cell lines. *Prostate* (2010) 70 (14):1563–74. doi: 10.1002/pros.21192

42. Lv DB, Zhang JY, Gao K, Yu ZH, Sheng WC, Yang G, et al. MicroRNA-765 targets MTUS1 to promote the progression of osteosarcoma via mediating ERK/EMT pathway. *Eur Rev Med Pharmacol Sci* (2019) 23(11):4618–28. doi: 10.26355/eurrev_201906_18040

frontiers | Frontiers in Pharmacology

TYPE Original Research
PUBLISHED 06 December 2023
DOI 10.3389/fphar.2023.1324339

OPEN ACCESS

EDITED BY
Duoyi Zhao,
Fourth Affiliated Hospital of China Medical University, China

REVIEWED BY
Giuliano Marchetti Bedoschi,
University of Sao Paulo, Brazil
Seiji Takashima,
Shinshu University, Japan

*CORRESPONDENCE
Teppei Takeshima,
teppei_t@yokohama-cu.ac.jp

RECEIVED 19 October 2023
ACCEPTED 24 November 2023
PUBLISHED 06 December 2023

CITATION
Takeshima T, Mimura N, Aoki S, Saito T, Karibe J, Usui K, Kuroda S, Komeya M and Yumura Y (2023), Pre- and post-chemotherapy spermatogenesis in male patients with malignant bone and soft tissue tumors.
Front. Pharmacol. 14:1324339.
doi: 10.3389/fphar.2023.1324339

Pre- and post-chemotherapy spermatogenesis in male patients with malignant bone and soft tissue tumors

Teppei Takeshima[1]*, Noboru Mimura[1], Shun Aoki[1], Tomoki Saito[1,2], Jurii Karibe[1,3], Kimitsugu Usui[1,4], Shinnosuke Kuroda[1,5], Mitsuru Komeya[1,6] and Yasushi Yumura[1]

[1]Department of Urology, Reproduction Center, Yokohama City University Medical Center, Yokohama, Kanagawa, Japan, [2]Department of Urology, Saiseikai Yokohama City Nanbu Hospital, Yokohama, Kanagawa, Japan, [3]Department of Urology, Sagami Rinkan Hospital, Sagamihara, Kanagawa, Japan, [4]Department of Urology, Kanagawa Cancer Center, Yokohama, Kanagawa, Japan, [5]Glickman Kidney and Urological Institute, Cleveland Clinic Foundation, Cleveland, OH, United States, [6]Department of Urology, Yokohama City University Hospital, Yokohama, Kanagawa, Japan

Introduction: Malignant bone and soft tissue tumors, commonly called sarcomas, predominantly originate in bone and soft tissues and typically affect individuals at a younger age. Following the resection of the primary tumor, treatment often necessitates radiation therapy and gonadotoxic chemotherapy, the specifics of which depend on the disease's stage Conversely, there is a notable concern regarding the potential loss of fertility due to these treatments. Consequently, it is recommended that men consider sperm cryopreservation before initiating treatment. This study aims to assess spermatogenesis in male patients diagnosed with malignant bone and soft tissue tumors before and after chemotherapy.

Methods: This study involved 34 male patients diagnosed with malignant bone and soft tissue tumors and subsequently underwent sperm cryopreservation before initiating treatment. Medical records included details about the primary disease, age, marital status at presentation, semen analysis results, treatment regimen and number of courses, post-treatment semen analysis, renewal status and outcomes.

Results: The mean age at the time of sperm cryopreservation was 22.8 years. The median semen volume was 2.5 mL, sperm concentration was 32.6 million/ml, and sperm motility was 38.5%. Following chemotherapy, semen analysis was conducted on 12 patients, with ifosfamide being the predominant drug used in all cases. Among these 12 patients, eight retained viable spermatozoa, and two successfully achieved spontaneous pregnancies resulting in live births. In one of the remaining four cases where no sperm were detected in ejaculate, a live birth was achieved through intracytoplasmic sperm injection using cryopreserved sperm.

Discussion: While ifosfamide, the primary chemotherapy drug for patients with malignant bone and soft tissue tumors, was associated with severe impairments in spermatogenesis, recovery of spermatogenesis was observed in many cases. However, there were instances of prolonged azoospermia. Even in such cases,

assisted reproduction using cryopreserved sperm remained viable for achieving parenthood. In light of these findings, offering patients the opportunity for fertility preservation is advisable.

KEYWORDS

sperm, sperm cryopreservation, malignant bone tumor, malignant soft tissue tumor, sarcoma, fertility preservation, ifosfamide

1 Introduction

Malignant bone and soft tissue tumors (BSTT), known as sarcomas, represent rare non-epithelial malignancies originating in bone and various bodily tissues, including muscles, fat, blood vessels, nerves, and connective tissues. These malignancies encompass several subtypes, including osteosarcoma, chondrosarcoma, Ewing's sarcoma, leiomyosarcoma, liposarcoma, rhabdomyosarcoma, and synovial sarcoma. These malignancies are uncommon, comprising only 1% of all malignant tumors (Siegel et al., 2022; Siegel et al., 2023) Notably, most cases of malignant BSTT manifest in younger age groups. For instance, osteosarcoma exhibits a bimodal peak of incidence in individuals in their 20s and after age 65. Osteosarcoma is the third most prevalent cancer type among children and adolescents aged 12–18, following leukemia and lymphoma.

The prognosis of these diseases has seen significant Improvement with the advent of multidisciplinary treatment approaches. The primary treatment approach is surgery; however, radiation therapy or chemotherapy may be indicated in those with more-severe malignancy grades. Notably, chemotherapy often involves alkylating agents with high testicular toxicity (Hiraga and Ozaki, 2021; Tanaka and Ozaki, 2021). Alkylating agents tend to cross-link sperm DNA double strands, impeding DNA synthesis and RNA transcription and eventually resulting in DNA breakage (Qiu et al., 1995; Ledingham et al., 2020). Damage to spermatogonia DNA within the seminiferous tubules can temporarily halt spermatogenesis, leading to azoospermia. The likelihood of permanent azoospermia or spermatogenesis restoration depends on the drug dose. For instance, doses exceeding 7.5 g/m^2 for cyclophosphamide and 60 g/m^2 for ifosfamide (Meistrich et al., 1992; Williams et al., 2008) increase the risk of permanent azoospermia. Use of doxorubicin-based chemotherapy regimens as alternatives to ifosfamide for malignant soft tissue tumors may induce testicular histopathological deformities, oligozoospermia, and abnormal sperm morphology. These drugs can affect the physiological role of Leydig and Sertoli cells, potentially causing chromosome abnormalities and DNA synthesis disruptions (Mohan et al., 2021a). Cisplatin (CDDP), used in osteosarcoma treatment, is associated with an increased risk of permanent azoospermia when cumulative doses exceed 400 mg/m^2 (DeSantis et al., 1999). Given that many individuals diagnosed with malignant BSTT are young, these adverse effects can lead to the loss of opportunities for significant life events like marriage, pregnancy, and childbirth. Consequently, sperm cryopreservation emerges as a crucial facet of fertility preservation before initiating treatment, particularly for male patients, due to the elevated risk of azoospermia and severe spermatogenesis dysfunction (Oktay et al., 2018).

The American Society for Clinical Oncology (ASCO) practice guideline identifies alkylating agents as high-risk drugs for causing permanent azoospermia and advocates for sperm cryopreservation as a means of fertility preservation. Regrettably, the urgency of treatment and limited awareness of fertility preservation among orthopedic surgeons often result in missed opportunities for pretreatment fertility preservation. In such cases, the timeline for recovering spermatogenesis also becomes a critical concern. Despite these risks, no prior studies have investigated spermatogenesis following chemotherapy for malignant BSTT. Thus, the primary objective of this study is to investigate spermatogenesis function during pretreatment sperm cryopreservation and assess the recovery of spermatogenesis following gonadotoxic treatments in patients afflicted with malignant BSTT.

2 Materials and methods

2.1 Study design

This retrospective study evaluated patients with malignant BSTT who underwent sperm cryopreservation for fertility preservation at the Reproduction Center of Yokohama City University Medical Center between September 2012 and August 2023. Data extracted from medical records encompassed details such as age, marital status, disease type, planned treatment, pretreatment and post-treatment semen parameters, and the status of cryopreservation maintenance.

Furthermore, for patients who could follow-up on semen analysis during annual cryopreservation follow-ups at the outpatient clinic, we analyzed spermatogenesis recovery in ejaculate and the time required for this recovery. The appearance of sperm in the ejaculate, even if scarce, was considered a marker of successful recovery. For this retrospective observational study, patient consent was assumed, utilizing an opt-out approach. The study's design received approval from the institutional review board of Yokohama City University Medical Center (IRB No: F211100008).

2.2 Semen analysis and sperm cryopreservation

Semen samples were collected through masturbation at our hospital after varying intervals of sexual abstinence. Following a 30-min liquefaction period at room temperature, semen analyses were conducted as per the World Health Organization (WHO) 2021 recommendations (World Health Organization, 2021), using the Sperm Motility Analyzing System (SMAS™: DITECT Corp.,

TABLE 1 Patient characteristics.

Mean age (SD), years		22.8 (7.3)
Maritai status (%), n	married	3 (8.8)
	unmarried	31 (91.2)
Diseases (%), n	osteosarcoma	11 (32.4)
	synovial sarcoma	6 (17.6)
	Ewing's sarcoma	5 (14.7)
	rhabdomyosarcoma	3 (8.8)
	epithlioid sarcoma	3 (8.8)
	leiomyosarcoma	2 (5.9)
	liposarcoma	2 (5.9)
	other	2 (5.9)
Median semen analysis (IQR)	semen volume, ml	2.5 (1.5, 3.6)
	sperm concentration, million/ml	32.5 (15.7, 54.5)
	sperm motility, %	38.5 (19.2, 52.7)
Regimen (%), n	ifosfamide-based	29 (85.3)
	cisplatin-based	3 (8.8)
	no chemotherapy	2 (5.9)
Cycles (%), n	1–5	21 (65.6)
	6–10	9 (28.1)
	11-	1 (3.1)
	unknown	1 (3.1)

Tokyo, Japan).The freezing procedure involved diluting the semen sample with an equal volume of freezing medium (Sperm Freeze™, Kitazato, Co. Ltd., Tokyo, Japan) and transferring it into a straw tube. Both ends of the straw tube were then sealed using a sealer. These sealed straw tubes were arranged in a column suspended in vapor-phase nitrogen for 5 min before being placed in liquid nitrogen for long-term storage.

2.3 Maintenance and usage for cryopreserved sperm

Patients undergo an annual reservation for follow-up in the outpatient clinic and are inquired about their preference regarding the retention or disposal of cryopreserved sperm. Semen analysis is conducted upon the patient's request to verify the presence of spermatozoa, thereby confirming spermatogenesis function.

In cases where a patient desires to discard the cryopreserved sperm or in the unfortunate event of their passing, the cryopreserved sperm is appropriately discarded. Alternatively, when the cryopreserved sperm is utilized to conceive a child, the frozen-thawed sperm is typically employed alongside intracytoplasmic sperm injection (ICSI) within our facility.

2.4 Data analysis

Summary statistics were computed, and the data are presented as mean values with standard deviation or median values with interquartile range (IQR) for continuous variables. The proportion of individual elements related to the total is expressed as a percentage (%).

3 Results

In this study, 34 patients were included, with a mean age of 22.8 years. The distribution of diseases among these patients was as follows, listed in descending order of frequency: osteosarcoma (11/34; 32.4%), synovial sarcoma (6/34; 17.6%), Ewing's sarcoma (5/34; 14.7%), rhabdomyosarcoma (3/34; 8.8%), epithelioid sarcoma (3/34; 8.8%), leiomyosarcoma (2/34; 5.9%), and liposarcoma (2/34; 5.9%).

All patients underwent tumor resection, and the majority (32 patients) received anticancer drugs, except for one case under surveillance and one undergoing radiotherapy. Of those who received chemotherapy, 29 patients were treated with ifosfamide-based regimens, except three patients with osteosarcoma who received cisplatin-based chemotherapy. Notably, all 34 patients had successfully ejaculated sperm and were deemed eligible for sperm cryopreservation.

At the time of cryopreservation, the median semen volume was 2.45 mL, with a sperm concentration of 32.5×10^6/mL and a motility rate of 38.5% (see Table 1).

Excluding the 7 patients who were followed for less than 1 year, the outcomes of 27 patients were as follows: death in 8, another 8 requested their frozen sperm be discarded, 7 kept their sperm under cryopreservation, and 4 were lost to follow-up. The median post-cryopreservation sperm survival for those who died was 2 years (IQR: 1–3 years), indicating that the prognosis for patients with malignant BSTT remains poor.

Among the 13 cases with available semen analysis follow-up data, 12 were examined, all of which involved ifosfamide-based chemotherapy, except for one case where chemotherapy was not administered. Spermatogenesis successfully recovered in eight cases (66.7%), with an average recovery time of 3 years (see Table 2). At the time of sperm cryopreservation, these eight cases demonstrated a median sperm concentration of 20.3×10^6/mL (IQR: 17.4–27.5) and median motility of 38.5% (IQR: 14.1–45.7). For the best findings after anticancer drug administration, the median sperm concentration was 32.1×10^6/mL (IQR: 11.8–44.9) and the median motility was 38.5% (IQR: 28.1–59.7) (see Table 3). Notably, six cases exhibited improved semen parameters compared to those during cryopreservation.

Additionally, among these cases, seven patients (one of whom had sadly passed due to disease progression) opted to discard their cryopreserved sperm. Remarkably, in two of these instances, the partners of the patients achieved spontaneous pregnancies and gave birth to their children (see Table 2). One of the patients had synovial sarcoma, and the other patient had Ewing's sarcoma; their sperm concentrations were 14.5×10^6/mL and 21.2×10^6/mL and motilities were 40.2% and 41.9% at the time of sperm cryopreservation, respectively. After 7 and 12 courses of ifosfamide and a doxorubicin-centered regimen, spermatogenesis was recovered in

TABLE 2 Outcome of patients whose spermatogenesis could be tracked.

Case	Age, years	Key drug*	Number of cycle	Time to evaluate, years	Spermatogenesis recovery	Delivery	Follow-up duration, years	Outome
1	16	IFM	2	1	-	-	1	died
2	18	IFM	unknown	7	-	-	7	ongoing
3	21	IFM	10	3	-	+**	7	ongoing
4	27	IFM	7	1	-	-	1	lost to follow
5	16	IFM	3	7	+	-	8	discarded
6	20	IFM	8	3	+	-	7	discarded
7	20	IFM	5	2	+	-	3	discarded
8	21	IFM	12	3	+	+	7	discarded
9	22	IFM	4	3	+	-	3	discarded
10	24	IFM	7	2	+	+	6	discarded
11	26	IFM	4	2	+	-	4	discarded
12	34	IFM	5	2	+	-	5	died

* IFM, ifosfamide.
** delivery with assisted reproduction.

TABLE 3 Pre- and post-chmotherapy semen analysis of patients with malignant BSTT.

	Sperm recovery	Prolonged azoospermia
Patients, n	8	4
Mean age, years	22.9	20.5
Median number of cycles (range), n	5 (4–12)	7 (2–10)*
Median semen analysis		
Pre-chemotherapy		
Concentration, 10^6/mL	20.3	28.8
Motility, %	38.5	49.5
Post-chemotherapy		
Concentration, 106/mL	32.1	0.0
Motility, %	38.5	0.0

* excluding one case with unkown number of cycles.

2 and 3 years. The maximum sperm concentrations of these patients were 1.8×10^6/mL and 42.9×10^6/mL, and the maximum motilities were 29.0% and 45.0%, respectively.

4 Discussion

This is the first retrospective observational study to assess pre- and post-chemotherapy spermatogenesis in patients with malignant BSTT. This issue is rarely studied as malignant BSTT is a rare condition, with a poor prognosis. Follow-ups for spermatogenesis are difficult to conduct as young patients often resist these evaluations.

Notably, the patients in this study were relatively young at the time of cryopreservation compared to individuals with other malignant diseases like testicular tumors and leukemia. Unfortunately, the prognosis remains unfavorable, with 8 out of 27 patients who could be followed for more than a year succumbing during the follow-up period.

The urgency of diagnosis and treatment often compels clinicians to initiate treatment without sufficient explanations about fertility preservation, potentially resulting in fertility loss. Some orthopedic oncologists have recommended pretreatment sperm cryopreservation for malignant BSTT patients under 45, with significant interest shown by unmarried and childless patients (Hoshi et al., 2014). Nevertheless, there is a paucity of reports summarizing spermatogenesis outcomes before and after chemotherapy for this condition.

In a previous study conducted in rabbits, a decrease in testicular weight and sperm count was observed with an increase in the dose of ifosfamide. Although prolonged spermatogenesis dysfunction was noted in response to dose, recovery was achieved by 8 weeks among

rabbits who received 240 mg/kg of ifosfamide. (Ypsilantis et al., 2003). In humans, 1.5–3 g/m^2, or 30–60 mg/kg is usually administered over 3–5 days for malignant BSTT. However, the abovementioned study was a single-dose study, with no examination of how spermatogenesis recovers over time and after multiple treatment cycles. Thus, it is clinically important to evaluate spermatogenesis recovery following ifosfamide treatment in humans.

In our study, sperm parameters during cryopreservation were notably favorable compared to other reported diseases (Yumura et al., 2018). We also analyzed 12 patients who underwent semen analysis after treatment. In all these cases, ifosfamide was the key drug used, and spermatogenesis recovery was observed in 8/12 patients. However, among the four cases where sperm did not appear in the ejaculate, one patient passed away due to disease progression after a semen analysis 1 year post-cryopreservation, and another had no sperm in the semen analysis 1-year post-cryopreservation, subsequently being lost to follow-up. Hence, many patients who underwent semen analysis after chemotherapy experienced spermatogenesis recovery, with seven out of eight patients choosing to discard their cryopreserved sperm, except for one who passed away during the disease. Remarkably, spontaneous pregnancies and live births were achieved by two patients who had received 7 and 12 courses of regimens containing ifosfamide, respectively, suggesting that spermatogenesis may recover even with extended treatment durations. However, the patient cohort was too small to draw any conclusions, and there were cases of prolonged azoospermia (even following short treatment cycles) and poor prognosis requiring immediate multidisciplinary treatment. Consequently, there remains a great need for sperm cryopreservation for fertility. Use of doxorubicin-based chemotherapy regimens as alternatives to ifosfamide for malignant soft tissue tumors may induce testicular histopathological deformities, oligozoospermia, and abnormal sperm morphology. These drugs can affect the physiological role of Leydig and Sertoli cells, potentially causing chromosome abnormalities and DNA synthesis disruptions (Mohan et al., 2021b).

However, one patient who did not experience spermatogenesis recovery achieved pregnancy and live birth through ICSI using cryopreserved sperm during the first blastocyst transfer. This also underscores the critical importance of sperm cryopreservation for fertility preservation before chemotherapy. Given that many malignant BSTT patients are younger, clinicians should present the option of sperm cryopreservation for future family planning with thorough informed consent (Tozawa et al., 2022). The prognosis for malignant BSTT remains unfavorable (2), necessitating prompt treatment. Hence, the seamless preservation of fertility becomes imperative. To achieve this, orthopedic oncologists and reproductive health specialists should be aware of the need to devote sustainable resources to improve accessibility (Bedoschi and Navarro, 2022) by addressing factors like patient navigation, psychological supports, and administrative and financial supports. Establishment of regional networks may also help facilitate seamless collaboration between facilities (Furui et al., 2016).

This study presents several limitations. First, it was conducted at a single institution, and the sample size was relatively small. Malignant BSTT is a rare disease, and within this patient group, the subset of individuals considered for fertility preservation at a single institution was limited. Consequently, it is crucial to accumulate and analyze national data from multiple centers in Japan to enhance the robustness of the findings.

Second, the number of patients who requested semen testing was relatively low, which hindered a more precise assessment of spermatogenesis recovery after treatment. This could be attributed, in part, to the fact that many young patients may not opt for semen analysis because they do not currently intend to start a family. It would have been beneficial to incorporate semen analysis as part of routine follow-up outpatient care, ensuring regular checkups to provide a more comprehensive evaluation.

5 Conclusion

This study represents the first dedicated examination of spermatogenic function before and after chemotherapy for malignant BSTT. Despite the gonadotoxic properties of ifosfamide, it is noteworthy that spermatogenesis made a remarkable recovery in numerous cases. However, given prolonged azoospermia in specific instances, the importance of sperm cryopreservation before treatment cannot be overstated. Furthermore, it underscores the necessity for seamless collaboration between orthopedic oncologists and reproductive specialists to preserve fertility.

Data availability statement

The raw data supporting the conclusion of this article will be made available by the authors, without undue reservation.

Ethics statement

The studies involving humans were approved by institutional review board of Yokohama City University Medical Center. The studies were conducted in accordance with the local legislation and institutional requirements. Written informed consent for participation was not required from the participants or the participants' legal guardians/next of kin in accordance with the national legislation and institutional requirements.

Author contributions

TT: Conceptualization, Investigation, Writing–original draft, Writing–review and editing. NM: Supervision, Writing–review and editing. SA: Supervision, Writing–review and editing. TS: Supervision, Writing–review and editing. JK: Supervision, Writing–review and editing. KU: Data curation, Resources, Writing–review and editing. SK: Supervision, Writing–review and

editing. MK: Supervision, Writing–review and editing. YY: Supervision, Writing–review and editing.

Funding

The author(s) declare that no financial support was received for the research, authorship, and/or publication of this article.

Acknowledgments

We would like to thank the students of the School of Medicine, Yokohama City University, for their cooperation in collecting the data for this study.

Conflict of interest

The authors declare that the research was conducted in the absence of any commercial or financial relationships that could be construed as a potential conflict of interest.

Publisher's note

All claims expressed in this article are solely those of the authors and do not necessarily represent those of their affiliated organizations, or those of the publisher, the editors and the reviewers. Any product that may be evaluated in this article, or claim that may be made by its manufacturer, is not guaranteed or endorsed by the publisher.

References

Bedoschi, G., and Navarro, P. A. (2022). Oncofertility programs still suffer from insufficient resources in limited settings. *J. Assist. Reprod. Genet.* 39 (4), 953–955. doi:10.1007/s10815-022-02452-w

DeSantis, M., Albrecht, W., Höltl, W., and Pont, J. (1999). Impact of cytotoxic treatment on long-term fertility in patients with germ-cell cancer. *Int. J. Cancer* 83, 864–865. doi:10.1002/(sici)1097-0215(19991210)83:6<864::aid-ijc33>3.0.co;2-e

Furui, T., Takenaka, M., Makino, H., Terazawa, K., Yamamoto, A., and Morishige, K. I. (2016). An evaluation of the Gifu Model in a trial for a new regional oncofertility network in Japan, focusing on its necessity and effects. *Reprod. Med. Biol.* 15, 107–113. doi:10.1007/s12522-015-0219-3

Hiraga, H., and Ozaki, T. (2021). Adjuvant and neoadjuvant chemotherapy for osteosarcoma: JCOG bone and soft tissue tumor study group. *Jpn. J. Clin. Oncol.* 51, 1493–1497. doi:10.1093/jjco/hyab120

Hoshi, M., Oebisu, N., Takada, J., Iwai, T., Tsuruta, R., and Nakamura, H. (2014). Pre-chemotherapy preservation of fertility in male patients with high-grade malignant bone and soft tissue tumors. *Mol. Clin. Oncol.* 2, 1111–1114. doi:10.3892/mco.2014.367

Ledingham, D., Plant, M., Mustafa, F., and Patil, B. (2020). Preserving fertility: using cyclophosphamide and other cytotoxics in young people. *Pract. Neurol.* 20, 148–153. doi:10.1136/practneurol-2019-002247

Meistrich, M. L., Wilson, G., Brown, B. W., da Cunha, M. F., and Lipshultz, L. I. (1992). Impact of cyclophosphamide on long-term reduction in sperm count in men treated with combination chemotherapy for Ewing and soft tissue sarcomas. *Cancer* 70 (11), 2703–2712. doi:10.1002/1097-0142(19921201)70:11<2703::aid-cncr2820701123>3.0.co;2-x

Mohan, U. P., Iqbal, S. T. A., and Arunachalam, S. (2021a). Mechanisms of doxorubicin-mediated reproductive toxicity - a review. *Reprod. Toxicol.* 102, 80–89. doi:10.1016/j.reprotox.2021.04.003

Mohan, U. P., Iqbal, S. T. A., and Arunachalam, S. (2021b). Mechanisms of doxorubicin-mediated reproductive toxicity - a review. *Reprod. Toxicol.* 102, 80–89. doi:10.1016/j.reprotox.2021.04.003

Oktay, K., Harvey, B. E., Partridge, A. H., Quinn, G. P., Reinecke, J., Taylor, H. S., et al. (2018). Fertility preservation in patients with cancer: ASCO clinical practice guideline update. *J. Clin. Oncol.* 36, 1994–2001. doi:10.1200/JCO.2018.78.1914

Qiu, J., Hales, B. F., and Robaire, B. (1995). Damage to rat spermatozoal DNA after chronic cyclophosphamide exposure. *Biol. Reprod.* 53, 1465–1473. doi:10.1095/biolreprod53.6.1465

Siegel, R. L., Miller, K. D., Fuchs, H. E., and Jemal, A. (2022). Cancer statistics. *CA Cancer J. Clin.* 72, 7–30. doi:10.3322/caac.21332

Siegel, R. L., Miller, K. D., Wagle, N. S., and Jemal, A. (2023). Cancer statistics, 2023. *CA Cancer J. Clin.* 73, 17–48. doi:10.3322/caac.21763

Tanaka, K., and Ozaki, T. (2021). Adjuvant and neoadjuvant chemotherapy for soft tissue sarcomas: JCOG bone and soft tissue tumor study group. *Jpn. J. Clin. Oncol.* 51, 180–184. doi:10.1093/jjco/hyaa231

Tozawa, A., Kimura, F., Takai, Y., Nakajima, T., Ushijima, K., Kobayashi, H., et al. (2022). Japan Society of Clinical Oncology Clinical Practice Guidelines 2017 for fertility preservation in childhood, adolescent, and young adult cancer patients: part 2. *Int. J. Clin. Oncol.* 27, 281–300. doi:10.1007/s10147-021-02076-7

World Health Organization (2021). *WHO laboratory manual for the examination and processing of human semen*. Geneva, Switzerland: WHO.

Williams, D., Crofton, P. M., and Levitt, G. (2008). Does ifosfamide affect gonadal function? *Pediatr. Blood Cancer* 50, 347–351. doi:10.1002/pbc.21323

Ypsilantis, P., Papaioannou, N., Psalla, D., Politou, M., and Simopoulos, C. (2003). Effects of single dose administration of ifosfamide on testes and semen characteristics in the rabbit. *Reprod. Toxicol.* 17, 237–245. doi:10.1016/s0890-6238(02)00127-2

Yumura, Y., Tsujimura, A., Okada, H., Ota, K., Kitazawa, M., Suzuki, T., et al. (2018). Current status of sperm banking for young cancer patients in Japanese nationwide survey. *Asian J. Androl.* 20, 336–341. doi:10.4103/aja.aja_74_17

frontiers | Frontiers in Pharmacology

TYPE Review
PUBLISHED 24 January 2024
DOI 10.3389/fphar.2024.1350187

OPEN ACCESS

EDITED BY
Duoyi Zhao,
Fourth Affiliated Hospital of China Medical University, China

REVIEWED BY
Zou Zhen Wei,
Huazhong University of Science and Technology, China
Bing Yang,
Tianjin Medical University, China

*CORRESPONDENCE
Hong Sun,
sunhong002@126.com
Hua Yang,
yanghua0203@gmc.edu.cn
Xu Ning,
179451982@qq.com

†These authors have contributed equally to this work

RECEIVED 05 December 2023
ACCEPTED 10 January 2024
PUBLISHED 24 January 2024

CITATION
Zhou J, Lan F, Liu M, Wang F, Ning X, Yang H and Sun H (2024), Hypoxia inducible factor-1α as a potential therapeutic target for osteosarcoma metastasis.
Front. Pharmacol. 15:1350187.
doi: 10.3389/fphar.2024.1350187

Hypoxia inducible factor-1α as a potential therapeutic target for osteosarcoma metastasis

Jianghu Zhou[1†], Fengjun Lan[2†], Miao Liu[1], Fengyan Wang[1], Xu Ning[1*], Hua Yang[1*] and Hong Sun[1*]

[1]Department of Orthopaedics, Affiliated Hospital of Guizhou Medical University, Guiyang, China, [2]Department of Orthopaedics, West China Hospital, Sichuan University, Chengdu, China

Osteosarcoma (OS) is a malignant tumor originating from mesenchymal tissue. Pulmonary metastasis is usually present upon initial diagnosis, and metastasis is the primary factor affecting the poor prognosis of patients with OS. Current research shows that the ability to regulate the cellular microenvironment is essential for preventing the distant metastasis of OS, and anoxic microenvironments are important features of solid tumors. During hypoxia, hypoxia-inducible factor-1α (HIF-1α) expression levels and stability increase. Increased HIF-1α promotes tumor vascular remodeling, epithelial-mesenchymal transformation (EMT), and OS cells invasiveness; this leads to distant metastasis of OS cells. HIF-1α plays an essential role in the mechanisms of OS metastasis. In order to develop precise prognostic indicators and potential therapeutic targets for OS treatment, this review examines the molecular mechanisms of HIF-1α in the distant metastasis of OS cells; the signal transduction pathways mediated by HIF-1α are also discussed.

KEYWORDS

osteosarcoma, HIF-1α, metastasis, cellular microenvironment, signaling pathways, therapy

1 Introduction

Osteosarcoma (OS) is the most common primary bone malignancy, derived from primitive bone-forming mesenchymal cell, for which there are two peak periods of incidence in adolescents and older adults (Shoaib et al., 2022). OS typically develops near the end of the long bone in the lower limbs, with high local invasiveness, rapid infiltration, and early metastasis (Vailas et al., 2019; Li K. et al., 2023a). The pathogenic

Abbreviations: OS, Osteosarcoma; HIF-1α, Hypoxia-inducible factor-1α; PHD, Proly Hydroxylase Domain; VHL, VonHippel-Lindaup; HRE, Hypoxia response element; PI3K, Phosphoinositide 3-Kinase; PKB/AKT, Protein Kinase B; ERK 1/2, Extracellular regulated protein kinases 1/2; EMT, Epithelial-mesenchymal transformation; CCL4, Chemokine C motif ligand 4; FAK, Focal adhesion kinase; GRM4, Glutamate metabotropic receptor 4; CXCR4, C-X-C chemokine receptor type-4; PHF 2, PHD Finger Protein 2; ANGPTL 4, Angiotensin like 4; MMP 2, Matrix metalloproteinase-2; VEGF, Vascular endothelial growth factor; SENP 1, SUMO-specificprotease1; TWIST 1, TWIST family bHLH transcription factor 1; ROS, Reactive oxygen species; TME, Tumor microenvironment; PRMT9, Promotes protein arginine methyltransferases 9; GIT1, G-protein-coupled receptor interacting protein 1; MCP 1, Monocyte chemoattractant protein-1; TUG 1, Taurine upregulated gene 1; ICAM-1, Intercellular adhesion molecule-1; PD-1, Programmed cell death protein 1; CTLA-4, Cytotoxic T lymphocyte-associated antigen-4; PD-L1, Programmed death ligand-1.

characteristic of OS, a spindle stromal cell tumor, is the direct conversion of proliferating tumor cells into bone or tissue that resembles bone from the perspective of pathomorphology (Dong et al., 2022). Histologically, OS encompasses various subtypes including conventional, telangiectatic, small cell, high-grade surface, secondary, low-grade central, periosteal, and parosteal variants. The conventional type of OS (intramedullary high-grade) accounts for approximately 85% of all cases, making it the most prevalent subtype (Rickel et al., 2017). Neoadjuvant radiotherapy and chemotherapy combined with limb salvage surgery is the primary OS treatment method at present (Anderson, 2016). In recent years, with the improvement of chemotherapy and the introduction of immunotherapy and targeted therapy, the prognosis and overall survival of OS patients have improved (Yang G. et al., 2021a). The prognostic survival rate of OS patients with distant metastasis, nevertheless, remains significantly low (Berner et al., 2015; Bläsius et al., 2022).

Metastasis means that the cells from an original tumor location invade the surrounding tissue and colonize a new site, through the vascular system or lymphatic duct (Valastyan and Weinberg, 2011). Metastasis, tumor location, and size are the main factors affecting the poor prognosis of OS, especially metastasis (Smeland et al., 2019). A significant proportion of individuals diagnosed with OS, ranging from 20%–30%, already presented with lung metastases at the time of their initial diagnosis (Chen et al., 2021). Patients with metastasis at diagnosis or recurrence was only a 20% 5-year survival rate (Meazza and Scanagatta, 2016). Significantly, recently conducted studies have demonstrated a robust correlation between modifications in the cellular microenvironment and the occurrence of OS metastasis (Jin J. et al., 2023a).

The tumor cells are experiencing hypoxia as a result of their rapid cellular proliferation, heightened oxygen demand, vascular remodeling, and compromised blood supply (Li Y. et al., 2021a). The heterogeneity of hypoxia in tumor cells is characterized by varying degrees, ranging from minimal to mild to severe, and the regulatory mechanism varies depending on the degree of hypoxia (Hompland et al., 2021). Hypoxia-induced modifications in the cellular microenvironment can lead to the activation of multiple signaling pathways (Wu et al., 2023). The presence of the intricate mechanisms regulating hypoxia undoubtedly presents greater challenges in the treatment of malignancies. It is widely acknowledged that the hypoxia-inducible factor-1α (HIF-1α) is one of the most critical regulators in cellular microenvironment (Ildiz et al., 2023). The activation of HIF-1α facilitates rapid tumor cell adaptation to hypoxic environments, thereby contributing to the metastasis process of various malignant tumors (Ma et al., 2021). The regulation of the anoxic microenvironment is also associated with the mechanism of OS metastasis, enabling control over tumor cell invasion and metastasis by manipulating the hypoxic cellular microenvironment to modulate tumor cell heterogeneity (Mohamed et al., 2023) (Figure 1).

In this review, we comprehensively reviewed the molecular mechanisms of HIF-1α in the progression of OS metastasis, alongside the intricate correlation between HIF-1α and the prognosis of patients with metastatic OS as well as relevant therapeutic strategies. Deep insights into the underlying mechanisms implicated in OS metastasis would help improve the prognosis, and provide novel therapeutic targets for patients with metastatic OS.

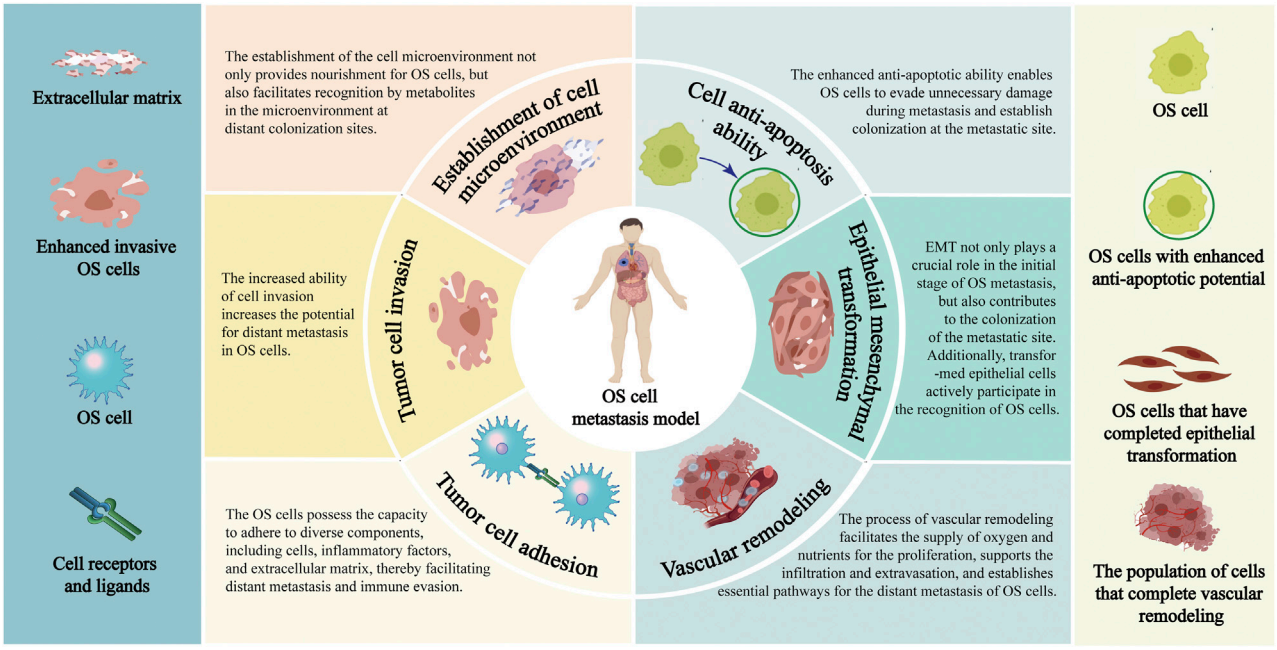

FIGURE 1
Pathological process of distant metastasis of OS. Annotation: The pathological mechanisms of distant metastasis of OS include: Enhance the invasiveness of OS cells; Facilitate the EMT process; Reduce the adhesion ability of OS cells; Enhance the anti-apoptosis characteristics of OS cells; Reconstruction of extracellular environment; Vascular remodeling process of OS cells.

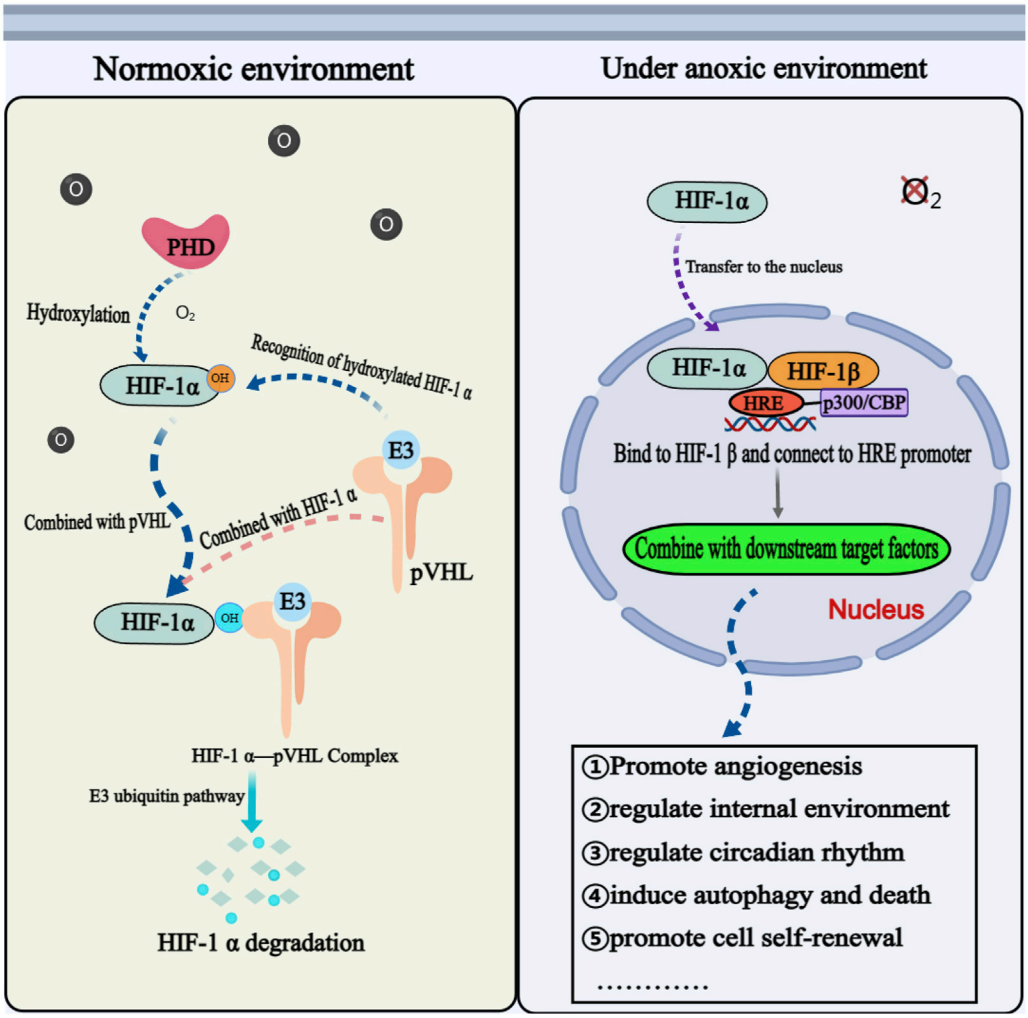

FIGURE 2
The physiological mechanism of HIF-1α in normoxic and hypoxic environments. Annotation: The mechanism of HIF-1α is different under anoxic and aerobic conditions. Under aerobic condition, HIF-1α cannot exist stably and needs to be degraded through related mechanisms. Under anoxic condition, HIF-1α is activated and participates in the physiological and pathological process of cells through corresponding signal pathways.

2 Biological characteristics and functions of HIF-1α

The equilibrium of oxygen content in extracellular fluid is crucial for cell survival and normal metabolism (Tao et al., 2021). Under severe hypoxic stress, cells precisely regulate the expression of certain coding genes or non-coding RNA through oxygen receptors and signal transduction, thereby participating in a variety of physiological and pathological processes (Duan et al., 2024). The hypoxia-inducible factors are members of the basic helix-loop-helix Per-Arnt-Sim transcription factor superfamily. This heterodimer consists of an oxygen concentration-sensitive HIF-α subunit and a constitutively-expressed HIF-β subunit (Semenza and Wang, 1992; Wang and Semenza, 1993). HIF-α subunit includes three subtypes: HIF-1α, HIF-2α, and HIF-3α (Nangaku and Eckardt, 2007). At present, the role and function of HIF-1α have been extensively studied compared to other subtypes (Ravenna et al., 2016).

Under normoxic conditions, HIF-1α is unstable, continuously degraded, and maintained at a relatively low basal level (Li L. et al., 2023b). The prolyl hydroxylase domain (PHD) catalyzes the hydroxylation of proline residues at positions 402 and 564 on the HIF-1α subunit. Hydroxylated HIF-1α is recognized by an E3 ubiquitin ligase complex, that includes the tumor suppressor protein von Hippel-Lindau (VHL), leading to its rapid degradation via the ubiquitin-proteasome pathway. The hydroxylase activity of PHD and HIF-1α is inhibited under hypoxia. After translocation into the nucleus, HIF-1α binds to HIF-1β, forming a transcriptional complex that binds to the hypoxia response element (HRE) in the promoter region of its target gene, which initiates the transcriptional expression of many downstream genes and participates in a variety of physiological and pathological processes (Haase, 2017). In addition to being regulated by oxygen concentration, HIF-1α is also subject to regulation by various other factors, including the antisense transcription factor aHIF-1α, which has a negative regulatory effect on the transcription of the HIF-1α gene (Bertozzi et al., 2011). Certain growth factors, inflammatory factors, and oncogenes can also regulate HIF-1α protein stability through signal pathways, such as phosphoinositide 3-kinase (PI3K)/protein kinase B (PKB/AKT) and extracellular regulated protein kinases 1/2 (ERK1/2)

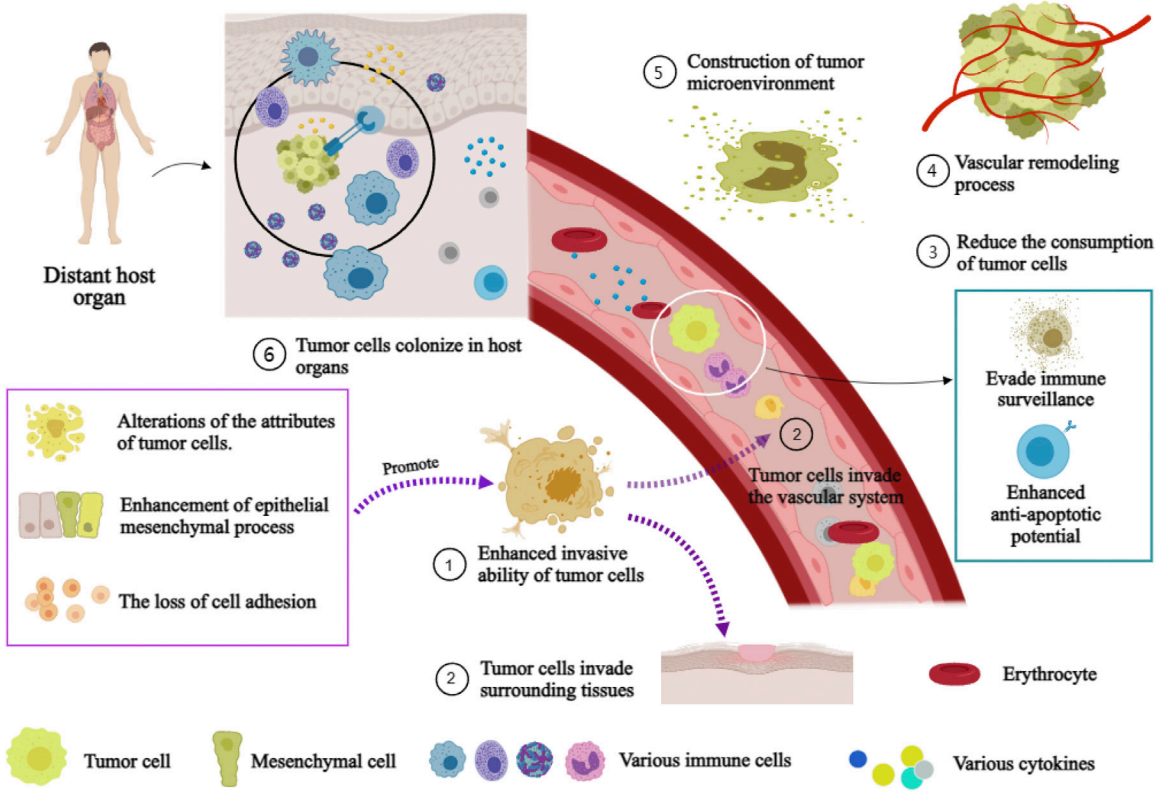

FIGURE 3
Mechanism of distant Metastasis of malignant tumor. Annotation: The mechanism of distant metastasis in malignant tumors: Firstiy, the enhancement of cell invasiveness, enabling tumor cells to invade surrounding tissues and the vascular system. Subsequently, tumor cells infiltrate the vascular system and surrounding tissues. Immune escape and anti-apoptosis mechanisms within the vasculature while reducing their loss. Finally, host organ microenvironments facilitate tumor cell colonization.

(Zhao et al., 2024). Additionally, multiple miRNAs are also involved in regulating the expression of HIF-1α (Lee et al., 2015).

Many studies have shown that HIF-1α is implicated in a majority of biological functions, such as promoting angiogenesis, regulating the internal environment, regulating circadian rhythm, inducing autophagy and programmed cell death, and promoting self-renewal and differentiation of mesenchymal stem cells (Adamovich et al., 2017; Wu et al., 2017) (Figure 2). The elevated expression level of HIF-1α has been observed in various primary and secondary malignant tumors, making it a valuable biomarker and potential target for clinical diagnosis, targeted treatment, and prognosis evaluation in numerous diseases (Semenza, 2012; Zeng et al., 2014; Tuomisto et al., 2016). Studies also indicated that HIF-1α plays a crucial role in regulating various molecular stages of OS metastasis and demonstrates significant prognostic implications (Khojastehnezhad et al., 2022). Therefore, HIF-1α may serve as a prognostic indicator for OS metastasis and a potential therapeutic target to enhance the prognosis and survival rate of patients with OS.

3 Mechanisms of malignant tumor metastasis

The molecular mechanism underlying the initiation and sustenance the metastasis of tumor is intricate (Tanaka and Sakamoto, 2023). The mechanism encompasses the establishment of a tumor microenvironment, the process of vascular remodeling, the acquisition of tumor cell invasiveness, and the reduction in tumor cell consumption (Figure 3). The initiation and maintenance of the metastatic process in malignant tumor cells involve the coordinated interaction and mutual influence of multiple pathways.

3.1 Acquisition of cell invasiveness

The acquisition of invasiveness is the primary determinant influencing distant metastasis in tumor cells. As a result of alterations in cellular characteristics, the facilitation of epithelial-mesenchymal transition (EMT), and the disruption of intercellular adhesion, there is an augmentation in the invasive capacity of tumor cells (Zepeda-Enríquez et al., 2023). After the enhancement of the invasive ability of tumor cells, they can invade the vascular system or surrounding tissue through the extracellular matrix (Huang et al., 2020). EMT is a process of transformation from polarized epithelial cells to mesenchymal cells, which drives tumor progression by enhancing the invasive ability of tumor cells (Huang et al., 2023). The process of EMT is crucial for facilitating the infiltration of OS cells into the local vascular system and promoting their migration to distant organs (Sinha et al., 2020). Additionally, the presence of established epithelial phenotypic cells further facilitates the

proliferation of secondary tumors in distant organs (Hinton et al., 2023). Cell adhesion is also an important factors in tumor cell metastasis. Cell adhesion molecules plays a pivotal role in adhesion, triggers intracellular signal transduction, and participates in the regulation of EMT, thereby participating in the progression of distant metastasis of tumor cells (Ruan et al., 2022).

3.2 Reduced consumption of tumor cells

Evading immune system monitoring is a crucial process in minimizing tumor cell elimination and facilitating their metastasis (Elanany et al., 2023). It has been shown that disrupting the tumor vascular system and recruiting aPDL1-loaded platelets can coordinate the response of tumor cells to immune factors and control malignant tumor metastasis (Li H. et al., 2021b). The anti-apoptosis mechanism enables tumor cell survival in the circulation through the vascular system is another way to reduce the consumption of tumor cells (Zhou et al., 2023). The presence of the immune escape and anti-apoptosis mechanism can attenuate the consumption of tumor cells during metastasis, giving tumor cells a better chance to travel to and populate the metastatic location.

3.3 Construction of tumor microenvironment

The establishment of a tumor cell ecological environment involves the coexistence of tumor cells with other tumor cells or host cells within the same microenvironment. From a holistic perspective, the tumor cell environment can be regarded as a complex tumor ecosystem consisting of diverse biological and abiotic factors that interact with each other, and influencing the progression of tumor development through various mechanisms (Bullman, 2023; Gong et al., 2023). The initiation of metastasis is accompanied by alterations in the cellular microenvironment, which enables tumor cells to become more invasive (Chen and Song, 2022). Prior to the infiltration of metastatic tumor cells into the host organ, the coordinated actions of cytokines, exosomes, and metabolites help to create a pre-metastatic milieu in particular organs prior to the entry of metastatic tumor cells and aid circulating tumor cells in completing colonization (Peinado et al., 2017). Surprisingly, the acidification milieu and elevated extracellular lactate levels also play a vital role in the immunological regulation of tumor cells and the promotion of neovascularization (Gottfried et al., 2006; Végran et al., 2011; Brand et al., 2016; Rastogi et al., 2023).

3.4 Vascular remodeling effect

The neovascularization of solid tumors is considered as a pivotal process in the advancement and dissemination of tumors (Kikuchi et al., 2019). Tumor cells, tumor-associated stromal cells, and their bioactive products collectively contribute to the regulation of angiogenesis within tumor tissues (De Palma et al., 2017). On vascular remodeling, vascular endothelial growth factor (VEGF) is one of them that has a significant impact (Alsina-Sanchis et al., 2021). In tumors, the secretion of VEGF is typically continuous, leading to aberrant angiogenesis and structural disarray within the vascular system. As a consequence, tumor tissue hemoperfusion is compromised, along with intercellular junction integrity is missing. This dysfunctional vascular network further facilitates hypoxia and immunosuppression, ultimately fostering tumor progression (Khan and Kerbel, 2018). In another aspect, the remodeling of tumor vasculature plays a significant role in EMT, cell invasion, cellular infiltration, immunosuppression, and regulation of the cellular microenvironment (Tzeng and Huang, 2023). Moreover, a remodeled endothelium within capillaries can promote the metastatic colonization of tumor cells (Karreman et al., 2023).

In brief, the process of tumor cell distant metastasis is a multifaceted and intricate multistage phenomenon, encompassing numerous pivotal steps (Liu QL. et al., 2021a). Regulation involves multiple factors that interact with each other. Finding significant targets is crucial for exploring the mechanism of OS distant metastasis. The majority of the aforementioned processes are regulated by HIF-1α, which may serve as a crucial hub in controlling OS metastasis.

4 Molecular mechanisms of HIF-1α in OS

HIF-1α, the most significant regulator of the cellular response to anoxic environments, is associated with OS cell occurrence, development, and treatment resistance (Han and Shen, 2020). Keratin 17 is a vital component of keratin, and is capable of inducing OS cell development and glycolysis, which are indispensable for cellular energy supply by activating the AKT/mTOR/HIF-1α pathway in the underlying mechanism of OS growth (Yan et al., 2020). During the process of OS cell proliferation, mitochondrial H_2O_2 signal transduction promotes tumor cell proliferation through HIF-1α-dependent and HIF-1α-independent manners (Sabharwal et al., 2023). Another study revealed that HIF-1α and VEGF regulate OS cell apoptosis under hypoxia, and any disruption to one substance may subsequently affect the existence of the other, demonstrating the critical function that HIF-1α and VEGF play in OS apoptosis (Yang SY. et al., 2021b). Moreover, the mechanism of HIF-1α inducing OS cells growth was confirmed through the urothelial cancer associated 1/protein tyrosine phosphatase/AKT signal pathway (Li T. et al., 2018a).

Furthermore, there is also a strong association between the expression of HIF-1α and the mechanism of drug resistance in OS cells. Visfatin can enhance miRNA expression through HIF-1α-induced transcription. However, visfatin does not affect zinc finger e-box binding homeobox 1 mRNA expression but significantly increases its protein stability. Decreasing visfatin levels can ameliorate the sensitivity of drug-resistant OS cells to cisplatin (Wang D. et al., 2019a). HIF-1α is directly targeted by miR-199a, and there is an inverse correlation between miR-199a and HIF-1α mRNA. Overexpression of MiR-199a resensitizes cisplatin resistant OS cells to cisplatin by inhibiting HIF-1α both *in vitro* and *in vivo*

TABLE 1 The role of HIF-1α signaling pathway in the metastasis mechanism of OS cells.

Classification	Signal pathway	Mechanism	References
Invasive potential	CXCR4/HIF-1α	Increases OS cell invasiveness	Zhang et al. (2018)
	CCL4/HIF-1α/integrin αvβ3	Induces cell migration	Lan et al. (2017)
	HIF-1α/miR-18b-5p/ PHF2	Increases cell invasion	Wang et al. (2019b)
	HIF-1α/NUSAP1	Enhances cell migration and invasion	Liu et al. (2016)
	GRM4/CBX4/HIF-1α	OS cell proliferation, migration and invasion	Nieto et al. (2016)
	HIF-1α/FOXD2-AS1/p21	Increases cell invasiveness	Wu et al. (2019)
	miR-33b/HIF-1α	OS cell proliferation and migration	Zhou and He (2022)
	HIF-1α/ANGPTL4	Enhances OS cell proliferation and migration	Tan and Zhao (2019)
	HIF-1α/ANGPTL2	Enhances the invasive ability	Sun et al. (2015)
	miR-20b/HIF-1α/VEGF pathway	OS cell invasion and proliferation	Thüring et al. (2023)
	DEC2/HIF-1α	Facilitates OS cells in response to hypoxia; invasion and metastasis	Shen et al. (2023)
EMT process	HIF-1α/BNIP3/LC3B	Mitochondrial autophagy	Ren et al. (2019)
	HIF-1α/VEGF	Enhances migration and invasion ability	Hamidi and Ivaska (2018)
	lncRNA NEAT1/miR-186-5p/HIF-1α	Enhances proliferation, invasion, and EMT	Harjunpää et al. (2019)
	SENP1/HIF-1α	Enhances EMT process	Janiszewska et al. (2020)
	AKT/mTOR/ HIF-1α	Enhances EMT process	Leng et al. (2016)
	p38/MAPK/HIF-1α		
	HIF-1α/Snail/MMP-9	Enhances EMT process	Itoh et al. (2018)
Adhesion ability	MEK/ERK1/2/HIF-1α/ICAM-1	Lung colonization; promotes glycolysis; adhesion	Feng et al. (2016)
Anti-apoptosis	HIF-1α/FoxO1/Mn SOD/catalase/Sesn3	Promotes cell growth and migration while inhibiting apoptosis	Zhang et al. (2023)
Metabolism	HIF-1α/Hsa-circ-0000566/VHLE3	Promotes OS cells glycolysis	Zhang et al. (2017d)
	miR-543/PRMT9/HIF-1α	OS cells glycolysis	Dou et al. (2021)
	MiR-186/ HIF-1	Glucose uptake, and lactic acid production in OS cells	Yu et al. (2019)
Vascular remodeling	GIT1/ p-ERK/HIF-1α	VEGF release and angiogenesis	Li et al. (2018b)
	WISP-1/FAK/JNK/HIF-1α/VEGF-A	Promotes angiogenesis	Watson et al. (2021)
	CCL5/CCR5/PKC/c-Src/HIF-1α	Promotes angiogenesis	Sukumar et al. (2013)
	LncRNA MALAT1/mTOR/HIF-1α	Promotes angiogenesis	Liao et al. (2020)
	LncRNA TUG1/miR-143-5p/HIF-1α	Promotes angiogenesis	Zhao et al. (2015)

(Keremu et al., 2019). The following study presented that miR-216b enhances cisplatin induced apoptosis by regulating the JMJD2C/HIF-1α/Hairy and enhancer of split 1 signal axis in OS cells, which may be a potential strategy for overcoming chemical resistance in OS (Yang et al., 2020). In another interesting study, transforming growth factor β downregulates the expression of succinate dehydrogenase by reducing the levels of transcription factor STAT1. This leads to upregulation of HIF-1α, which disrupts glucose metabolism and exacerbates chemical resistance in OS cells (Xu et al., 2021). However, the involvement of HIF-1α extends beyond its role in the occurrence and drug resistance of OS, as it also exhibits a close association with the progression and metastasis of OS (Shang et al., 2022).

5 HIF-1α and the mechanism of OS metastasis

In normoxic and hypoxic environments, HIF-1α exhibits distinct pathological mechanisms and actively participates in molecular mechanism regulation of tumor cells through corresponding signaling pathways (Jin Z. et al., 2023b; Ceranski et al., 2023; Li Y. et al., 2023c; Xie et al., 2023). Recent studies have shown that HIF-1α genes-related and signal pathways are significantly associated with OS cells metastasis (Zhao et al., 2019; He G. et al., 2023a). It can induce and sustain distant metastasis of OS cells by modulating the invasive and metastatic potential of tumor cells, promoting the EMT process, enhancing

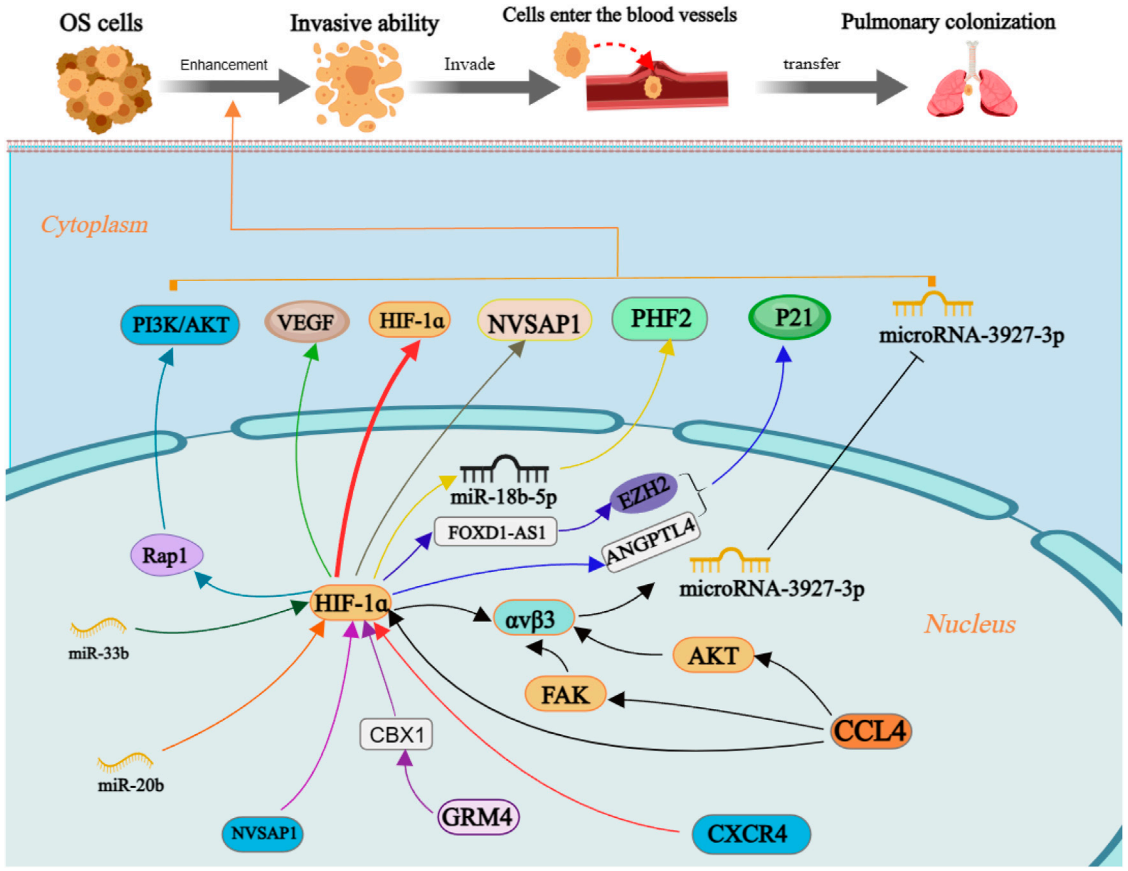

FIGURE 4
The molecular mechanism of enhancement invasiveness of OS cells by HIF-1α. Annotation: HIF-1α is regulated by many factors and regulates the level of downstream target factors, which can enhance the invasive ability of OS cells and increase the risk of distant metastasis.

cellular adhesion, increasing anti-apoptotic properties, inducing immune evasion, facilitating tumor angiogenesis, and fostering microenvironmental remodeling (Table 1).

5.1 Invasion ability and OS metastasis

Tumor cells possess the capacity for invasion and migration during the early stages of metastasis, enabling them to detach from the primary tumor mass and infiltrate neighboring and distant host tissues (Kushwaha et al., 2019). The initial phase of metastasis can be completed by HIF-1α by increasing the invasive ability of OS cells (Figure 4). It was established that hBMSC-MVs augment the invasiveness of OS cells under hypoxic conditions through activation of the HIF-1α pathway (Lin et al., 2019). An intriguing study unveiled a correlation between HIF-1α and C-X-C chemokine receptor type 4 (CXCR4), a chemokine receptor, in the context of OS metastasis. Hypoxia-induced high-metastatic potential OS cells exhibit heightened invasiveness compared to low-metastatic potential counterparts, with their induction being sensitive to CXCR4 antagonists and HIF-1α inhibitors (Guan et al., 2015).

Moreover, OS clinical stage and lung metastasis are positively linked with Chemokine C-C motif ligand 4 (CCL4) and integrin αvβ3 expression. CCL4 promotes the development of integrin αvβ3 and enhances cell migration potential in OS by activating the HIF-1α, PKB, and focal adhesion kinase (FAK) signaling pathways while suppressing miRNA-3927-3p expression (Tsai et al., 2021). Hypoxia-induced upregulation of miR-18b-5p through HIF-1α transcriptional control inhibits tumor suppressor gene PHD finger protein 2 (PHF2) expression at the post-transcriptional level; its suggested that the miR-18b-5p-PHF2 signal axis is involved in the HIF-1α-mediated metastasis of OS (Luo et al., 2022). The upregulation of both HIF-1α and nucleolar and spindle associated protein 1 (NUSAP1) in OS cells positively correlates with their invasive capacity under hypoxic conditions (Zhang et al., 2021). Although bioinformatics analysis did not show significant differences in glutamate metabotropic receptor 4 (GRM4) expression between OS and normal tissue. However, subsequent cell tests revealed that the interaction between GRM4 and Chromobox 4 had a notable impact on the transcriptional activity of HIF-1α. Overexpressing GRM4 resulted in a substantial reduction in cell proliferation, migration, and invasion ability (Zhang et al., 2020).

The P21 protein is a cell cycle-dependent protein related to the invasive ability of cells (Cao et al., 2020). In OS cells, the interaction between FOXD1-AS1 and ZEST homologous enhancer 2 suppresses the level of p21 protein. Simultaneously, the expression of

FOXD1AS1 is regulated by the transcription factor HIF-1α, which plays a crucial role in augmenting the malignant biological characteristics of OS cells (Ren et al., 2019). MiR-33b has been identified as targeting HIF-1α, and its downregulation in OS cells enhances cell proliferation and migration. Overexpression of HIF-1α reverses the inhibitory effect of miR-33b on cell proliferation and migration (Zhou et al., 2017). Suppressing CircRNA-103801 expression can reduce OS cell proliferation, migration, and invasion capacity. Downregulation of miR-338-3p may lead to upregulation of CircRNA-103801 expression in OS cells through primarily involving the circRNA_103801-miR-338-3p-HIF-1/Rap1/PI3K-Akt pathway; unfortunately, it is not clear which subtype of HIF-1 was involved in this study (Li ZQ. et al., 2021c).

Angiotensin like 4 (ANGPTL4) is associated with the vascular remodeling and regeneration (Fernández-Hernando and Suárez, 2020). The expression of ANGPTL4 is upregulated by HIF-1α and thus enhances OS cell proliferation and migration (Z et al., 2018). Quercetin can suppress OS cell migration and invasion in a dose- and time-dependent manner by decreasing HIF-1α, VEGF, matrix metalloproteinase 2 (MMP2) and MMP9 expression (Lan et al., 2017). It has been indicated that the expression of angiopoietin Like 2 (ANGPTL2) is upregulated in HIF-1α-induced OS cells, and ANGPTL2 overexpression increased OS cells' capacity for invasion (Wang X. et al., 2019b). Meanwhile, miR-20b significantly decreases in OS cells, resulting in overexpression of the target gene HIF-1α and subsequent upregulation of the VEGF pathway. Thereby promoting cell proliferation and invasion (Liu et al., 2016). Consequently, acquisition of invasive capacity in OS cells trigger the initiation of distant metastasis.

5.2 EMT and OS cells metastasis

EMT is commonly recognized as a critical step in the development of malignant tumors, characterized by the downregulation of epithelial markers and upregulation of mesenchymal proteins. Consequently, EMT results in the loss of epithelial polarity, relaxation of intercellular junctions, and recombination of cytoskeleton proteins, ultimately facilitating tumor invasion and metastasis (Nieto et al., 2016). Remarkably, HIF-1α has been demonstrated implicated in regulating the progression of EMT (Figure 5).

Under hypoxia, the expression of E-cadherin is upregulated, while the expression of Vimentin, N-cadherin, and snail protein is downregulated; all these proteins serve as markers for EMT (Zhang et al., 2020). With the expression of HIF-1α and TWIST family bHLH transcription factor 1 is upregulated, while the expression of e-cadherin is downregulated, leading to altered EMT process in OS cells (Fujiwara et al., 2020). Previous studies have reported that HIF-1α can interact with β-catenin to form HIF-1α/β-catenin complex, promoting tumor cell proliferation and metastasis (Wu et al., 2019). Interestingly, a cellular investigation has revealed a phenomena that defies the foregoing conclusion has been discovered. Their research findings suggested that the regulation of OS cell metastasis involved the mitochondrial autophagy degradation pathway, which was mediated by HIF-1α/BCL2/adenovirus E1B interacting protein 3/light chain 3 beta. The aforementioned mechanism may provide an explanation for the underlying cause of this apparent contradiction (He G. et al., 2023a). Research has shown significant variations in the expression levels of VEGF, E-cadherin, and N-cadherin in OS cells, corresponding to changes in HIF-1α level, thereby leading to a substantial enhancement in their migratory and invasive capabilities. However, *sauchinone* effectively mitigates the detrimental effects of hypoxia-induced EMT on OS cells (Zhou and He, 2022). miR-186-5p functions as a downstream target of nuclear enriched abundant transcript 1 which targets HIF-1α. It inhibits proliferation, invasion, and EMT through miR-186-5p/HIF-1α axis in OS cells (Tan and Zhao, 2019).

In the anoxic microenvironment, both HIF-1α and UMO specific-protease 1 (SENP1) exhibit upregulation in OS cells. Interestingly, inhibition of HIF-1α result in the suppression of SENP1 enhancement. Subsequent inhibition of SENP1 leads to the upregulation of E-cadherin and downregulation of vimentin and N-cadherin, thereby regulating EMT and attenuating the invasive potential of tumor cells (Wang et al., 2018). *Tetrahydrocurcumin (THC)* reduces HIF-1α levels under hypoxic conditions by blocking the Akt/mTOR and p38/MAPK pathways, thus improving the EMT process (Zhang Y. et al., 2017a). Another study found that *Melatonin* inhibits EMT in OS cells through HIF-1α/Snail/MMP-9 signal transduction, thereby inhibiting OS metastasis (Chen et al., 2020). When exposed to hypoxia, silencing of HIF-1α restore the upregulation of E-cadherin expression and downregulates vimentin expression in OS cells, significantly impacting their proliferative and invasive abilities. *Resveratrol* prevented the development of HIF-1α protein without altering HIF-1α mRNA levels (Sun et al., 2015).

The process of EMT assumes a paramount significance in enabling tumor cells to acquire invasive abilities, thus serving as an essential node in initiating and spreading malignant tumors. The cytokine HIF-1α plays a crucial role in regulating the process of EMT. Therefore, focusing on modulating the HIF-1α-regulated EMT process will offer a novel therapeutic approach for treatment of metastatic OS.

5.3 Cell adhesion and OS metastasis

Adhesive changes are an important feature of malignant tumors (Liu et al., 2022; Thüring et al., 2023). Due to the lack of cellular adhesion, tumor cells possess the capacity to infiltrate neighboring tissues as individual cells or small clusters, thereby enhancing their potential for distant metastasis (Gkretsi and Stylianopoulos, 2018; Cao et al., 2023). Cell adhesion encompasses cell-cell, cell-extracellular matrix, and cell-protein interactions (Hamidi and Ivaska, 2018). Integrin, cadherin, selectin, and IgCAM are the key regulators involved in cell adhesion (Harjunpää et al., 2019). E-cadherin, integrin, and epithelial cell adhesion molecules are closely related to EMT and tumor cell migration; selectin and IgCAM may serve as important factors enabling tumor cells to evade immune surveillance (Janiszewska et al., 2020). Targeting cell adhesion molecules is a popular approach in antitumor therapy, particularly focusing on inhibiting integrins (Hamidi and Ivaska, 2018). Surprisingly, the mechanism of cellular adhesion has been elucidated in the dissemination of certain malignant tumors (Leng

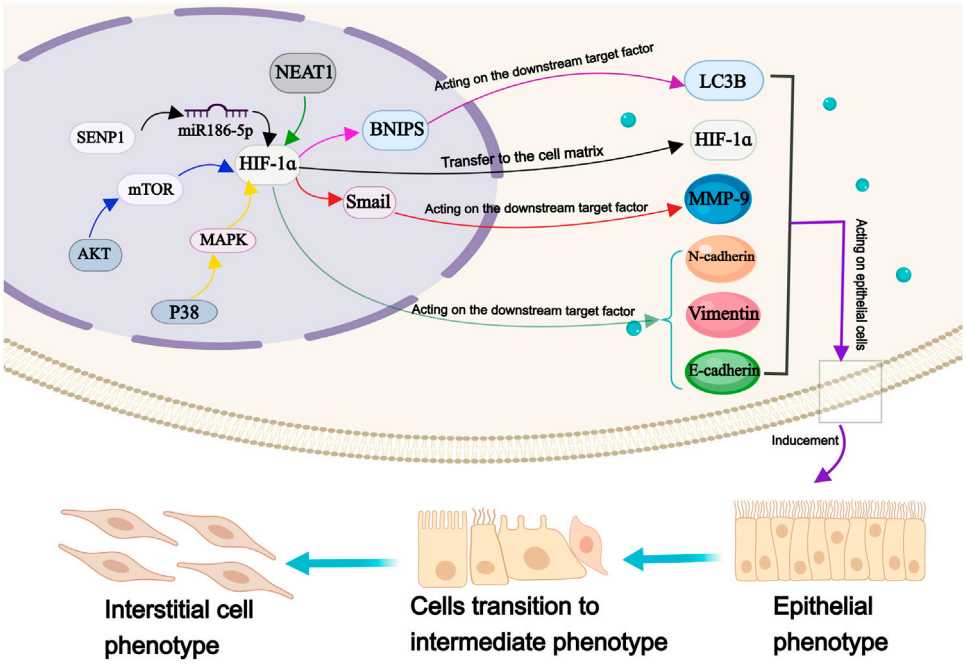

FIGURE 5
The molecular mechanism of HIF-1α in epithelial mesenchymal transformation of OS cells. Annotation: HIF-1 α is involved in the regulation of many factors, which metastasis to the cell matrix, induce the EMT of OS cells and maintain the transformation process.

et al., 2016). The discovery offers promising prospects for the management of metastatic malignant tumors.

In the mechanism of bone tumor metastasis (Figure 6), intercellular adhesion molecule-1 (ICAM-1) expression is connected to HIF-1α, IL-6 enhances ICAM-1 expression through activation of the MEK/ERK1/2/HIF-1α pathway in OS cells, and Tet methylcytosine dioxygenase 2 contributes to demethylation and IL-6 upregulation in tumor cells (Itoh et al., 2018). The alteration in the process of EMT, as indicated by the change in cadherin expression, frequently occurs concurrently with loss of cellular adhesion (Almotiri et al., 2021; Fujisaki and Futaki, 2022). These findings suggest a potential association between OS cell adhesion, EMT process and OS cells invasiveness.

5.4 Cell apoptosis and OS metastasis

Apoptosis is one of the main pathways of programmed cell death, which can be triggered by multiple extracellular and intracellular factors (Pihán et al., 2017). Enhanced antiapoptotic properties alter tumor cell characteristics and elevate the risk of distant metastasis events (Figure 6). It has been shown that HIF-1α can directly regulate ForkheadboxClassO1 in OS cells, prevent the accumulation of reactive oxygen species (ROS), and inhibit manganese-dependent superoxide dismutase, catalase, and Sesn3. Hypoxia-induced ROS formation and apoptosis in OS cells are associated with interference in the cytochrome P450 enzyme system. The HIF-1α inhibitor 2-mercaptoethanol and ROS inducer arsenic oxide inhibit OS cell proliferation and migration while promoting apoptosis (Sun et al., 2019). *In vitro* experiments have confirmed that HIF-1α downregulates caspase-3 expression, promotes OS cell growth, and inhibits apoptosis processes (Lv et al., 2016).

The transcription factor DEC2 gene is associated with a shortened sleep rhythm and plays a role in regulating tumor pathology as a transcriptional suppressor (He et al., 2009). It has been demonstrated that DEC2 expression is significantly correlated with HIF-1α levels. In OS cell lines, knockdown of DEC2 reduces HIF-1α accumulation and compromise the ability of HIF-1α to activate its target genes in response to hypoxia. Increased expression of DEC2 causes OS cells to accumulate HIF-1α more quickly, which aids their adaptation to anoxic environments (Hu et al., 2015). Additionally, the death mechanism of OS cells is supplemented by HIF-1α-induced autophagy. As a result of prolyl hydroxylase being inhibited by ROS and Zn, autophagy is demonstrated to be triggered in OS cells via the connection between HIF-1α and the autophagy-zinc-ROS autophagy cycle axis (He et al., 2020).

Radiation therapy is a treatment modality employed for the management of malignant tumor cells. The administration of HIF-1α siRNA treatment significantly diminishes the hypoxia-induced antiradiation potential of OS cells (Jin et al., 2015). Under hypoxic conditions, HIF-1αoverexpression expedites ROS clearance through autophagy induction in OS cells, thereby conferring radiation resistance to these cells (Feng et al., 2016). Targeting the HIF-1α pathway may enhance radiation resistance induced by hypoxia (von et al., 2021). Anti-apoptotic properties increase the potential of OS distant metastasis. The HIF-1α signaling pathway plays an important role in regulating OS cell apoptosis. Regulating related signal factors in order to promote tumor cell apoptosis allows for new treatments for metastatic OS.

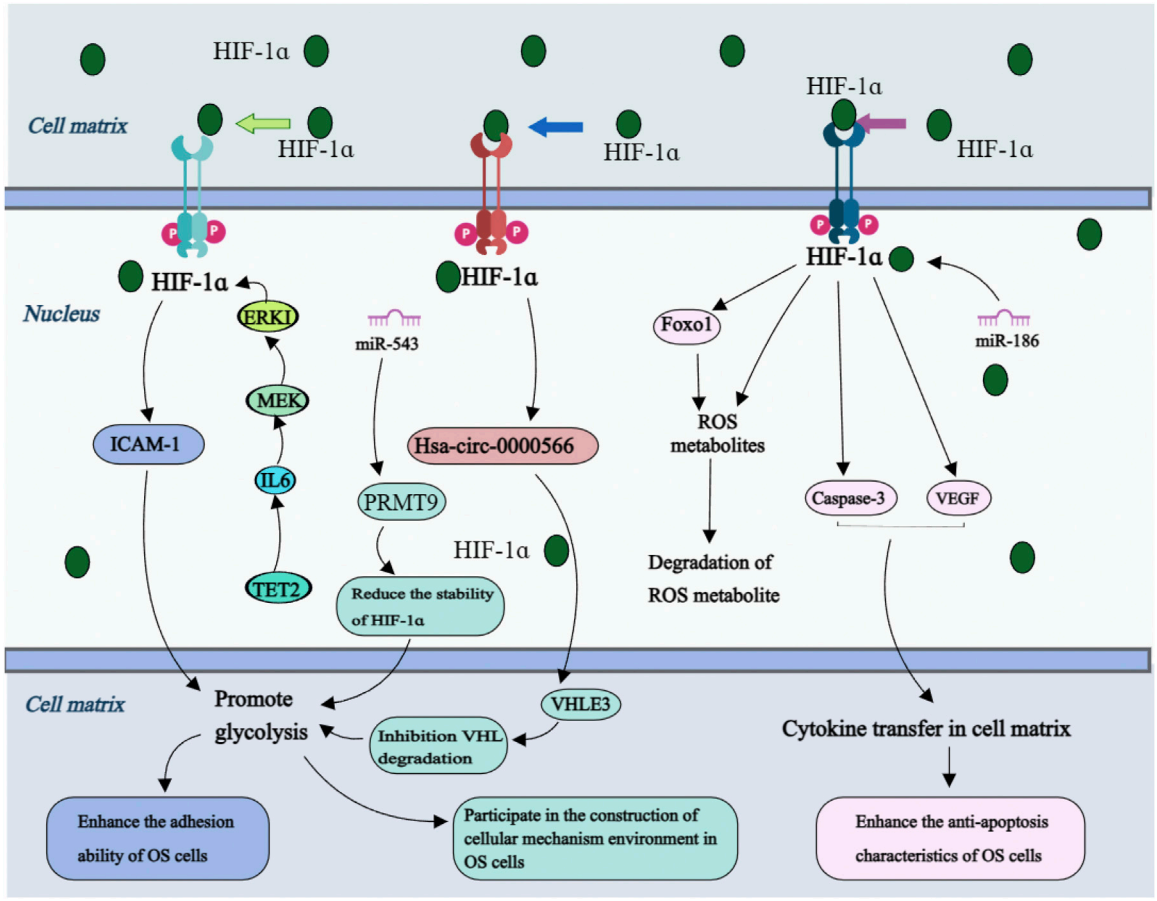

FIGURE 6
Molecular mechanism of HIF-1α receptor in OS cell adhesion, anti-apoptotic properties and matrix environment construction. Annotation: On the one hand, changes in the level of downstream factors regulated by HIF-1α and changes in the cellular matrix environment such as the degradation of reactive oxygen species enhance the ability of cells to resist apoptosis. On the other hand, the downstream factors regulated by HIF-1α participate in the glycolysis process of OS cells, enhance cell adhesion and participate in the construction of a suitable environment for OS cell growth, guide OS cells to break through local lesions, colonization, and complete the process of metastasis.

5.5 Establishment of microenvironment and OS metastasis

Malignant tumors can proliferate rapidly, and the increasing oxygen consumption of tumor cells perpetuates their hypoxic environment. Within this hypoxic milieu, tumor cells obtain energy through glycolysis, i.e., the Warburg effect (Liberti and Locasale, 2016). Cell metabolism undergoes different stages during distant malignant tumor cell metastasis, providing energy and essential metabolites for the continuous growth and proliferation of cancer cells (Phan et al., 2014). The metabolic activity of tumor cells fosters an advantageous environment for the biological activities of malignant cells (Zhang et al., 2023). Simultaneously, through a dynamic multi-step metastasis cascade, the communication between the structural and cellular components within the tumor microenvironment (TME) induces cancer cells to disseminate from their primary site to distant areas (Neophytou et al., 2021). Following colonization in distant organs, metastatic cells interact with the TME, which involves angiogenesis and other processes, and the metabolic process is reprogrammed to achieve metastatic tumor cell growth (De Palma et al., 2017; Zanconato et al., 2019).

In the process of OS metastasis (Figure 6), Hsa-circ-0000566 is regulated by HIF-1α, and both directly binds to VHLE3 ubiquitin ligase protein to inhibit VHL-mediated ubiquitin degradation, thereby promoting their pivotal role in glycolysis of OS cells (Shen et al., 2023). Mechanistically, protein arginine methyltransferase 9 (PrMT9) exerts control over HIF-1α through a distinct mechanism. miR-543 suppresses oxidative phosphorylation, which is promoted by PrMT9, and deletion of miR-543 enhances the PrMT9-induced destabilization of HIF-1α, leading to inhibition of glycolysis in OS cells (Zhang H. et al., 2017b). It has been shown that miR-186 regulates the expression of HIF-1α by targeting pituitary tumor transforming gene 1, thus facilitating glucose uptake and promoting lactic acid generation (Xiao et al., 2018).

The remodeling of the cellular microenvironment, as mentioned in the mechanism of malignant tumor metastasis, not only facilitates the acquisition of invasive ability by tumor cells but also plays a crucial role in sustaining metastasis and facilitating host organ colonization. This substantiates that the TME induced by HIF-1α is related to maintaining the stability of all OS cell metastasis stages, HIF-1α regulation is an important way to inhibit distant OS metastasis.

10.3389/fphar.2024.1350187

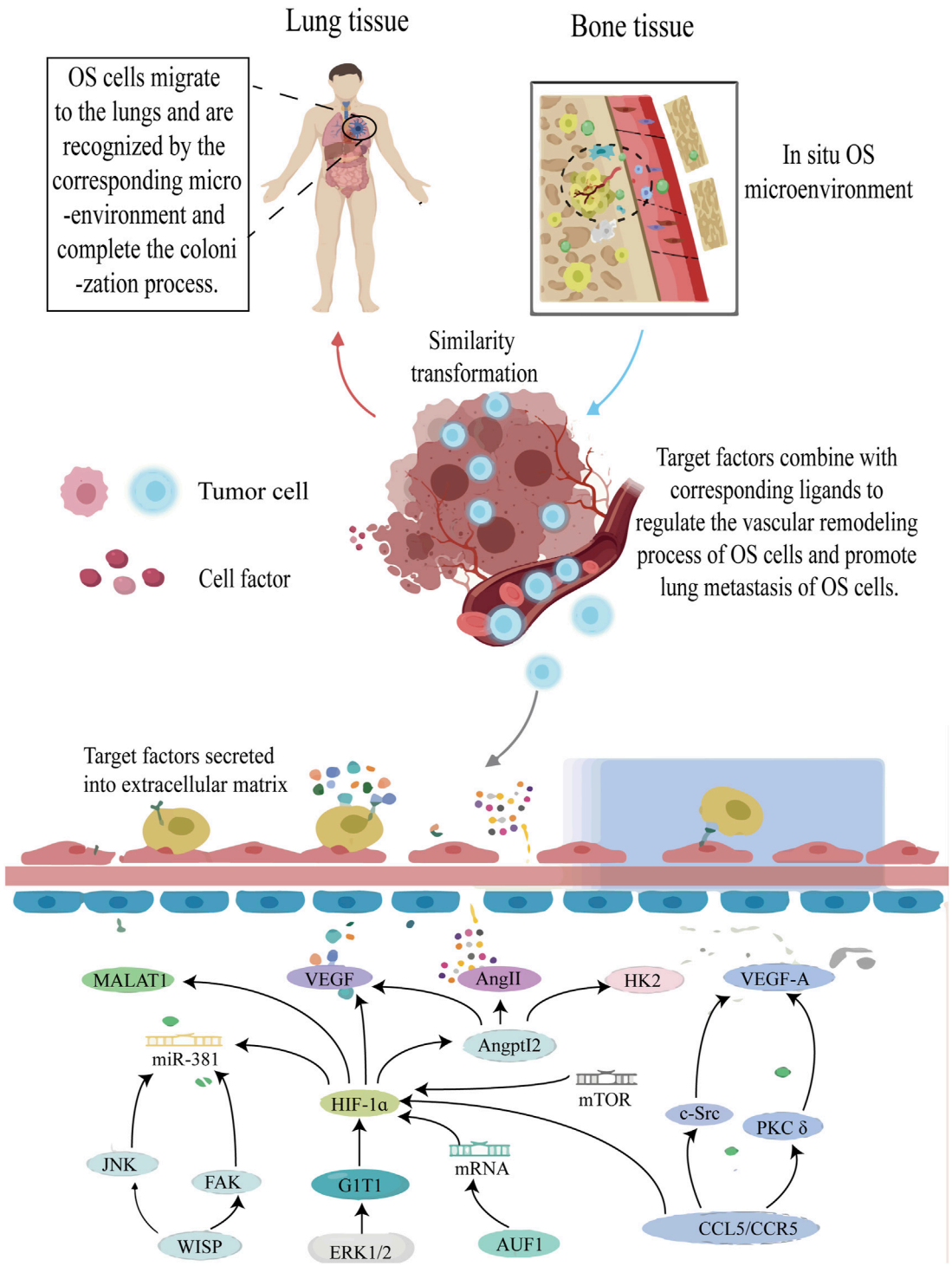

FIGURE 7
The roles of HIF-1α in vascular remodeling of OS cells. Annotation: HIF-1α-induced signal pathway regulates the vascular remodeling process of OS tissue and improves the anoxic environment of OS cells. At the same time, the vascular remodeling process will undoubtedly increase the risk of metastasis of OS cells.

5.6 Vascular remodeling and OS metastasis

Vascular remodeling is an important factor that impacts tumor cell growth and metastasis by facilitating oxygen and nutrient supply to the cancer cells, as well as supporting their infiltration and extravasation. Tumor angiogenesis is triggered by environmental stress, with hypoxia being the most significant contributor. Environmental stress leads to the imbalance of promoting/anti-angiogenesis, which leads to increased expression of angiogenic factors (Corre et al., 2020). Although OS is a highly vascularized

bone tumor, the mechanism of neovascularization in OS remains unknown. Studies have shown that HIF-1α plays an important role in vascular remodeling of OS (Figure 7).

The research findings confirmed that in addition to increasing OS cell invasion capacity, HIF-1α mediates ANGPTL2 expression and promotes VEGF, Angie, and Hexokinase 2 synthesis *in vitro* and *in vivo*. These factors are related to vascular remodeling in OS cells (Wang X. et al., 2019b). ERK1/2 is a key player in G-protein-coupled receptor interacting protein 1 (GIT1)-mediated VEGF secretion and angiogenesis, while HIF-1α acts as the primary transcription factor controlling VEGF production. Under hypoxia, HIF-1α expression can be observed; however, its deletion by GIT1 drastically reduces its expression by preventing ERK1/2 activation. In such circumstances, although VEGF levels also decrease, the downregulation of HIF-1α expression occurs. Therefore, the researchers hypothesized that the ERK1/2/HIF-1α pathway could be utilized to elucidate this mechanism (Zhang et al., 2018).

The transcriptional activities of HIF-1α and activator protein-1 (AP-1) are regulated by α-CaMKII. By encouraging the binding of VEGF transcript with HIF-1α and AP-1, VEGF expression is increased, which aids in the neovascularization of OS (Daft et al., 2015). HIF-1α, FAK, and Jun N-terminal kinase signal pathways are activated upon stimulation of WNT1-induced signal pathway protein-1 (WISP-1). The interaction between integrin and WISP-1 contributes to the control of vascular regulation, increase VEGA production in human OS cells and stimulate angiogenesis and migration in human endothelial progenitor cells (Tsai et al., 2017). Additionally, HIF-1α gene suppression through siRNA can drastically lower VEGF protein levels and VEGF mRNA expression at the transcriptional level, effectively suppressing angiogenesis (Zhang XD. et al., 2017c). In previous studies, ribonucleic acid binding protein AUF1 directly binds and stabilizes the positive regulatory factor HIF-1α and VEGF-A gene, and positively regulates the expression of both genes, which enhances the angiogenic ability of OS cells *in vitro* and *in vivo*. This effect is caused by inoculating AUF1 protein into the sequence of VEGF-A and HIF-1α (Al-Khalaf and Aboussekhra, 2019).

Interestingly, the involvement of THC in the HIF-1α-mediated EMT process is not only evident but also demonstrates a partial inhibitory effect on OS vascular remodeling (Zhang Y. et al., 2017a). It has been indicated that the HIF-1α-mediated PKC/c-Src/HIF-1α signaling pathway is activated by Cmurc chemokine ligand 5/C-C chemokine receptor 5, leading to an increase in tumor angiogenesis dependent on VEGF in the OS microenvironment (Wang et al., 2015). In a fascinating study, the involvement of HIF-1α in the regulation of the rapamycin mTOR/HIF-1α/metastasis-related lung adenocarcinoma transcript 1 signaling axis has been confirmed, highlighting its significance in vascular remodeling in OS (Zhang ZC. et al., 2017d). Subsequent research revealed increased expression of HIF-1α, monocyte chemoattractant protein-1 (MCP1), MCP2, MCP3, Lmur6, and VEGF in OS cells associated with vascular remodeling along the osteosarcoma's metastatic pathway (Dou et al., 2021). Furthermore, the process of vascular remodeling in OS is regulated by taurine upregulation of gene 1 (TUG1), which is owing to a competitive binding mechanism, TUG1 competitively protected HIF-1α from miR-143-5p, and is expected to be the prognostic indicator and therapeutic target of OS (Yu et al., 2019).

Another mechanism of vascular remodeling in tumor cell metastasis is tumor cell infiltration and extravasation. During a specific stage of capillary endothelial cell remodeling, cancer cells successfully exudate and form new capillary rings, which is characteristic of invasive malignant tumor metastasis (Giordo et al., 2022; Karreman et al., 2023). Unfortunately, limited knowledge exists regarding this pathway in terms of OS metastasis.

Vascular remodeling plays a crucial role in the adaptive development of tumor cells, contributing to the establishment of a metastatic microenvironment for solid tumors (Li X. et al., 2018b). Inhibition of angiogenesis in solid tumors can induce apoptosis in OS cells; thus, preventing vascular remodeling represents a promising strategy to enhance the prognosis of metastatic OS.

5.7 Immune escape and OS metastasis

As previously mentioned, the majority of solid tumor cells are in a hypoxic state due to their malignant characteristics. The hypoxia of microenvironment is associated with immune escape and immune cell apoptosis (Vito et al., 2020). During glycolysis, lactic acid is produced in the extracellular matrix, and increased lactic acid levels can inhibit T cell function and enhance tumor cell anti-immune response (DePeaux and Delgoffe, 2021; Watson et al., 2021). Hypoxic metabolism induces an immunosuppressive TME that augments T cell hyperresponsiveness. Specifically, HIF-1α specifically inhibits immune cell function in the TME (Multhoff and Vaupel, 2020). This enables the tumor to escape immune-mediated killing, thus reducing the efficacy of many immunotherapy methods (Vito et al., 2020). Conversely, HIF-1α inhibition can enhance T cell anti-tumor activity and inhibit glycolysis, and reducing HIF-1α levels in the TME can increase memory T cell production and improve anti-tumor function (Sukumar et al., 2013). The aforementioned phenomenon accelerates the metastasis of tumor cells and reduces their consumption involved in the metastatic process (Liao et al., 2020). Unfortunately, the mechanism of immune evasion in HIF-1α-mediated OS transmission has not been reported and requires further investigation.

6 Therapeutic prospect of targeting HIF-1α in the treatment of metastatic OS

Metastatic events are crucial factors influencing the unfavorable prognosis in OS, and effective management of metastatic risk holds particular significance for prognosis. It is worth considering that when OS undergoes metastasis, treatment should not solely focus on the primary tumor but also aim to inhibit its invasion and metastasis. This underscores the necessity to comprehend the shared characteristics of primary tumors, tumor metastasis, and secondary sites of metastasis (Du et al., 2023). Research has showed that HIF-1α participates in nearly all processes involved in OS metastasis and serves as a pivotal target within the respective molecular mechanisms. Modulating HIF-1α levels may potentially achieve inhibition of OS metastasis. Interestingly, COX regression analysis confirmed again that HIF-1α expression

is a prognostic indicator for the survival of patients with OS. It promotes OS cell invasion by increasing the production of VEGF, which is a promising therapeutic target for metastatic OS prognosis (Zhao et al., 2015).

6.1 HIF-1α and gene therapy

In targeted gene therapy, HDACIs are traditionally considered as effective tumor inhibitors as their effect via loosening tightly-wound chromatin to inhibit a variety of tumor suppressor genes. bSAHA, an FDA-approved I/IIb/IV HDACI drug, effectively inhibits the nuclear translocation of HIF-1α by directly acetylating Hsp90 and significantly reduces its transcriptional activity (Zhang C. et al., 2017e). However, it is important to investigate whether SAHA can also inhibit OS metastasis. While current research is limited to autophagy, paclitaxel has demonstrated its ability to target HIF-1α and reduce its activity in OS cells (Guo et al., 2015). Furthermore, px-478 has been reported to modulate the transcriptional level of HIF-1α (Koh et al., 2008). Similarly, the compound YC-1 possesses the capacity to inhibit HIF-1α's transcriptional activity and effectively impede protein accumulation (Hu et al., 2020). A potent inhibitor of HIF-1, echinomycin is a small-molecule antibiotic derived from the bacterium *Streptomyces*. It competitively hinders the function of HIF-1α by binding to the HRE region. Unfortunately, subsequent research revealed its hazardous nature (Infantino et al., 2021; Zhao et al., 2024). Currently, the creation of echinococcin liposomes has the potential to improve drug accessibility and safety while reducing tumor growth and metastasis (Bailey et al., 2020). The aforementioned statement exemplifies the feasibility of developing HIF-1α-targeted inhibitors that exhibit both advantageous and safe effects.

6.2 HIF-1α and vascular remodeling

Inhibiting tumor vascular remodeling is a crucial approach employed to suppress OS metastasis. VEGF serves as an important target of OS in anti-vascular remodeling, which affects almost every step of metastasis. The therapeutic options for OS anti-angiogenesis encompass VEGF monoclonal antibody (bevacizumab), tyrosine kinase inhibitors (sorafenib, apatinib, pazopanil and rigofinib), and recombinant human endostatin (Endostar) (Liu Y. et al., 2021b). Interestingly, bevacizumab not only inhibits vascular remodeling but also participates in immune mechanism regulation (Park et al., 2023). Recent studies have shown that proprietary Chinese medicines can effectively inhibit vascular remodeling in OS. For instance, the synthesis of vancomycin derivative T-methyl chloride can stabilize HIF-1α protein and activate its transcriptional activity, thereby inducing gene expression of downstream targets such as VEGF and GLUT-1 (Magae et al., 2019). Moreover, curcumin exerts multiple inhibitory effects on OS metastatic cells including cell adhesion and vascular remodeling (Zahedipour et al., 2021). Therefore, anti-angiogenesis may simultaneously target multiple molecular mechanisms involved in the process of OS metastasis, making it the most promising therapeutic approach for inhibiting OS metastasis.

6.3 HIF-1α and immunotherapy

Immunotherapy is a novel approach employed in the treatment of OS in recent years, and yielding promising outcomes (Tian et al., 2023). OS cells are enveloped by a complex immune microenvironment wherein HIF-1α plays a crucial role in regulating immune factors such as interleukins, transforming growth factor, VEGF, and other elements that significantly contribute to OS metastasis. In the OS cell model, immunotherapy has been observed to augment the efficacy of chemotherapeutic drugs to some extent (Wang H. et al., 2023a; Zhong et al., 2023). Therefore, modulation of the cellular immune microenvironment assumes paramount importance in the management of metastatic OS (Huang et al., 2022; Kuo et al., 2023).

It has been reported that T cells are capable of expressing cytotoxic T lymphocyte-associated antigen-4 (CTLA-4) and programmed cell death protein 1 (PD-1), which are considered as the primary targets of immune checkpoint inhibitors for tumor cells (Conforti et al., 2018). The expression of CTLA-4 exhibits a positive correlation with the prognosis of OS, and the expression level of CTLA-4 is related to the signal pathway of PD-1 activation. Administration of CTLA-4 blockers and antagonists has the potential to restore anti-tumor immunity by activating B7 and CD28 signal transduction pathways (Tian et al., 2023). PD-1 is the key nodes of immune escape of tumor cells, and the expression of PD-1 and its receptor programmed death ligand-1 (PD-L1) is negatively associated with OS prognosis (Zheng et al., 2015; Yang W. et al., 2021c). Treatment with PD-1 inhibitors in OS mice model results in a significant reduction in the probability of lung metastasis (Zheng et al., 2018). Although the role of HIF-1α on PD-1/PD-L1 in OS cells remains unconfirmed, inhibiting the expression of HIF-1α can effectively reduce the expression level of PD-1 in glioma and prostate cancer cells (Ding et al., 2021; Shen et al., 2022). Decreased expression of HIF-1α and PD-L1 promotes the infiltration of CD8 T cells, and increases the levels of TNF-α, IFN-γ, thereby significantly enhancing the efficacy of anti-PD-1 therapy in gastric cancer cells (Wang Z. et al., 2023b). Significantly, PD-L1 has been proved to be a downstream target of HIF-1α in hepatocellular carcinoma (Yao et al., 2023). Interestingly, the HIF-1α inhibitor echinomycin not only augments the therapeutic efficacy of anti-CTLA-4 therapy in immunotherapy, but also enhances the immune tolerance function of PD-1/PD-L1 checkpoints in normal tissues. This dual effects serves to eliminate the immune escape mechanism within the tumor microenvironment, thereby facilitating a safer and more effective approach to immunotherapy (Bailey et al., 2022). Thus, the immune escape mechanism mediated by HIF-1α may be involved in the metastatic process of OS. More researches are demanded to investigate the potential role of HiF-1a in the immunotherapy of metastatic OS.

6.4 HIF-1α and ROS level regulation

The level of ROS and the activation of HIF-1α exhibit a significant correlation. The primary focus of research on the regulatory mechanism of HIF-1α lies in elucidating the connection between the HIF-1α pathway and ROS, particularly in terms of modulating environmental ROS levels to maintain optimal HIF-1α expression. N-acetylcysteine is an inhibitor of ROS that can inhibit the apoptosis of diosgenin-related p38/MAPK signal transduction. This indicates that ROS plays an important role in diosgenin-induced apoptosis (Zheng et al., 2023). In addition, the class I HDAC inhibitor MS-275 enhances the vulnerability of ROS in sarcoma cells. Acetylhistological analysis showed that MS-275 promotes rapid acetylation of lysine RNA binding proteins and blocked the binding and translation activation of NFE2L2 and the corresponding mRNA target HIF-1α to stress granule nucleator G3BP1, thus promoting translation control of key cytoprotective factors and inhibiting the metastatic activity of OS cells (El-Naggar et al., 2019). Increased ROS levels not only promoted the iron death process of OS cells but were also significantly correlated with cisplatin resistance (He P. et al., 2023b). D-arginine is the inert metabolic enantiomer of L-arginine, which can produce nitric oxide, enhance oxygen activity in the cell matrix, downregulate HIF-1α, reduce tumor hypoxia, and increase the sensitivity of OS to radiotherapy, as well as enhance the effect of tumor ablation and effectively prevent lung metastasis (Du et al., 2021).

Gene therapy, immunotherapy and optimization of the cellular microenvironment (including regulation of angiogenesis and ROS concentration) can effectively regulate the level of HIF-1α, which is very important to improve the prognosis of metastatic OS. It is conceivable to develop therapeutic targets or interventions that are both safe and efficient, albeit the research in this domain is still in its nascent stages. This underscores the imperative for conducting a substantial amount of research to establish efficacious and targeted therapy options for successful treatment of metastatic OS.

7 Conclusion

The development and subsequent metastasis not solely determined by genetic alterations within the tumor cells, but also by the adaptive advantages conferred by these mutations in the particular environment (Tarin, 2013). Anoxic microenvironment can promote tumor cells invasion and facilitate the formation of a “pre-metastatic niche” resembling “soil” in distant organs, which serves as a colonization site for circulating tumor cells and leads to the occurrence of metastatic lesions (Kakkad et al., 2019; Hussain et al., 2020). The involvement of HIF-1α in facilitating the rapid adaptation of tumor cells to the anoxic microenvironment and thus plays crucial roles in OS metastasis. During these processes, HIF-1α is engaged in activating several important signaling pathways, including FAK, AKT, PI3K-Akt, VEGF, ERK1/2. These findings of the current study suggest that HIF-1α orchestrates the process of OS metastasis through a highly intricate network, encompassing the initiation, maintenance, and distant colonization of metastatic lesions. For better prediction and treatment for OS metastasis, further investigation into the link between HIF-1α and OS metastasis is imperative.

Targeting HIF-1α as a strategy to reverse the metastatic process in OS demonstrates significant potential; however, current challenges still persist. Recent studies indicate that HIF-1α levels can be modulated through appropriate interventions and the utilization of specific pharmaceutical agents. Therefore, the development of HIF-1α inhibitors is expected to offer more promising therapeutic options for patients with metastatic OS in the future. However, the current understanding of HIF-1α in the tumor microenvironment and its corresponding small-molecule inhibitors is still in the developmental phase, yet to progress to the clinical trial stage. In order to facilitate the clinical application of HIF-1α, it is imperative to determine its efficacy, bioavailability, and potential adverse effects in patients with metastatic OS.

In a word, it can be concluded that HIF-1α promotes the initiation and development of OS metastasis though facilitating cell invasion, vascular remodeling, EMT, and immune escape. Targeting HIF-1α has the potential to decelerate the progression of OS metastasis. Hence, it is essential to elucidate of the precise mechanism underlying HIF-1α in OS metastasis. Moreover, further investigation of associated molecular mechanisms may facilitate the development of efficient and safe small-molecule inhibitors for HIF-1α in treatment of patients of metastatic OS.

Author contributions

JZ: Data curation, Investigation, Visualization, Writing–original draft. FL: Data curation, Software, Visualization, Writing–original draft. ML: Formal Analysis, Project administration, Writing–review and editing. FW: Project administration, Supervision, Writing–review and editing. XN: Conceptualization, Methodology, Supervision, Writing–review and editing. HY: Conceptualization, Funding acquisition, Project administration, Resources, Writing–review and editing. HS: Conceptualization, Funding acquisition, Resources, Writing–review and editing.

Funding

The author(s) declare financial support was received for the research, authorship, and/or publication of this article. The study was funded by the Science and Technology Fund of Guizhou Science and Technology Department (QKH-ZK [2021] 391; QKH-ZK [2023] 344), Science and Technology Fund of Guizhou Provincial Health Commission (gzwjkj 2020-1-120; gzwkj 2021-261), the Youth Fund cultivation program of National Natural Science Foundation of Affiliated Hospital of Guizhou Medical University (gyfynsfc-2021-12), and Graduate Scientific Research Fund project of Guizhou (YJSKYJJ [2021]157).

Conflict of interest

The authors declare that the research was conducted in the absence of any commercial or financial relationships that could be construed as a potential conflict of interest.

Publisher's note

References

Adamovich, Y., Ladeuix, B., Golik, M., Koeners, M. P., and Asher, G. (2017). Rhythmic oxygen levels reset circadian clocks through HIF1α. *Cell Metab.* 25, 93–101. doi:10.1016/j.cmet.2016.09.014

Al-Khalaf, H. H., and Aboussekhra, A. (2019). AUF1 positively controls angiogenesis through mRNA stabilization-dependent up-regulation of HIF-1α and VEGF-A in human osteosarcoma. *Oncotarget* 10, 4868–4879. doi:10.18632/oncotarget.27115

Almotiri, A., Alzahrani, H., Menendez-Gonzalez, J. B., Abdelfattah, A., Alotaibi, B., Saleh, L., et al. (2021). Zeb1 modulates hematopoietic stem cell fates required for suppressing acute myeloid leukemia. *J. Clin. Invest.* 131, e129115. doi:10.1172/JCI129115

Alsina-Sanchis, E., Mülfarth, R., and Fischer, A. (2021). Control of tumor progression by angiocrine factors. *Cancers (Basel)* 13, 2610. doi:10.3390/cancers13112610

Anderson, M. E. (2016). Update on survival in osteosarcoma. *Orthop. Clin. North Am.* 47, 283–292. doi:10.1016/j.ocl.2015.08.022

Bailey, C. M., Liu, Y., Liu, M., Du, X., Devenport, M., Zheng, P., et al. (2022). Targeting HIF-1α abrogates PD-L1-mediated immune evasion in tumor microenvironment but promotes tolerance in normal tissues. *J. Clin. Invest.* 132, 132. doi:10.1172/jci150846

Bailey, C. M., Liu, Y., Peng, G., Zhang, H., He, M., Sun, D., et al. (2020). Liposomal formulation of HIF-1α inhibitor echinomycin eliminates established metastases of triple-negative breast cancer. *Nanomedicine* 29, 102278. doi:10.1016/j.nano.2020.102278

Berner, K., Johannesen, T. B., Berner, A., Haugland, H. K., Bjerkehagen, B., Bøhler, P. J., et al. (2015). Time-trends on incidence and survival in a nationwide and unselected cohort of patients with skeletal osteosarcoma. *Acta Oncol.* 54, 25–33. doi:10.3109/0284186X.2014.923934

Bertozzi, D., Iurlaro, R., Sordet, O., Marinello, J., Zaffaroni, N., and Capranico, G. (2011). Characterization of novel antisense HIF-1α transcripts in human cancers. *Cell Cycle* 10, 3189–3197. doi:10.4161/cc.10.18.17183

Bläsius, F., Delbrück, H., Hildebrand, F., and Hofmann, U. K. (2022). Surgical treatment of bone sarcoma. *Cancers (Basel)* 14, 2694. doi:10.3390/cancers14112694

Brand, A., Singer, K., Koehl, G. E., Kolitzus, M., Schoenhammer, G., Thiel, A., et al. (2016). LDHA-associated lactic acid production blunts tumor immunosurveillance by T and NK cells. *Cell Metab.* 24, 657–671. doi:10.1016/j.cmet.2016.08.011

Bullman, S. (2023). The intratumoral microbiota: from microniches to single cells. *Cell* 186, 1532–1534. doi:10.1016/j.cell.2023.03.012

Cao, J., Yang, Z., An, R., Zhang, J., Zhao, R., Li, W., et al. (2020). lncRNA IGKJ2-MALLP2 suppresses LSCC proliferation, migration, invasion, and angiogenesis by sponging miR-1911-3p/p21. *Cancer Sci.* 111, 3245–3257. doi:10.1111/cas.14559

Cao, Y., Chen, E., Wang, X., Song, J., Zhang, H., and Chen, X. (2023). An emerging master inducer and regulator for epithelial-mesenchymal transition and tumor metastasis: extracellular and intracellular ATP and its molecular functions and therapeutic potential. *Cancer Cell Int.* 23, 20. doi:10.1186/s12935-023-02859-0

Ceranski, A. K., Carreño-Gonzalez, M. J., Ehlers, A. C., Colombo, M. V., Cidre-Aranaz, F., and Grünewald, T. G. P. (2023). Hypoxia and HIFs in Ewing sarcoma: new perspectives on a multi-facetted relationship. *Mol. Cancer* 22, 49. doi:10.1186/s12943-023-01750-w

Chen, B., Zeng, Y., Liu, B., Lu, G., Xiang, Z., Chen, J., et al. (2021). Risk factors, prognostic factors, and nomograms for distant metastasis in patients with newly diagnosed osteosarcoma: a population-based study. *Front. Endocrinol. (Lausanne)* 12, 672024. doi:10.3389/fendo.2021.672024

Chen, X., and Song, E. (2022). The theory of tumor ecosystem. *Cancer Commun. (Lond)* 42, 587–608. doi:10.1002/cac2.12316

Chen, Y., Zhang, T., Liu, X., Li, Z., Zhou, D., and Xu, W. (2020). Melatonin suppresses epithelial-to-mesenchymal transition in the MG-63 cell line. *Mol. Med. Rep.* 21, 1356–1364. doi:10.3892/mmr.2019.10902

Conforti, F., Pala, L., Bagnardi, V., De Pas, T., Martinetti, M., Viale, G., et al. (2018). Cancer immunotherapy efficacy and patients' sex: a systematic review and meta-analysis. *Lancet Oncol.* 19, 737–746. doi:10.1016/S1470-2045(18)30261-4

Corre, I., Verrecchia, F., Crenn, V., Redini, F., and Trichet, V. (2020). The osteosarcoma microenvironment: a complex but targetable ecosystem. *Cells* 9, 976. doi:10.3390/cells9040976

Daft, P. G., Yang, Y., Napierala, D., and Zayzafoon, M. (2015). The growth and aggressive behavior of human osteosarcoma is regulated by a CaMKII-controlled autocrine VEGF signaling mechanism. *PLoS One* 10, e0121568. doi:10.1371/journal.pone.0121568

De Palma, M., Biziato, D., and Petrova, T. V. (2017). Microenvironmental regulation of tumour angiogenesis. *Nat. Rev. Cancer* 17, 457–474. doi:10.1038/nrc.2017.51

DePeaux, K., and Delgoffe, G. M. (2021). Metabolic barriers to cancer immunotherapy. *Nat. Rev. Immunol.* 21, 785–797. doi:10.1038/s41577-021-00541-y

Ding, X. C., Wang, L. L., Zhang, X. D., Xu, J. L., Li, P. F., Liang, H., et al. (2021). The relationship between expression of PD-L1 and HIF-1α in glioma cells under hypoxia. *J. Hematol. Oncol.* 14, 92. doi:10.1186/s13045-021-01102-5

Dong, Z., Liao, Z., He, Y., Wu, C., Meng, Z., Qin, B., et al. (2022). Advances in the biological functions and mechanisms of miRNAs in the development of osteosarcoma. *Technol. Cancer Res. Treat.* 21, 15330338221117386. doi:10.1177/15330338221117386

Dou, B., Chen, T., Chu, Q., Zhang, G., and Meng, Z. (2021). The roles of metastasis-related proteins in the development of giant cell tumor of bone, osteosarcoma and Ewing's sarcoma. *Technol. Health Care* 29, 91–101. doi:10.3233/THC-218010

Du, C., Zhou, M., Jia, F., Ruan, L., Lu, H., Zhang, J., et al. (2021). D-arginine-loaded metal-organic frameworks nanoparticles sensitize osteosarcoma to radiotherapy. *Biomaterials* 269, 120642. doi:10.1016/j.biomaterials.2020.120642

Du, X., Wei, H., Zhang, B., Wang, B., Li, Z., Pang, L. K., et al. (2023). Molecular mechanisms of osteosarcoma metastasis and possible treatment opportunities. *Front. Oncol.* 13, 1117867. doi:10.3389/fonc.2023.1117867

Duan, M., Liu, H., Xu, S., Yang, Z., Zhang, F., Wang, G., et al. (2024). IGF2BPs as novel m(6)A readers: diverse roles in regulating cancer cell biological functions, hypoxia adaptation, metabolism, and immunosuppressive tumor microenvironment. *Genes Dis.* 11, 890–920. doi:10.1016/j.gendis.2023.06.017

Elanany, M. M., Mostafa, D., and Hamdy, N. M. (2023). Remodeled tumor immune microenvironment (TIME) parade via natural killer cells reprogramming in breast cancer. *Life Sci.* 330, 121997. doi:10.1016/j.lfs.2023.121997

El-Naggar, A. M., Somasekharan, S. P., Wang, Y., Cheng, H., Negri, G. L., Pan, M., et al. (2019). Class I HDAC inhibitors enhance YB-1 acetylation and oxidative stress to block sarcoma metastasis. *EMBO Rep.* 20, e48375. doi:10.15252/embr.201948375

Feng, H., Wang, J., Chen, W., Shan, B., Guo, Y., Xu, J., et al. (2016). Hypoxia-induced autophagy as an additional mechanism in human osteosarcoma radioresistance. *J. Bone Oncol.* 5, 67–73. doi:10.1016/j.jbo.2016.03.001

Fernández-Hernando, C., and Suárez, Y. (2020). ANGPTL4: a multifunctional protein involved in metabolism and vascular homeostasis. *Curr. Opin. Hematol.* 27, 206–213. doi:10.1097/MOH.0000000000000580

Fujisaki, H., and Futaki, S. (2022). Epithelial-mesenchymal transition induced in cancer cells by adhesion to type I collagen. *Int. J. Mol. Sci.*, 24. doi:10.3390/ijms24010198

Fujiwara, S., Kawamoto, T., Kawakami, Y., Koterazawa, Y., Hara, H., Takemori, T., et al. (2020). Acquisition of cancer stem cell properties in osteosarcoma cells by defined factors. *Stem Cell Res. Ther.* 11, 429. doi:10.1186/s13287-020-01944-9

Giordo, R., Wehbe, Z., Paliogiannis, P., Eid, A. H., Mangoni, A. A., and Pintus, G. (2022). Nano-targeting vascular remodeling in cancer: recent developments and future directions. *Semin. Cancer Biol.* 86, 784–804. doi:10.1016/j.semcancer.2022.03.001

Gkretsi, V., and Stylianopoulos, T. (2018). Cell adhesion and matrix stiffness: coordinating cancer cell invasion and metastasis. *Front. Oncol.* 8, 145. doi:10.3389/fonc.2018.00145

Gong, Y., Bao, L., Xu, T., Yi, X., Chen, J., Wang, S., et al. (2023). The tumor ecosystem in head and neck squamous cell carcinoma and advances in ecotherapy. *Mol. Cancer* 22, 68. doi:10.1186/s12943-023-01769-z

Gottfried, E., Kunz-Schughart, L. A., Ebner, S., Mueller-Klieser, W., Hoves, S., Andreesen, R., et al. (2006). Tumor-derived lactic acid modulates dendritic cell activation and antigen expression. *Blood* 107, 2013–2021. doi:10.1182/blood-2005-05-1795

Guan, G., Zhang, Y., Lu, Y., Liu, L., Shi, D., Wen, Y., et al. (2015). The HIF-1α/CXCR4 pathway supports hypoxia-induced metastasis of human osteosarcoma cells. *Cancer Lett.* 357, 254–264. doi:10.1016/j.canlet.2014.11.034

Guo, Y., Huang, C., Li, G., Chen, T., Li, J., and Huang, Z. (2015). Paxilitaxel induces apoptosis accompanied by protective autophagy in osteosarcoma cells through hypoxia-inducible factor-1α pathway. *Mol. Med. Rep.* 12, 3681–3687. doi:10.3892/mmr.2015.3860

Haase, V. H. (2017). HIF-prolyl hydroxylases as therapeutic targets in erythropoiesis and iron metabolism. *Hemodial. Int.* 21 (1), S110–s124. doi:10.1111/hdi.12567

Hamidi, H., and Ivaska, J. (2018). Every step of the way: integrins in cancer progression and metastasis. *Nat. Rev. Cancer* 18, 533–548. doi:10.1038/s41568-018-0038-z

Han, J., and Shen, X. (2020). Long noncoding RNAs in osteosarcoma via various signaling pathways. *J. Clin. Lab. Anal.* 34, e23317. doi:10.1002/jcla.23317

Harjunpää, H., Llort Asens, M., Guenther, C., and Fagerholm, S. C. (2019). Cell adhesion molecules and their roles and regulation in the immune and tumor microenvironment. *Front. Immunol.* 10, 1078. doi:10.3389/fimmu.2019.01078

He, G., Nie, J. J., Liu, X., Ding, Z., Luo, P., Liu, Y., et al. (2023a). Zinc oxide nanoparticles inhibit osteosarcoma metastasis by downregulating β-catenin via HIF-1α/BNIP3/LC3B-mediated mitophagy pathway. *Bioact. Mater* 19, 690–702. doi:10.1016/j.bioactmat.2022.05.006

He, G., Pan, X., Liu, X., Zhu, Y., Ma, Y., Du, C., et al. (2020). HIF-1α-Mediated mitophagy determines ZnO nanoparticle-induced human osteosarcoma cell death both *in vitro* and *in vivo*. *ACS Appl. Mater Interfaces* 12, 48296–48309. doi:10.1021/acsami.0c12139

He, P., Xu, S., Miao, Z., Que, Y., Chen, Y., Li, S., et al. (2023b). Anti-Her2 affibody-decorated arsenene nanosheets induce ferroptosis through depleting intracellular GSH to overcome cisplatin resistance. *J. Nanobiotechnology* 21, 203. doi:10.1186/s12951-023-01963-7

He, Y., Jones, C. R., Fujiki, N., Xu, Y., Guo, B., Holder, J. L., Jr., et al. (2009). The transcriptional repressor DEC2 regulates sleep length in mammals. *Science* 325, 866–870. doi:10.1126/science.1174443

Hinton, K., Kirk, A., Paul, P., and Persad, S. (2023). Regulation of the epithelial to mesenchymal transition in osteosarcoma. *Biomolecules*, 13. doi:10.3390/biom13020398

Hompland, T., Fjeldbo, C. S., and Lyng, H. (2021). Tumor hypoxia as a barrier in cancer therapy: why levels matter. *Cancers (Basel)* 13, 499. doi:10.3390/cancers13030499

Hu, H., Miao, X. K., Li, J. Y., Zhang, X. W., Xu, J. J., Zhang, J. Y., et al. (2020). YC-1 potentiates the antitumor activity of gefitinib by inhibiting HIF-1α and promoting the endocytic trafficking and degradation of EGFR in gefitinib-resistant non-small-cell lung cancer cells. *Eur. J. Pharmacol.* 874, 172961. doi:10.1016/j.ejphar.2020.172961

Hu, T., He, N., Yang, Y., Yin, C., Sang, N., and Yang, Q. (2015). DEC2 expression is positively correlated with HIF-1 activation and the invasiveness of human osteosarcomas. *J. Exp. Clin. Cancer Res.* 34, 22. doi:10.1186/s13046-015-0135-8

Huang, H., Li, T., Meng, Z., Zhang, X., Jiang, S., Suo, M., et al. (2023). A risk model for prognosis and treatment response prediction in colon adenocarcinoma based on genes associated with the characteristics of the epithelial-mesenchymal transition. *Int. J. Mol. Sci.*, 24. doi:10.3390/ijms241713206

Huang, X., Han, L., Wang, R., Zhu, W., Zhang, N., Qu, W., et al. (2022). Dual-responsive nanosystem based on TGF-β blockade and immunogenic chemotherapy for effective chemoimmunotherapy. *Drug Deliv.* 29, 1358–1369. doi:10.1080/10717544.2022.2069877

Huang, X. Y., Huang, Z. L., Huang, J., Xu, B., Huang, X. Y., Xu, Y. H., et al. (2020). Exosomal circRNA-100338 promotes hepatocellular carcinoma metastasis via enhancing invasiveness and angiogenesis. *J. Exp. Clin. Cancer Res.* 39, 20. doi:10.1186/s13046-020-1529-9

Hussain, S., Peng, B., Cherian, M., Song, J. W., Ahirwar, D. K., and Ganju, R. K. (2020). The roles of stroma-derived chemokine in different stages of cancer metastases. *Front. Immunol.* 11, 598532. doi:10.3389/fimmu.2020.598532

Ildiz, E. S., Gvozdenovic, A., Kovacs, W. J., and Aceto, N. (2023). Travelling under pressure - hypoxia and shear stress in the metastatic journey. *Clin. Exp. Metastasis* 40, 375–394. doi:10.1007/s10585-023-10224-8

Infantino, V., Santarsiero, A., Convertini, P., Todisco, S., and Iacobazzi, V. (2021). Cancer cell metabolism in hypoxia: role of HIF-1 as key regulator and therapeutic target. *Int. J. Mol. Sci.*, 22. doi:10.3390/ijms22115703

Itoh, H., Kadomatsu, T., Tanoue, H., Yugami, M., Miyata, K., Endo, M., et al. (2018). TET2-dependent IL-6 induction mediated by the tumor microenvironment promotes tumor metastasis in osteosarcoma. *Oncogene* 37, 2903–2920. doi:10.1038/s41388-018-0160-0

Janiszewska, M., Primi, M. C., and Izard, T. (2020). Cell adhesion in cancer: beyond the migration of single cells. *J. Biol. Chem.* 295, 2495–2505. doi:10.1074/jbc.REV119.007759

Jin, J., Cong, J., Lei, S., Zhang, Q., Zhong, X., Su, Y., et al. (2023a). Cracking the code: deciphering the role of the tumor microenvironment in osteosarcoma metastasis. *Int. Immunopharmacol.* 121, 110422. doi:10.1016/j.intimp.2023.110422

Jin, Z., Aixi, Y., Baiwen, Q., Zonghuan, L., and Xiang, H. (2015). Inhibition of hypoxia-inducible factor-1 alpha radiosensitized MG-63 human osteosarcoma cells *in vitro*. *Tumori* 101, 578–584. doi:10.5301/tj.5000243

Jin, Z., Xiang, R., Dai, J., Wang, Y., and Xu, Z. (2023b). HIF-1α mediates CXCR4 transcription to activate the AKT/mTOR signaling pathway and augment the viability and migration of activated B cell-like diffuse large B-cell lymphoma cells. *Mol. Carcinog.* 62, 676–684. doi:10.1002/mc.23515

Kakkad, S., Krishnamachary, B., Jacob, D., Pacheco-Torres, J., Goggins, E., Bharti, S. K., et al. (2019). Molecular and functional imaging insights into the role of hypoxia in cancer aggression. *Cancer Metastasis Rev.* 38, 51–64. doi:10.1007/s10555-019-09788-3

Karreman, M. A., Bauer, A. T., Solecki, G., Berghoff, A. S., Mayer, C. D., Frey, K., et al. (2023). Active remodeling of capillary endothelium via cancer cell-derived MMP9 promotes metastatic brain colonization. *Cancer Res.* 83, 1299–1314. doi:10.1158/0008-5472.CAN-22-3964

Keremu, A., Aini, A., Maimaitirexiati, Y., Liang, Z., Aila, P., Xierela, P., et al. (2019). Overcoming cisplatin resistance in osteosarcoma through the miR-199a-modulated inhibition of HIF-1α. *Biosci. Rep.* 39. doi:10.1042/BSR20170080

Khan, K. A., and Kerbel, R. S. (2018). Improving immunotherapy outcomes with anti-angiogenic treatments and vice versa. *Nat. Rev. Clin. Oncol.* 15, 310–324. doi:10.1038/nrclinonc.2018.9

Khojastehnezhad, M. A., Seyedi, S. M. R., Raoufi, F., and Asoodeh, A. (2022). Association of hypoxia-inducible factor 1 expressions with prognosis role as a survival prognostic biomarker in the patients with osteosarcoma: a meta-analysis. *Expert Rev. Mol. Diagn* 22, 1099–1106. doi:10.1080/14737159.2022.2157719

Kikuchi, S., Yoshioka, Y., Prieto-Vila, M., and Ochiya, T. (2019). Involvement of extracellular vesicles in vascular-related functions in cancer progression and metastasis. *Int. J. Mol. Sci.* 20, 2584. doi:10.3390/ijms20102584

Koh, M. Y., Spivak-Kroizman, T., Venturini, S., Welsh, S., Williams, R. R., Kirkpatrick, D. L., et al. (2008). Molecular mechanisms for the activity of PX-478, an antitumor inhibitor of the hypoxia-inducible factor-1alpha. *Mol. Cancer Ther.* 7, 90–100. doi:10.1158/1535-7163.MCT-07-0463

Kuo, C. L., Chou, H. Y., Lien, H. W., Yeh, C. A., Wang, J. R., Chen, C. H., et al. (2023). A Fc-VEGF chimeric fusion enhances PD-L1 immunotherapy via inducing immune reprogramming and infiltration in the immunosuppressive tumor microenvironment. *Cancer Immunol. Immunother.* 72, 351–369. doi:10.1007/s00262-022-03255-9

Kushwaha, P. P., Gupta, S., Singh, A. K., and Kumar, S. (2019). Emerging role of migration and invasion enhancer 1 (MIEN1) in cancer progression and metastasis. *Front. Oncol.* 9, 868. doi:10.3389/fonc.2019.00868

Lan, H., Hong, W., Fan, P., Qian, D., Zhu, J., and Bai, B. (2017). Quercetin inhibits cell migration and invasion in human osteosarcoma cells. *Cell Physiol. Biochem.* 43, 553–567. doi:10.1159/000480528

Lee, S. H., Jee, J. G., Bae, J. S., Liu, K. H., and Lee, Y. M. (2015). A group of novel HIF-1α inhibitors, glyceollins, blocks HIF-1α synthesis and decreases its stability via inhibition of the PI3K/AKT/mTOR pathway and Hsp90 binding. *J. Cell Physiol.* 230, 853–862. doi:10.1002/jcp.24813

Leng, C., Zhang, Z. G., Chen, W. X., Luo, H. P., Song, J., Dong, W., et al. (2016). An integrin beta4-EGFR unit promotes hepatocellular carcinoma lung metastases by enhancing anchorage independence through activation of FAK-AKT pathway. *Cancer Lett.* 376, 188–196. doi:10.1016/j.canlet.2016.03.023

Li, H., Wang, Z., Chen, Z., Ci, T., Chen, G., Wen, D., et al. (2021b). Disrupting tumour vasculature and recruitment of aPDL1-loaded platelets control tumour metastasis. *Nat. Commun.* 12, 2773. doi:10.1038/s41467-021-22674-3

Li, K., Huo, Q., Dimmitt, N. H., Qu, G., Bao, J., Pandya, P. H., et al. (2023a). Osteosarcoma-enriched transcripts paradoxically generate osteosarcoma-suppressing extracellular proteins. *Elife* 12, 12. doi:10.7554/elife.83768

Li, L., Shen, S., Bickler, P., Jacobson, M. P., Wu, L. F., and Altschuler, S. J. (2023b). Searching for molecular hypoxia sensors among oxygen-dependent enzymes. *Elife* 12, 12. doi:10.7554/elife.87705

Li, T., Xiao, Y., and Huang, T. (2018a). HIF-1α-induced upregulation of lncRNA UCA1 promotes cell growth in osteosarcoma by inactivating the PTEN/AKT signaling pathway. *Oncol. Rep.* 39, 1072–1080. doi:10.3892/or.2018.6182

Li, X., Lu, Q., Xie, W., Wang, Y., and Wang, G. (2018b). Anti-tumor effects of triptolide on angiogenesis and cell apoptosis in osteosarcoma cells by inducing autophagy via repressing Wnt/β-Catenin signaling. *Biochem. Biophys. Res. Commun.* 496, 443–449. doi:10.1016/j.bbrc.2018.01.052

Li, Y., Zhang, M. Z., Zhang, S. J., Sun, X., Zhou, C., Li, J., et al. (2023c). HIF-1α inhibitor YC-1 suppresses triple-negative breast cancer growth and angiogenesis by targeting PlGF/VEGFR1-induced macrophage polarization. *Biomed. Pharmacother.* 161, 114423. doi:10.1016/j.biopha.2023.114423

Li, Y., Zhao, L., and Li, X. F. (2021a). Hypoxia and the tumor microenvironment. *Technol. Cancer Res. Treat.* 20, 15330338211036304. doi:10.1177/15330338211036304

Li, Z. Q., Wang, Z., Zhang, Y., Lu, C., Ding, Q. L., Ren, R., et al. (2021c). CircRNA_103801 accelerates proliferation of osteosarcoma cells by sponging miR-338-3p and regulating HIF-1/Rap1/PI3K-Akt pathway. *J. Biol. Regul. Homeost. Agents* 35, 1021–1028. doi:10.23812/20-725-A

Liao, K., Zhang, X., Liu, J., Teng, F., He, Y., Cheng, J., et al. (2020). The role of platelets in the regulation of tumor growth and metastasis: the mechanisms and targeted therapy. *MedComm* 2023 (4), e350. doi:10.1002/mco2.350

Liberti, M. V., and Locasale, J. W. (2016). The Warburg effect: how does it benefit cancer cells? *Trends Biochem. Sci.* 41, 211–218. doi:10.1016/j.tibs.2015.12.001

Lin, S., Zhu, B., Huang, G., Zeng, Q., and Wang, C. (2019). Microvesicles derived from human bone marrow mesenchymal stem cells promote U2OS cell growth under hypoxia: the role of PI3K/AKT and HIF-1α. *Hum. Cell* 32, 64–74. doi:10.1007/s13577-018-0224-z

Liu, M., Wang, D., and Li, N. (2016). MicroRNA-20b downregulates HIF-1α and inhibits the proliferation and invasion of osteosarcoma cells. *Oncol. Res.* 23, 257–266. doi:10.3727/096504016X14562725373752

Liu, Q. L., Luo, M., Huang, C., Chen, H. N., and Zhou, Z. G. (2021a). Epigenetic regulation of epithelial to mesenchymal transition in the cancer metastatic cascade: implications for cancer therapy. *Front. Oncol.* 11, 657546. doi:10.3389/fonc.2021.657546

Liu, Y., Huang, N., Liao, S., Rothzerg, E., Yao, F., Li, Y., et al. (2021b). Current research progress in targeted anti-angiogenesis therapy for osteosarcoma. *Cell Prolif.* 54, e13102. doi:10.1111/cpr.13102

Liu, Y., Wang, Y., Sun, S., Chen, Z., Xiang, S., Ding, Z., et al. (2022). Understanding the versatile roles and applications of EpCAM in cancers: from bench to bedside. *Exp. Hematol. Oncol.* 11, 97. doi:10.1186/s40164-022-00352-4

Luo, P., Zhang, Y. D., He, F., Tong, C. J., Liu, K., Liu, H., et al. (2022). HIF-1α-mediated augmentation of miRNA-18b-5p facilitates proliferation and metastasis in osteosarcoma through attenuation PHF2. *Sci. Rep.* 12, 10398. doi:10.1038/s41598-022-13660-w

Lv, F., Du, R., Shang, W., Suo, S., Yu, D., and Zhang, J. (2016). HIF-1α silencing inhibits the growth of osteosarcoma cells by inducing apoptosis. *Ann. Clin. Lab. Sci.* 46, 140–146.

Ma, Z., Wang, L. Z., Cheng, J. T., Lam, W. S. T., Ma, X., Xiang, X., et al. (2021). Targeting hypoxia-inducible factor-1-mediated metastasis for cancer therapy. *Antioxid. Redox Signal* 34, 1484–1497. doi:10.1089/ars.2019.7935

Magae, J., Furukawa, C., Kuwahara, S., Jeong, Y. J., Nakajima, H., and Chang, Y. C. (2019). 4-O-methylascochlorin stabilizes hypoxia-inducible factor-1 in a manner different from hydroxylase inhibition by iron chelating or substrate competition. *Biosci. Biotechnol. Biochem.* 83, 2244–2248. doi:10.1080/09168451.2019.1651626

Meazza, C., and Scanagatta, P. (2016). Metastatic osteosarcoma: a challenging multidisciplinary treatment. *Expert Rev. Anticancer Ther.* 16, 543–556. doi:10.1586/14737140.2016.1168697

Mohamed, O. A. A., Tesen, H. S., Hany, M., Sherif, A., Abdelwahab, M. M., and Elnaggar, M. H. (2023). The role of hypoxia on prostate cancer progression and metastasis. *Mol. Biol. Rep.* 50, 3873–3884. doi:10.1007/s11033-023-08251-5

Multhoff, G., and Vaupel, P. (2020). Hypoxia compromises anti-cancer immune responses. *Adv. Exp. Med. Biol.* 1232, 131–143. doi:10.1007/978-3-030-34461-0_18

Nangaku, M., and Eckardt, K. U. (2007). Hypoxia and the HIF system in kidney disease. *J. Mol. Med. Berl.* 85, 1325–1330. doi:10.1007/s00109-007-0278-y

Neophytou, C. M., Panagi, M., Stylianopoulos, T., and Papageorgis, P. (2021). The role of tumor microenvironment in cancer metastasis: molecular mechanisms and therapeutic opportunities. *Cancers (Basel)* 13, 2053. doi:10.3390/cancers13092053

Nieto, M. A., Huang, R. Y., Jackson, R. A., and Thiery, J. P. (2016). EMT: 2016. *Cell* 166, 21–45. doi:10.1016/j.cell.2016.06.028

Park, J. A., Espinosa-Cotton, M., Guo, H. F., Monette, S., and Cheung, N. V. (2023). Targeting tumor vasculature to improve antitumor activity of T cells armed *ex vivo* with T cell engaging bispecific antibody. *J. Immunother. Cancer*, 11. doi:10.1136/JITC-2023-006680

Peinado, H., Zhang, H., Matei, I. R., Costa-Silva, B., Hoshino, A., Rodrigues, G., et al. (2017). Pre-metastatic niches: organ-specific homes for metastases. *Nat. Rev. Cancer* 17, 302–317. doi:10.1038/nrc.2017.6

Phan, L. M., Yeung, S. C., and Lee, M. H. (2014). Cancer metabolic reprogramming: importance, main features, and potentials for precise targeted anti-cancer therapies. *Cancer Biol. Med.* 11, 1–19. doi:10.7497/j.issn.2095-3941.2014.01.001

Pihán, P., Carreras-Sureda, A., and Hetz, C. (2017). BCL-2 family: integrating stress responses at the ER to control cell demise. *Cell Death Differ.* 24, 1478–1487. doi:10.1038/cdd.2017.82

Rastogi, S., Aldosary, S., Saeedan, A. S., Ansari, M. N., Singh, M., and Kaithwas, G. (2023). NF-κB mediated regulation of tumor cell proliferation in hypoxic microenvironment. *Front. Pharmacol.* 14, 1108915. doi:10.3389/fphar.2023.1108915

Ravenna, L., Salvatori, L., and Russo, M. A. (2016). HIF3α: the little we know. *Febs J.* 283, 993–1003. doi:10.1111/febs.13572

Ren, Z., Hu, Y., Li, G., Kang, Y., Liu, Y., and Zhao, H. (2019). HIF-1α induced long noncoding RNA FOXD2-AS1 promotes the osteosarcoma through repressing p21. *Biomed. Pharmacother.* 117, 109104. doi:10.1016/j.biopha.2019.109104

Rickel, K., Fang, F., and Tao, J. (2017). Molecular genetics of osteosarcoma. *Bone* 102, 69–79. doi:10.1016/j.bone.2016.10.017

Ruan, Y., Chen, L., Xie, D., Luo, T., Xu, Y., Ye, T., et al. (2022). Mechanisms of cell adhesion molecules in endocrine-related cancers: a concise outlook. *Front. Endocrinol. (Lausanne)* 13, 865436. doi:10.3389/fendo.2022.865436

Sabharwal, S. S., Dudley, V. J., Landwerlin, C., and Schumacker, P. T. (2023). HH_2O_2 transit through the mitochondrial intermembrane space promotes tumor cell growth in vitro and in vivo. *J. Biol. Chem.* 299, 104624. doi:10.1016/j.jbc.2023.104624

Semenza, G. L. (2012). Hypoxia-inducible factors in physiology and medicine. *Cell* 148, 399–408. doi:10.1016/j.cell.2012.01.021

Semenza, G. L., and Wang, G. L. (1992). A nuclear factor induced by hypoxia via *de novo* protein synthesis binds to the human erythropoietin gene enhancer at a site required for transcriptional activation. *Mol. Cell Biol.* 12, 5447–5454. doi:10.1128/mcb.12.12.5447

Shang, C., Ou, X., Zhang, H., Wei, D., Wang, Q., and Li, G. (2022). Activation of PGRN/MAPK axis stimulated by the hypoxia-conditioned mesenchymal stem cell-derived HIF-1α facilitates osteosarcoma progression. *Exp. Cell Res.* 421, 113373. doi:10.1016/j.yexcr.2022.113373

Shen, S., Xu, Y., Gong, Z., Yao, T., Qiao, D., Huang, Y., et al. (2023). Positive feedback regulation of circular RNA Hsa_circ_0000566 and HIF-1α promotes osteosarcoma progression and glycolysis metabolism. *Aging Dis.* 14, 529–547. doi:10.14336/AD.2022.0826

Shen, Z., Pei, Q., Zhang, H., Yang, C., Cui, H., Li, B., et al. (2022). Hypoxia-inducible factor-1α inhibition augments efficacy of programmed cell death 1 antibody in murine prostatic cancer models. *Anticancer Drugs* 33, 587–594. doi:10.1097/CAD.0000000000001294

Shoaib, Z., Fan, T. M., and Irudayaraj, J. M. K. (2022). Osteosarcoma mechanobiology and therapeutic targets. *Br. J. Pharmacol.* 179, 201–217. doi:10.1111/bph.15713

Sinha, D., Saha, P., Samanta, A., and Bishayee, A. (2020). Emerging concepts of hybrid epithelial-to-mesenchymal transition in cancer progression. *Biomolecules* 10, 1561. doi:10.3390/biom10111561

Smeland, S., Bielack, S. S., Whelan, J., Bernstein, M., Hogendoorn, P., Krailo, M. D., et al. (2019). Survival and prognosis with osteosarcoma: outcomes in more than 2000 patients in the EURAMOS-1 (European and American Osteosarcoma Study) cohort. *Eur. J. Cancer* 109, 36–50. doi:10.1016/j.ejca.2018.11.027

Sukumar, M., Liu, J., Ji, Y., Subramanian, M., Crompton, J. G., Yu, Z., et al. (2013). Inhibiting glycolytic metabolism enhances CD8+ T cell memory and antitumor function. *J. Clin. Invest.* 123, 4479–4488. doi:10.1172/JCI69589

Sun, W., Wang, B., Qu, X. L., Zheng, B. Q., Huang, W. D., Sun, Z. W., et al. (2019). Metabolism of reactive oxygen species in osteosarcoma and potential treatment applications. *Cells* 9, 87. doi:10.3390/cells9010087

Sun, Y., Wang, H., Liu, M., Lin, F., and Hua, J. (2015). Resveratrol abrogates the effects of hypoxia on cell proliferation, invasion and EMT in osteosarcoma cells through downregulation of the HIF-1α protein. *Mol. Med. Rep.* 11, 1975–1981. doi:10.3892/mmr.2014.2913

Tan, H., and Zhao, L. (2019). lncRNA nuclear-enriched abundant transcript 1 promotes cell proliferation and invasion by targeting miR-186-5p/HIF-1α in osteosarcoma. *J. Cell Biochem.* 120, 6502–6514. doi:10.1002/jcb.27941

Tanaka, N., and Sakamoto, T. (2023). MT1-MMP as a key regulator of metastasis. *Cells*, 12. doi:10.3390/cells12172187

Tao, B., Shi, J., Shuai, S., Zhou, H., Zhang, H., Li, B., et al. (2021). CYB561D2 up-regulation activates STAT3 to induce immunosuppression and aggression in gliomas. *J. Transl. Med.* 19, 338. doi:10.1186/s12967-021-02987-z

Tarin, D. (2013). Role of the host stroma in cancer and its therapeutic significance. *Cancer Metastasis Rev.* 32, 553–566. doi:10.1007/s10555-013-9438-4

Thüring, E. M., Hartmann, C., Schwietzer, Y. A., Ebnet, K., and TMIGD1 (2023). TMIGD1: emerging functions of a tumor supressor and adhesion receptor. *Oncogene* 42, 1777–1785. doi:10.1038/s41388-023-02696-5

Tian, H., Cao, J., Li, B., Nice, E. C., Mao, H., Zhang, Y., et al. (2023). Managing the immune microenvironment of osteosarcoma: the outlook for osteosarcoma treatment. *Bone Res.* 11, 11. doi:10.1038/s41413-023-00246-z

Tsai, H. C., Lai, Y. Y., Hsu, H. C., Fong, Y. C., Lien, M. Y., and Tang, C. H. (2021). CCL4 stimulates cell migration in human osteosarcoma via the mir-3927-3p/integrin αvβ3 Axis. *Int. J. Mol. Sci.*, 22. doi:10.3390/ijms222312737

Tsai, H. C., Tzeng, H. E., Huang, C. Y., Huang, Y. L., Tsai, C. H., Wang, S. W., et al. (2017). WISP-1 positively regulates angiogenesis by controlling VEGF-A expression in human osteosarcoma. *Cell Death Dis.* 8, e2750. doi:10.1038/cddis.2016.421

Tuomisto, A., García-Solano, J., Sirniö, P., Väyrynen, J., Pérez-Guillermo, M., Mäkinen, M. J., et al. (2016). HIF-1α expression and high microvessel density are characteristic features in serrated colorectal cancer. *Virchows Arch.* 469, 395–404. doi:10.1007/s00428-016-1988-8

Tzeng, H. T., and Huang, Y. J. (2023). Tumor vasculature as an emerging pharmacological target to promote anti-tumor immunity. *Int. J. Mol. Sci.*, 24. doi:10.3390/ijms24054422

Vailas, M., Syllaios, A., Hashemaki, N., Sotiropoulou, M., Schizas, D., Papalampros, A., et al. (2019). Irreversible electroporation and sarcomas: where do we stand? *J. buon* 24, 1354–1359.

Valastyan, S., and Weinberg, R. A. (2011). Tumor metastasis: molecular insights and evolving paradigms. *Cell* 147, 275–292. doi:10.1016/j.cell.2011.09.024

Végran, F., Boidot, R., Michiels, C., Sonveaux, P., and Feron, O. (2011). Lactate influx through the endothelial cell monocarboxylate transporter MCT1 supports an NF-κB/IL-8 pathway that drives tumor angiogenesis. *Cancer Res.* 71, 2550–2560. doi:10.1158/0008-5472.CAN-10-2828

Vito, A., El-Sayes, N., and Mossman, K. (2020). Hypoxia-driven immune escape in the tumor microenvironment. *Cells* 9, 992. doi:10.3390/cells9040992

von Fallois, M., Kosyna, F. K., Mandl, M., Landesman, Y., Dunst, J., and Depping, R. (2021). Selinexor decreases HIF-1α via inhibition of CRM1 in human osteosarcoma and hepatoma cells associated with an increased radiosensitivity. *J. Cancer Res. Clin. Oncol.* 147, 2025–2033. doi:10.1007/s00432-021-03626-2

Wang, D., Qian, G., Wang, J., Wang, T., Zhang, L., Yang, P., et al. (2019a). Visfatin is involved in the cisplatin resistance of osteosarcoma cells via upregulation of Snail and Zeb1. *Cancer Biol. Ther.* 20, 999–1006. doi:10.1080/15384047.2019.1591675

Wang, G. L., and Semenza, G. L. (1993). Characterization of hypoxia-inducible factor 1 and regulation of DNA binding activity by hypoxia. *J. Biol. Chem.* 268, 21513–21518. doi:10.1016/s0021-9258(20)80571-7

Wang, H., Chen, Y., Wei, R., Zhang, J., Zhu, J., Wang, W., et al. (2023a). Synergistic chemoimmunotherapy augmentation via sequential nanocomposite hydrogel-mediated reprogramming of cancer-associated fibroblasts in osteosarcoma. *Adv. Mater* 2023, e2309591. doi:10.1002/adma.202309591

Wang, S. W., Liu, S. C., Sun, H. L., Huang, T. Y., Chan, C. H., Yang, C. Y., et al. (2015). CCL5/CCR5 axis induces vascular endothelial growth factor-mediated tumor angiogenesis in human osteosarcoma microenvironment. *Carcinogenesis* 36, 104–114. doi:10.1093/carcin/bgu218

Wang, X., Hu, Z., Wang, Z., Cui, Y., and Cui, X. (2019b). Angiopoietin-like protein 2 is an important facilitator of tumor proliferation, metastasis, angiogenesis and glycolysis in osteosarcoma. *Am. J. Transl. Res.* 11, 6341–6355.

Wang, X., Liang, X., Liang, H., and Wang, B. (2018). SENP1/HIF-1α feedback loop modulates hypoxia-induced cell proliferation, invasion, and EMT in human osteosarcoma cells. *J. Cell Biochem.* 119, 1819–1826. doi:10.1002/jcb.26342

Wang, Z., Zhu, M., Dong, R., Cao, D., Li, Y., Chen, Z., et al. (2023b). TH-302-loaded nanodrug reshapes the hypoxic tumour microenvironment and enhances PD-1 blockade efficacy in gastric cancer. *J. Nanobiotechnology* 21, 440. doi:10.1186/s12951-023-02203-8

Watson, M. J., Vignali, P. D. A., Mullett, S. J., Overacre-Delgoffe, A. E., Peralta, R. M., Grebinoski, S., et al. (2021). Metabolic support of tumour-infiltrating regulatory T cells by lactic acid. *Nature* 591, 645–651. doi:10.1038/s41586-020-03045-2

Wu, H., Lu, X. X., Wang, J. R., Yang, T. Y., Li, X. M., He, X. S., et al. (2019). TRAF6 inhibits colorectal cancer metastasis through regulating selective autophagic CTNNB1/β-catenin degradation and is targeted for GSK3B/GSK3β-mediated phosphorylation and degradation. *Autophagy* 15, 1506–1522. doi:10.1080/15548627.2019.1586250

Wu, Y., Kou, Q., Sun, L., and Hu, X. (2023). Effects of anoxic prognostic model on immune microenvironment in pancreatic cancer. *Sci. Rep.* 13, 9104. doi:10.1038/s41598-023-36413-9

Wu, Y., Tang, D., Liu, N., Xiong, W., Huang, H., Li, Y., et al. (2017). Reciprocal regulation between the circadian clock and hypoxia signaling at the genome level in mammals. *Cell Metab.* 25, 73–85. doi:10.1016/j.cmet.2016.09.009

Xiao, Q., Wei, Z., Li, Y., Zhou, X., Chen, J., Wang, T., et al. (2018). miR-186 functions as a tumor suppressor in osteosarcoma cells by suppressing the malignant phenotype and aerobic glycolysis. *Oncol. Rep.* 39, 2703–2710. doi:10.3892/or.2018.6394

Xie, X., Zhu, Y., Cheng, H., Li, H., Zhang, Y., Wang, R., et al. (2023). BPA exposure enhances the metastatic aggression of ovarian cancer through the ERα/AKT/mTOR/HIF-1α signaling axis. *Food Chem. Toxicol.* 176, 113792. doi:10.1016/j.fct.2023.113792

Xu, Y., Li, Y., Chen, X., Xiang, F., Deng, Y., Li, Z., et al. (2021). TGF-β protects osteosarcoma cells from chemotherapeutic cytotoxicity in a SDH/HIF1α dependent manner. *BMC Cancer* 21, 1200. doi:10.1186/s12885-021-08954-7

Yan, X., Yang, C., Hu, W., Chen, T., Wang, Q., Pan, F., et al. (2020). Knockdown of KRT17 decreases osteosarcoma cell proliferation and the Warburg effect via the AKT/mTOR/HIF1α pathway. *Oncol. Rep.* 44, 103–114. doi:10.3892/or.2020.7611

Yang, D., Xu, T., Fan, L., Liu, K., and Li, G. (2020). microRNA-216b enhances cisplatin-induced apoptosis in osteosarcoma MG63 and SaOS-2 cells by binding to JMJD2C and regulating the HIF1α/HES1 signaling axis. *J. Exp. Clin. Cancer Res.* 39, 201. doi:10.1186/s13046-020-01670-3

Yang, G., Wu, Y., Wan, R., Sang, H., Liu, H., Huang, W., et al. (2021a). 1-Bromopropane-induced apoptosis in OVCAR-3 cells via oxidative stress and inactivation of Nrf2. *Int. J. Oncol.* 37, 59–67. doi:10.1177/0748233720979427

Yang, S. Y., Garcia, E., Xia, W., and Wang, A. (2021b). Effects of hypoxia on proliferation and apoptosis of osteosarcoma cells. *Anticancer Res.* 41, 4781–4787. doi:10.21873/anticanres.15293

Yang, W., Lei, C., Song, S., Jing, W., Jin, C., Gong, S., et al. (2021c). Immune checkpoint blockade in the treatment of malignant tumor: current statue and future strategies. *Cancer Cell Int.* 21, 589. doi:10.1186/s12935-021-02299-8

Yao, B., Lu, Y., Li, Y., Bai, Y., Wei, X., Yang, Y., et al. (2023). BCLAF1-induced HIF-1α accumulation under normoxia enhances PD-L1 treatment resistances via BCLAF1-CUL3 complex. *Cancer Immunol. Immunother.* 72, 4279–4292. doi:10.1007/s00262-023-03563-8

Yu, X., Hu, L., Li, S., Shen, J., Wang, D., Xu, R., et al. (2019). Long non-coding RNA Taurine upregulated gene 1 promotes osteosarcoma cell metastasis by mediating HIF-1α via miR-143-5p. *Cell Death Dis.* 10, 280. doi:10.1038/s41419-019-1509-1

Zahedipour, F., Bolourinezhad, M., Teng, Y., and Sahebkar, A. (2021). The multifaceted therapeutic mechanisms of curcumin in osteosarcoma: state-of-the-art. *J. Oncol.* 2021, 3006853. doi:10.1155/2021/3006853

Zanconato, F., Cordenonsi, M., Piccolo, S., and Yap and, T. A. Z. (2019). YAP and TAZ: a signalling hub of the tumour microenvironment. *Nat. Rev. Cancer* 19, 454–464. doi:10.1038/s41568-019-0168-y

Zeng, D., Wang, J., Kong, P., Chang, C., Li, J., and Li, J. (2014). Ginsenoside Rg3 inhibits HIF-1α and VEGF expression in patient with acute leukemia via inhibiting the activation of PI3K/Akt and ERK1/2 pathways. *Int. J. Clin. Exp. Pathol.* 7, 2172–2178.

Zepeda-Enríquez, P., Silva-Cázares, M. B., and López-Camarillo, C. (2023). Novel insights into circular RNAs in metastasis in breast cancer: an update. *Noncoding RNA*, 9. doi:10.3390/NCRNA9050055

Zhang, C., Yang, C., Feldman, M. J., Wang, H., Pang, Y., Maggio, D. M., et al. (2017e). Vorinostat suppresses hypoxia signaling by modulating nuclear translocation of hypoxia inducible factor 1 alpha. *Oncotarget* 8, 56110–56125. doi:10.18632/oncotarget.18125

Zhang, H., Guo, X., Feng, X., Wang, T., Hu, Z., Que, X., et al. (2017b). MiRNA-543 promotes osteosarcoma cell proliferation and glycolysis by partially suppressing PRMT9 and stabilizing HIF-1α protein. *Oncotarget* 8, 2342–2355. doi:10.18632/oncotarget.13672

Zhang, L., Song, J., Xin, X., Sun, D., Huang, H., Chen, Y., et al. (2021). Hypoxia stimulates the migration and invasion of osteosarcoma via up-regulating the NUSAP1 expression. *Open Med. (Wars)* 16, 1083–1089. doi:10.1515/med-2020-0180

Zhang, T., Kastrenopoulou, A., Larrouture, Q., Athanasou, N. A., and Knowles, H. J. (2018). Angiopoietin-like 4 promotes osteosarcoma cell proliferation and migration and stimulates osteoclastogenesis. *BMC Cancer* 18, 536. doi:10.1186/s12885-018-4468-5

Zhang, X. D., Wu, Q., and Yang, S. H. (2017c). Effects of siRNA-mediated HIF-1α gene silencing on angiogenesis in osteosarcoma. *Pak J. Med. Sci.* 33, 341–346. doi:10.12669/pjms.332.12587

Zhang, Y., Liu, Y., Zou, J., Yan, L., Du, W., Zhang, Y., et al. (2017a). Tetrahydrocurcumin induces mesenchymal-epithelial transition and suppresses angiogenesis by targeting HIF-1α and autophagy in human osteosarcoma. *Oncotarget* 8, 91134–91149. doi:10.18632/oncotarget.19845

Zhang, Y., Sun, S., Qi, Y., Dai, Y., Hao, Y., Xin, M., et al. (2023). Characterization of tumour microenvironment reprogramming reveals invasion in epithelial ovarian carcinoma. *J. Ovarian Res.* 16, 200. doi:10.1186/s13048-023-01270-7

Zhang, Z., Hu, P., Xiong, J., and Wang, S. (2018). Inhibiting GIT1 reduces the growth, invasion, and angiogenesis of osteosarcoma. *Cancer Manag. Res.* 10, 6445–6455. doi:10.2147/CMAR.S181066

Zhang, Z., Li, N., Wei, X., Chen, B., Zhang, Y., Zhao, Y., et al. (2020). GRM4 inhibits the proliferation, migration, and invasion of human osteosarcoma cells through interaction with CBX4. *Biosci. Biotechnol. Biochem.* 84, 279–289. doi:10.1080/09168451.2019.1673147

Zhang, Z. C., Tang, C., Dong, Y., Zhang, J., Yuan, T., Tao, S. C., et al. (2017d). Targeting the long noncoding RNA MALAT1 blocks the pro-angiogenic effects of osteosarcoma and suppresses tumour growth. *Int. J. Biol. Sci.* 13, 1398–1408. doi:10.7150/ijbs.22249

Zhao, B., Liu, K., and Cai, L. (2019). LINK-A lncRNA functions in the metastasis of osteosarcoma by upregulating HIF1α. *Oncol. Lett.* 17, 5005–5011. doi:10.3892/ol.2019.10177

Zhao, H., Wu, Y., Chen, Y., and Liu, H. (2015). Clinical significance of hypoxia-inducible factor 1 and VEGF-A in osteosarcoma. *Int. J. Clin. Oncol.* 20, 1233–1243. doi:10.1007/s10147-015-0848-x

Zhao, Y., Xing, C., Deng, Y., Ye, C., and Peng, H. (2024). HIF-1α signaling: essential roles in tumorigenesis and implications in targeted therapies. *Genes Dis.* 11, 234–251. doi:10.1016/j.gendis.2023.02.039

Zheng, B., Ren, T., Huang, Y., Sun, K., Wang, S., Bao, X., et al. (2018). PD-1 axis expression in musculoskeletal tumors and antitumor effect of nivolumab in osteosarcoma model of humanized mouse. *J. Hematol. Oncol.* 11, 16. doi:10.1186/s13045-018-0560-1

Zheng, G. Z., Zhang, Q. H., Chang, B., Xie, P., Liao, H., Du, S. X., et al. (2023). Dioscin induces osteosarcoma cell apoptosis by upregulating ROS-mediated P38 MAPK signaling. *Drug Dev. Res.* 84, 25–35. doi:10.1002/ddr.22009

Zheng, W., Xiao, H., Liu, H., and Zhou, Y. (2015). Expression of programmed death 1 is correlated with progression of osteosarcoma. *Apmis* 123, 102–107. doi:10.1111/apm.12311

Zhong, C., Yang, D., Zhong, L., Xie, W., Sun, G., Jin, D., et al. (2023). Single-cell and bulk RNA sequencing reveals Anoikis related genes to guide prognosis and immunotherapy in osteosarcoma. *Sci. Rep.* 13, 20203. doi:10.1038/s41598-023-47367-3

Zhou, D., and He, L. (2022). Sauchinone inhibits hypoxia-induced invasion and epithelial-mesenchymal transition in osteosarcoma cells via inactivation of the sonic hedgehog pathway. *J. Recept Signal Transduct. Res.* 42, 173–179. doi:10.1080/10799893.2021.1881556

Zhou, J. S., Liu, Z. N., Chen, Y. Y., Liu, Y. X., Shen, H., Hou, L. J., et al. (2023). New advances in circulating tumor cell-mediated metastasis of breast cancer (Review). *Mol. Clin. Oncol.* 19, 71. doi:10.3892/mco.2023.2667

Zhou, Y., Yang, C., Wang, K., Liu, X., and Liu, Q. (2017). MicroRNA-33b inhibits the proliferation and migration of osteosarcoma cells via targeting hypoxia-inducible factor-1α. *Oncol. Res.* 25, 397–405. doi:10.3727/096504016X14743337535446

frontiers | Frontiers in Oncology

TYPE Original Research
PUBLISHED 16 April 2024
DOI 10.3389/fonc.2024.1325794

OPEN ACCESS

EDITED BY
Zhiyu Zhang,
Fourth Affiliated Hospital of China Medical University, China

REVIEWED BY
Fiona E. Freeman,
University College Dublin, Ireland
Fanyuan Yu,
Sichuan University, China

*CORRESPONDENCE
Eiichi Hinoi
hinoi-e@gifu-pu.ac.jp

†These authors have contributed equally to this work and share first authorship

RECEIVED 22 October 2023
ACCEPTED 03 April 2024
PUBLISHED 16 April 2024

CITATION
Osumi R, Sugihara K, Yoshimoto M, Tokumura K, Tanaka Y and Hinoi E (2024) Role of proteoglycan synthesis genes in osteosarcoma stem cells. *Front. Oncol.* 14:1325794. doi: 10.3389/fonc.2024.1325794

Role of proteoglycan synthesis genes in osteosarcoma stem cells

Ryoma Osumi[1†], Kengo Sugihara[1†], Makoto Yoshimoto[1], Kazuya Tokumura[1], Yuki Tanaka[1] and Eiichi Hinoi[1,2,3*]

[1]Department of Bioactive Molecules, Pharmacology, Gifu Pharmaceutical University, Gifu, Japan, [2]United Graduate School of Drug Discovery and Medical Information Sciences, Gifu University, Gifu, Japan, [3]Center for One Medicine Innovative Translational Research, Division of Innovative Modality Development, Gifu University, Gifu, Japan

Osteosarcoma stem cells (OSCs) contribute to the pathogenesis of osteosarcoma (OS), which is the most common malignant primary bone tumor. The significance and underlying mechanisms of action of proteoglycans (PGs) and glycosaminoglycans (GAGs) in OSC phenotypes and OS malignancy are largely unknown. This study aimed to investigate the role of PG/GAG biosynthesis and the corresponding candidate genes in OSCs and poor clinical outcomes in OS using scRNA-seq and bulk RNA-seq datasets of clinical OS specimens, accompanied by biological validation by *in vitro* genetic and pharmacological analyses. The expression of *β-1,3-glucuronyltransferase 3* (*B3GAT3*), one of the genes responsible for the biosynthesis of the common core tetrasaccharide linker region of PGs, was significantly upregulated in both OSC populations and OS tissues and was associated with poor survival in patients with OS with high stem cell properties. Moreover, the genetic inactivation of *B3GAT3* by RNA interference and pharmacological inhibition of PG biosynthesis abrogated the self-renewal potential of OSCs. Collectively, these findings suggest a pivotal role for *B3GAT3* and PG/GAG biosynthesis in the regulation of OSC phenotypes and OS malignancy, thereby providing a potential target for OSC-directed therapy.

KEYWORDS

osteosarcoma, osteosarcoma stem cell, proteoglycan, glycosaminoglycan, *β-1, 3glucuronyltransferase 3*

1 Introduction

Osteosarcoma (OS) is the most common primary malignant bone tumor with a high risk of bone and lung metastases (1–4). The incidence of OS shows a bimodal age distribution, peaking in adolescents and young adults, and adults older than 65 years, and is slightly more common in men than in women (5, 6). OS is characterized by marked

malignancy, strong invasiveness, rapid disease progression, and a high mortality rate (7, 8). OS commonly occurs in the knee joint (the metaphysis of the long tubular bones: the distal femur and the proximal tibia) (9, 10). The 5-year survival rate of OS stands at approximately 70% in the absence of metastases and decreases to 30% in patients with metastatic disease (11, 12). The exact cell origin of OS remains to be defined; however, it is believed to be cells of the osteoblast lineage, ranging from mesenchymal stem cells (MSCs) to osteoblast progenitors (13, 14). Osteosarcoma stem cells (OSCs) are functionally delineated based on their intrinsic properties, including self-renewal potential and multilineage differentiation capacity (15). OSCs also play a pivotal role in tumor initiation, recurrence, metastasis, and chemoresistance (16). Accumulating evidence suggests that targeting OSCs is an efficacious strategy for improving OS treatment (17, 18). Therefore, understanding the underlying molecular mechanisms governing the function of OSCs is necessary for developing novel therapeutic strategies for OS.

All mammalian glycosaminoglycans (GAGs), except hyaluronan (HA), attach to core proteins to form proteoglycans (PGs) (19–21). PGs/GAGs are abundantly distributed on the cell surface and in the extracellular matrix (22). GAGs have various biological functions and play important roles in numerous physiological and pathological conditions (23–25). Among them, the biosynthesis of chondroitin sulfate (CS); dermatan sulfate (DS), which is derived from CS by C5-epimerization of the β-D-glucuronic acid residue; and heparan sulfate (HS) begins with the formation of a common tetrasaccharide linker region to the core protein, followed by repeated addition of disaccharide units (26–28). The biosynthesis of the tetrasaccharide linker region in CS, DS, and HS is initiated by the enzymatic transfer of xylose to specific serine residues located in the core proteins of PGs within the endoplasmic reticulum by xylosyltransferase-I (XylT-I) and -II (XylT-II), encoded by *xylosyltransferase 1* (*XYLT1*) and *XYLT2*, respectively (29–31). Subsequently, two galactoses and a glucuronic acid are successively added to the xylose residues within the Golgi apparatus through the concerted actions of galactosyltransferase-I (GalT-I), galactosyltransferase-II (GalT-II), and glucuronyltransferase-I (GlcAT-I), which are encoded by *β-1,4-galactosyltransferase 7* (*B4GALT7*), *β-1,3-galactosyltransferase 6* (*B3GALT6*), and *β-1,3-glucuronyltransferase 3* (*B3GAT3*), respectively (32, 33).

PGs/GAGs not only play fundamental and diverse roles in the progression, malignancy, metastasis, and refractoriness of various types of cancer, but are also implicated in the cellular properties of cancer stem cells (CSCs) in some cancers, including glioblastoma, triple-negative breast cancer, and colorectal cancer (34, 35). Although some studies have been conducted to understand the role of PGs/GAGs in the pathogenesis of OS, limited data are available on the significance of enzymes related to PG/GAG biosynthesis in OSCs and OS malignancy. This study aimed to investigate the role of PG/GAG biosynthesis and corresponding candidate genes in OSCs and poor clinical outcomes in OS by combining bioinformatics analysis of clinical OS specimens with independent cohorts and *in vitro* genetic and pharmacological analyses.

2 Materials and methods

2.1 scRNA-seq data analysis

We analyzed two scRNA-seq datasets (GSE152048 and GSE162454) (36, 37). The GSE152048 dataset included 11 patients (five men and six women, 11–38 years). The data of five patients with primary osteoblastic OS lesions were used in subsequent analyses. The GSE162454 dataset included six primary OS patients (four men and two women, 13–45 years). The data of all six patients were used in subsequent analyses.

Data were analyzed using the "Seurat" package (version 4.3.0.1) in R (version 4.3.0) (38–40). First, the data were read using the Read10X function. In the preprocessing of each dataset, cells with > 6,000 and < 300 expressed genes with more than 10% mitochondrial RNA counts were considered low-quality and filtered out. The gene expression levels of the remained cells were normalized by regressing mitochondrial mapping rates on glmGamPoi using the SCTransform function. To remove batch effects, integration of the five sample datasets in GSE152048, and the six sample datasets in GSE152048, was performed using the SelectIntegrationFeatures, PrepSCTIntegration, RunPCA, FindIntegrationAnchors, and IntegrateData functions. Accordingly, 59,738 cells in GSE152048 and 32,681 cells in GSE162454 were used for downstream analysis, respectively. For dimensional reduction, principal component analysis (PCA) and t-distributed stochastic neighbor embedding (t-SNE) were performed using the RunPCA and RunTSNE functions. To cluster cell populations, k.param nearest neighbors were calculated using the FindNeighbors function using the first 50 principal components. Clusters were identified using theFindClusters function at a resolution of 0.2. Each cluster was manually annotated based on violin plots of the expression of established cell-specific marker genes. Detailed information on these marker genes is provided in Figure 1C and Supplementary Figure 1B. Osteoblasts, proliferating cells, and MSCs were extracted as OS cells from the identified clusters (n = 26,249 in GSE152048, n = 7,650 in GSE162454).

OS cells were divided into two groups, OSCs and non-OSCs, for downstream analysis. In GSE152048, *ABCG1*, *KLF4*, and *MYC* co-expressing cells were defined as OSCs (n = 58) and others as non-OSCs (n = 26,191). Similarly, *ABCG1*, *KLF4*, and *MYC* co-expressing cells were defined as OSCs (n = 10) and others as non-OSCs (n = 26,239). In GSE162454, *SOX2*, *NES*, and *MYC* co-expressing cells were defined as OSCs (n = 150) and others as non-OSCs (n = 7,500).

Sixty-three human PG/GAG biosynthesis-related genes were obtained by integrating four gene sets (KEGG_GLYCOSAMINOGLYCAN_BIOSYNTHESIS_CHONDROITIN_SULFATE, KEGG_GLYCOSAMINOGLYCAN_BIOSYNTHESIS_HEPARAN_SULFATE, KEGG_GLYCOSAMINOGLYCAN_BIOSYNTHESIS_KERATAN_SULFATE, and WP_PROTEOGLYCAN_BIOSYNTHESIS) registered in the MSigDB database (http://gsea-msigdb.org/gsea/msigdb/index.jsp). Differentially expressed genes (DEGs) were identified among these 63 genes using Wilcoxon's

10.3389/fonc.2024.1325794

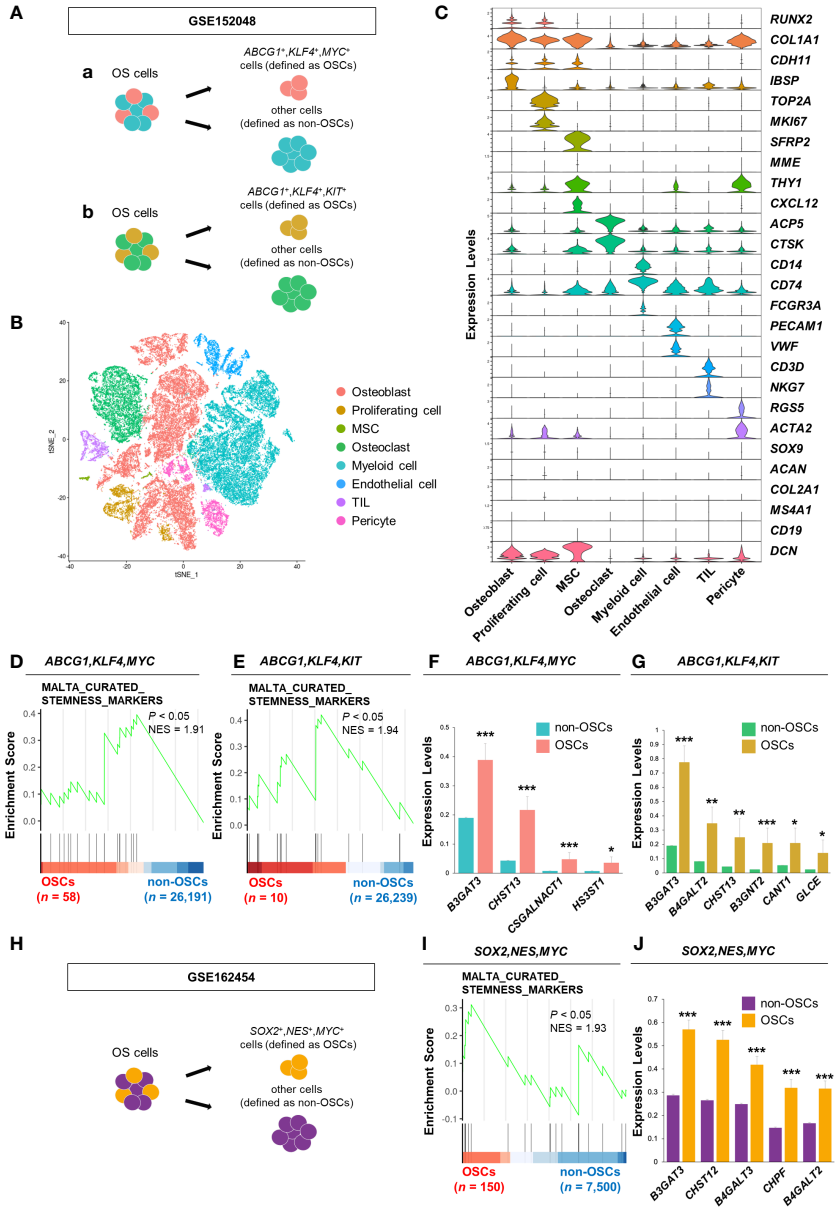

FIGURE 1
B3GAT3 is upregulated in the OSC population of patients with OS. **(A)** Schematic of the identification of the OSC population in GSE152048. (a) *ABCG1*, *KLF4*, and *MYC* co-expressing cells or (b) *ABCG1*, *KLF4*, and *KIT* co-expressing cells were defined as OSCs, respectively. **(B)** t-SNE plot of cell clusters classified in OS tissues. **(C)** Violin plots showing the normalized expression levels of 27 representative marker genes across 8 clusters. **(D, E)** Enrichment plot for a gene set related to "stemness" between OSCs ([D] *ABCG1*, *KLF4*, and *MYC* or [E] *ABCG1*, *KLF4*, and *KIT* co-expressing cells) and non-OSCs. **(F, G)** Barplot showing the expression levels of PG/GAG biosynthesis genes between OSCs ([F] *ABCG1*, *KLF4*, and *MYC* or [G] *ABCG1*, *KLF4*, and *KIT* co-expressing cells) and non-OSCs. (*$P < 0.05$, **$P < 0.01$, ***$P < 0.001$). **(H)** Schematic of the identification of the OSC population in GSE162454. *SOX2*, *NES*, and *MYC* co-expressing cells were defined as OSCs. **(I)** Enrichment plot for a gene set related to "stemness" between OSCs and non-OSCs. **(J)** Barplot showing the expression levels of PG/GAG biosynthesis genes between OSCs and non-OSCs. The top five most highly expressed genes in OSCs are shown (***$P < 0.001$).

rank-sum test ($P < 0.05$) using the wilcoxauc function in the "presto" package (version 1.0.0). Gene Set Enrichment Analysis (GSEA) was performed using the GSEA function (minGSsize, 5; maxGSsize, 500; eps, 0; pvalueCutoff, 0.05) in the "clusterProfiler" package (version 4.8.3). The gene sets used in GSEA were obtained from the C2 and C5 collections in the MSigDB database using the msigdbr function in the "msigdbr" package (version 7.5.1). Gene sets with NES > 0 and $P < 0.05$ were considered significantly enriched. Visualization was performed using the gseaplot2 function in the "enrichplot" package (version 1.20.1).

2.2 Bulk RNA-seq data analysis

We analyzed the RNA-seq dataset (PRJNA539828) obtained from OS ($n = 16$) and non-tumor ($n = 4$) tissues from patients with

OS (41). Fastq files were downloaded using "SRA Toolkit" (version 3.0.1). Trimming was performed using "Trim_Galore" (version 0.6.7). Quality control after trimming was performed using "FASTQC" (version 0.12.1). Mapping to the hg38 human genome assembly was performed using "STAR" (version 2.7.10b). Expression levels were calculated from the bam files generated by mapping using "RSEM" (version 1.3.3). GSEA was performed using the "clusterProfiler" package (version 4.8.3) in R (version 4.3.0). Visualization of the GSEA results was performed using the "enrichplot" package (version 1.20.3).

2.3 Survival analysis

Clinical data from patients with OS were downloaded from the TARGET-OS database. Patients were divided into high and low expression groups based on median gene expression values. Survival analysis was conducted with the log-rank test using the "survival" package (version 4.8.3). Kaplan–Meier curves were plotted using the "survminer" package (version 0.4.9).

2.4 Cell culture

HEK293T cells were obtained from the RIKEN Cell Bank (Saitama, Japan) and cultured in DMEM (FUJIFILM Wako Pure Chemical) supplemented with 10% FBS (Hyclone) and 1% penicillin/streptomycin (Thermo Fisher Scientific) at 37°C in 5% CO_2 (42). The patient-derived OS cell line 143B was obtained from the ATCC (Manassas, USA) and cultured in adherent medium containing DMEM supplemented with 10% FBS, 110 µg/mL sodium pyruvate (FUJIFILM Wako Pure Chemical), and 1% penicillin/streptomycin. Both cell types were cultured in tissue culture dishes (SARSTEDT) to ensure optimal adherence and expansion. To enrich stem-like cells, 143B cells were harvested using trypsin (BD Bioscience) and EDTA (FUJIFILM Wako Pure Chemical), then cultured in osteosphere medium containing DMEM/F12 (FUJIFILM Wako Pure Chemical) supplemented with 20 ng/mL recombinant human EGF (FUJIFILM Wako Pure Chemical), 20 ng/mL recombinant human basic FGF (FUJIFILM Wako Pure Chemical), B27 supplement without vitamin A (Gibco), GlutaMAX (Thermo Fisher Scientific), and 1% penicillin/streptomycin. Under these conditions, the cells were incubated in Ultra-Low Attachment Surface culture dishes (Corning). To assess the differentiation potential of OSCs, the cells were transferred from osteosphere to adherent medium, and from Ultra-Low Attachment Surface to tissue culture dishes, to promote adherence and differentiation.

2.5 Lentiviral transfection

To introduce vectors into HEK293T cells, the calcium phosphate method was employed (43). Lentiviral vectors containing expression constructs, pRRE and pREV packaging plasmids, and VSVG envelope plasmids were transfected into HEK293T cells for packaging. After 48 h of transfection, viral supernatants were harvested and subsequently incubated with 143B cells for 24 h. Following this, 143B cells were selected by culturing them for 4 days in the presence of 0.5 µg/mL puromycin prior to their use in experiments. Plasmid pLKO.1-sh*B3GAT3* (TRCN0000035610) was purchased from Sigma-Aldrich; pLKO.1 puro plasmid (#8453) was purchased from Addgene.

2.6 Sphere formation and limiting dilution assay

For sphere formation assay, 143B cells (1,000 cells) were seeded in ultra-low attachment 96-well plates (Corning) and cultured in osteosphere medium supplemented with 1% methylcellulose (FUJIFILM Wako Pure Chemical). The number of spheres was calculated on the fifth day using a BZ-X800 microscope (KEYENCE). Sphere formation ability was assessed by enumerating the quantity of spheres with a diameter > 30 µm (44). For limiting dilution assay, cells were seeded in 96-well plates at a density of 1, 5, 10, 20, 40, or 80 cells/well with five replicates per density. The presence of spheres in each well was determined after 5 days. Wells containing spheres with a diameter > 50 µm were considered positive, while those without spheres were considered negative. The frequency of sphere formation was assessed using an extreme limiting dilution algorithm (ELDA software; http://bioinf.wehi.edu.au/software/elda/).

2.7 Reverse transcription quantitative PCR

Total cellular RNA was isolated. cDNA was synthesized using reverse transcriptase and oligo-dT primers (45). RT-qPCR analysis was performed using gene-specific primers and THUNDERBIRD SYBR qPCR Mix (TOYOBO) on an MX3000P instrument (Agilent Technologies). mRNA expression levels were standardized using *GAPDH* as an internal control (46). The primer sequences used in this study are listed in the Supplementary Table.

2.8 Flow cytometry

143B cells (1,000,000 cells) were incubated with Fixable Viability Stain 780 (1:1000, #565388, BD) for 10 minutes at room temperature in the dark, followed by incubation with APC-CD133 (1:50, #566597, BD) for 30 minutes at 4°C in the dark. Samples were analyzed using a CytoFLEX S (Beckman).

2.9 Xenograft model of OS

Animal experiments were performed in accordance with the Guidelines for the Care and Use of Laboratory Animals of Gifu Pharmaceutical University. Four-week-old female BALB/c nu/nu mice were obtained from Japan SLC (Hamamatsu, Japan). Mice were injected subcutaneously with 5×10^6 143B cells. Tumor length

and width were measured with calipers. Tumor volume was calculated as (length × width^2)/2. Mice were euthanized before the tumor length exceeded 20 mm.

2.10 Statistical analysis

Unless otherwise specified, data are expressed as mean ± SE. Statistical significance was assessed using Student's *t*-test. A $P < 0.05$ was considered statistically significant.

3 Results

3.1 *B3GAT3* is upregulated in the OSC population of OS patient specimens

First, we analyzed a scRNA-seq dataset of clinical OS specimens deposited in the GEO database (GSE152048), to profile the properties of OSCs (Figure 1A). Eight clusters were identified through t-SNE analysis based on the genetic profiles of the cells (Figure 1B). Canonical markers were used to annotate the different cell types: osteoblasts (*RUNX2*$^+$,*COL1A1*$^+$,*CDH11*$^+$,*IBSP*$^+$), proliferating cells (*TOP2A*$^+$,*MKI67*$^+$), MSCs (*SFRP2*$^+$,*MME*$^+$, *THY1*$^+$,*CXCL12*$^+$), osteoclasts (*ACP5*$^+$,*CTSK*$^+$), myeloid cells (*CD14*$^+$,*CD74*$^+$,*FCGR3A*$^+$), endothelial cells (*PECAM1*$^+$,*VWF*$^+$), tumor infiltrating lymphocytes (TILs; *CD3D*$^+$,*NKG7*$^+$), and pericytes (*RGS5*$^+$,*ACTA2*$^+$) (Figure 1C). Malignant cells were distinguished from non-malignant cells using CNV inference (data not shown). The OS cell population was further divided into two groups, OSCs and non-OSCs, based on the co-expression of three stem cell markers, *ABCG1*, *KLF4*, and *MYC* (Figure 1Aa). The enrichment of the gene set involved in "stemness" in OSCs was confirmed by GSEA (Figure 1D). Consistent results were obtained when another cell population with co-expression of stem cell markers (*ABCG1*, *KLF4*, and *KIT*) was defined as OSCs (Figures 1Ab, E), allowing us to define these cells as the OSC population. Under these experimental conditions, we identified DEGs related to the biosynthesis of PGs/GAGs between OSCs and non-OSCs. Sixty-three DEGs related to the biosynthesis of PGs/GAGs were screened, with four and six significantly upregulated genes in OSCs defined by co-expression of *ABCG1*/*KLF4*/*MYC*, and *ABCG1*/*KLF4*/*KIT*, respectively (Figures 1F, G). Among the significantly upregulated genes, *B3GAT3*, one of the genes responsible for the biosynthesis of the common core tetrasaccharide linker region of PGs (47), was the most highly expressed gene in both *ABCG1*/*KLF4*/*MYC* and *ABCG1*/*KLF4*/*KIT* OSC populations (Figures 1F, G).

To confirm the results obtained from GSE152048, we analyzed a different scRNA-seq dataset (GSE162454) (Supplementary Figures 1A, B). The OS cell population was divided into two groups, OSCs and non-OSCs, based on the co-expression of three stem cell markers, *SOX2*, *NES*, and *MYC* (Figure 1H). The enrichment of the gene set involved in "stemness" in OSCs was confirmed by GSEA (Figure 1I). Among the 63 genes related to the biosynthesis of PGs/GAGs, *B3GAT3* was significantly upregulated in OSCs defined by co-expression of *SOX2*/*NES*/*MYC* (Figure 1J, Supplementary Figure 1C), with consistent results from two independent cohorts of clinical specimens.

3.2 *B3GAT3* is associated with poor prognosis in patients with OS with high stem cell properties

Next, we determined the expression levels of genes related to the biosynthesis of the common core tetrasaccharide linker region of PGs in clinical OS tissues. The expression levels of *B3GAT3*, *XYLT1, XYLT2, B4GALT7*, and *B3GALT6* were significantly upregulated in OS tissues compared to those in non-tumor tissues, according to the analysis of the bulk RNA-seq dataset (PRJNA539828) (Figure 2A). GSEA revealed significant enrichment of gene sets related to the "PG metabolic process", "PG biosynthetic process", and "GAG biosynthesis (HS)" (Figure 2B), which contain the above five PG biosynthesis genes. Contrary to the significant upregulation of *B3GAT3* in OSC populations (Figures 1F, G, J), the expression levels of *XYLT1, XYLT2, B4GALT7*, and *B3GALT6* did not differ significantly between OSCs and non-OSCs, even when OSC populations were defined under three different conditions (Figure 2C).

Next, we assessed whether the expression levels of *B3GAT3*, *XYLT1, XYLT2, B4GALT7*, and *B3GALT6* affected the survival of patients with OS using the TARGET-OS database. Kaplan–Meier analysis revealed that patients with OS with higher *B3GAT3* expression had significantly shorter survival than those with lower *B3GAT3* expression (Figure 2D). In contrast, the expression levels of *XYLT1*, *XYLT2*, *B4GALT7*, and *B3GALT6* were not significantly correlated with the prognosis of patients with OS (Figure 2D). Given that only *B3GAT3* expression was correlated with poor prognosis in patients with OS, we next assessed whether *B3GAT3* expression was associated with poor prognosis in patients with OS harboring higher stem cell properties. Kaplan–Meier analysis demonstrated that high *B3GAT3* expression was significantly associated with poor prognosis in patients with high expression of stemness markers, such as *PROM1*, *POU5F1*, *KLF4*, *BMI1*, *NGFR*, *ABCG1*, and *ABCG2* (Figure 2E).

3.3 Targeting *B3GAT3* impairs the self-renewal potential of 143B OS cells *in vitro*

To validate the results of the bioinformatics analysis, 143B cells were cultured under floating or adherent conditions, followed by determination of *B3GAT3* expression (Figure 3A). First, we confirmed the stemness and tumorigenicity of 143B cells *in vitro* and *in vivo* as previously demonstrated (48, 49). Under floating condition, 143B cells formed tumorspheres and exhibited self-renewal potential in the sphere formation and limited dilution assays, respectively (Supplementary Figures 2A, B), along with higher expression levels of the stem cell markers, *KLF4*, *ABCG1*, *SOX2*, and *BMI1* (Figure 3B). The proportion of CD133$^+$ cells were markedly increased in 143B tumorspheres (Supplementary Figure 2C). 143B tumorspheres

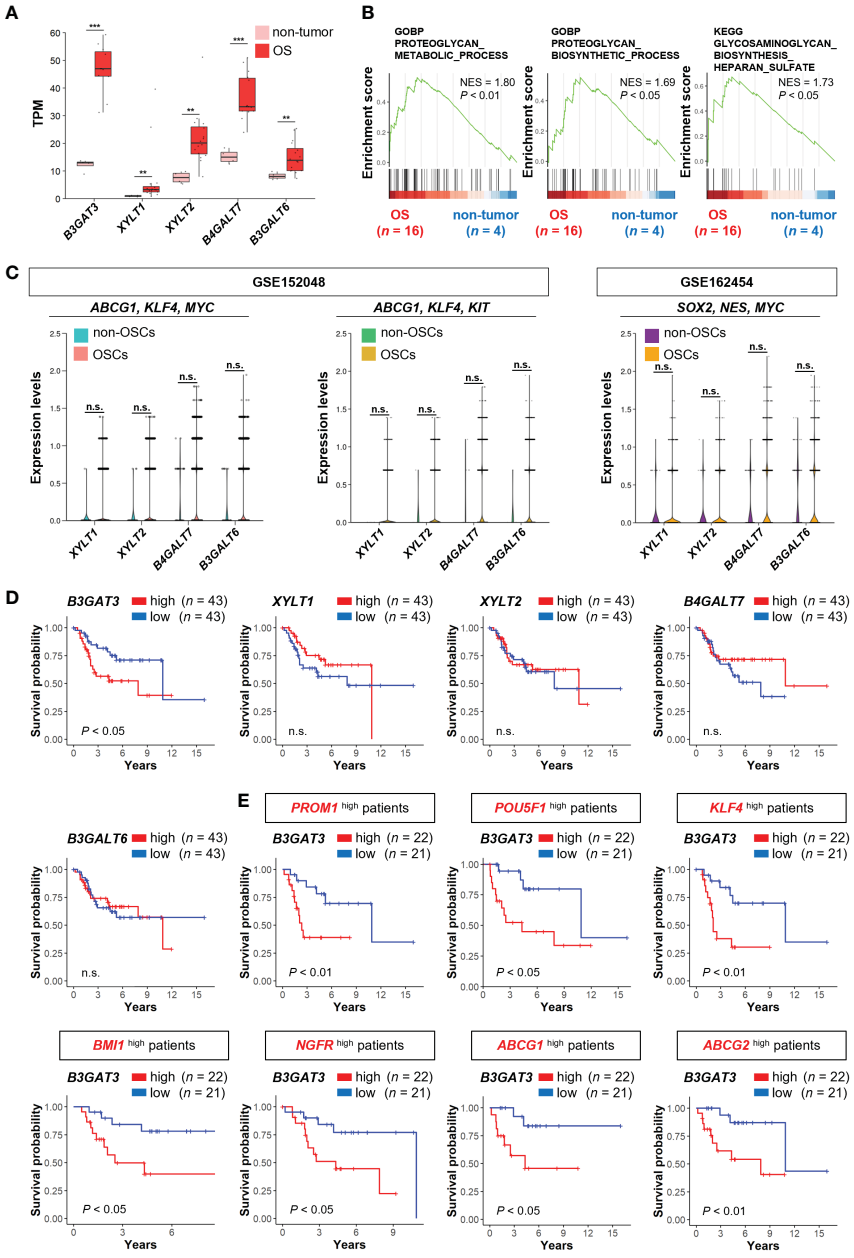

FIGURE 2
B3GAT3 is associated with poor prognosis in OS patients with high stemness. **(A)** The expression levels of *B3GAT3*, *XYLT1*, *XYLT2*, *B4GALT7*, and *B3GALT6* in OS (n = 16) and non-tumor (n = 4) tissues using bulk RNA-seq dataset (PRJNA539828) (**P < 0.01, ***P < 0.001). **(B)** The enrichment plots for gene sets related to "PG metabolic process", "PG biosynthetic process", and "GAG biosynthesis" in OS (n = 16) and non-tumor (n = 4) tissues. **(C)** The expression levels of *XYLT1*, *XYLT2*, *B4GALT7*, and *B3GALT6* in OSCs and non-OSCs using scRNA-seq datasets (GSE152048 and GSE162454). **(D)** Kaplan–Meier curves comparing patients with OS with high (n = 43) and low (n = 43) expression levels of *B3GAT3*, *XYLT1*, *XYLT2*, *B4GALT7*, and *B3GALT6* respectively. **(E)** Kaplan–Meier curves comparing high (n = 22) and low (n = 21) *B3GAT3* expression levels in patients with OS with high stemness. n.s., not significant.

differentiated into 143B cells under adherent conditions (Supplementary Figure 2D). The tumorigenicity of 143B cells was confirmed in an orthotopic xenograft mouse model (Supplementary Figure 2E). Under these conditions, *B3GAT3* expression was significantly upregulated in 143B tumorspheres compared to differentiated 143B cells (Figure 3C).

Next, we elucidated the functional significance of GlcAT-I/*B3GAT3* in 143B cells *in vitro* by targeting *B3GAT3* expression using lentiviral shRNA. *B3GAT3* mRNA levels were markedly reduced by sh*B3GAT3* in 143B cells (Figure 3D). Disruption of *B3GAT3* with shRNA significantly decreased tumorsphere formation ability of 143B cells (Figure 3E). Furthermore, *B3GAT3* knockdown resulted in a significant downregulation of the stem cell markers, *KLF4*, *ABCG1*, *SOX2*, and *BMI1* in 143B tumorspheres (Figure 3F). Next, we determined whether the pharmacological inhibition of PG biosynthesis by 4-nitrophenyl β-D-xylopyranoside (β-D-xyloside), an inhibitor of GAG chain attachment to the core protein (50), could confirm the genetic inhibition of *B3GAT3* in

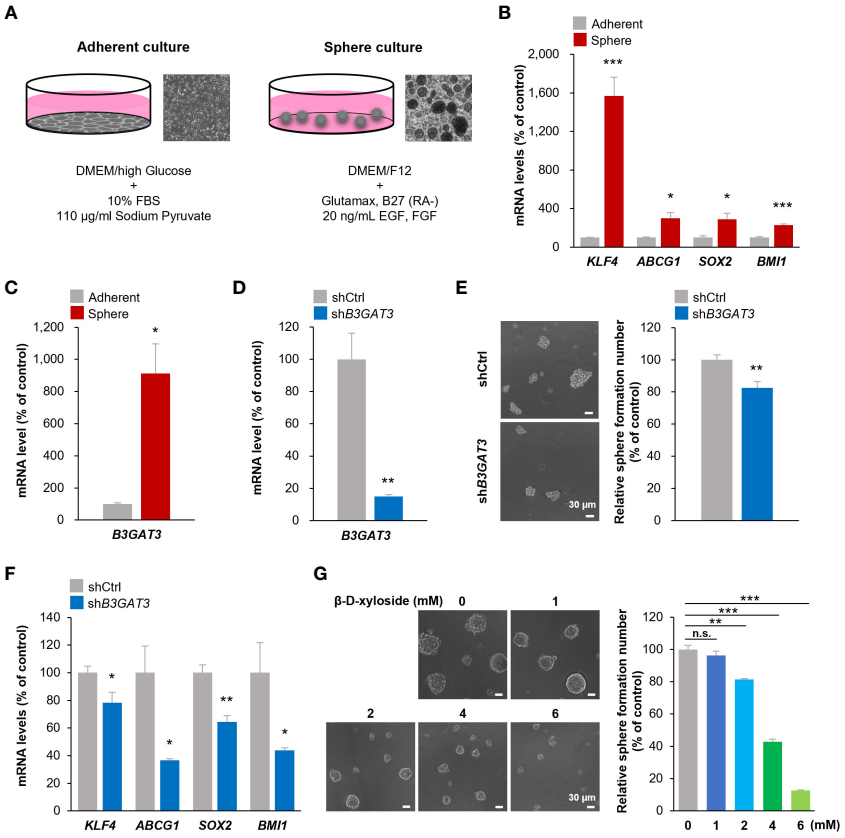

FIGURE 3
Inhibition of *B3GAT3* suppresses the self-renewal ability of 143B OS cells *in vitro*. **(A)** 143B cells were cultured under sphere or adherent conditions. **(B)** The mRNA expression levels of *KLF4*, *ABCG1*, *SOX2*, and *BMI1* were determined in sphere and adherent cells using RT-qPCR ($n = 4$. $^{*}P < 0.05$, $^{***}P < 0.001$). **(C)** The mRNA expression level of *B3GAT3* was determined in sphere and adherent cells using RT-qPCR ($n = 4$. $^{*}P < 0.05$). **(D)** *B3GAT3* knockdown was verified via RT-qPCR ($n = 5$. $^{**}P < 0.01$). **(E)** The sphere formation ability of 143B cells was assessed following *B3GAT3* knockdown. Representative images are presented (left, scale bar = 30 μm). The number of spheres was counted (right, $n = 8$. $^{**}P < 0.01$). **(F)** The mRNA expression levels of *KLF4*, *ABCG1*, *SOX2*, and *BMI1* were determined in *B3GAT3* knockdown 143B cells ($n = 4$. $^{*}P < 0.05$, $^{**}P < 0.01$). **(G)** 143B cells were treated with β-D-xyloside (0, 1, 2, 4, 6 mM), and sphere formation ability was assessed. Representative images are presented (left, scale bar = 30 μm). The number of spheres was counted (right, $n = 5$. $^{**}P < 0.01$, $^{***}P < 0.001$ using Student's *t*-test with Holm-Sidak correction for multiple comparisons). The mRNA expression level (normalized to *GAPDH*) is presented relative to that in **(B, C)** adherent cells and **(D, F)** cells treated with shCtrl. n.s., not significant.

143B cells. β-D-xyloside significantly decreased the tumorsphere formation ability of 143B cells at concentrations > 2 mM in a concentration-dependent manner (Figure 3G). Although further studies should be performed to demonstrate the pivotal role of *B3GAT3* on OSC properties by purifying stem cells from 143B tumorspheres because of their heterogeneous population including a subset exhibiting OSC markers, these genetic and pharmacological analyses indicate that *B3GAT3* and PG/GAG biosynthesis could be implicated in the regulation of stem cell properties of 143B *in vitro*.

4 Discussion

PGs/GAGs are widely recognized as important regulators of stem cell function in embryonic development and tissue regeneration (51, 52). Moreover, the aberrant functions of PGs/GAGs have recently been shown to contribute to CSC phenotypes, tumor initiation, recurrence, metastasis, and chemoresistance (35). The assembly of HS, CS, and DS is initiated by the formation of a common tetrasaccharide structure (Xyl-Gal-Gal-GlcA), catalyzed by XylT-I, XylT-II, GalT-I, GalT-II, and GlcAT-I, encoded by *XYLT1*, *XYLT2*, *B4GALT7*, *B3GALT6*, and *B3GAT3*, respectively (26–28). Mutations in these genes can cause inherited diseases that result in various bone, skin, and connective tissue abnormalities (53, 54). For instance, mutations in *B3GAT3* have been implicated in multiple joint dislocations, short stature, and craniofacial dysmorphism, with or without congenital heart defects (47). However, the importance of PG/GAG biosynthesis and the functional roles of the corresponding genes (*XYLT1*, *XYLT2*, *B4GALT7*, *B3GALT6*, and *B3GAT3*) in OSC properties and OS pathogenesis are largely unknown. Although further *in vivo* analyses should be performed to validate our findings, to our knowledge, this is the first study to reveal, using integrated bioinformatics analysis and *in vitro* genetic and pharmacological studies, that the PG/GAG biosynthesis pathway and corresponding enzyme, GlcAT-I/*B3GAT3*, may be associated with the maintenance of OSC characteristics and OS malignancy.

Notably, the expression analysis of DEGs related to the biosynthesis of PGs/GAGs revealed the potential involvement of

alternative candidate genes in OSC properties. Carbohydrate sulfotransferase 13 (*CHST13*), which catalyzes the transfer of sulfate to position 4 of the GalNAc residue of chondroitin (55), was the commonly significantly upregulated gene in all three OSC populations defined by the co-expression of *ABCG1*/*KLF4*/*MYC*, and *ABCG1*/*KLF4*/*KIT*, and *SOX2*/*NES*/*MYC* (Figures 1F, G, J, Supplementary Figure 1C). In addition to *B3GAT3* and *CHST13*, there were several significantly upregulated genes in each OSC population without overlap, indicating that these additional genes require further exploration. OS is highly heterogeneous in terms of molecular pathogenesis, which is at least in part due to the genetic and phenotypic variation in OSCs, suggesting that optimal biomarkers vary slightly between patients and cancer types (56, 57). For that reason, different OSC markers were used for each of the datasets: GSE152048 and GSE162454. It is also noteworthy that there were discrepancies in the expression of PG biosynthesis genes between OSC populations and OS tissues. Only *B3GAT3* was significantly upregulated in OSC populations (Figures 1F, G, J, 2C). However, all five PG biosynthesis genes (*XYLT1*, *XYLT2*, *B4GALT7*, *B3GALT6*, and *B3GAT3*) were significantly upregulated in OS tissues (Figure 2A), in which the proportion of OSC is small. Therefore, it can be speculated that XylT-I/*XYLT1*, XylT-II/*XYLT2*, GalT-I/*B4GALT7*, and GalT-II/*B3GALT6* may have functional roles in differentiated OS cell properties rather than in OSC properties, providing an incentive to pursue further research to determine their roles in OS pathogenesis in cell culture studies.

The primary therapeutic approach for OS is a combination of surgical intervention and chemotherapy. Effective treatments for OS have not improved over the past four decades (3, 4). Although accumulating evidence suggests that mutations in the tumor suppressor genes, *RB1* and *TP53*, are associated with the development of OS, cytogenetic analysis suggests that genomic profiles differ significantly among patients with OS, without specific patterns, resulting in difficulties in the development of new and effective drugs and innovative treatment strategies (58–62). Our findings contribute to the improvement of our understanding of the molecular mechanisms underlying OS development and progression, as well as OSC properties, and suggest that PG/GAG biosynthesis and the corresponding genes expressed by OSCs may represent novel and effective targets for drug development to treat OS in humans.

Data availability statement

The datasets presented in this study can be found in online repositories. The names of the repository/repositories and accession number(s) can be found in the article/Supplementary Material.

Ethics statement

Ethical approval was not required for the studies on humans in accordance with the local legislation and institutional requirements because only commercially available established cell lines were used.

Author contributions

EH: Writing – original draft, Writing – review & editing, Conceptualization, Funding acquisition, Supervision. RO: Writing – original draft, Writing – review & editing, Conceptualization, Formal analysis, Investigation, Visualization. KS: Writing – original draft, Writing – review & editing, Conceptualization, Formal analysis, Investigation, Visualization. MY: Writing – original draft, Writing – review & editing, Formal analysis, Investigation, Methodology, Validation, Visualization. KT: Writing – original draft, Writing – review & editing, Formal analysis, Investigation, Methodology, Validation, Visualization. YT: Writing – original draft, Formal analysis, Investigation, Methodology, Validation.

Funding

The author(s) declare financial support was received for the research, authorship, and/or publication of this article. This work was partly supported by the Japan Society for the Promotion of Science (20H03407 to EH).

Acknowledgments

Bioinformatics analyses were performed using the super-computing resource provided by the Human Genome Center, Institute of Medical Science, University of Tokyo.

Conflict of interest

EH received grants from the Japan Society for the Promotion of Science for this study.

The remaining authors declare that the research was conducted in the absence of any commercial or financial relationships that could be constructed as a potential conflict of interest.

Publisher's note

Supplementary material

The Supplementary Material for this article can be found online at: https://www.frontiersin.org/articles/10.3389/fonc.2024.1325794/full#supplementary-material

References

1. Panez-Toro I, Muñoz-García J, Vargas-Franco JW, Renodon-Cornière A, Heymann MF, Lézot F, et al. Advances in osteosarcoma. *Curr osteoporosis Rep*. (2023) 21:330–43. doi: 10.1007/s11914-023-00803-9

2. Rickel K, Fang F, Tao J. Molecular genetics of osteosarcoma. *Bone*. (2017) 102:69–79. doi: 10.1016/j.bone.2016.10.017

3. Beird HC, Bielack SS, Flanagan AM, Gill J, Heymann D, Janeway KA, et al. Osteosarcoma. *Nat Rev Dis Primers*. (2022) 8:77. doi: 10.1038/s41572-022-00409-y

4. Gill J, Gorlick R. Advancing therapy for osteosarcoma. *Nat Rev Clin Oncol*. (2021) 18:609–24. doi: 10.1038/s41571-021-00519-8

5. Brown HK, Schiavone K, Gouin F, Heymann MF, Heymann D. Biology of bone sarcomas and new therapeutic developments. *Calcified Tissue Int*. (2018) 102:174–95. doi: 10.1007/s00223-017-0372-2

6. Xie D, Wang Z, Li J, Guo DA, Lu A, Liang C. Targeted delivery of chemotherapeutic agents for osteosarcoma treatment. *Front Oncol*. (2022) 12:843345. doi: 10.3389/fonc.2022.843345

7. Berner K, Johannesen TB, Berner A, Haugland HK, Bjerkehagen B, Bøhler PJ, et al. Time-trends on incidence and survival in a nationwide and unselected cohort of patients with skeletal osteosarcoma. *Acta Oncol (Stockholm Sweden)*. (2015) 54:25–33. doi: 10.3109/0284186x.2014.923934

8. Ji Z, Shen J, Lan Y, Yi Q, Liu H. Targeting signaling pathways in osteosarcoma: Mechanisms and clinical studies. *MedComm*. (2023) 4:e308. doi: 10.1002/mco2.308

9. Yang Z, Li X, Yang Y, He Z, Qu X, Zhang Y. Long noncoding RNAs in the progression, metastasis, and prognosis of osteosarcoma. *Cell Death Dis*. (2016) 7:e2389. doi: 10.1038/cddis.2016.272

10. Pang H, Wu T, Peng Z, Tan Q, Peng X, Zhan Z, et al. Baicalin induces apoptosis and autophagy in human osteosarcoma cells by increasing ROS to inhibit PI3K/Akt/mTOR, ERK1/2 and β-catenin signaling pathways. *J Bone Oncol*. (2022) 33:100415. doi: 10.1016/j.jbo.2022.100415

11. Zhao X, Wu Q, Gong X, Liu J, Ma Y. Osteosarcoma: a review of current and future therapeutic approaches. *Biomed Eng Online*. (2021) 20:24. doi: 10.1186/s12938-021-00860-0

12. Kansara M, Teng MW, Smyth MJ, Thomas DM. Translational biology of osteosarcoma. *Nat Rev Cancer*. (2014) 14:722–35. doi: 10.1038/nrc3838

13. Mutsaers AJ, Walkley CR. Cells of origin in osteosarcoma: mesenchymal stem cells or osteoblast committed cells? *Bone*. (2014) 62:56–63. doi: 10.1016/j.bone.2014.02.003

14. Franceschini N, Verbruggen B, Tryfonidou MA, Kruisselbrink AB, Baelde H, de Visser KE, et al. Transformed canine and murine mesenchymal stem cells as a model for sarcoma with complex genomics. *Cancers*. (2021) 13:1126. doi: 10.3390/cancers13051126

15. Yan GN, Lv YF, Guo QN. Advances in osteosarcoma stem cell research and opportunities for novel therapeutic targets. *Cancer Lett*. (2016) 370:268–74. doi: 10.1016/j.canlet.2015.11.003

16. Fujiwara S, Kawamoto T, Kawakami Y, Koterazawa Y, Hara H, Takemori T, et al. Acquisition of cancer stem cell properties in osteosarcoma cells by defined factors. *Stem Cell Res Ther*. (2020) 11:429. doi: 10.1186/s13287-020-01944-9

17. Abarrategi A, Tornin J, Martinez-Cruzado L, Hamilton A, Martinez-Campos E, Rodrigo JP, et al. Osteosarcoma: cells-of-origin, cancer stem cells, and targeted therapies. *Stem Cells Int*. (2016) 2016:3631764. doi: 10.1155/2016/3631764

18. Menéndez ST, Gallego B, Murillo D, Rodríguez A, Rodríguez R. Cancer stem cells as a source of drug resistance in bone sarcomas. *J Clin Med*. (2021) 10. doi: 10.3390/jcm10122621

19. Muir H. Proteoglycans of cartilage. *J Clin Pathol*. (1978) 31:67–81. doi: 10.1136/jcp.31.Suppl_12.67

20. Kjellén L, Lindahl U. Proteoglycans: structures and interactions. *Annu Rev Biochem*. (1991) 60:443–75. doi: 10.1146/annurev.bi.60.070191.002303

21. Couchman JR. Transmembrane signaling proteoglycans. *Annu Rev Cell Dev Biol*. (2010) 26:89–114. doi: 10.1146/annurev-cellbio-100109-104126

22. Esko JD, Kimata K, Lindahl U. Proteoglycans and sulfated glycosaminoglycans. In: Varki A, Cummings RD, Esko JD, Freeze HH, Stanley P, Bertozzi CR, et al, editors. *Essentials of glycobiology*. Cold Spring Harbor Laboratory Press Copyright © 2009, The Consortium of Glycobiology Editors, La Jolla, California, Cold Spring Harbor (NY (2009).

23. Mizumoto S, Yamada S, Sugahara K. Molecular interactions between chondroitin-dermatan sulfate and growth factors/receptors/matrix proteins. *Curr Opin Struct Biol*. (2015) 34:35–42. doi: 10.1016/j.sbi.2015.06.004

24. Miller GM, Hsieh-Wilson LC. Sugar-dependent modulation of neuronal development, regeneration, and plasticity by chondroitin sulfate proteoglycans. *Exp Neurol*. (2015) 274:115–25. doi: 10.1016/j.expneurol.2015.08.015

25. Soares da Costa D, Reis RL, Pashkuleva I. Sulfation of glycosaminoglycans and its implications in human health and disorders. *Annu Rev Biomed Eng*. (2017) 19:1–26. doi: 10.1146/annurev-bioeng-071516-044610

26. Kreuger J, Kjellén L. Heparan sulfate biosynthesis: regulation and variability. *J Histochem cytochemistry: Off J Histochem Soc*. (2012) 60:898–907. doi: 10.1369/0022155412464972

27. Mikami T, Kitagawa H. Biosynthesis and function of chondroitin sulfate. *Biochim Biophys Acta*. (2013) 1830:4719–33. doi: 10.1016/j.bbagen.2013.06.006

28. Sugahara K, Kitagawa H. Recent advances in the study of the biosynthesis and functions of sulfated glycosaminoglycans. *Curr Opin Struct Biol*. (2000) 10:518–27. doi: 10.1016/s0959-440x(00)00125-1

29. Götting C, Kuhn J, Brinkmann T, Kleesiek K. Xylosylation of alternatively spliced isoforms of Alzheimer APP by xylosyltransferase. *J Protein Chem*. (1998) 17:295–302. doi: 10.1023/a:1022549121672

30. Hinsdale ME. Xylosyltransferase I, II (XYLT1,2). In: Taniguchi N, Honke K, Fukuda M, Narimatsu H, Yamaguchi Y, Angata T, editors. *Handbook of glycosyltransferases and related genes*. Springer Japan, Tokyo (2014). p. 873–83.

31. Briggs DC, Hohenester E. Structural basis for the initiation of glycosaminoglycan biosynthesis by human xylosyltransferase 1. *Structure (London England: 1993)*. (2018) 26:801–9.e3. doi: 10.1016/j.str.2018.03.014

32. Wen J, Xiao J, Rahdar M, Choudhury BP, Cui J, Taylor GS, et al. Xylose phosphorylation functions as a molecular switch to regulate proteoglycan biosynthesis. *Proc Natl Acad Sci United States America*. (2014) 111:15723–8. doi: 10.1073/pnas.1417993111

33. Koike T, Izumikawa T, Tamura J, Kitagawa H. FAM20B is a kinase that phosphorylates xylose in the glycosaminoglycan-protein linkage region. *Biochem J*. (2009) 421:157–62. doi: 10.1042/bj20090474

34. Ibrahim SA, Hassan H, Vilardo L, Kumar SK, Kumar AV, Kelsch R, et al. Syndecan-1 (CD138) modulates triple-negative breast cancer stem cell properties via regulation of LRP-6 and IL-6-mediated STAT3 signaling. *PloS One*. (2013) 8:e85737. doi: 10.1371/journal.pone.0085737

35. Vitale D, Kumar Katakam S, Greve B, Jang B, Oh ES, Alaniz L, et al. Proteoglycans and glycosaminoglycans as regulators of cancer stem cell function and therapeutic resistance. *FEBS J*. (2019) 286:2870–82. doi: 10.1111/febs.14967

36. Zhou Y, Yang D, Yang Q, Lv X, Huang W, Zhou Z, et al. Single-cell RNA landscape of intratumoral heterogeneity and immunosuppressive microenvironment in advanced osteosarcoma. *Nat Commun*. (2020) 11:6322. doi: 10.1038/s41467-020-20059-6

37. Liu Y, Feng W, Dai Y, Bao M, Yuan Z, He M, et al. Single-cell transcriptomics reveals the complexity of the tumor microenvironment of treatment-naive osteosarcoma. *Front Oncol*. (2021) 11:709210. doi: 10.3389/fonc.2021.709210

38. Horie T, Fukasawa K, Yamada T, Mizuno S, Iezaki T, Tokumura K, et al. Erk5 in bone marrow mesenchymal stem cells regulates bone homeostasis by preventing osteogenesis in adulthood. *Stem Cells (Dayton Ohio)*. (2022) 40:411–22. doi: 10.1093/stmcls/sxac011

39. Yoshimoto M, Sadamori K, Tokumura K, Tanaka Y, Fukasawa K, Hinoi E. Bioinformatic analysis reveals potential relationship between chondrocyte senescence and protein glycosylation in osteoarthritis pathogenesis. *Front Endocrinol*. (2023) 14:1153689. doi: 10.3389/fendo.2023.1153689

40. Tokumura K, Sadamori K, Yoshimoto M, Tomizawa A, Tanaka Y, Fukasawa K, et al. The bioinformatics identification of potential protein glycosylation genes associated with a glioma stem cell signature. *BioMedInformatics*. (2024) 4:75–88. doi: 10.3390/biomedinformatics4010005

41. Wang X, Qin G, Liang X, Wang W, Wang Z, Liao D, et al. Targeting the CK1α/CBX4 axis for metastasis in osteosarcoma. *Nat Commun*. (2020) 11:1141. doi: 10.1038/s41467-020-14870-4

42. Fukasawa K, Lyu J, Kubo T, Tanaka Y, Suzuki A, Horie T, et al. MEK5-ERK5 axis promotes self-renewal and tumorigenicity of glioma stem cells. *Cancer Res Commun*. (2023) 3:148–59. doi: 10.1158/2767-9764.crc-22-0243

43. Hiraiwa M, Fukasawa K, Iezaki T, Sabit H, Horie T, Tokumura K, et al. SMURF2 phosphorylation at Thr249 modifies glioma stemness and tumorigenicity by regulating TGF-β receptor stability. *Commun Biol*. (2022) 5:22. doi: 10.1038/s42003-021-02950-0

44. Fukasawa K, Kadota T, Horie T, Tokumura K, Terada R, Kitaguchi Y, et al. CDK8 maintains stemness and tumorigenicity of glioma stem cells by regulating the c-MYC pathway. *Oncogene*. (2021) 40:2803–15. doi: 10.1038/s41388-021-01745-1

45. Hinoi E, Iezaki T, Ozaki K, Yoneda Y. Nuclear factor-κB is a common upstream signal for growth differentiation factor-5 expression in brown adipocytes exposed to pro-inflammatory cytokines and palmitate. *Biochem Biophys Res Commun*. (2014) 452:974–9. doi: 10.1016/j.bbrc.2014.09.022

46. Nakamura Y, Hinoi E, Iezaki T, Takada S, Hashizume S, Takahata Y, et al. Repression of adipogenesis through promotion of Wnt/β-catenin signaling by TIS7 up-regulated in adipocytes under hypoxia. *Biochim Biophys Acta*. (2013) 1832:1117–28. doi: 10.1016/j.bbadis.2013.03.010

47. Yauy K, Tran Mau-Them F, Willems M, Coubes C, Blanchet P, Herlin C, et al. B3GAT3-related disorder with craniosynostosis and bone fragility due to a unique mutation. *Genet medicine: Off J Am Coll Med Genet*. (2018) 20:269–74. doi: 10.1038/gim.2017.109

48. Gibbs CP, Kukekov VG, Reith JD, Tchigrinova O, Suslov ON, Scott EW, et al. Stem-like cells in bone sarcomas: implications for tumorigenesis. *Neoplasia (New York NY)*. (2005) 7:967–76. doi: 10.1593/neo.05394

49. Rainusso N, Man TK, Lau CC, Hicks J, Shen JJ, Yu A, et al. Identification and gene expression profiling of tumor-initiating cells isolated from human osteosarcoma cell lines in an orthotopic mouse model. *Cancer Biol Ther*. (2011) 12:278–87. doi: 10.4161/cbt.12.4.15951

50. Stevens RL, Austen KF. Effect of p-nitrophenyl-beta-D-xyloside on proteoglycan and glycosaminoglycan biosynthesis in rat serosal mast cell cultures. *J Biol Chem*. (1982) 257:253–9. doi: 10.1016/S0021-9258(19)68354-7

51. Kraushaar DC, Yamaguchi Y, Wang L. Heparan sulfate is required for embryonic stem cells to exit from self-renewal. *J Biol Chem*. (2010) 285:5907–16. doi: 10.1074/jbc.M109.066837

52. Chen J, Sun T, You Y, Wu B, Wang X, Wu J. Proteoglycans and glycosaminoglycans in stem cell homeostasis and bone tissue regeneration. *Front Cell Dev Biol*. (2021) 9:760532. doi: 10.3389/fcell.2021.760532

53. Mizumoto S, Ikegawa S, Sugahara K. Human genetic disorders caused by mutations in genes encoding biosynthetic enzymes for sulfated glycosaminoglycans. *J Biol Chem*. (2013) 288:10953–61. doi: 10.1074/jbc.R112.437038

54. Taylan F, Mäkitie O. Abnormal proteoglycan synthesis due to gene defects causes skeletal diseases with overlapping phenotypes. *Hormone Metab Res = Hormon- und Stoffwechselforschung = Hormones metabolisme*. (2016) 48:745–54. doi: 10.1055/s-0042-118706

55. Kang HG, Evers MR, Xia G, Baenziger JU, Schachner M. Molecular cloning and characterization of chondroitin-4-O-sulfotransferase-3. A novel member of the HNK-1 family of sulfotransferases. *J Biol Chem*. (2002) 277:34766–72. doi: 10.1074/jbc.M204907200

56. Nassar D, Blanpain C. Cancer stem cells: basic concepts and therapeutic implications. *Annu Rev Pathol*. (2016) 11:47–76. doi: 10.1146/annurev-pathol-012615-044438

57. Lindsey BA, Markel JE, Kleinerman ES. Osteosarcoma overview. *Rheumatol Ther*. (2017) 4:25–43. doi: 10.1007/s40744-016-0050-2

58. Toguchida J, Ishizaki K, Sasaki MS, Nakamura Y, Ikenaga M, Kato M, et al. Preferential mutation of paternally derived RB gene as the initial event in sporadic osteosarcoma. *Nature*. (1989) 338:156–8. doi: 10.1038/338156a0

59. Wunder JS, Gokgoz N, Parkes R, Bull SB, Eskandarian S, Davis AM, et al. TP53 mutations and outcome in osteosarcoma: a prospective, multicenter study. *J Clin oncology: Off J Am Soc Clin Oncol*. (2005) 23:1483–90. doi: 10.1200/jco.2005.04.074

60. Stephens PJ, Greenman CD, Fu B, Yang F, Bignell GR, Mudie LJ, et al. Massive genomic rearrangement acquired in a single catastrophic event during cancer development. *Cell*. (2011) 144:27–40. doi: 10.1016/j.cell.2010.11.055

61. Savage SA, Mirabello L, Wang Z, Gastier-Foster JM, Gorlick R, Khanna C, et al. Genome-wide association study identifies two susceptibility loci for osteosarcoma. *Nat Genet*. (2013) 45:799–803. doi: 10.1038/ng.2645

62. Chen X, Bahrami A, Pappo A, Easton J, Dalton J, Hedlund E, et al. Recurrent somatic structural variations contribute to tumorigenesis in pediatric osteosarcoma. *Cell Rep*. (2014) 7:104–12. doi: 10.1016/j.celrep.2014.03.003

frontiers | Frontiers in Pharmacology

TYPE Review
PUBLISHED 06 May 2024
DOI 10.3389/fphar.2024.1390361

OPEN ACCESS

EDITED BY
Duoyi Zhao,
Fourth Affiliated Hospital of China Medical University, China

REVIEWED BY
Borislav Belev,
University Hospital Centre Zagreb, Croatia
Weilin Zhang,
Affiliated Hospital of Guangdong Medical University, China
Li Suoyuan,
Suzhou Municipal Hospital, China, in collaboration with reviewer WZ

*CORRESPONDENCE
Jiuwei Cui,
cuijw@jlu.edu.cn

RECEIVED 23 February 2024
ACCEPTED 22 April 2024
PUBLISHED 06 May 2024

CITATION
Yang R, Jia L and Cui J (2024), Mechanism and clinical progression of solid tumors bone marrow metastasis.
Front. Pharmacol. 15:1390361.
doi: 10.3389/fphar.2024.1390361

Mechanism and clinical progression of solid tumors bone marrow metastasis

Ruohan Yang, Lin Jia and Jiuwei Cui *

Cancer Center, The First Hospital of Jilin University, Changchun, China

The rich blood supply of the bone marrow provides favorable conditions for tumor cell proliferation and growth. In the disease's early stages, circulating tumor cells can escape to the bone marrow and form imperceptible micro metastases. These tumor cells may be reactivated to regain the ability to grow aggressively and eventually develop into visible metastases. Symptomatic bone marrow metastases with abnormal hematopoiesis solid tumor metastases are rare and have poor prognoses. Treatment options are carefully chosen because of the suppression of bone marrow function. In this review, we summarized the mechanisms involved in developing bone marrow metastases from tumor cells and the clinical features, treatment options, and prognosis of patients with symptomatic bone marrow metastases from different solid tumors reported in the literature.

KEYWORDS

solid tumor, bone marrow metastases, clinical manifestations, prognosis, therapy regimens

1 Introduction

Symptomatic bone marrow metastases (BMM) from solid tumors imply severe myelosuppression and a poorer prognosis. Bone marrow is a blood-rich soft connective tissue in the cancellous space of bone and the cavity of long bone marrow and is an essential source of hematopoietic cell production. Because of its unique environment, non-hematological solid tumor cells are less likely to invade the bone marrow. However, a tiny percentage of malignant tumor cells in extramedullary organs can metastasize via blood or lymphatic routes leading to symptomatic BMM (Wang et al., 2019). As normal bone marrow tissue is replaced by tumor tissue, patients usually present with suppression of hematopoietic functions such as anemia, thrombocytopenia, and abnormal coagulation. Some patients may also present with life-threatening disseminated intravascular coagulation (DIC) in gastric and colorectal cancers (Yoshioka et al., 1992; Nakashima et al., 2014; Hanamura et al., 2016; Seki and Wakaki, 2016; Zhai et al., 2022). Bone marrow aspiration biopsy(BMAB) reveals typical tumor cell infiltration and immunohistochemical staining helps to determine the origin of the tumor (Khan et al., 2019). Li et al. retrospectively studied 101 pathological specimens of patients with BMM, and the primary tumor sites were most common in the stomach (11 cases, 22%), lung (11 cases, 22%), and breast (9 cases, 18%) (Xiao et al., 2009). This is consistent with the findings of Hung et al. (2014).

In patients presenting with BMM, cytopenia frequently emerges as the principal clinical manifestation, constraining the dosage selection for chemotherapeutic agents and compromising the therapeutic efficacy (Kopp et al., 2011). Complicating the clinical

landscape is the challenge of differentiating BMM from cytopenia induced by chemotherapy, a distinction that often eludes clinicians (Fumet et al., 2018). The bone marrow-blood barrier (MBB) further impedes the efficacy of certain chemotherapeutic drugs, particularly large molecules, which struggle to infiltrate the bone marrow milieu (Tavassoli, 2008). Owing to the covert progression of BMM, timely diagnosis and effective treatment are impeded, leading to a more dire prognosis for patients with solid tumor BMM as compared to those with metastases originating from other sites (Cardoso et al., 2020).

The published articles are mainly retrospective studies with small samples. Sakin et al. found that in 30 patients with BMM of breast cancer, the median overall survival (mOS) was 9 months (Sakin et al., 2020). And mOS of 31 weeks in 28 patients with small cell lung cancer (SCLC) with BMM (Zych et al., 1993). In a study of 39 cases of gastric cancer (GC) combined with BMM, the authors found that mOS was only 20–67 days (Kim et al., 2007).

Papac, in 1994, summarized the common tumor types of BMM and the application of new techniques for detecting tumors in the bone marrow (Papac, 1994). In recent years, as oncology treatment continues to evolve, the choice and application of drugs have become more diverse, and patients with BMM from solid tumors have gained survival benefits. In this review, we describe the factors involved in the bone marrow microenvironment that promote tumor metastasis and summarize the clinical features, treatment options, and prognosis of symptomatic BMM from different solid tumors.

2 Molecular mechanisms of BMM

BMM can be classified as micro metastases, symptomatic metastases, and bone marrow necrosis (BMN). Micro metastases are infiltrations and dormancy of circulating tumor cells (DCTs) in the bone marrow, which are not typical of patients' symptoms and are easily overlooked by clinicians (Wang et al., 2019). The invasion of DCTs into blood vessels and the spread of blood circulation to organs throughout the body is the basic process of metastatic development, and DCTs are only "seeded" where "suitable soil" is available (Croucher et al., 2016). BM is characterized by having a large number of blood vessels, which allows tumor cells to enter the bone marrow cavity, BM microenvironment confers enhanced tumor metastasis capacity on tumor cells (Weilbaecher et al., 2011). Simultaneous recognition and interaction of adhesion molecules on tumor cells with bone marrow endothelial cells (ECs), stromal cells, and extracellular matrix. Adhesion to the BM endothelial intima also enhances tumor cell angiogenesis and bone resorption factor secretion, which favors the survival and growth of cancer cells (Weilbaecher et al., 2011). Bone metastases have been shown to occur more frequently in breast, prostate, and lung cancers (Coghlin and Murray, 2010). BM-derived hematopoietic stem cells expressing vascular endothelial growth factor receptor-1 (VEGFR-1) were demonstrated in a tumor-specific premetastatic niche and formed receptor clusters before the arrival of metastatic tumor cells in a mouse model. Blocking VEGFR-1 function specifically prevents the formation of premetastatic niches and tumor metastasis in BM (Kaplan et al., 2005; Kaplan et al., 2006a) (Figure 1).

Cytotoxic chemotherapy regimens will likely fail to eliminate such dormant, non-proliferating DTCs (Braun et al., 2003); this explains why some patients with early solid tumors develop distant metastases after several years (Ghajar et al., 2013). KAMBY et al. found microfiltration of tumor cells in the bone marrow of 87 (23%) of 320 patients with postoperative recurrent breast cancer (Kamby et al., 1987). Braun et al. also saw a poor prognosis for those with bone marrow micro metastases (Braun et al., 2005). Very rare symptomatic BMM resulting from early occult DCTs that spread hematogenous and invade highly vascularized bone marrow under certain conditions (Hung et al., 2014). When the expanding growth of proliferating tumor cells within the noncompliant space of the bone marrow cavity obstructs blood flow, leading to more severe ischemic BMN (Miyoshi et al., 2005). It is characterized by massive necrosis of the marrow and myeloid tissue of the hematopoietic bone marrow, forming an amorphous eosinophilic background, ill-defined necrotic cells, and preserved cortical bone (Maisel et al., 1988). BMN is very rare in solid tumors, and the prognosis for patients is poor (Wool and Deucher, 2015). The mechanisms of symptomatic bone marrow metastasis and bone marrow necrosis are unclear. Some studies have found that specific factors can promote bone marrow micro metastasis in solid tumor cells, so we summarized the molecular mechanisms.

2.1 Bone marrow-derived mesenchymal stem cells

Bone marrow-derived mesenchymal stem cells (BMSCs) influence the formation and development of tumor metastases. Mouse models of bone marrow metastasis confirm the involvement of BMSC in tumor invasion and metastasis (Kawai et al., 2018). BMSCs are a scarce cell type in the bone marrow, accounting for 0.01%–0.001% of all mononuclear cells (Pittenger et al., 1999). Studies have found that proteins regulating bone tissue homeostases such as Angiopoietin-2 (ANGPT2), WNT1-inducible-signalling pathway protein 1 (WISP1), and Osteoprotegerin (OPG) are increased in the blood of mice in a mouse model of breast cancer, and further studies have found that the morphology of the humeral blood vessels of mice with breast cancer is altered, as evidenced by a reduction in the diameter volume and length of vascular endothelial cells, and that MSCs are no longer distributed around the endothelium of the blood vessels, but are located away from the blood vessels and are close touched to the hematopoietic stem cells. This suggests that the endothelial ecological niche in which hematopoietic stem cells reside is remodeled. In addition, *in vitro* experiments have also shown that MSCs derived from mice with breast cancer can promote the expansion of hematopoietic stem cells and their differentiation to myeloid cells, affecting the myeloid system (Gerber-Ferder et al., 2023). Primary and metastatic tumor cells can release tumor necrosis factor (TGF), Interleukin(IL)-8, and Neurotrophin-3 (NT-3) to recruit BMSCs to the tumor site. BMSCs recruited to the tumor microenvironment differentiate into tumor-associated fibroblasts (TAF), which release IL-6, IL-10, C-C chemokine ligand 5 (CCL5), and extracellular matrix remodeling enzymes in the tumor microenvironment to affect tumor cell survival and angiogenesis (Bergfeld and DeClerck, 2010). In the bone marrow, however, BMSCs produce chemoattractant proteins such as stromal cell-derived factor-1(SDF-1) and monocyte chemoattractant protein-1 (MCP-1)

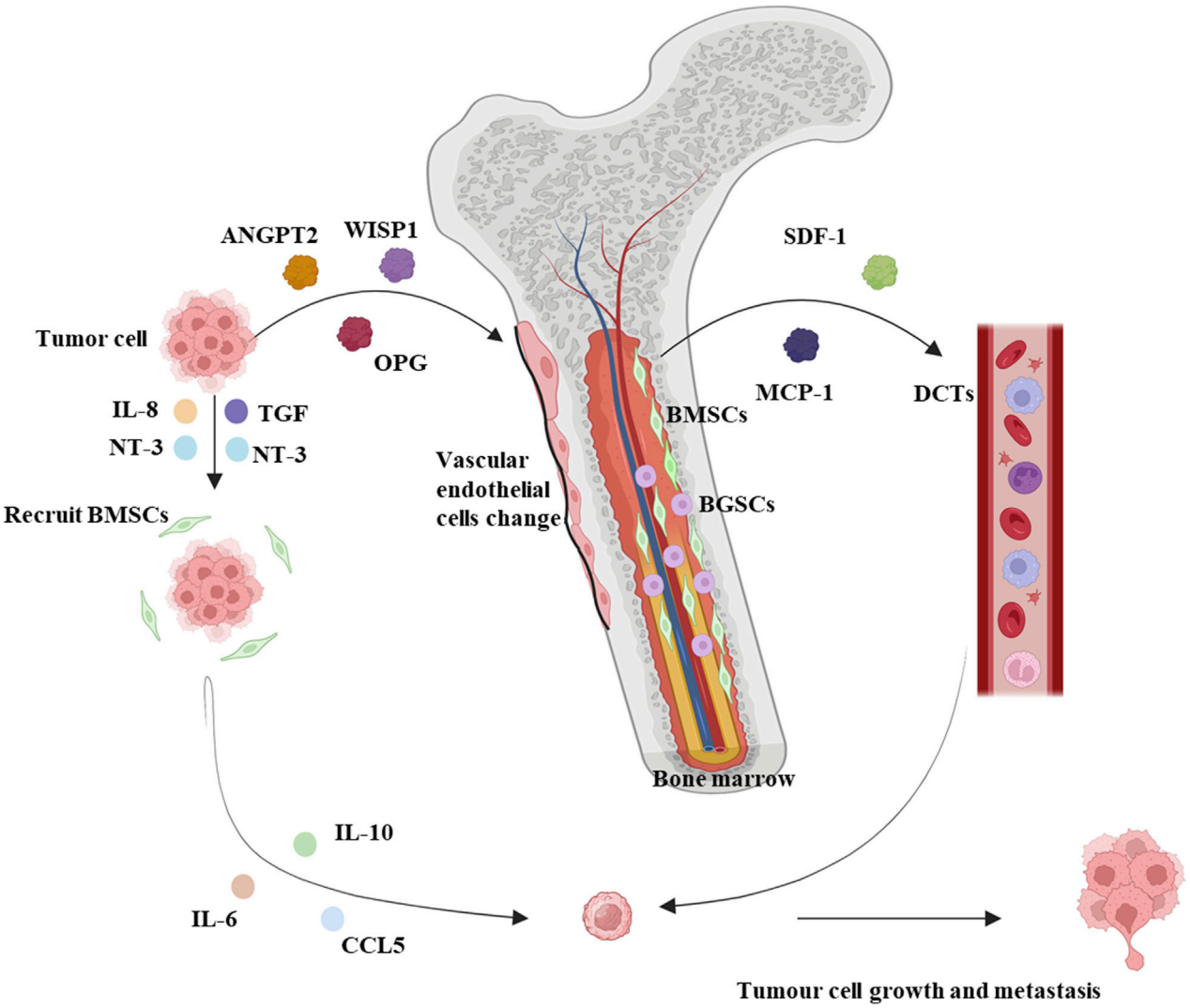

FIGURE 1
Summary mechanistic map between solid tumors and bone marrow microenvironment. Solid tumors lead to increased blood levels of proteins regulating bone tissue homeostasis such as ANGPT2, WISP1, and OPG, along with a reduction in the diameter volume and length of vascular endothelial cells, and MSCs are no longer distributed around the vascular endothelium, moving away from the blood vessels and near hematopoietic stem cells. Solid tumors secrete IL-8, TGF, and NT-3 to recruit BMSCs to the peritumoral area and release IL-6, IL-10, and CCL5 to promote tumor cell metastasis. Meanwhile, BMSCs promote the secretion of proteins such as SDF-1 and MCP-1, which stimulate circulating DCTs to promote tumor cell metastasis. BMSCs: Bone marrow-derived mesenchymal stem cells. BCSCs: Blood-generating stem cells. Interleukin: IL. DCTs: SDF-1: Stromal cell-derived factor-1. MCP-1: Monocyte chemoattractant protein-1. TGF: Tumor necrosis factor. CCL5: C-C chemokine ligand 5. NT3: Neurotrophin-3. Schematic in a created using BioRender (www.biorender.com).

that attract DCTs and promote tumor growth and drug resistance in the microenvironment (Bergfeld and DeClerck, 2010). Some reports suggest that BMSCs promote phagocytosis and vascularization of primary tumor development, thereby increasing the metastatic capacity of tumor cells (Kaplan et al., 2006b; Amé-Thomas et al., 2007) (Figure 1).

2.2 Bone marrow angiogenesis

The bone marrow is an extensively vascularized tissue, suggesting that blood vessels may play an essential role in the metastatic process of tumors (Kusumbe, 2016). It has been demonstrated that stable micro vessels in the bone marrow provide an ecological niche for dormant breast cancer cells. In a mouse model of breast cancer, dormant DCTs reside on the microvasculature of the bone marrow and sprout new vessels that stimulate the growth of breast tumor micro metastases (Ghajar et al., 2013). Similar results were found in the human study, where 19 of 42 patients (45%) with a bone marrow biopsy for breast cancer had bone marrow tumor cell infiltration. They found that patients with bone marrow micro metastases had significantly higher micro vessel density and had disease progression or recurrence at a substantially higher rate than patients with negative bone marrow puncture (Chavez-Macgregor et al., 2005).

Yip et al. (2021) found that in a mouse model of breast cancer, tumor cells preferentially enter a pre-existing epiphyseal domain rich in H-type blood vessels. Metastatic tumor growth can rapidly remodel the local microvascular system, establishing a microenvironment that promotes tumor growth (Yip et al., 2021). Similarly, it has been shown that endothelial cells and perivascular cells appear to promote the proliferation of tumor cells in BM in mouse models (Ghajar et al., 2013), These blood vessels release growth factors that promote tumor growth in mouse model BM (Ghajar, 2015).

2.3 Bone marrow chemokines

Chemokines secreted by different cells of the bone marrow play an essential role in forming the bone marrow ecotone system (Ahmadzadeh et al., 2015). Based on the position of the two conserved cysteine residues at the NH2 terminus, these low molecular weight peptides or proteins are classified into four groups, CXC, CC, C, and CX3C (Ahmadzadeh et al., 2015). In particular, the CXCL12-CXCR4 axis is vital in assisting the bone marrow in regulating tumor development (Shi et al., 2014). Chemokine CXCL12 is a highly conserved chemokine, and its receptor CXCR4 is a G protein-coupled receptor associated with intracellular heterotrimeric G proteins (Teicher and Fricker, 2010; Tanaka et al., 2012). CXCL12 and CXCR4 are involved in developing tumor progression and distant metastases and can lead to resistance to chemotherapy in solid tumors (Shi et al., 2014). One study found that CXCL12 expression in the bone marrow in a lung cancer model provided a displacement signal for CXCR4 tumor cells, increasing their invasion of the environment (Ahmadzadeh et al., 2015). In ovarian cancer, CXCR4 and CCR9 chemokine receptors cause resistance of tumor cells to apoptosis, promote their escape from the immune system, and increase angiogenesis (Singh et al., 2011). CXCR4, CCR2, and CX3CR1 are chemokines that play a prominent role in breast cancer metastasis to the bone marrow and in the proliferation of tumor cells (Müller et al., 2001; Lu and Kang, 2009; Jamieson-Gladney et al., 2011). The CXCR4 inhibitor AMD3100 has been shown to enhance the sensitivity of chemotherapy in a mouse model of multiple myeloma. At the same time, the CXCL12-CXCR4 axis can exert anti-tumor effects through inhibition of the CXCL12-CXCR4 axis (de Nigris et al., 2012). In addition to the CXCL12-CXCR4 axis, chemokines CCL12 and CCL22 enhance tumor cell formation in the bone marrow microenvironment and are involved in tumor transformation, growth, and metastasis (Kulbe et al., 2004).

2.4 Other factors in the bone marrow microenvironment

In addition, regulatory T cells (Tregs), closely associated with tumor development, are also widely stored in the bone marrow. It has been shown that Tregs infiltration into tumors is a poor prognostic marker and that depletion of Tregs in a 4T1 mouse model inhibits the development of lung metastases (Hong et al., 2010).

Bone marrow adipocytes (BMAs) are abundant in the bone marrow microenvironment and account for approximately 70% of the adult bone marrow volume (Luo et al., 2018). It has been suggested that BMAs may act as an energy source during tumor progression (Luo et al., 2018). BMAs secrete adipocytokines such as leptin, adiponectin, IL-1β, IL-6, VCAM-1, TNF-α, and VEGF to promote tumor cell metastasis (Shin and Koo, 2020).

3 Clinical features and diagnosis of patients with symptomatic BMM from solid tumors

Li et al. found 101 cases (1.0%) of solid tumor metastases in a review of 10,112 bone marrow samples, with lung, gastric, breast, and prostate cancers being the most common. In addition to the typical peripheral blood changes described previously, this study found patients with non-specific clinical symptoms such as skeletal pain (24.75%) and unexplained fever (4.95%) (Xiao et al., 2009). The number of patients limits published studies, and clinical characteristics still need to be systematically summarized. We searched the published literature for clinical characteristics of patients with bone marrow metastases from different solid tumors such as gastric, lung, and breast cancer and summarized them (Figure 2).

3.1 Gastric cancer

Gastric cancer (GC) is the fifth most common cancer and the fourth leading cause of cancer-related death worldwide (Qiu et al., 2021; Sung et al., 2021). GC combination with BMM significantly shortens the survival (Kim et al., 2007). There is a lack of prospective studies in this area, with small retrospective samples and case reports predominating. In addition to typical peripheral blood changes such as anemia and thrombocytopenia, patients with GC are more likely to present clinically with DIC, and BMAB reveals tumor cells with markedly heterogeneous staining (Kim et al., 2007; Iguchi, 2015; Zhai et al., 2022). Kim et al. retrospectively studied 39 cases of BMM of GC. The clinical features included mostly young male patients with elevated serum alkaline phosphatase (ALP) and/or lactate dehydrogenase (LDH) levels in laboratory tests and pathological types of hypo-f fractionated adenocarcinoma or indolent cell carcinoma (Kim et al., 2007). This is consistent with the studies reported (Kwon et al., 2011; Iguchi, 2015; Zhai et al., 2022) (Table 1). It has been found that bone metastases tend to occur in the hematopoietic bone; therefore, bone marrow involvement is considered a prerequisite for bone metastases (Papac, 1994). Our literature review revealed that BMM of GC is most often associated with extensive bone metastases. Of the 39 patients with BMM, 69.23% had multiple bone metastases (Kim et al., 2007). In another study, 57.7% of patients had a combination of bone metastases (Kwon et al., 2011). Significant expression of RANKL, a primary regulator of osteoclast differentiation and activation, plays an essential role in the bone marrow dissemination of GC (Kusumoto et al., 2006).

3.2 Breast cancer

Studies have shown that symptomatic BMM is rare in metastatic breast cancer (Kopp et al., 2011). We screened the published

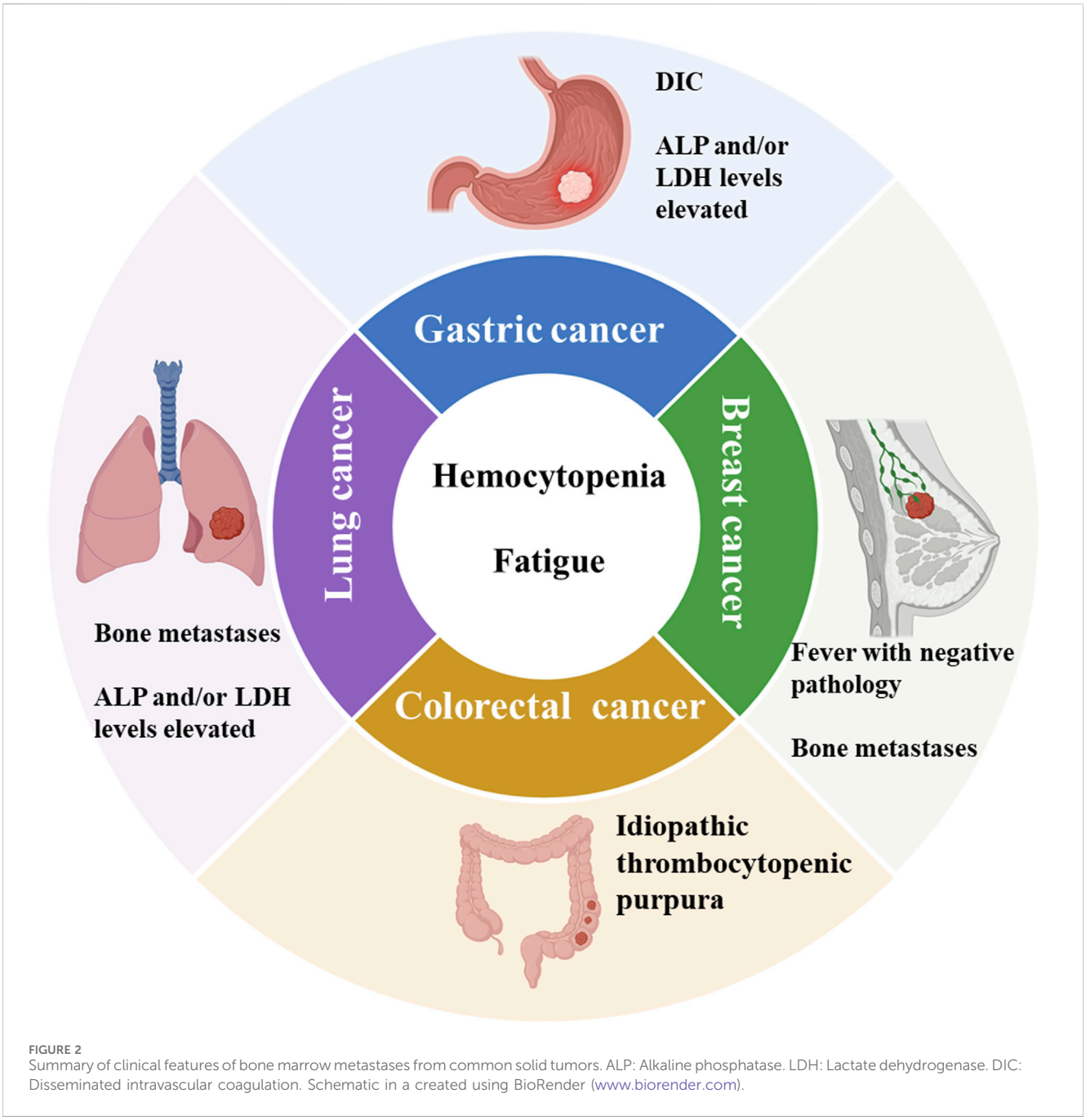

FIGURE 2
Summary of clinical features of bone marrow metastases from common solid tumors. ALP: Alkaline phosphatase. LDH: Lactate dehydrogenase. DIC: Disseminated intravascular coagulation. Schematic in a created using BioRender (www.biorender.com).

literature and summarized the clinical characteristics of patients with BMM (Table 1). Kopp et al. retrospectively studied 22 patients with BMM of breast cancer, 50% (11/22) were molecularly typed as hormone receptor (HR) positive and human epidermal growth factor receptor 2 (HER-2) negative (Kopp et al., 2011), Sakin et al. found similar results (21/30, 70%) (Sakin et al., 2020). Invasive ductal carcinoma is the primary pathological type constituting BMM, followed by invasive lobular carcinoma (Kopp et al., 2011; Sakin et al., 2020), Documented histological grading of 2–3 (Bjelic-Radisic et al., 2006; Rahmat and Ikhwan, 2018). Patients mostly present with clinical weakness (Ardavanis et al., 2008; Akagi et al., 2021). Our previous study found nearly 76% of patients had a pathogenically negative fever. We also found a combination of bone metastases in all patients, with spinal metastases being the most common (78.78%) (Yang et al., 2022a). This may be due to higher levels of the chemokine CXC3L1/CXC3R1 in the spine than in other bones, which can promote adhesion and migration of breast cancer cells (Meng et al., 2022).

3.3 Colorectal cancer

Colorectal cancer is the third leading cause of cancer-related death, with common distant metastases usually occurring in the liver and lungs, and symptomatic BMM is extremely rare in colorectal cancer (Assi et al., 2016; Alghandour et al., 2020). Similar to BMM

TABLE 1 Summary of treatment modalities and prognosis of different solid tumors.

Treatment	Tumor type	Pathological type	Molecular type	Use of medications	OS/mOS	Results
Chemotherapy	Breast cancer	Invasive ductal carcinoma Invasive lobular carcinoma	Triple-negative HR positive, HER-2 negative Her-2 overexpression	Adriamycin, doxorubicin, cyclophosphamide	6–38 months	Chemotherapy significantly prolongs survival in breast cancer patients with bone marrow metastases. Among them, paclitaxel treatment achieved the best survival rate Freyer et al. (2000), Kopp et al. (2011), Sakin et al. (2020)
	Gastric cancer	Poorly differentiated/ signet ring cell	NA	FOLFOX, FOLFIRI	67–137 days	Gastric cancer patients with bone marrow metastases should receive more tailored therapies for risk factors to enhance survival. Kim et al. (2007), Ubukata et al. (2011)
		Well/moderately differentiated				
	Gastric cancer	Hypo fractionated adenocarcinoma	NA	Tegafur	8.1 ± 2.7 months	Due to the low incidence of BMM in gastric cancer, it has not received sufficient attention, and the prognosis has not improved much Iguchi (2015)
		Indolent cell carcinoma, Tubular adenocarcinoma				
	Colorectal cancer	Moderately to poorly differentiated adenocarcinoma	NA	FOLFOX, FOLFIRI, Bevacizumab, 5-fluorouracil, Adriamycin	15 days-10 months	Clinical bone marrow involvement limits the clinician's ability to tailor chemotherapy regimens. Early diagnosis is critical in future treatment and therapeutic decisions Ozkan et al. (2007), Arslan et al. (2015), Assi et al. (2016), Hanamura et al. (2016)
	Lung Cancer	Small cell lung cancer	NA	NA	31 week	The presence of BMM is associated with a shorter time to progression and survival Zych et al. (1993)
	Rhabdomyosarcoma	Embryonal, Alveolar	NA	NA	18–27 months	RMS with BMM has a low survival rate and new therapies are needed to alleviate the disease Aida et al. (2015), Bailey and Wexler (2020), Huang et al. (2021)
Endocrine therapy	Breast cancer	Invasive lobular carcinoma	HR positive, HER-2 negative	Palbociclib + Letrozole + ovarian suppression	26 months	A combination of endocrine therapy and CDK4/6 inhibitor may have more extended clinical benefit than chemotherapy, and a combination therapy of ET and CDK4/6 inhibitor is less toxic and leads to a better quality of life than chemotherapy Garufi et al. (2021)
	Breast cancer	Invasive lobular carcinoma	HR positive, HER-2 negative	Aromatase inhibitor	7 months	After hormonal treatment with the aromatase inhibitor, the patient's condition improved Rahmat and Ikhwan (2018)
Target therapy	Breast cancer	Invasive ductal carcinoma	HER-2 overexpression	Trastuzumab	11 months	Trastuzumab may be a beneficial treatment option for patients with Her-2-positive bone marrow metastases Xu et al. (2014)

(Continued on following page)

TABLE 1 (*Continued*) Summary of treatment modalities and prognosis of different solid tumors.

Treatment	Tumor type	Pathological type	Molecular type	Use of medications	OS/mOS	Results
	Lung Cancer	lung adenocarcinoma	NA	Anti- EGFR therapy	422 days	Patients with BMM from lung adenocarcinoma have a short survival period, which can be prolonged by targeted drugs Wang et al. (2019)

NA, not applicable; HR, Hormone Receptor; FOLFOX, paclitaxel; 5-fluorouracil, calcium folinic acid, and oxaliplatin FOLFIRI:5-fluorouracil, calcium folinic acid, irinotecan. EGFR, Epidermal growth factor receptor. DIC, disseminated intravascular coagulation. mOS, median Overall survival.

from other malignancies, the common signs and symptoms have been shown to include malaise, fever, and complete blood cytopenia (Assi et al., 2016). Occasionally life-threatening DIC and idiopathic thrombocytopenic purpura (TTP) (Lee et al., 2004; Hanamura et al., 2016). The published articles are case reports. The patient was an elderly male with a predominantly low to moderately differentiated adenocarcinoma of the rectum and sigmoid colon as the main pathological feature (Arslan et al., 2015; Assi et al., 2016; Alghandour et al., 2020). Only OZKAN et al. reported one patient with the pathology of a highly differentiated neuroendocrine tumor of the rectum combined with BMM (Table 1) (Ozkan et al., 2007).

3.4 Lung cancer

In recent years, radiotherapy, chemotherapy, and molecular targeted therapy have become essential treatment strategies for patients with advanced lung cancer (Jones and Baldwin, 2018). However, the prognosis for patients with BMM from lung adenocarcinoma remains unsatisfactory (Wang et al., 2019). Wang et al. retrospectively studied 12 patients with lung adenocarcinoma BMM and found that the patient population was predominantly middle-aged and older men. For the more malignant small cell lung cancer (SCLC) BMM, the patient population was also middle-aged and elderly males (21 cases, 75%) (Zych et al., 1993). The patients' hematology showed decreased blood cells and ALP and LDH levels. They also found that most patients had a combination of bone metastases (Zych et al., 1993; Wang et al., 2019).

3.5 Other solid tumors

Apart from the solid tumors mentioned above, other solid tumors of BMM are less frequently reported. The published articles are retrospective studies of small samples, and we summarized their clinical features in the following sections.

3.5.1 Prostate cancer

Prostate cancer is one of the most common malignancies in men worldwide and the leading cause of death in men worldwide, and metastatic prostate cancer implies a poor prognosis (Table 1) (Morash et al., 2015). There are few reports related to BMM in prostate cancer clinical features. Shahait et al. retrospectively studied 189 patients with prostate cancer, of whom 11 (6%) had a diagnosis of BMM (Shahait et al., 2022). BMAB reveals many scattered or clumped metastatic cancer cells with clinical features such as anemia, elevated ALP, and poor ECOG fitness status (Shahait et al., 2022).

3.5.2 Rhabdomyosarcoma

Rhabdomyosarcoma (RMS) is the most common soft tissue sarcoma in adolescence and childhood (Bailey and Wexler, 2020). Bone marrow is a common site of distant metastases in RMS, with an incidence of 6% (Weiss et al., 2013). Some studies have confirmed that alveolar RMS is the most common type of pathology, with no significant specificity for age or sex (Table 1) (Bailey and Wexler, 2020; Huang et al., 2021).

For BMM in hepatocellular carcinoma, nasopharyngeal carcinoma, glioma, and renal carcinoma, the number of published articles is small, and they are all case reports, so we do not summarize their clinical features in this article.

4 Treatment options and prognosis

The prognosis of patients with advanced solid tumors has improved with advances in treatment options. However, the prognosis for patients with symptomatic BMM remains poor compared to metastases from other sites. Chemotherapy remains an important treatment option for BMM in the remaining solid tumors, except breast and lung adenocarcinoma. We summarized the treatment options and prognosis of patients with documented BMM from gastric, lung, breast, and colorectal cancers.

4.1 Chemotherapy

4.1.1 Gastric cancer

Limited data on BMM treatment options for GC and poor patient prognosis (Iguchi, 2015). We summarized the reported treatment regimens and prognosis (Table 1). Dittus et al. reported one male BMM patient treated with epirubicin, oxaliplatin, and capecitabine (EOX) chemotherapy. The patient's prognosis and the associated adverse events were not recorded at (Dittus et al., 2014). In a study of five patients who received a combination of platinum, 5-fluorouracil, and docetaxel chemotherapy, overall survival (OS) was only 20–53 days (Ekinci et al., 2014).

Studies have shown a survival benefit of chemotherapy in patients with BMM of GC. And mOS was 67 days in patients treated with paclitaxel, 5-fluorouracil, calcium folinic acid, and

oxaliplatin (FOLFOX) and 5-fluorouracil, calcium folinic acid, irinotecan (FOLFIRI) chemotherapy with no treatment-related adverse events recorded by Kim et al. (2007). Kwon et al. found an mOS of 121 days in 16 patients receiving platinum, paclitaxel, irinotecan, and 5-fluorouracil chemotherapy, respectively. Patients had higher leukocyte, neutrophil, and platelet levels after cytotoxic treatment, improved bone marrow function, and no treatment-related deaths (Kwon et al., 2011). A 2015 study in Japan summarized 14 cases treated with Tegafur with OS for up to 8.1 months and well-tolerated by patients (Iguchi, 2015).

BMM of GC combined with DIC means a worse prognosis. An 80-year-old man diagnosed with BMM combined with DIC and thrombotic microangiopathy did not receive antineoplastic treatment and died on the third day after admission to hospital (Seki and Wakaki, 2016). Zhai et al. examined 36 patients with concurrent BMM and DIC receiving chemotherapy based on 5-fluorouracil, paclitaxel, and platinum drugs. They found that survival time after chemotherapy was strongly correlated with remission of DIC. mOS was 7.2 months in the DIC remission group and only 0.93 months in the no remission group (Zhai et al., 2022).

Our literature review found that Tegafur chemotherapy may be the best option for BMM in GC and may provide a survival benefit to patients. In the case of frequent life-threatening DIC, the effectiveness of chemotherapy is a critical factor in the survival time of patients. Future prospective studies are needed to compare the efficacy of different chemotherapeutic agents in BMM of GC.

4.1.2 Small-cell lung cancer

Small cell lung cancer (SCLC) is highly malignant, and approximately 2/3 of SCLC patients have distant metastases to the brain, liver, adrenal glands, bone, and bone marrow at the time of initial diagnosis, with studies showing that the frequency of bone marrow involvement in SCLC ranges from 32% to 46% (Ihde et al., 1979). Zych et al. studied 28 patients with symptomatic BMM from SCLC treated with cyclophosphamide, Adriamycin, methotrexate, and etoposide. 60.7% of patients were assessed to be in complete or partial remission after chemotherapy, with an mOS of 31 weeks and no treatment-related adverse events recorded (Zych et al., 1993). In a study of 14 patients receiving cyclophosphamide chemotherapy, an mOS of 8 months was found. However, BMM patients required more red blood cell infusion, and up to 29% developed severe infections (sepsis and pneumonia) (Ihde et al., 1979). Asai et al. (2013) reported one case treated with small incremental doses of Adriamycin in which the patient remained in complete remission after a 6-month follow-up period. Still, unfortunately, the authors did not record data on his overall survival and adverse effects. Patients with SCLC combined with BMM have a poor prognosis, and small studies have not identified safe and effective treatment options for patients with SCLC combined with BMM.

4.1.3 Breast cancer

Symptomatic BMM from breast cancer is rapidly progressive and has a poor prognosis (Cardoso et al., 2020). The 5th ESO-ESMO International Consensus Guidelines for Advanced Breast Cancer recommend chemotherapy for rapid and effective symptomatic relief regardless of the patient's receptor expression (Cardoso et al., 2020). However, there are differences in treatment tolerability and prognosis with different drugs, which we have summarized.

Combining anthracyclines and anti-microtubule drugs is one of the most effective therapies for treating metastatic breast cancer (OBrien et al., 2004). It is also widely used in BMM. In a retrospective study of 22 patients, the best response rate was found in the adriamycin combined with the doxorubicin treatment group, as evidenced by increased white blood cells, platelets, and hemoglobin and an overall mOS of 11 months (Kopp et al., 2011). However, five patients developed febrile neutropenia, and four developed bleeding-related adverse events (three grade 3 and one grade 4) during treatment (Kopp et al., 2011). Another study found that one patient discontinued due to a severe adverse neurotoxic event during treatment with Adriamycin and cyclophosphamide in combination with docetaxel (Akagi et al., 2021). Pahouja et al. reported that a patient with BMM treated with adriamycin monotherapy survived 44 months. However, a granulocyte deficiency fever occurred in the second treatment cycle, reducing drug dosage (Pahouja et al., 2015). Sakin et al. found that of 30 patients with BMM of breast cancer, 18 treated with paclitaxel achieved the best survival with an mOS of 9.0 months and no treatment-related adverse events (Sakin et al., 2020).

In addition to the cytotoxic chemotherapeutic agents mentioned above, Ardavanis et al. reported on five patients with BMM treated with low-dose capecitabine oral chemotherapy, two patients with OS over 22 months and well-tolerated drug with no serious adverse events (Ardavanis et al., 2008). A 62-year-old female patient diagnosed with BMM due to thrombocytopenia was subsequently treated with docetaxel, Adriamycin, capecitabine, CMF, vincristine, gemcitabine, and carboplatin, respectively, and had OS of 57 months with increased platelet levels after treatment onset. However, multiple recurrent grade 3 or four neutropenia and leukopenia adverse events occurred during treatment (Bjelic-Radisic et al., 2006).

Cytotoxic chemotherapy delays the progression of BMM disease, and an increase in blood cell count is the main indication that the disease is under control. However, the hematological toxicity and neurotoxicity caused by chemotherapy cannot be ignored.

4.1.4 Colorectal cancer

Chemotherapy is also the treatment of choice for BMM patients with colorectal cancer (Assi et al., 2016). The published articles were small sample studies with variable drug choices. Assi et al. reported on three patients with colon cancer combined with BMM. One was treated with 12 cycles of FOLFOX and achieved complete clinical remission. While the other two had an OS of 4 and 6 months, respectively, no adverse events from the drug were recorded (Assi et al., 2016). ÖZKAN et al. reported rectal cancer combined with BMM treated with systemic chemotherapy using a modified FOLFOX(mFOLFOX) regimen, in which the patient's hematocrit improved after three treatment cycles. Bevacizumab combination therapy was added in cycle five. Still, the patient experienced significant fatigue and decreased ability to perform daily activities due to chemotherapy and died at 4 months of diagnosis (Nakashima et al., 2014). HANAMURA et al. reported a patient with sigmoid BMM treated with mFOLFOX, capecitabine in combination with

oxaliplatin, irinotecan, and panitumumab, respectively, with survival of up to 10 months (Hanamura et al., 2016).

4.2 Molecular targeted therapy

In recent years, targeted drugs for different targets of malignant tumors have been introduced, significantly prolonging survival and improving quality of life (Lee et al., 2018a). For patients with HER-2 overexpression, molecularly targeted anti-HER-2 therapy substantially prolongs survival (Ekinci et al., 2014). Of the 12 patients with HER-2 overexpressing lung adenocarcinoma, they were treated with platinum-based chemotherapy, chemotherapy, and targeted drug tyrosine kinase inhibitor (TKI) therapy, TKI therapy alone or best supportive care in separate cases. TKI-targeted patients had a significantly better survival time than chemotherapy alone and palliative care ($p = 0.031$) (Wang et al., 2019). Wu et al. reported a case of a 62-year-old female patient with HER-2 overexpressed lung adenocarcinoma BMM combined with DIC who opted for molecularly targeted therapy with pyrrolizidine. After 2 months of treatment, the patient's hematocrit symptoms improved (Wu et al., 2020). The authors did not count adverse events of the drug or the OS of patients. Molecularly targeted therapy also significantly prolonged survival in patients with HER-2 overexpressing metastatic breast cancer (Modi et al., 2020). XU et al. reported a case of a 41-year-old female with HR-negative, HER-2-positive breast cancer BMM who was first treated with trastuzumab followed by paclitaxel-concurrent chemotherapy; the patient had an OS of 19 months and no associated adverse events were recorded (Xu et al., 2014).

Sorafenib inhibits multiple targets of tumor cells (CRAF, BRAF, etc.) and tumor vessels (CRAF, VEGFR-2, etc.) and significantly treats advanced hepatocellular carcinoma (Cheng et al., 2020). In a case of symptomatic BMM in combination with HCC reported by Hong et al., the patient was treated with sorafenib molecular targeting. However, OS was 2.3 months due to the patient's poor physical strength and discontinuation of treatment for diarrhea (Hong et al., 2016).

Targeted epidermal growth factor (EGFR) therapy also plays a prominent role in solid tumor BMM. Zhang et al. reported a case of a patient receiving gemcitabine, cisplatin, and cetuximab chemotherapy in combination with targeted therapy, sequential capecitabine, and sintilimab maintenance chemotherapy and immunotherapy. At publication, the patient had sustained complete remission of BMM (Zhang et al., 2022). A 45-year-old patient with rectal cancer BMM received cetuximab, FOLFIRI-targeted combination chemotherapy with partial disease remission after four cycles and OS of 8 months, with no treatment-related adverse events reported in either patient (Arslan et al., 2015).

4.3 Endocrine therapy/endocrine therapy combined with chemotherapy

Endocrine therapy (ET) is best for patients with HR positive, HER-2 negative breast cancer. Data are currently sparse in BMM due to its slow onset of action. One female BMM patient had an OS of 7 months after selecting a single aromatase inhibitor and tolerated treatment well (Rahmat and Ikhwan, 2018). Freyer et al. used tamoxifen in combination with or without gonadotropin-releasing hormone agonists or aromatase inhibitors in combination with weekly low-dose anthracycline chemotherapy in five patients with BMM breast cancer who had excellent disease control with OS of 12–38 months and no treatment-related adverse events (Freyer et al., 2000). It has been suggested that combining endocrine therapy and cell cycle protein-dependent kinase (CDK) 4/6 inhibitors may provide longer clinical benefits than chemotherapy in treating advanced breast cancer. Both the MONALEESA-3 (Slamon et al., 2021) and MONALEESA-7 (Lu et al., 2022) trials demonstrated that ribociclib combined with ET significantly prolonged disease-free progression survival and overall survival in patients with advanced HR positive, HER-2 negative breast cancer. Giovanna et al. reported a case of a woman receiving letrozole, leuprolide, and palbociclib for BMM of breast cancer who achieved a complete remission at 26 months (Garufi et al., 2021). Our previous study also found that of 33 patients with BMM breast cancer, 13 used ET combined with CDK4/6 inhibitors for mOS of 18.0 months, which was better than any previous study and had lower side effects (Yang et al., 2022a; Yang et al., 2022b). At the 2022 San Antonio Breast Cancer Symposium, the RIGHT Choice study found that receiving the CDK4/6 inhibitor ribociclib combined with ET in contrast to combination chemotherapy significantly prolonged PFS (24.0 vs. 12.3 months) in patients with visceral crisis, including those with symptomatic BMM, which was similar to our findings (Yang et al., 2022a; Yang et al., 2022b). This further supports the idea that CDK4/6 inhibitors in combination with ET could be the treatment of choice for breast cancer patients with HR positive, HER-2 negative.

5 Treatment modalities and prognosis of BMM in other solid tumors

Other solid tumors have a lower incidence of BMM, and fewer studies are available. The following summarized their treatment modalities and prognosis for different solid tumors.

5.1 Prostate cancer

Kaplan et al. (2012) reported a case of a patient with BMM of prostate cancer who received radiotherapy; however, tumor lysis syndrome occurred during radiotherapy with an OS of 11 days. In a study of 11 patients with prostate cancer combined with BMM, the authors found an mOS of 18.1 months after doxorubicin/abiraterone or systemic therapy, a significantly shorter survival time than the 42.2 months in patients without BMM (Shahait et al., 2022).

5.2 Rhabdomyosarcoma

Lee et al. retrospectively studied 51 pediatric patients with RMS and found that bone marrow involvement mOS was significantly shorter than in patients without BMM (17 vs. 61 months, $p = 0.033$).

However, treatment modalities were not documented in the study (Lee et al., 2018). Bailey et al. found no significant improvement in prognosis despite patients receiving aggressive chemotherapy, with an mOS of approximately 18 months (Bailey and Wexler, 2020). And Huang et al., 2021 located in a single-center retrospective study that 13 patients with RMS combined with BMM received various treatment regimens, including chemotherapy, radiotherapy, and surgery, respectively, with an mOS of 27 months (Huang et al., 2021).

5.3 Glioblastoma multiforme

Less than 2% of patients with central nervous system (CNS) tumors are expected to develop extra-neurological metastases, with the bone marrow being an even rarer site for extra-neurological metastase (Didelot et al., 2006). Didelot et al. reported a glioblastoma multiforme (GBM) patient who presented with postoperative allogeneic cytopenia and subsequent BMM confirmed by BMAB. The patient was treated with one course of lomustine chemotherapy. However, the results were insignificant, with an OS of only 2 months (Didelot et al., 2006). Rajagopalan et al. reported a case of a 60-year-old man with BMM diagnosed after a BMAB for low back pain, thrombocytopenia, and hemoglobin reduction, who died after 1 month due to disease progression despite palliative radiotherapy (Rajagopalan et al., 2005). In the DEMASTER et al. study, patients did not receive anti-tumor therapy and died on day 5 and day 17 of the diagnosis of BMM, respectively (Kleinschmidt-Demasters, 1996).

5.4 Astrocytoma

LoRusso et al. first reported a patient with diffuse bone marrow involvement in astrocytoma who received concurrent intracranial radiotherapy and carmustine chemotherapy and died of sepsis 24 weeks after diagnosis (LoRusso et al., 1988). Hsu et al. found that patients treated with multiple lines of chemotherapy with etoposide, cyclophosphamide, cisplatin, carmustine, carboplatin, tamoxifen, and paclitaxel, respectively, had an OS of 21 months (Hsu et al., 1998).

5.5 Neuroblastoma

Hirano et al. reported a case of a patient presenting with left hip pain with hypothermia, initially diagnosed as septic osteomyelitis. However, subsequent negative pathogenic tests and aggressive anti-infective therapy did not significantly improve the fever symptoms. Further, BMAB confirmed a BMM from a neuroblastoma (Hirano et al., 2020). She was treated with chemotherapy, autologous peripheral blood hematopoietic stem cell transplantation, surgery, and radiation and went into remission. Overall survival time and adverse effects during treatment were not analyzed (Hirano et al., 2020).

5.6 Renal cell carcinoma

The common distant metastatic renal cell carcinoma organs are lungs, bones, and lymph nodes (Umer et al., 2018). BMM is very rare (Khan et al., 2019). Khan et al. identified a male patient with renal clear cell carcinoma in whom laboratory tests suggested that he did not have significant hematopoietic suppression. Cytopathy was found in the bone on computed tomography, and a bone marrow biopsy was performed, suggesting tumor cell infiltration. However, the authors did not report on the treatment and prognosis of patient (Khan et al., 2019).

6 Bone marrow necrosis

Hematological malignancies are the most common underlying disease of BMN, and caused by a solid tumor is very rare (Lee et al., 2004). Only two of the 101 smears of bone marrow metastases from solid tumors showed BMN (Xiao et al., 2009). Laboratory tests usually show suppression of bone marrow hematopoiesis (Wang et al., 2009). Common symptoms include fever, pancytopenia, and back pain (Janssens et al., 2000). This is similar to symptomatic BMM. In non-hematological malignancies, Lee et al. reported a case of a 67-year-old male with colorectal cancer BMN combined with thrombotic thrombocytopenic purpura, who received combination chemotherapy with oxaliplatin and 5-fluorouracil after diagnosis. After two treatment cycles, the patient's hematological results improved. His hematology remains stable 4.5 months after diagnosis (Lee et al., 2004). However, a 37-year-old male with colon cancer BMN was treated with cetuximab in combination with oxaliplatin and fluorouracil. The patient's disease went into remission in the first month after the start of treatment. Unfortunately, the patient died 3 months later due to disease progression (Wang et al., 2009).

7 Conclusion

In the early stages of malignancy, chemotherapy cannot wholly destroy the resting, dormant DCTs. At the same time, the bone marrow microenvironment with bone marrow-derived cells, microvasculature, and chemokines can promote the growth and metastasis of DCTs, resulting in symptomatic bone marrow metastases with allogeneic cytopenia in some patients. When the tumor cells in the bone marrow continue to proliferate and compress the microvasculature in the bone marrow, the result is impaired microcirculation and bone marrow necrosis. The suppression of bone marrow hematopoiesis and hemocytopenia characterizes this. DIC can also be life-threatening in some patients with gastric and colorectal cancers. Our literature review shows that most patients with solid tumors have BMM in combination with bone metastases, suggesting that bone marrow metastases may be a prerequisite for bone metastases. Symptomatic BMM and BMN have a poor prognosis. For patients with different types of tumors, cytotoxic chemotherapy can rapidly alleviate the symptoms of bone marrow infiltration. Still, its toxic side effects can significantly affect patients' quality of life. We found that in patients with HER-2 overexpressed lung and breast cancers, chemotherapy combined with molecularly targeted therapy resulted in a survival benefit for patients with BMM, and in patients with

HR positive, HER-2 negative breast cancers, CDK4/6 inhibitor with ET may be a better option for patients as its excellent great superiority due to its low toxicity and high efficiency. The bone marrow microenvironment can be disrupted by intervention to promote the metastatic drive of tumor cells. It is expected to prevent systemic metastasis in the later stage and control the tumor within a relatively easy treatment range. Future prospective studies with large samples are needed to explore the safety and efficacy of new agents in treating symptomatic BMM from different solid tumors.

Author contributions

RY: Writing–original draft. LJ: Conceptualization, Investigation, Writing–original draft, Writing–review and editing. JC: Conceptualization, Investigation, Writing–review and editing.

Funding

The author(s) declare that financial support was received for the research, authorship, and/or publication of this article. This article was supported by the Fund of Jilin Provincial Science and Technology Department (20210101311JC).

Acknowledgments

We thank all the patients and the authors involved in this study.

Conflict of interest

The authors declare that the research was conducted in the absence of any commercial or financial relationships that could be construed as a potential conflict of interest.

Publisher's note

All claims expressed in this article are solely those of the authors and do not necessarily represent those of their affiliated organizations, or those of the publisher, the editors and the reviewers. Any product that may be evaluated in this article, or claim that may be made by its manufacturer, is not guaranteed or endorsed by the publisher.

References

Ahmadzadeh, A., Kast, R. E., Ketabchi, N., Shahrabi, S., Shahjahani, M., Jaseb, K., et al. (2015). Regulatory effect of chemokines in bone marrow niche. *Cell Tissue Res.* 361 (2), 401–410. doi:10.1007/s00441-015-2129-4

Aida, Y., Ueki, T., Kirihara, T., Takeda, W., Kurihara, T., Sato, K., et al. (2015). Bone marrow metastasis of rhabdomyosarcoma mimicking acute leukemia: a case report and review of the literature. *Intern Med.* 54 (6), 643–650. doi:10.2169/internalmedicine.54.2473

Akagi, H., Shimada, A., Chin, K., and Domoto, H. (2021). Successful stabilization of symptomatic bone marrow metastasis two times in a breast cancer patient. *Anticancer Res.* 41 (6), 3139–3144. doi:10.21873/anticanres.15099

Alghandour, R., Saleh, G. A., Shokeir, F. A., and Zuhdy, M. (2020). Metastatic colorectal carcinoma initially diagnosed by bone marrow biopsy: a case report and literature review. *J. Egypt Natl. Canc Inst.* 32 (1), 30. doi:10.1186/s43046-020-00040-6

Amé-Thomas, P., Maby-El Hajjami, H., Monvoisin, C., Jean, R., Monnier, D., Caulet-Maugendre, S., et al. (2007). Human mesenchymal stem cells isolated from bone marrow and lymphoid organs support tumor B-cell growth: role of stromal cells in follicular lymphoma pathogenesis. *Blood* 109 (2), 693–702. doi:10.1182/blood-2006-05-020800

Ardavanis, A., Kountourakis, P., Orphanos, G., and Rigatos, G. (2008). Low-dose capecitabine in breast cancer patients with symptomatic bone marrow infiltration: a case study. *Anticancer Res.* 28 (1b), 539–541.

Arslan, C., Sen, C. A., and Ortac, R. (2015). A case of rectal carcinoma with skin and bone marrow metastasis with concurrent extensive visceral involvement; unusual and dismal co-incidence. *Expert Rev. Gastroenterol. Hepatol.* 9 (6), 727–730. doi:10.1586/17474124.2015.1025053

Asai, N., Ohkuni, Y., Matsuda, M., Narita, M., and Kaneko, N. (2013). Incremental low doses of amrubicin for the treatment of bone marrow metastasis in small cell lung cancer. *J. Bras. Pneumol.* 39 (1), 108–110. doi:10.1590/s1806-37132013000100016

Assi, R., Mukherji, D., Haydar, A., Saroufim, M., Temraz, S., and Shamseddine, A. (2016). Metastatic colorectal cancer presenting with bone marrow metastasis: a case series and review of literature. *J. Gastrointest. Oncol.* 7 (2), 284–297. doi:10.3978/j.issn.2078-6891.2015.092

Bailey, K. A., and Wexler, L. H. (2020). Pediatric rhabdomyosarcoma with bone marrow metastasis. *Pediatr. Blood Cancer* 67 (5), e28219. doi:10.1002/pbc.28219

Bergfeld, S. A., and DeClerck, Y. A. (2010). Bone marrow-derived mesenchymal stem cells and the tumor microenvironment. *Cancer Metastasis Rev.* 29 (2), 249–261. doi:10.1007/s10555-010-9222-7

Bjelic-Radisic, V., Stöger, H., Winter, R., Beham-Schmid, C., and Petru, E. (2006). Long-term control of bone marrow carcinosis and severe thrombocytopenia with standard-dose chemotherapy in a breast cancer patient: a case report. *Anticancer Res.* 26 (2b), 1627–1630.

Braun, S., Vogl, F. D., Janni, W., Marth, C., Schlimok, G., and Pantel, K. (2003). Evaluation of bone marrow in breast cancer patients: prediction of clinical outcome and response to therapy. *Breast* 12 (6), 397–404. doi:10.1016/s0960-9776(03)00143-7

Braun, S., Vogl, F. D., Naume, B., Janni, W., Osborne, M. P., Coombes, R. C., et al. (2005). A pooled analysis of bone marrow micrometastasis in breast cancer. *N. Engl. J. Med.* 353 (8), 793–802. doi:10.1056/NEJMoa050434

Cardoso, F., Paluch-Shimon, S., Senkus, E., Curigliano, G., Aapro, M. S., Andre, F., et al. (2020). 5th ESO-ESMO international consensus guidelines for advanced breast cancer (ABC 5). *Ann. Oncol.* 31 (12), 1623–1649. doi:10.1016/j.annonc.2020.09.010

Chavez-Macgregor, M., Aviles-Salas, A., Green, D., Fuentes-Alburo, A., Gómez-Ruiz, C., and Aguayo, A. (2005). Angiogenesis in the bone marrow of patients with breast cancer. *Clin. Cancer Res.* 11 (15), 5396–5400. doi:10.1158/1078-0432.Ccr-04-2420

Cheng, Z., Wei-Qi, J., and Jin, D. (2020). New insights on sorafenib resistance in liver cancer with correlation of individualized therapy. *Biochim. Biophys. Acta Rev. Cancer* 1874 (1), 188382. doi:10.1016/j.bbcan.2020.188382

Coghlin, C., and Murray, G. I. (2010). Current and emerging concepts in tumour metastasis. *J. Pathol.* 222 (1), 1–15. doi:10.1002/path.2727

Croucher, P. I., McDonald, M. M., and Martin, T. J. (2016). Bone metastasis: the importance of the neighbourhood. *Nat. Rev. Cancer* 16 (6), 373–386. doi:10.1038/nrc.2016.44

de Nigris, F., Schiano, C., Infante, T., and Napoli, C. (2012). CXCR4 inhibitors: tumor vasculature and therapeutic challenges. *Recent Pat. Anticancer Drug Discov.* 7 (3), 251–264. doi:10.2174/157489212801820039

Didelot, A., Taillandier, L., Grignon, Y., Vespignani, H., and Beauchesne, P. (2006). Concomitant bone marrow metastasis of a glioblastoma multiforme revealed at the diagnosis. *Acta Neurochir. (Wien)* 148 (9), 997–1000. doi:10.1007/s00701-006-0854-x

Dittus, C., Mathew, H., Malek, A., and Negroiu, A. (2014). Bone marrow infiltration as the initial presentation of gastric signet ring cell adenocarcinoma. *J. Gastrointest. Oncol.* 5 (6), E113–E116. doi:10.3978/j.issn.2078-6891.2014.050

Ekinci, A. S., Bal, O., Ozatli, T., Turker, I., Esbah, O., Demirci, A., et al. (2014). Gastric carcinoma with bone marrow metastasis: a case series. *J. Gastric Cancer* 14 (1), 54–57. doi:10.5230/jgc.2014.14.1.54

Freyer, G., Ligneau, B., and Trillet-Lenoir, V. V. (2000). Palliative hormone therapy, low-dose chemotherapy, and bisphosphonate in breast cancer patients with bone marrow involvement and pancytopenia: report of a pilot experience. *Eur. J. Intern. Med.* 11 (6), 329–333. doi:10.1016/s0953-6205(00)00121-7

Fumet, J. D., Wickre, M., Jacquot, J. P., Bizollon, M. H., Melis, A., Vanoli, A., et al. (2018). Successfully treatment by eribulin in visceral crisis: a case of lymphangitic carcinomatosis from metastatic breast cancer. *BMC Cancer* 18 (1), 839. doi:10.1186/s12885-018-4725-7

Garufi, G., Carbognin, L., Orlandi, A., Palazzo, A., Tortora, G., and Bria, E. (2021). The therapeutic challenge of disseminated bone marrow metastasis from HR-positive HER2-negative breast cancer: case report and review of the literature. *Front. Oncol.* 11, 651723. doi:10.3389/fonc.2021.651723

Gerber-Ferder, Y., Cosgrove, J., Duperray-Susini, A., Missolo-Koussou, Y., Dubois, M., Stepaniuk, K., et al. (2023). Breast cancer remotely imposes a myeloid bias on haematopoietic stem cells by reprogramming the bone marrow niche. *Nat. Cell Biol.* 25 (12), 1736–1745. doi:10.1038/s41556-023-01291-w

Ghajar, C. M. (2015). Metastasis prevention by targeting the dormant niche. *Nat. Rev. Cancer* 15 (4), 238–247. doi:10.1038/nrc3910

Ghajar, C. M., Peinado, H., Mori, H., Matei, I. R., Evason, K. J., Brazier, H., et al. (2013). The perivascular niche regulates breast tumour dormancy. *Nat. Cell Biol.* 15 (7), 807–817. doi:10.1038/ncb2767

Hanamura, F., Shibata, Y., Shirakawa, T., Kuwayama, M., Oda, H., Ariyama, H., et al. (2016). Favorable control of advanced colon adenocarcinoma with severe bone marrow metastasis: a case report. *Mol. Clin. Oncol.* 5 (5), 579–582. doi:10.3892/mco.2016.1029

Hirano, N., Goto, H., Suenobu, S., and Ihara, K. (2020). Bone marrow metastasis of neuroblastoma mimicking purulent osteomyelitis. *Jpn. J. Clin. Oncol.* 50 (10), 1227–1228. doi:10.1093/jjco/hyaa046

Hong, H., Gu, Y., Zhang, H., Simon, A. K., Chen, X., Wu, C., et al. (2010). Depletion of CD4+CD25+ regulatory T cells enhances natural killer T cell-mediated anti-tumour immunity in a murine mammary breast cancer model. *Clin. Exp. Immunol.* 159 (1), 93–99. doi:10.1111/j.1365-2249.2009.04018.x

Hong, Y. M., Yoon, K. T., Cho, M., Kang, D. H., Kim, H. W., Choi, C. W., et al. (2016). Bone marrow metastasis presenting as bicytopenia originating from hepatocellular carcinoma. *Clin. Mol. Hepatol.* 22 (2), 267–271. doi:10.3350/cmh.2015.0017

Hsu, E., Keene, D., Ventureyra, E., Matzinger, M. A., Jimenez, C., Wang, H. S., et al. (1998). Bone marrow metastasis in astrocytic gliomata. *J. Neurooncol* 37 (3), 285–293. doi:10.1023/a:1005909127196

Huang, C., Jian, B., Su, Y., Xu, N., Yu, T., He, L., et al. (2021). Clinical features and prognosis of paediatric rhabdomyosarcoma with bone marrow metastasis: a single Centre experiences in China. *BMC Pediatr.* 21 (1), 463. doi:10.1186/s12887-021-02904-9

Hung, Y. S., Chou, W. C., Chen, T. D., Chen, T. C., Wang, P. N., Chang, H., et al. (2014). Prognostic factors in adult patients with solid cancers and bone marrow metastases. *Asian Pac J. Cancer Prev.* 15 (1), 61–67. doi:10.7314/apjcp.2014.15.1.61

Iguchi, H. (2015). Recent aspects for disseminated carcinomatosis of the bone marrow associated with gastric cancer: what has been done for the past, and what will be needed in future? *World J. Gastroenterol.* 21 (43), 12249–12260. doi:10.3748/wjg.v21.i43.12249

Ihde, D. C., Simms, E. B., Matthews, M. J., Cohen, M. H., Bunn, P. A., and Minna, J. D. (1979). Bone marrow metastases in small cell carcinoma of the lung: frequency, description, and influence on chemotherapeutic toxicity and prognosis. *Blood* 53 (4), 677–686. doi:10.1182/blood.v53.4.677.bloodjournal534677

Jamieson-Gladney, W. L., Zhang, Y., Fong, A. M., Meucci, O., and Fatatis, A. (2011). The chemokine receptor CX3CR1 is directly involved in the arrest of breast cancer cells to the skeleton. *Breast Cancer Res.* 13 (5), R91. doi:10.1186/bcr3016

Janssens, A. M., Offner, F. C., and Van Hove, W. Z. (2000). Bone marrow necrosis. *Cancer* 88 (8), 1769–1780. doi:10.1002/(sici)1097-0142(20000415)88:8<1769::aid-cncr3>3.3.co;2-8

Jones, G. S., and Baldwin, D. R. (2018). Recent advances in the management of lung cancer. *Clin. Med. (Lond)* 18 (Suppl. 2), s41–s46. doi:10.7861/clinmedicine.18-2-s41

Kamby, C., Guldhammer, B., Vejborg, I., Rossing, N., Dirksen, H., Daugaard, S., et al. (1987). The presence of tumor cells in bone marrow at the time of first recurrence of breast cancer. *Cancer* 60 (6), 1306–1312. doi:10.1002/1097-0142(19870915)60:6<1306::aid-cncr2820600624>3.0.co;2-x

Kaplan, M. A., Kucukoner, M., Alpagat, G., and Isikdogan, A. (2012). Tumor lysis syndrome during radiotherapy for prostate cancer with bone and bone marrow metastases without visceral metastasis. *Ann. Saudi Med.* 32 (3), 306–308. doi:10.5144/0256-4947.2012.306-308

Kaplan, R. N., Psaila, B., and Lyden, D. (2006b). Bone marrow cells in the 'pre-metastatic niche': within bone and beyond. *Cancer metastasis Rev.* 25 (4), 521–529. doi:10.1007/s10555-006-9036-9

Kaplan, R. N., Rafii, S., and Lyden, D. (2006a). Preparing the "soil": the premetastatic niche. *Cancer Res.* 66 (23), 11089–11093. doi:10.1158/0008-5472.Can-06-2407

Kaplan, R. N., Riba, R. D., Zacharoulis, S., Bramley, A. H., Vincent, L., Costa, C., et al. (2005). VEGFR1-positive haematopoietic bone marrow progenitors initiate the pre-metastatic niche. *Nature* 438 (7069), 820–827. doi:10.1038/nature04186

Kawai, H., Tsujigiwa, H., Siar, C. H., Nakano, K., Takabatake, K., Fujii, M., et al. (2018). Characterization and potential roles of bone marrow-derived stromal cells in cancer development and metastasis. *Int. J. Med. Sci.* 15 (12), 1406–1414. doi:10.7150/ijms.24370

Khan, S., Awan, S. A., Jahangir, S., Kamran, S., and Ahmad, I. N. (2019). Bone marrow metastasis in clear cell renal cell carcinoma: a case study. *Cureus* 11 (3), e4181. doi:10.7759/cureus.4181

Kim, H. S., Yi, S. Y., Jun, H. J., Lee, J., Park, J. O., Park, Y. S., et al. (2007). Clinical outcome of gastric cancer patients with bone marrow metastases. *Oncology* 73 (3-4), 192–197. doi:10.1159/000127386

Kleinschmidt-Demasters, B. K. (1996). Diffuse bone marrow metastases from glioblastoma multiforme: the role of dural invasion. *Hum. Pathol.* 27 (2), 197–201. doi:10.1016/s0046-8177(96)90376-7

Kopp, H. G., Krauss, K., Fehm, T., Staebler, A., Zahm, J., Vogel, W., et al. (2011). Symptomatic bone marrow involvement in breast cancer--clinical presentation, treatment, and prognosis: a single institution review of 22 cases. *Anticancer Res.* 31 (11), 4025–4030.

Kulbe, H., Levinson, N. R., Balkwill, F., and Wilson, J. L. (2004). The chemokine network in cancer--much more than directing cell movement. *Int. J. Dev. Biol.* 48 (5-6), 489–496. doi:10.1387/ijdb.041814hk

Kusumbe, A. P. (2016). Vascular niches for disseminated tumour cells in bone. *J. Bone Oncol.* 5 (3), 112–116. doi:10.1016/j.jbo.2016.04.003

Kusumoto, H., Haraguchi, M., Nozuka, Y., Oda, Y., Tsuneyoshi, M., and Iguchi, H. (2006). Characteristic features of disseminated carcinomatosis of the bone marrow due to gastric cancer: the pathogenesis of bone destruction. *Oncol. Rep.* 16 (4), 735–740. doi:10.3892/or.16.4.735

Kwon, J. Y., Yun, J., Kim, H. J., Kim, K. H., Kim, S. H., Lee, S. C., et al. (2011). Clinical outcome of gastric cancer patients with bone marrow metastases. *Cancer Res. Treat.* 43 (4), 244–249. doi:10.4143/crt.2011.43.4.244

Lee, D. H., Park, C. J., Jang, S., Cho, Y. U., Seo, J. J., Im, H. J., et al. (2018b). Clinical and cytogenetic profiles of rhabdomyosarcoma with bone marrow involvement in Korean children: a 15-year single-institution experience. *Ann. Lab. Med.* 38 (2), 132–138. doi:10.3343/alm.2018.38.2.132

Lee, J. L., Lee, J. H., Kim, M. K., Cho, H. S., Bae, Y. K., Cho, K. H., et al. (2004). A case of bone marrow necrosis with thrombotic thrombocytopenic purpura as a manifestation of occult colon cancer. *Jpn. J. Clin. Oncol.* 34 (8), 476–480. doi:10.1093/jjco/hyh082

Lee, Y. T., Tan, Y. J., and Oon, C. E. (2018a). Molecular targeted therapy: treating cancer with specificity. *Eur. J. Pharmacol.* 834, 188–196. doi:10.1016/j.ejphar.2018.07.034

LoRusso, P. M., Tapazoglou, E., Zarbo, R. J., Cullis, P. A., Austin, D., and Al-Sarraf, M. (1988). Intracranial astrocytoma with diffuse bone marrow metastasis: a case report and review of the literature. *J. Neurooncol* 6 (1), 53–59. doi:10.1007/bf00163541

Lu, X., and Kang, Y. (2009). Chemokine (C-C motif) ligand 2 engages CCR2+ stromal cells of monocytic origin to promote breast cancer metastasis to lung and bone. *J. Biol. Chem.* 284 (42), 29087–29096. doi:10.1074/jbc.M109.035899

Lu, Y. S., Im, S. A., Colleoni, M., Franke, F., Bardia, A., Cardoso, F., et al. (2022). Updated overall survival of ribociclib plus endocrine therapy versus endocrine therapy alone in pre- and perimenopausal patients with hr+/HER2- advanced breast cancer in MONALEESA-7: a phase III randomized clinical trial. *Clin. cancer Res. official J. Am. Assoc. Cancer Res.* 28 (5), 851–859. doi:10.1158/1078-0432.CCR-21-3032

Luo, G., He, Y., and Yu, X. (2018). Bone marrow adipocyte: an intimate partner with tumor cells in bone metastasis. *Front. Endocrinol. (Lausanne)* 9, 339. doi:10.3389/fendo.2018.00339

Maisel, D., Lim, J. Y., Pollock, W. J., Yatani, R., and Liu, P. I. (1988). Bone marrow necrosis: an entity often overlooked. *Ann. Clin. Lab. Sci.* 18 (2), 109–115.

Meng, Q., Zhou, L., Liang, H., Hu, A., Zhou, H., Zhou, J., et al. (2022). Spine-specific downregulation of LAPTM5 expression promotes the progression and spinal metastasis of estrogen receptor-positive breast cancer by activating glutamine-dependent mTOR signaling. *Int. J. Oncol.* 60 (4), 47. doi:10.3892/ijo.2022.5337

Miyoshi, I., Daibata, M., Ohtsuki, Y., and Taguchi, H. (2005). Bone marrow necrosis. *Br. J. Haematol.* 130 (4), 467. doi:10.1111/j.1365-2141.2005.05532.x

Modi, S., Saura, C., Yamashita, T., Park, Y. H., Kim, S. B., Tamura, K., et al. (2020). Trastuzumab deruxtecan in previously treated HER2-positive breast cancer. *N. Engl. J. Med.* 382 (7), 610–621. doi:10.1056/NEJMoa1914510

Morash, C., Tey, R., Agbassi, C., Klotz, L., McGowan, T., Srigley, J., et al. (2015). Active surveillance for the management of localized prostate cancer: guideline recommendations. *Can. Urol. Assoc. J.* 9 (5-6), 171–178. doi:10.5489/cuaj.2806

Müller, A., Homey, B., Soto, H., Ge, N., Catron, D., Buchanan, M. E., et al. (2001). Involvement of chemokine receptors in breast cancer metastasis. *Nature* 410 (6824), 50–56. doi:10.1038/35065016

Nakashima, Y., Takeishi, K., Guntani, A., Tsujita, E., Yoshinaga, K., Matsuyama, A., et al. (2014). Rectal cancer with disseminated carcinomatosis of the bone marrow: report of a case. *Int. Surg.* 99 (5), 518–522. doi:10.9738/INTSURG-D-13-00130.1

OBrien, M. E., Wigler, N., Inbar, M., Rosso, R., Grischke, E., Santoro, A., et al. (2004). Reduced cardiotoxicity and comparable efficacy in a phase III trial of pegylated liposomal doxorubicin HCl (CAELYX/Doxil) versus conventional doxorubicin for

first-line treatment of metastatic breast cancer. *Ann. Oncol.* 15 (3), 440–449. doi:10.1093/annonc/mdh097

Ozkan, M., Er, O., Karahan, I. O., Deniz, K., Coşkun, R., Küçük, C., et al. (2007). Rectal carcinoid tumor with bone marrow and osteoblastic bone metastasis: a case report. *Turk J. Gastroenterol.* 18 (2), 111–114.

Pahouja, G., Wesolowski, R., Reinbolt, R., Tozbikian, G., Berger, M., Mangini, N., et al. (2015). Stabilization of bone marrow infiltration by metastatic breast cancer with continuous doxorubicin. *Cancer Treat. Commun.* 3, 28–32. doi:10.1016/j.ctrc.2014.11.002

Papac, R. J. (1994). Bone marrow metastases. A review. *Cancer* 74 (9), 2403–2413. doi:10.1002/1097-0142(19941101)74:9<2403::Aid-cncr2820740904>3.0.Co;2-f

Pittenger, M. F., Mackay, A. M., Beck, S. C., Jaiswal, R. K., Douglas, R., Mosca, J. D., et al. (1999). Multilineage potential of adult human mesenchymal stem cells. *Science* 284 (5411), 143–147. doi:10.1126/science.284.5411.143

Qiu, H., Cao, S., and Xu, R. (2021). Cancer incidence, mortality, and burden in China: a time-trend analysis and comparison with the United States and United Kingdom based on the global epidemiological data released in 2020. *Cancer Commun. (Lond)* 41 (10), 1037–1048. doi:10.1002/cac2.12197

Rahmat, C., and Ikhwan, R. (2018). Hormonal treatment for symptomatic bone marrow metastasis in breast cancer patients. *Maedica (Bucur)* 13 (3), 238–240. doi:10.26574/maedica.2018.13.3.238

Rajagopalan, V., El Kamar, F. G., Thayaparan, R., and Grossbard, M. L. (2005). Bone marrow metastases from glioblastoma multiforme--A case report and review of the literature. *J. Neurooncol* 72 (2), 157–161. doi:10.1007/s11060-004-3346-y

Sakin, A., Sakalar, T., Sahin, S., Yasar, N., Demir, C., Geredeli, C., et al. (2020). Factors affecting survival and treatment efficacy in breast cancer patients with bone marrow metastasis. *Breast J.* 26 (4), 815–818. doi:10.1111/tbj.13647

Seki, Y., and Wakaki, K. (2016). Pathological findings in a case of bone marrow carcinosis due to gastric cancer complicated by disseminated intravascular coagulation and thrombotic microangiopathy. *Int. J. Hematol.* 104 (4), 506–511. doi:10.1007/s12185-016-2051-x

Shahait, M., Abu-Hijlih, R., Salamat, A., Abou Heidar, N., Sharaf, B., Abuhijla, F., et al. (2022). Bone marrow involvement in patients with metastatic castration sensitive prostate cancer. *PLoS One* 17 (7), e0270956. doi:10.1371/journal.pone.0270956

Shi, J., Wei, Y., Xia, J., Wang, S., Wu, J., Chen, F., et al. (2014). CXCL12-CXCR4 contributes to the implication of bone marrow in cancer metastasis. *Future Oncol.* 10 (5), 749–759. doi:10.2217/fon.13.193

Shin, E., and Koo, J. S. (2020). The role of adipokines and bone marrow adipocytes in breast cancer bone metastasis. *Int. J. Mol. Sci.* 21 (14), 4967. doi:10.3390/ijms21144967

Singh, R., Stockard, C. R., Grizzle, W. E., Lillard, J. W., Jr., and Singh, S. (2011). Expression and histopathological correlation of CCR9 and CCL25 in ovarian cancer. *Int. J. Oncol.* 39 (2), 373–381. doi:10.3892/ijo.2011.1059

Slamon, D. J., Neven, P., Chia, S., Jerusalem, G., De Laurentiis, M., Im, S., et al. (2021). Ribociclib plus fulvestrant for postmenopausal women with hormone receptor-positive, human epidermal growth factor receptor 2-negative advanced breast cancer in the phase III randomized MONALEESA-3 trial: updated overall survival. *Ann. Oncol.* 32 (8), 1015–1024. doi:10.1016/j.annonc.2021.05.353

Sung, H., Ferlay, J., Siegel, R. L., Laversanne, M., Soerjomataram, I., Jemal, A., et al. (2021). Global cancer statistics 2020: GLOBOCAN estimates of incidence and mortality worldwide for 36 cancers in 185 countries. *CA Cancer J. Clin.* 71 (3), 209–249. doi:10.3322/caac.21660

Tanaka, G., Nakase, I., Fukuda, Y., Masuda, R., Oishi, S., Shimura, K., et al. (2012). CXCR4 stimulates macropinocytosis: implications for cellular uptake of arginine-rich cell-penetrating peptides and HIV. *Chem. Biol.* 19 (11), 1437–1446. doi:10.1016/j.chembiol.2012.09.011

Tavassoli, M. (2008). The marrow-blood barrier. *Br. J. Haematol.* 41 (3), 297–302. doi:10.1111/j.1365-2141.1979.tb05862.x

Teicher, B. A., and Fricker, S. P. (2010). CXCL12 (SDF-1)/CXCR4 pathway in cancer. *Clin. Cancer Res.* 16 (11), 2927–2931. doi:10.1158/1078-0432.Ccr-09-2329

Ubukata, H., Motohashi, G., Tabuchi, T., Nagata, H., Konishi, S., and Tabuchi, T. (2011). Overt bone metastasis and bone marrow micrometastasis of early gastric cancer. *Surg. Today* 41 (2), 169–174. doi:10.1007/s00595-010-4389-7

Umer, M., Mohib, Y., Atif, M., and Nazim, M. (2018). Skeletal metastasis in renal cell carcinoma: a review. *Ann. Med. Surg. (Lond)* 27, 9–16. doi:10.1016/j.amsu.2018.01.002

Wang, D., Luo, Y., Shen, D., Yang, L., Liu, H. Y., and Che, Y. Q. (2019). Clinical features and treatment of patients with lung adenocarcinoma with bone marrow metastasis. *Tumori* 105 (5), 388–393. doi:10.1177/0300891619839864

Wang, Y. C., Chang, P. Y., and Yao, N. S. (2009). Bone marrow necrosis caused by metastatic colon cancer. *J. Clin. Oncol.* 27 (23), e48. doi:10.1200/JCO.2008.21.3140

Weilbaecher, K. N., Guise, T. A., and McCauley, L. K. (2011). Cancer to bone: a fatal attraction. *Nat. Rev. Cancer* 11 (6), 411–425. doi:10.1038/nrc3055

Weiss, A. R., Lyden, E. R., Anderson, J. R., Hawkins, D. S., Spunt, S. L., Walterhouse, D. O., et al. (2013). Histologic and clinical characteristics can guide staging evaluations for children and adolescents with rhabdomyosarcoma: a report from the Children's Oncology Group Soft Tissue Sarcoma Committee. *J. Clin. Oncol.* 31 (26), 3226–3232. doi:10.1200/JCO.2012.44.6476

Wool, G. D., and Deucher, A. (2015). Bone marrow necrosis: ten-year retrospective review of bone marrow biopsy specimens. *Am. J. Clin. Pathol.* 143 (2), 201–213. doi:10.1309/AJCP0TN1MCMOLMPK

Wu, Y., Ni, J., Chang, X., Zhang, X., and Zhang, L. (2020). Successful treatment of pyrotinib for bone marrow metastasis induced pancytopenia in a patient with non-small-cell lung cancer and ERBB2 mutation. *Thorac. Cancer* 11 (7), 2051–2055. doi:10.1111/1759-7714.13480

Xiao, L., Luxi, S., Ying, T., Yizhi, L., Lingyun, W., and Quan, P. (2009). Diagnosis of unknown nonhematological tumors by bone marrow biopsy: a retrospective analysis of 10,112 samples. *J. Cancer Res. Clin. Oncol.* 135 (5), 687–693. doi:10.1007/s00432-008-0503-2

Xu, L., Guo, F., Song, S., Zhang, G., Liu, Y., and Xie, X. (2014). Trastuzumab monotherapy for bone marrow metastasis of breast cancer: a case report. *Oncol. Lett.* 7 (6), 1951–1953. doi:10.3892/ol.2014.1999

Yang, R., Jia, L., Lu, G., Lv, Z., and Cui, J. (2022a). Symptomatic bone marrow metastases in breast cancer: a retrospective cohort study. *Front. Oncol.* 12, 1042773. doi:10.3389/fonc.2022.1042773

Yang, R., Lu, G., Lv, Z., Jia, L., and Cui, J. (2022b). Different treatment regimens in breast cancer visceral crisis: a retrospective cohort study. *Front. Oncol.* 12, 1048781. doi:10.3389/fonc.2022.1048781

Yip, R. K. H., Rimes, J. S., Capaldo, B. D., Vaillant, F., Mouchemore, K. A., Pal, B., et al. (2021). Mammary tumour cells remodel the bone marrow vascular microenvironment to support metastasis. *Nat. Commun.* 12 (1), 6920. doi:10.1038/s41467-021-26556-6

Yoshioka, K., Shimizu, H., Yokoo, S., and Andachi, H. (1992). Disseminated carcinomatosis of bone marrow from submucosal carcinoma in adenoma of the rectum. *Intern Med.* 31 (8), 1056–1059. doi:10.2169/internalmedicine.31.1056

Zhai, X., Wang, C., Li, S., Cao, T., Du, G., Zhang, Y., et al. (2022). Bone marrow metastasis from advanced gastric cancer complicated with disseminated intravascular coagulation: a highly aggressive but manageable disease subtype. *Cancer Commun. (Lond)* 42 (4), 350–354. doi:10.1002/cac2.12277

Zhang, B., Zhang, T., Jin, L., Zhang, Y., and Wei, Q. (2022). Treatment strategy of metastatic nasopharyngeal carcinoma with bone marrow involvement-A case report. *Front. Oncol.* 12, 877451. doi:10.3389/fonc.2022.877451

Zych, J., Polowiec, Z., Wiatr, E., Broniek, A., and Rowinska-Zakrzewska, E. (1993). The prognostic significance of bone marrow metastases in small cell lung cancer patients. *Lung Cancer* 10 (3-4), 239–245. doi:10.1016/0169-5002(93)90184-y

Frontiers in Pharmacology

Explores the interactions between chemicals and living beings

The most cited journal in its field, which advances access to pharmacological discoveries to prevent and treat human disease.

Discover the latest Research Topics

See more →

Frontiers

Avenue du Tribunal-Fédéral 34
1005 Lausanne, Switzerland
frontiersin.org

Contact us

+41 (0)21 510 17 00
frontiersin.org/about/contact